TOPICS IN
STEREOCHEMISTRY

VOLUME 2

AN INTERSCIENCE SERIES

ADVISORY BOARD

TOPICS IN
STEREOCHEMISTRY

EDITORS

NORMAN L. ALLINGER

Professor of Chemistry
Wayne State University
Detroit, Michigan

ERNEST L. ELIEL

Professor of Chemistry
University of Notre Dame
Notre Dame, Indiana

VOLUME 2

INTERSCIENCE PUBLISHERS
A DIVISION OF JOHN WILEY & SONS
New York · London · Sydney

Library of Congress Catalog Card Number 67-13943
Printed in the United States of America

INTRODUCTION

During the last five years several texts in the areas of stereochemistry and conformational analysis have been published, including *Stereochemistry of Carbon Compounds* (Eliel, McGraw-Hill, 1962) and *Conformational Analysis* (Eliel, Allinger, Angyal, and Morrison, Interscience, 1965). While the writing of these books was stimulated by the high level of research activity in the area of stereochemistry, it has, in turn, spurred further activity. As a result, many of the details found in these texts are already inadequate or out of date, although the student of stereochemistry and conformational analysis may still learn the basic concepts of the subject from them.

For both human and economic reasons, standard textbooks can be revised only at infrequent intervals. Yet the spate of periodical publications in the field of stereochemistry is such that it is an almost hopeless task for anyone to update himself by reading all the original literature. The present series is designed to bridge the resulting gap.

If that were its only purpose, this series would have been called "Advances (or "Recent Advances") in Stereochemistry." It must be remembered, however, that the above-mentioned texts were themselves not treatises and did not aim at an exhaustive treatment of the field. Thus the present series has a second purpose, namely to deal in greater detail with some of the topics summarized in the standard texts. It is for this reason that we have selected the title *Topics in Stereochemistry*.

The series is intended for the advanced student, the teacher, and the active researcher. A background of the basic knowledge in the field of stereochemistry is assumed. Each chapter is written by an expert in the field and, hopefully, covers its subject in depth. We have tried to choose topics of fundamental import, aimed primarily at an audience of organic chemists (and, possibly, biochemists), but involved frequently with fundamental principles of physical chemistry and molecular physics. At a later time perhaps, we hope to devote more space to inorganic stereochemistry.

It is our present intention to bring out volumes at approximately annual intervals. The Editors will welcome suggestions as to suitable topics for future volumes.

We are fortunate in having been able to secure the help of an international board of Editorial Advisors who have been of great assistance by suggesting topics and authors for several articles and by helping us avoid duplication of topics appearing in other, related monograph series. We are grateful to the Editorial Advisors for this assistance, but the Editors and Authors alone must assume the responsibility for any shortcomings of *Topics in Stereochemistry.*

N. L. Allinger
E. L. Eliel

January 1967

PREFACE

In the present volume are brought together four chapters on diverse areas of current interest within the field of stereochemistry. In the first chapter, James H. Brewster discusses in some detail a method for the calculation of the optical rotations of organic molecules based on structure, configuration, and conformation. The method, first disclosed in 1959, has proved of considerable use—especially in those cases where the complementary methods of optical rotatory dispersion and circular dichroism (Vol. 1) are not accessible. In the present chapter, the original author of the method extends it and develops in some detail the underlying theory.

A mere twelve years have elapsed since the concept of a stereoregular polymer arose; in the intervening period there has been an explosive growth, not only in the theoretical understanding of such polymers and their formation, but also in their industrial applications. In the second chapter, Murray Goodman gives a comprehensive but concise review of the present status of polymer stereochemistry. The chapter is written for the organic chemist not thoroughly conversant with polymer chemistry and, besides familiarizing him with an important and active field, should serve to correlate the stereochemistry of polymers with that of smaller molecules.

The stereochemistry of addition reactions to saturated carbonyl compounds is just beginning to be understood. In the third chapter, Edmond Toromanoff discusses the related 1,2-addition to unsaturated carbonyl compounds, a topic which is of considerable practical importance, especially in the steroid field.

The final chapter in this volume, by Morton Raban and Kurt Mislow, is concerned with modern methods for the determination of optical purity. Since this subject was considered in a standard textbook a mere five years ago, two important and very convenient new methods have been developed—the gas chromatographic method and the NMR method for determining optical purity. In the fourth chapter these approaches are presented in detail, along with the older and more classical methods.

AUTHORS OF VOLUME 2

J. H. BREWSTER
Department of Chemistry
Purdue University
Lafayette, Indiana

M. GOODMAN
Department of Chemistry
Polytechnic Institute of Brooklyn
Brooklyn, New York

K. MISLOW
Department of Chemistry
Princeton University
Princeton, New Jersey

M. RABAN
Department of Chemistry
Wayne State University
Detroit, Michigan

E. TOROMANOFF
Centre de Recherches Roussel-Uclaf
Romainville, France

CONTENTS

Topics in Stereochemistry, Volume 2
Edited by Norman L. Allinger, Ernest L. Eliel

Helix Models of Optical Activity

JAMES H. BREWSTER

Department of Chemistry, Purdue University
Lafayette, Indiana

I. INTRODUCTION

The theoretical concepts necessary for the development of a simple but sound general model of optical activity have been available for many years (1) but no such model, suited to both the qualitative and quantitative needs of the ordinary organic chemist, appears to have been developed. Kauzmann (2) came close with a model that provides great enlightenment; however, this model was not reduced to the level at which useful numerical predictions could be made. A closely related model, developed on the principles of wave mechanics by Tinoco and Woody (3), gave numerical predictions but is, at least in this author's opinion, neither general enough nor mathematically simple enough to be of much use to the organic chemist.* We will attempt here to describe in some detail a model which one organic chemist finds useful. It stands in direct line of descent from the model of Kauzmann (2) and is collaterally related to that of Tinoco and Woody (3). Like all models it is subject to limitations imposed by the overriding need for simplicity and by the fact that it rests on a number of arguments by analogy. It seems best, then, to begin by summarizing its basic features and by pointing out what may prove to be the origins of some limitations.

We start with Fresnel's model, in which optical rotation is produced by differences in refractive index for right (n_r) and left (n_l) circular polarized light (4a):

$$[\Phi]_\lambda = (18\mathrm{MW}/\rho\lambda)(n_l - n_r) \tag{1}$$

where $[\Phi]$ is molecular rotation in degrees, MW is molecular weight, ρ is density or concentration (g/cc), and λ is wavelength (*in vacuo*) (cm). According to this model dextrorotation (at long wavelengths) results when left circular polarized light interacts more strongly with the medium than does right circular polarized light. This could occur, as shown by the use of classical electromagnetics, if electrons are constrained to helical paths, a right-handed helix conductor giving dextrorotation. Although Fresnel (4b) and Pasteur (5) suggested that helical units of molecular structure could produce optical rotation, the relationship between handedness of structure and direction of rotation was, apparently, first given by Gibbs (6) and then, in more detail, by Drude (7). Drude's model (7), however, was based on an interaction of matter only with the electric field of light and was shown to be in error by Born (8) and Kuhn (9); this objection can be overcome by taking into account the effects of both the electric and magnetic fields of light on a helix (1–3,10). The model we use is closely related to that of Kauzmann (2), but not identical to it. The derivation has been simplified

*This is to be regarded in part as a commentary on the deficiencies in the training of organic chemists, including the present author.

and is keyed to Kauzmann's text for the benefit of those wishing the more detailed mathematical insight he provides. Like Kauzmann (2), we use a simple classical electromagnetic wave model of light. Where he considers the motions of two electrons in a double stranded helix we [in common with Tinoco and Woody (3)] consider a single helix having the properties of a uniform macroscopic wire.

We depart somewhat from both models in allowing the helix to be irregular and arrive at an equation defining rotation in terms of the dimensions of the conductor system and the refractivities of its constituents:

$$[\Phi]_D = 652(LA/D^2)(\sum R_D)f(n) \qquad (2)$$

where D is the length of the conducting pathway (Å), L is the length of the helix axis (Å), A is the area subtended by projection on a plane perpendicular to the axis (Å^2), $\sum R_D$ is the sum of the refractions of the bonds composing the helix (cm^3/mole), and $f(n)$ is a function of the refractive index of the fluid medium.

This equation and its interpretation are comparable to that given by Kauzmann (2a); he has shown his equations to be in satisfactory correspondence with those obtained via quantum mechanics (2b). This correspondence does not constitute evidence for the theoretical validity of the model, but it does indicate that it can reasonably be expected to be reliable when used with due respect for its limitations and when empirically checked out against appropriate analogs. The obvious origins of limitations in such a model include: (*a*) use of the classical wave theory of light, (*b*) use of classical macroscopic electromagnetics, (*c*) use of refractivity as a measure of extent of interaction between light and matter, and (*d*) comparison of chemical bonds to copper wires.

We justify these features of the model on heuristic grounds, pointing out that the model does allow reasonably good estimates of rotatory power to be made in a simple way.

The conclusion that a right-handed helical conductor will be dextrorotatory at long wavelengths is not without relevance to studies of optical rotatory dispersion (ORD) (11,12) and circular dichroism (CD) (12,13). The general relationship between absorption and refraction [Kronig-Kramers theorem (14)] indicates that any unit of structure giving rise to a positive Cotton effect at its absorption band will make a positive contribution to rotation at longer wavelengths; a positive

Cotton effect is, therefore, also indicative of right-hand helicity. Admitting that there may sometimes be difficulty in comparing the details of an electronic transition to movement of current in a coil of wire, we suggest that useful insights of a qualitative nature can be obtained by use of such analogies. Indeed, they are most useful in ORD and CD work precisely because such measurements serve to pick out the contributions of particular units of structure, making it possible to say unequivocally which portion of a molecule must have the helicity indicated by the sign of the Cotton effect.

II. BASIC PRINCIPLES

A. Electromagnetic Rules and Conventions

We assume that the relationships to be described below are valid at the molecular level and can be applied as though covalent bonds have the properties of wires. Current will be described as a flow of positive charge unless an electronic interpretation is specifically required.

1. An electric field (E) will exert a force (F) on a positive charge (e):

$$F = eE \tag{3}$$

in the direction of the field.

2. A flow of positive charge (Fig. 1, light arrow) induces a magnetic field having circular "lines of force" (dark arrow) in planes perpendicular to the current. The direction of the magnetic field is related to the direction of the current as shown in Figure 1.

3. If the current flows in a loop the magnetic lines of force coalesce to produce a magnetic field as shown in Figure 2. This field is identical to

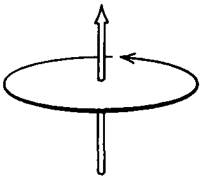

Fig. 1. Circular magnetic field induced by a linear current.

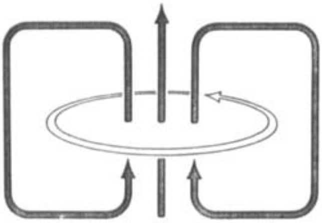

Fig. 2. Magnetic field induced by a circular current.

that produced by a small magnet having its axis perpendicular to the plane of the loop and having a magnetic moment (μ, in emu) equal to the product of the current (I, in esu) and the area of the loop (A, in cm^2) (Ampere's law):

$$\mu = IA/c \tag{4}$$

where c, the velocity of light, is the factor relating esu and emu.

4. When a loop conductor is held in a steady magnetic field no current will be induced in it. As the intensity of the magnetic field (H_0) increases there will be induced a current flowing so that it produces a magnetic field (H') opposing the change (Lenz's law) (Fig. 3).

B. Plane Polarized Light

A ray of light is considered to consist of an electric (E) and a magnetic (H) field oscillating at right angles to one another and to the direction of propagation (Fig. 4). The two fields are in phase, mutually sustaining,

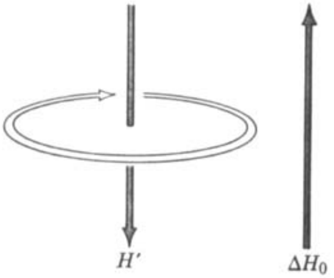

Fig. 3. Current induced in a loop conductor by a change (ΔH_0) of magnetic field.

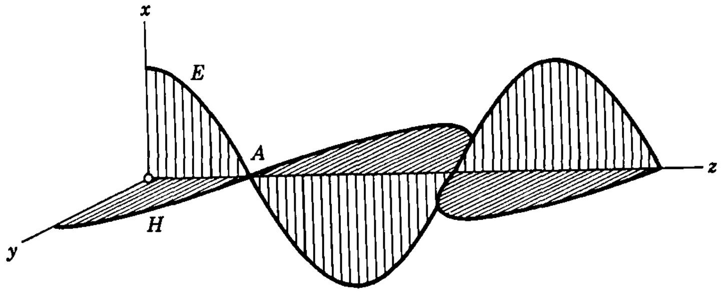

Fig. 4. A beam of plane polarized light. The electric field (E) oscillates in the xz plane while the magnetic field oscillates in the yz plane. At point A the electric field is increasing upward with time and the magnetic field is increasing toward the reader. The light beam is traveling in the direction of increasing z.

and oriented in accord with the Poynting diagram (Fig. 5). Figure 4 represents the structure of a part of the ray at one moment in time; the entire structure is to be pictured as moving to the right along the z axis with time. A beam of plane polarized light consists of a bundle of concurrent rays, all oriented in the same way.

C. Circular Polarized Light

A circular polarized ray can be pictured as the resultant of two equal and concurrent plane polarized rays which have their electric fields set at right angles and one-quarter wavelength out of phase (Fig. 6; the

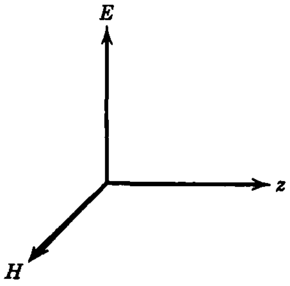

Fig. 5. The Poynting diagram.

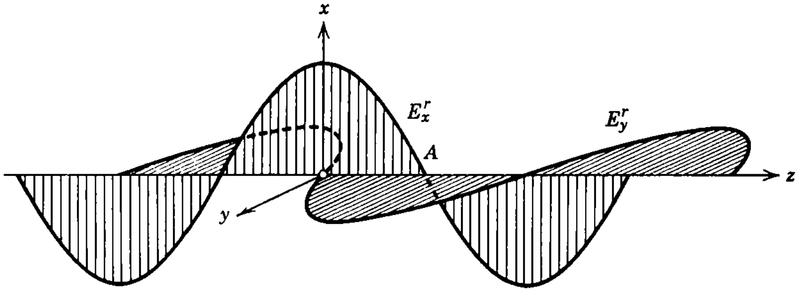

Fig. 6. A right circular polarized ray (electric fields only).

magnetic fields have been omitted for clarity). The ray shown here is described as right handed on the basis of its structure. Lines showing the direction of the electric field at quarter-wavelength intervals along the z axis, all at one specific moment (Fig. 7), define a right-handed helix (Fig. 8). An observer standing at, for example, the point where $z = \lambda/4$ (point A in Fig. 6), and facing the oncoming light, would find the electric field at his station (E_r) directed to the left (Fig. 9). With time, the orientation of this field at that point would rotate clockwise (this is a second basis for designating such a ray right handed), one complete rotation corresponding to motion through one wavelength (λ in vacuum, λ' in a material medium) along the z axis. The angle of rotation (φ_r) between E_r and E_0, both taken at the same instant (Fig. 9), can be expressed (in radians) as:

$$\varphi_r = -2\pi z/\lambda' \tag{5}$$

These angles are measured clockwise from the origin (E_0) so that φ_r will

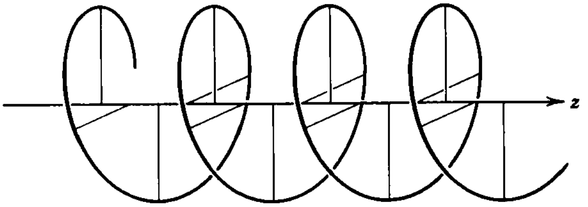

Fig. 7. Instantaneous electric field of a right circular polarized ray.

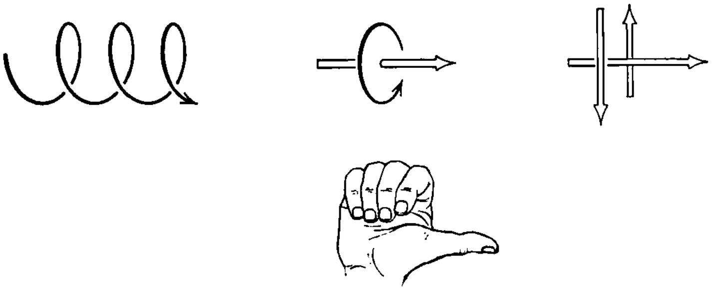

Fig. 8. Right-hand helicity.

be negative and the corresponding angle (φ_l) for a left circular polarized ray (Fig. 10) will be positive. For the case where the light is traversing a material medium these angles can also be expressed in terms of refractive index (n), since the frequency (ν) of the light is taken as constant:

$$n = c/v = \lambda/\lambda' \tag{6}$$

or,

$$\varphi_r = -2\pi z n_r/\lambda \tag{7a}$$

where λ is the wavelength of light in vacuum. (Recall that $c = \lambda\nu$.)

We will be particularly concerned with the interrelation of plane and circular polarized rays of light. It is readily seen that superposition of the rays shown in Figures 6 and 10 would produce an exact cancellation of the horizontal components (yz plane) and reinforcement of the vertical components (xz plane), giving a plane polarized ray (Fig. 4). Conversely a plane-polarized ray could, in principle, be broken down into two rays

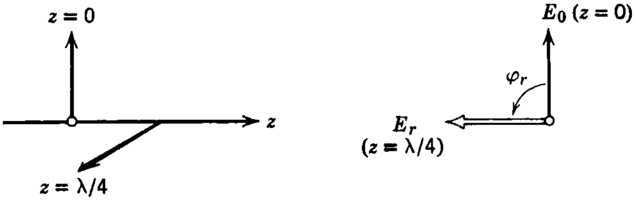

Fig. 9. Instantaneous electric field of a right circular ray (Fig. 6) at the origin ($z = 0$) and at point A ($z = \lambda/4$).

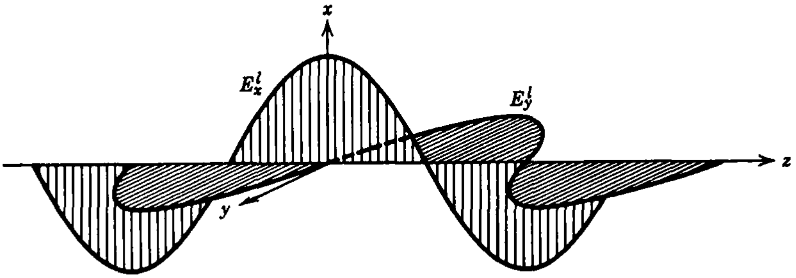

Fig. 10. A left circular polarized ray (electric fields only).

circular polarized in opposite senses but otherwise equal. This principle is central to Fresnel's picture (4a) of optical rotation (below) which, in turn, is central to the present model of optical activity.

D. Optical Rotation

If a medium has the same refractive index for right and left circular polarized light the electric fields (E_r and E_l) will be rotated (from E_0) through equal but opposite angles at every point along the z axis:

$$\varphi_l = -\varphi_r = 2\pi zn/\lambda \tag{7b}$$

The resultant of the electric fields will, then, always be oriented as was the original incident plane polarized ray. If, however, the refractive indices are different, then the angles of rotation will be different and recombination of the circular rays will now give a plane polarized ray (E_z) that has been rotated by some angle (φ) from the plane of the incident ray (E_0) (Fig. 11). The amount of this optical rotation is readily obtained:

$$\varphi = \varphi_l - (\varphi_l - \varphi_r)/2 = (\varphi_l + \varphi_r)/2 \tag{8}$$

(recall that φ_r is negative) or, in terms of refractive indices:

$$\varphi = (\pi z/\lambda)(n_l - n_r) \tag{9a}$$

This is the Fresnel equation (4a); it shows that dextrorotation (as seen in Fig. 11) occurs when the refractive index is greater for the left circular polarized ray.

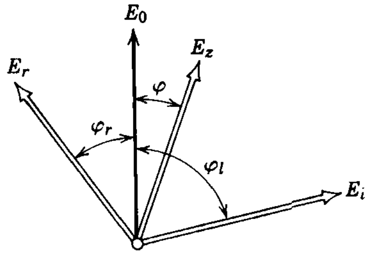

Fig. 11. Orientation of electric fields in an optically active medium (dextrorotatory).

It follows from this analysis that a set of prisms of, alternately, *d* and *l* quartz, arranged as in Figure 12, should be capable of splitting a plane-polarized ray into two opposite circular polarized rays. This has, in fact, been shown by Fresnel (4a), and, for liquids, by von Fleischl (15).

Equation (9a) gives the rotation in radians when the sample thickness (z) and the wavelength (λ) are in the same units. The specific rotation:

$$[\varphi] = \varphi/\rho l \tag{10}$$

where ρ is the density or concentration in g/cc and l is the length of the sample in decimeters, is, then, in degrees:

$$[\varphi] = (1800/\rho\lambda)(n_l - n_r) \tag{9b}$$

where λ is in centimeters.

Comparisons among compounds are generally made in terms of molecular rotation:

$$[\Phi] = [\varphi]\mathrm{MW}/100 \tag{11}$$

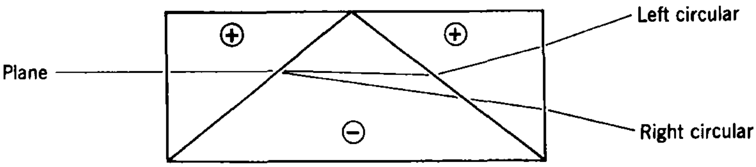

Fig. 12. Formation of circular polarized rays from a plane ray.

whence we obtain eq. (1):

$$[\Phi]_\lambda = (18\mathrm{MW}/\rho\lambda)(n_l - n_r) \tag{1}$$

It is of interest that an unexceptional molecular rotation of 46 could be produced at the sodium D line ($\lambda = 5893 \times 10^{-8}$ cm) by a substance with a molecular weight of 150, a density of 1, and a refractive index difference of 10^{-6}.

E. Polarizability

A molecular model of optical activity requires a connection between refractive index and bond structure. This is provided by the electrical polarizability (16), or sensitivity to deformation by electrical fields, and molecular refraction:

$$R = (4\pi N_0/3)\alpha \tag{12}$$

where α is the mean electrical polarizability of a molecule (spherical average), N_0 is Avogadro's number and R is the molecular refraction.

We use here the Lorentz-Lorenz refraction:

$$R = (\mathrm{MW}/\rho)[(n^2 - 1)/(n^2 + 2)] \tag{13a}$$

which already contains the "Lorentz factor" (17): $(n^2 + 2)/3$, that takes into account intermolecular interactions of induced dipoles. Equation (13a) can be rearranged to:

$$n^2 = (\mathrm{MW} + 2\rho R)/(\mathrm{MW} - \rho R) \tag{13b}$$

Letting $n_l = n + \Delta$ and $n_r = n - \Delta$ and distinguishing R_l and R_r we obtain:

$$4\Delta n = \frac{3\mathrm{MW}\rho(R_l - R_r)}{(\mathrm{MW} - \rho R_l)(\mathrm{MW} - \rho R_r)} \tag{14a}$$

but

$$(n^2 + 2)/3 = \mathrm{MW}/(\mathrm{MW} - \rho R) \tag{13c}$$

whence, to a very good approximation

$$4\Delta = (3\rho/\mathrm{MW})(R_l - R_r)[(n^2 + 2)/3][(n^2 + 2)/3n] \tag{14b}$$

Since

$$n_l - n_r = 2\Delta$$

and

$$R_l - R_r = (4\pi N_0/3)(\alpha_l - \alpha_r) \tag{12b}$$

we obtain

$$n_l - n_r = (2\pi N_0/\mathrm{MW})\rho(\alpha_l - \alpha_r)[(n^2 + 2)/3][(n^2 + 2)/3n] \qquad (15)$$

Letting

$$f(n) = [(n^2 + 2)/3][(n^2 + 2)/3n] \qquad (16)$$

the Fresnel equation [eq. (1)] becomes

$$[\Phi]_\lambda = (36\pi N_0/\lambda)(\alpha_l - \alpha_r)f(n) \qquad (17)$$

We digress at this point to note that terms related to $f(n)$ have long been recognized as contributing to the dependence of rotation on solvent, concentration and temperature; see particularly the work of Beckmann et al. (18) for the use of "rotivity":

$$\Omega = [\Phi]/(n^2 + 2) \qquad (18)$$

in dealing with solvent effects. Our expression [eq. (16)] is roughly equivalent to the "Lorentz factor," which is used in all recent models, since the term $(n^2 + 2)/3n$ is approximately unity for ordinary values of refractive index. The term $f(n)$ is required in the equations to be developed below; it will be left in this form for convenience and also to leave open the question of which form is better. In most solvents its numerical value is of the order of $\frac{4}{3}$.

III. THE HELIX MODEL OF OPTICAL ACTIVITY

A. The General Model

A beam of circular polarized light can be described as the resultant of two rays plane polarized at right angles and one quarter wavelength out of phase. For many purposes it is sufficient to focus attention on the electrical component alone (as, for example, in Figs. 6, 7, 9, and 10), it being understood that the magnetic component will be present and will be oriented in accord with Figures 4 and 5. We need now, however, to consider the relationships of the electric and magnetic fields in a plane along which the circular ray is being propagated.

Figure 13 is a representation of the electric (E_x^r) and magnetic (H_x^r) fields in the xz plane of the right circular polarized beam shown in Figure 6, the magnetic field being that of the plane ray whose electric field lies in the yz plane. Figure 14 shows the electric and magnetic fields

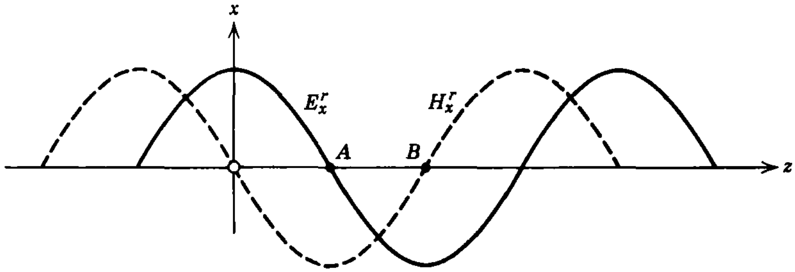

Fig. 13. Planar (xz) representation of right circular polarized light ($t = 0$). $E_x^r = \frac{1}{2}E_0 \cos \omega (t - z/c)$; $H_x^r = \frac{1}{2}H_0 \sin \omega (t - z/c)$; $\omega = 2\pi\nu = 2\pi c/\lambda$.

of the corresponding left circular polarized ray (Fig. 10) in the *xz* plane. Although the helicity and dissymmetry of these beams is not obvious in these drawings, it is evident that superposition of the two rays would leave only the electric field of the plane polarized ray shown in Figure 4.

When these rays (Figs. 13 and 14) are traversing a material medium, both will produce an upward flow of positive charge in the medium at point *A*. If the molecules of the medium are so constituted that this flow of charge also produces a parallel (upward) magnetic field then the left polarized ray (Fig. 14) will be reinforced in its interaction with the medium while the right ray (Fig. 13) will be opposed. In a similar fashion the left circular polarized ray has an increasingly positive magnetic flux at point *B*. If this should produce a downward flow of positive charge in the medium then this will augment the effect of the electric field at this point. On the principle that the magnitude of the

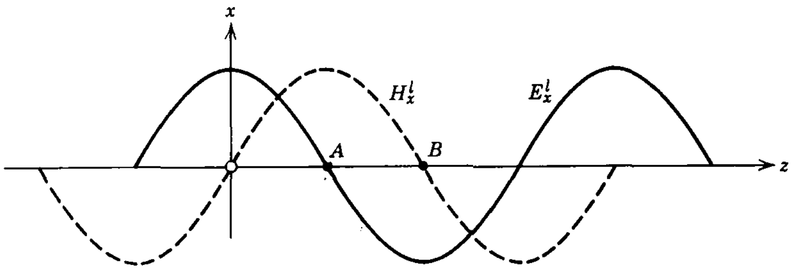

Fig. 14. Planar (xz) representation of left circular polarized light ($t = 0$). $E_x^l = \frac{1}{2}E_0 \cos \omega (t - z/c)$; $H_x^l = -\frac{1}{2}H_0 \sin \omega (t - z/c)$; $\omega = 2\pi\nu = 2\pi c/\lambda$.

refractive index is a reflection of the extent to which electric oscillations are induced in the medium by the light, we can say that n_l will be greater than n_r (the condition for dextrorotation) when:

a. The induced magnetic dipole moment (μ) is in the same direction as the change in electric field (point *A*, Fig. 14):

$$\mu = \frac{\gamma}{c}\frac{\partial E}{\partial t} \tag{19}$$

b. The induced electric dipole moment (m) is in the direction opposite that of the change in magnetic field (point *B*, Fig. 14)

$$m = -\frac{\beta}{c}\frac{\partial H}{\partial t} \tag{20}$$

where β and γ are molecular polarizability parameters (ref. 2a, p. 616).

From the laws of electromagnetics (Figs. 1–3) we can see that the requirement for dextrorotation will be met by a molecule having the characteristics of a right-handed helical conductor (Figs. 15a and 16a). At point *A* in Figure 14 such a conductor would experience an upward driving of positive charge; such motion would also require a circular component of motion which, from Figure 2, would give an upward magnetic field [eq. (19)]. The enantiomeric left-handed helical conductor (Figs. 15*b* and 16*b*) would, under the same influence, give a downward magnetic field. At point *B* in Figure 14 there is an upward magnetic flux. This, from Figure 3, will induce a circular motion in the conductors (Fig. 16), leading to a downward displacement of positive charge in the case of the right-handed conductor (16a) [eq. (20)].

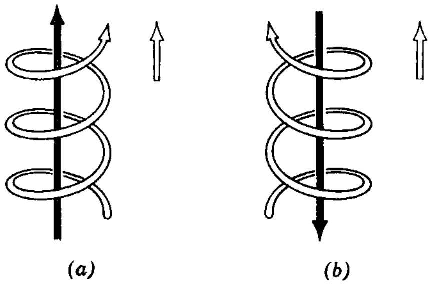

Fig. 15. Induced magnetic fields (dark arrows) in helical conductors at point *A* in Figure 14.

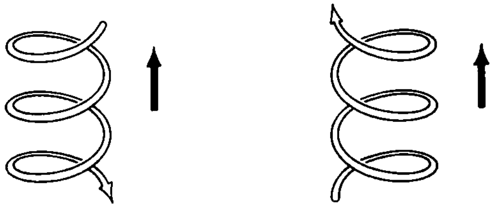

(a) *(b)*

Fig. 16. Induced currents (light arrows) in helical conductors at point *B* in Figure 14.

We conclude, thus, that a right-handed helical conductor will give dextrorotation when positive charge moves in phase with the electric field. By the same token, a right-handed helical conductor will give levorotation when positive charge moves out of phase with the electric field since then the magnetic effect at *A* or the electric effect at *B* would be greater with right than with left circular polarized light. This is a conclusion of some importance because in the classical model of light a charged particle is considered to respond to periodic perturbation in analogy with macroscopic mechanical systems:

$$\text{response} = \text{constant}/(\nu_i^2 - \nu^2)$$

where ν_i is the "natural frequency" of the *i*th particle and ν the applied frequency. Maximum response, corresponding to excitation, occurs at the "natural frequency"; the response becomes rapidly smaller at higher or lower frequencies. At low frequencies the response is in phase with the periodic perturber, but at high frequencies it is out of phase.* Equations of the form shown above accurately describe the variation of refractive index with frequency and indicate a relation of that property to strong absorption bands. The Drude (7) expression for optical rotation (recast in wavelength terms) $\varphi = k/(\lambda^2 - \lambda_i^2)$, is of the same form because it was derived from refractive dispersion equations; it is found to give a satisfactory description of the rotatory effects

---

*This effect is seen in driving on washboard roads. When the wheels hit the bumps at the "natural frequency" of the springs, mechanical resonance will occur and the vehicle may go out of control—in rough analogy to the excitation process. At higher speeds the wheels oscillate less vigorously, but now out of phase, hitting only the tops of the bumps, and giving a smoother ride.

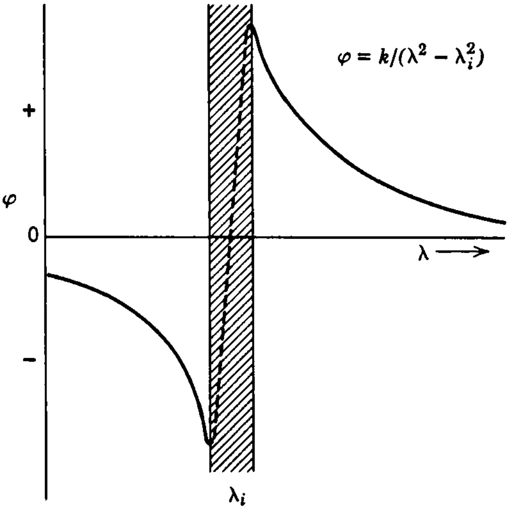

Fig. 17. Schematic optical rotatory effect related to a single absorption band (at λ_i) and following the Drude expression in regions of transparency (——).

(observed in regions of transparency) which are attributable to the absorption band at λ_i (19a) (Fig. 17, solid curve). Rotatory phenomena within the absorption band (Fig. 17, broken curve) [the Cotton effect (20)] can be accounted for (14,19b) on the basis of differential absorption of one form of circular polarized light (circular dichroism) (12,13). The form more strongly absorbed is that which interacts the better at long wavelengths (19b) corresponding, as seems reasonable, with a maximization of in-phase oscillation in the helix.

Model experiments (21–23) have shown that systems containing helices made of copper wire can rotate the plane of polarization of microwaves and even give "Cotton effects" at particular wavelengths. Right-handed helices give positive Cotton effects when set perpendicular to the axis of propagation, but negative Cotton effects when parallel to that axis (23). The rotatory effects reported first for irregular tetrahedra (21) could also be produced in other ways (22) and it seems likely that only helices are very effective.

The terms β and γ [eqs. (19) and (20)] can be related to the polarizability difference $(\alpha_l - \alpha_r)$ as follows.

The electric moment (m_x) induced in the direction x in a particle arises in part from the effect of the electric field and in part from that of the magnetic field. For the case of right circular polarized light (Fig. 13, and equations given in the legend) the contribution of the electrical component is:

$$m_x{}^E = \alpha_x{}^E(E_0/2)[\cos \omega(t - z/c)] \tag{21a}$$

where $\alpha_x{}^E$ is the directed electrical polarizability along the x axis, while that due to the magnetic component is:

$$m_x{}^H = -\frac{\beta}{c}\frac{dH}{dt} = -\frac{\beta\omega}{c}\frac{H_0}{2}\cos \omega(t - z/c) \tag{21b}$$

whence, since $H_0 = E_0$

$$m_x = \left(\alpha_x^E - \frac{\beta\omega}{c}\right)\frac{E_0}{2}\cos \omega(t - z/c) \tag{22}$$

From this equation it is seen that the net effective electric polarization toward right circular polarized light is

$$\alpha_{xr}^E = \alpha_x^E - (\beta\omega/c) \tag{23a}$$

Similarly for left circular polarized light (Fig. 14)

$$\alpha_{xl}^E = \alpha_x^E + (\beta\omega/c) \tag{23b}$$

or

$$(\alpha_l^E - \alpha_r^E)_x = 2\beta\omega/c = 4\pi\beta/\lambda \tag{24a}$$

In a similar fashion the relationship of γ to magnetic polarizability terms is found:

$$(\alpha_l^H - \alpha_r^H)_x = 4\pi\gamma/\lambda \tag{24b}$$

whence

$$(\alpha_l - \alpha_r)_x = (4\pi/\lambda)(\beta + \gamma) \tag{24c}$$

For a randomly oriented fluid system the mean polarizability difference will be the same in all directions and, from eq. (17):

$$[\Phi]_\lambda = (144\pi^2 N_0/\lambda^2)(\beta + \gamma)f(n) \tag{25}$$

This equation is the same as G-15 on p. 622 of Kauzmann's text (2) except for the fact that our $f(n)$ contains the additional term $(n^2 + 2)/3n$. This term arises from our use of the Lorentz-Lorenz refraction equation [eq. (13)]; it would not have appeared had we used the equivalent form of the Gladstone-Dale refraction equation:

$$R = \tfrac{2}{3}(\mathrm{MW}/\rho)(n - 1)$$

[see Kauzmann (2), pp. 600–604]. We have pointed out above that this additional term is, in any case, nearly unity for most values of n.

The derivation of this equation by means of quantum mechanics has been described (10) as providing, in principle, a solution of the problem of optical activity, and it is asserted (10) that any modern model must depart from this point.

B. A Uniform Conductor Model

The helicity of a chain of bonds can, as a rule, be established by simple inspection of molecular models that emphasize bond structure. One looks from one end atom along the straight line to the other end atom. In the simplest cases a single area will be subtended by projection along this axis, corresponding to one turn of a helix. If, overall, the pathway followed in tracing from the near end to the far end is clockwise then the helix is, overall, right handed. Thus the twisted system i–A–B–k (Fig. 18) subtends a triangular area when viewed along line (i–k) (or k–i) (Fig. 19). Progression from near to far along the bond system requires a clockwise motion so that this system can be described as a right-handed helix of bonds. The method of end-to-end projection is of special importance to the present model and it is desirable to identify its features. The straight-line distance from one end to the other will be termed L; this is the length along the axis of one helix turn and so corresponds to the pitch of the screw. The distance from end to end as measured along the bonds (a sum of bond distances) will be denoted D. The area subtended by the bonds when the structure is

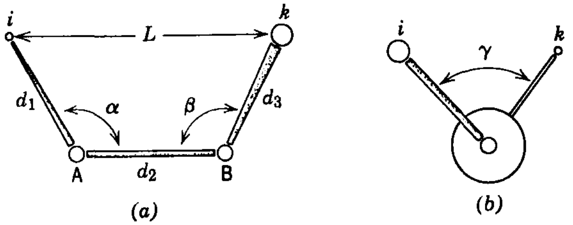

Fig. 18. A right-handed set of three bonds, viewed (*a*) from the side and (*b*) along the central bond.

projected on a plane perpendicular to L will be termed A; the perimeter length of the projected area will be designated P.

Imagine now that the entire bond system is replaced by a single uniform electrical conductor so that all parts have the same electrical properties and so that displacement of charge along the entire bond system will be uniform. This is not a hypothesis about the structure and properties of bonds but a stage in the construction of an artificial model. It allows an approximation to the inductive interactions along a chain of bonds under conditions where all parts of the system are being perturbed to about the same extent by light. It is probably a poor approximation for the case where only one portion of the helix is undergoing excitation but may be appropriate to the case where the whole helix corresponds to the "path" of an electron during excitation.

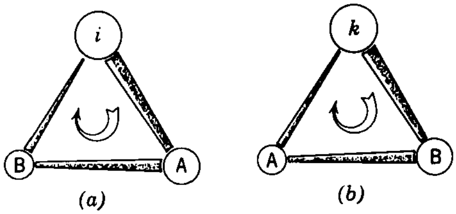

Fig. 19. A right-handed set of three bonds viewed from one end to the other: (*a*) from *i* to *k*, (*b*) from *k* to *i*.

We first place the helix at the origin of coordinates in Figures 13 and 14, with L along the x axis and therefore parallel to the noncancelling electric fields (Figs. 6 and 10). Given the uniform conductor hypothesis and the orientation of the bonds into exactly one turn of a helix, the net induced electrical dipole moment (m) will be directed parallel to L and will be related to the effective vertical displacement of charge (x_v):

$$m = ex_v = \alpha E \tag{26}$$

The equivalent effective displacement along the bonds (x_b) is, then:

$$x_b = (\alpha E/e)(L/D) \tag{27}$$

and the equivalent effective displacement horizontally around the projected perimeter (x_p) is:

$$x_p = x_b(P/D) = (\alpha E/e)(PL/D^2) \tag{28}$$

The current around the perimeter (I_p) is:

$$I_p = \frac{\mathscr{E}e}{P}\frac{dx_p}{dt} \tag{29}$$

where $\mathscr{E}$ is the number of unit charges that would pass a reference point in a hypothetical circulation of current around the perimeter (one full turn per charge). Accordingly:

$$I_p = \frac{\mathscr{E}\alpha L}{D^2}\frac{dE}{dt} \tag{30}$$

Given our artificial model the net magnetic moment will also parallel the x axis. From Ampere's law:

$$\mu = IA/c \tag{4}$$

$$\mu = \frac{\mathscr{E}\alpha}{c}\frac{LA}{D^2}\frac{dE}{dt} \tag{31}$$

but, since

$$\mu = \frac{\gamma}{c}\frac{dE}{dt} \tag{19}$$

$$\gamma = \mathscr{E}\alpha(LA/D^2) \tag{32}$$

We now place the helix at the origin with L parallel to the y axis, in the plane of the noncancelling magnetic fields. The magnetic oscillation will produce an oscillating potential (in esu) in a right-handed helix:

$$\Delta V = -\frac{A}{c}\frac{dH}{dt} \tag{33}$$

where A is the area in projection along L. The electric field along the bonds will be:

$$E_b = \Delta V/D \tag{34}$$

and the displacement of charge along the bonds:

$$x_b = \alpha E_b/e \tag{35}$$

The electric dipole along L (parallel to the y axis) is:

$$m = \mathscr{E}ex_b(L/D) \tag{36}$$

whence

$$m = -\frac{\mathscr{E}\alpha}{c}\frac{LA}{D^2}\frac{dH}{dt} \tag{37}$$

and, from eq. (19):

$$\beta = \mathscr{E}\alpha(LA/D^2) \tag{38}$$

It is seen that β and γ are equal. In a number of analyses the molecular rotatory parameter g is used; this is equivalent to β (or γ) and correlations among equations can be made by use of the factor: $2g = (\beta + \gamma)$.

The third major orientation of the helix, with L parallel to the axis of propagation, should not produce any rotation by the present mechanism. Intuitively, however, it seems possible that a purely electrical mechanism might provide some rotational effect and this is supported by work with copper helices and microwaves (23); in most chemical cases there will be a large disparity in size between L, the pitch of the molecular screw, and λ, the pitch of the optical screw. We will neglect this effect here, as does Kauzmann (2); the model of Tinoco and Woody (3) indicates that this coaxial rotatory effect will be opposite in sign but small.

More important at the present is the fact that the evaluation of β and γ indicates that they will not be operative in all directions relative to plane polarized light. When the axis (L) of the helix makes an angle ϕ with the "electrical" axis (x in the present diagrams, but actually a turning axis in an optically active medium) then the magnetic moment along the helix axis will be

$$\mu = \frac{\gamma}{c}\frac{dE}{dt}\cos\phi \tag{39a}$$

and the component of this directed along the "electrical" axis will be

$$\mu_e = \frac{\gamma}{c}\frac{dE}{dt}\cos^2\phi \tag{39b}$$

so that the average value of γ will be

$$\gamma_{av} = \gamma(\cos^2\phi)_{av} \tag{40}$$

Similarly,

$$\beta_{av} = \beta(\cos^2\phi)_{av} \tag{41}$$

For random orientations the average value of $\cos^2\phi$ is $\frac{1}{3}$, whence

$$(\beta + \gamma)_{av} = 2/3\mathscr{E}\alpha(LA/D^2) \tag{42}$$

Substituting into eq. (25) we obtain

$$[\Phi]_\lambda = (96\pi^2 N_0/\lambda^2)\mathscr{E}\alpha(LA/D^2)f(n) \tag{43a}$$

The term $\mathcal{E}\alpha$ as we have used it here can be related to the sum of bond refractions:

$$\sum \Delta R_\lambda = (4\pi N_0/3)\mathcal{E}\alpha \tag{44}$$

whence, for wavelengths relatively remote from absorption bands

$$[\Phi]_\lambda = (72\pi/\lambda^2)(LA/D^2)(\sum \Delta R_\lambda)f(n) \tag{43b}$$

(λ, L, A, and D in cm).

For the common case of the sodium D line (λ = 5893 Å) this becomes:

$$[\Phi]_\mathrm{D} = 652.4(L'A'/D'^2)(\sum \Delta R_D)f(n) \tag{43c}$$

(L', A', and D' in Ångstrom units).

The term $\mathcal{E}\alpha$ can also be related to frequencies of absorption bands by use of the relationship [Kauzmann (2), pp. 568–573]:

$$\mathcal{E}\alpha = (e^2/4\pi^2 m_e) \sum [f_i/(\nu_i^2 - \nu^2)] \tag{45a}$$

where m_e is the mass of the electron, ν_i the "natural frequency" of the absorption band i and f_i the "oscillator strength"; f_i reflects the fact that not all electrons contribute fully to polarizability. Since $\nu = c/\lambda$

$$\mathcal{E}\alpha = (e^2\lambda^2/4\pi^2 m_e c^2) \sum [\lambda_i^2 f_i/(\lambda^2 - \lambda_i^2)] \tag{45b}$$

or

$$[\Phi]_\lambda = (24N_0 e^2/m_e c^2)(LA/D^2) \sum [\lambda_i^2 f_i/(\lambda^2 - \lambda_i^2)]f(n) \tag{46a}$$

and

$$[\Phi]_\lambda = 4.06 \times 10^4 f(n)(L'A'/D'^2) \sum [\lambda_i^2 f_i/(\lambda^2 - \lambda_i^2)] \tag{46b}$$

This equation (L', A', D' in Å) reduces to that obtained by Kauzmann (2) for his double-stranded regular helix model (G-37, p. 630) when the appropriate substitutions are made:

$$L = 2\pi s$$
$$A = \pi r^2$$
$$D = 2\pi(r^2 + s^2)^{1/2}$$

(all in cm) and

$$\sum f_i = 2$$

and when allowance is made for differences in units and in the method of obtaining $f(n)$. The geometric term of the equations of Tinoco and Woody (3) is also equivalent.

Although eq. (46b) has the proper terms to express rotatory dispersion in regions of transparency it is of limited use because it contains the "oscillator strength" terms. It is to be noted that the helix under consideration will often consist of units having similar spectroscopic characteristics; in other cases the helix will be the "path" of an electron in a single transition. Under these circumstances there will be, to a good approximation, only one value for λ_i (the absorption wavelength) and:

$$\mathscr{E}\alpha = (e^2\lambda^2/4\pi^2 m_e c^2)[\sum \lambda_i^2 f_i/(\lambda^2 - \lambda_i^2)] \tag{45c}$$

or, expressing "oscillator strength" by use of empirical refraction values:

$$\mathscr{E}\alpha = (3 \sum \Delta R_D/4\pi N_0)[\lambda^2(\lambda_D^2 - \lambda_i^2)/(\lambda^2 - \lambda_i^2)\lambda_D^2] \tag{45d}$$

whence,

$$[\Phi]_\lambda = 652.4(L'A'/D'^2) \sum \Delta R_D[(\lambda_D^2 - \lambda_i^2)/(\lambda^2 - \lambda_i^2)]f(n) \tag{46c}$$

The molecular rotation of a compound will, then, be the sum of a number of terms of this form, taking into account all atoms (including hydrogen) of all major conformations.

The model described above is electric rather than electronic but it is easy to recast in electronic terms. When this is done it is seen that the required electric and magnetic moments can be provided by the motion of one electron within a chromophore or by cooperative motions of a number of electrons in a set of bonds. The strongest effects will occur when the helix structure is well developed so that both the electric and magnetic moment changes will be large. Significant rotations could, however, also be produced by nearly circular (weak electric, strong magnetic) or nearly linear (strong electric, weak magnetic) motions of electrons. The motions with appreciable linear character will produce strong refraction or strong absorption, depending on the wavelength of light. Polarizability models are appropriate for such systems and the Drude-type wavelength terms of eqs. (45) and (46) originate in the classical model for refractive dispersion. The nearly circular motions will give only weak refraction and absorption but they may give appreciable rotations. As a rule the equations given above will be difficult to apply in this case because the "pathway" of an electron in the relevant transition process becomes difficult to define. It is, however, to be expected that these rotatory effects will show Drude dependence on wavelength since they also arise from periodic perturbation of electrons.

IV. SOME SPECIFIC APPLICATIONS

A. The Skew Conformational Unit

The idea that twisted chains of atoms such as that shown in Figure 20 could make major and characteristic contributions to optical rotatory power was developed in a general way by Kuhn (see Sect. V-B-1), Kirkwood (see Sect. V-B-2) and Eyring (10). These workers appear to have been mainly concerned with properties of terminal atoms. Whiffen (24) and Kauzmann (2a) focused attention on the dissymmetry of the bond pattern. Whiffen (24) showed that the rotations ($[\Phi]_D$) of the cyclitols and carbohydrates could be expressed as sums of the characteristic contributions of a relatively small number of four atom units. The empirically determined rotatory contributions showed little regularity, however, and the treatment did not appear amenable to generalization. It was suggested (26) that axial hydroxyl groups dissymmetrically positioned with respect to the ring oxygen might make characteristic contributions of a different sort ("permolecular dissymmetry") (25). There were enough data available in the carbohydrate series to allow estimates of these effects to be made and, thus, a new set of empirical rotatory contributions for four atom (three bond) systems could be obtained. These new values fell into a simple pattern—the skew conformational unit shown in Figure 20 is dextrorotatory and the magnitude of its effect is a function of the polarizabilities (refractions) of the terminal atoms and of the sine of the dihedral angle γ:

$$[\Delta\Phi]_D = +k'f(R_x)f(R_y)\sin\gamma$$

or, more simply, for the important case where γ is 60°:

$$[\Delta\Phi]_D = +kXY \tag{47}$$

where X and Y are terms characteristic of the atoms X and Y.

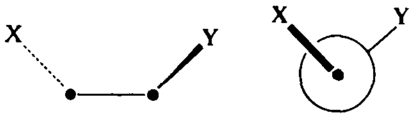

$[\Delta\Phi]_D = +kXY$

Fig. 20. The skew conformational unit.

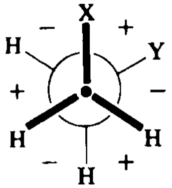

$$[\Phi]_D = k(XY - YH + HH - HH + HH - XH)$$
$$= k(X - H)(Y - H)$$

Fig. 21. One of the two enantiomeric gauche conformations of XCH_2CH_2Y, showing the six skew conformational units and the signs of their rotatory effects. In this case the enantiomeric conformations will be present to an equal extent, unless X or Y contains a center of dissymmetry.

Rotation values for the simple conformational units cannot be obtained empirically. Their factorial nature, however, allows their use in defining the net rotatory effect of a full conformation, as in Figure 21; the sign and magnitude of these effects can be obtained empirically. These contributions can, in turn, be manipulated arithmetically; thus, the rotation of the unit shown in Figure 21 can be calculated from the values for the three conformations shown in Figure 22:

$$k[X - H][Y - H]$$
$$= (k[CH_3 - H][X - H]k[CH_3 - H][Y - H])/k[CH_3 - H]^2$$

This allowed a more general application to a variety of open-chain (25,28,29) and cyclic (26,27,29) compounds. The wholly empirical nature of this approach led, however, to several difficulties. It was not possible to take longer range ("permolecular dissymmetry") effects

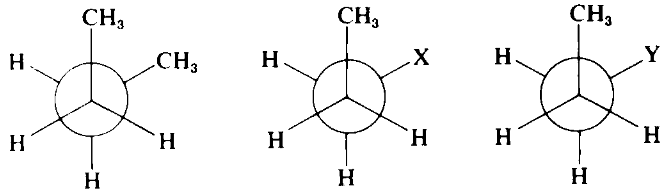

$+k(CH_3 - H)^2$ $+k(CH_3 - H)(X - H)$ $+k(CH_3 - H)(Y - H)$

Figure 22

into account in a general way, although the significance of such effects was recognized *ab initio* (25) and specifically taken into account in the carbohydrate series (26) (where there was enough empirical data to do so). That some such effects were common and of appreciable magnitude was nicely shown in an exhaustive study of the norbornane series (30), where significant rotations were observed although nearly complete cancellations of four-atom rotatory effects might have been expected. When models of such compounds are examined with a view to finding longer dissymmetric chains, it becomes at once evident that the norbornanes are not really very simple. In addition a number of phenyl compounds, in this and other series, showed large rotation shifts opposite in sign to those predicted by use of the original model (30–35). While it cannot be contended that we can now predict these phenyl rotation effects, it does seem possible to assert that the phenyl group can produce rogue rotational effects when not allowed to rotate freely (36,37); it can then act as a symmetrical chromophore in a dissymmetric environment (37) (see Sect. V-C-1) or become part of an inherently dissymmetric composite chromophore (36) (see Sect. V-C-2). The general insight provided by the one-electron theory (see Sect. V-C) now indicates that the original "conformational dissymmetry" model is not applicable to such cases, where chromophores with weak absorption bands are not conformationally free.

The general skew system (Fig. 18) has the character of a single turn of a right-hand screw (with a triangular cross section, Fig. 24). The helix model can be applied to this system if we can obtain the distance L between the terminal atoms, the sum of the three bond distances ($D = d_1 + d_2 + d_3$) and the area, A, subtended by these bonds in projection along line L (Fig. 24). It turns out that A and L can be expressed in such a way that neither need be calculated explicitly.

We first project the twisted system (Fig. 18*a*) along the line A–B (Fig. 18*b*) obtaining the dihedral angle γ. The projected lengths of bonds d_1 and d_3 are related to the bond angles α and β (Fig. 23). Since the area of a triangle is given by $\frac{1}{2}ab \sin C$ the projection area here (Fig. 23) is:

$$A' = \tfrac{1}{2}d_1 d_3 \sin\alpha \sin\beta \sin\gamma \qquad (48)$$

This is not, however, the projection of immediate interest to us. That is obtained by aligning the system in Figure 23 so that the line L' is horizontal and then rotating about the vertical axis which lies in the

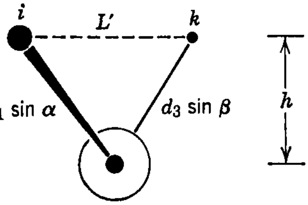

Fig. 23. Projection of Figure 18 on a plane perpendicular to the A–B axis.

plane of the paper until *i* and *k* are aligned (Fig. 24). The vertical distance *h* between the lines *i*–*k* and A–B in Figures 23 and 24 is the same. Accordingly the projection areas are related:

$$A' = (h/2)L' \tag{49a}$$

$$A'' = (h/2)d_2' \tag{49b}$$

$$A'' = A'(d_2'/L') \tag{49c}$$

If now, we project the system along the axis used for rotation of Figure 23 to form Figure 24 we obtain the Figure 25. Here *i* and *k* lie in one plane and A and B in a lower parallel one so that lines *L* and d_2 have their full values. It is readily seen from the plane geometry of sets of parallel and perpendicular lines that:

$$d_2'/d_2 = L'/L \tag{50}$$

or

$$A'' = A'(d_2/L) \tag{49d}$$

whence

$$A'' = (d_1 d_2 d_3/2L) \sin \alpha \sin \beta \sin \gamma \tag{51}$$

and

$$(LA/D^2) = \tfrac{1}{2}[d_1 d_2 d_3/(d_1 + d_2 + d_3)^2] \sin \alpha \sin \beta \sin \gamma \tag{52}$$

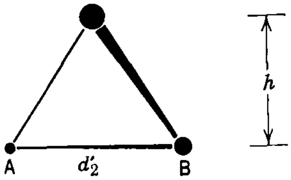

Fig. 24. Projection of Figure 18 on a plane perpendicular to the *i*–*k* axis.

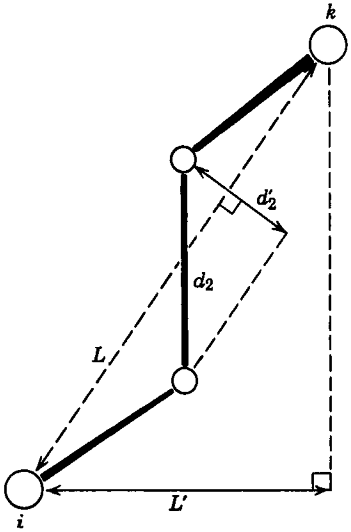

Fig 25. Projection of Figure 18 with A and B in the plane of the paper and *i* and *k* both in a plane parallel to the first.

Substitution of this expression into eq. (43c) shows that under the uniform conductor model the rotatory contribution of the skew conformational unit (Fig. 20) will be positive and proportional to the sine of the dihedral angle in accord with the intuitive and empirical "conformational dissymmetry" model (25).

TABLE I

Bond Distances[a]

Bond	Distance, Å	Bond	Distance, Å	Bond	Distance, Å
C—H	1.10	C—C	1.53	C—F	1.37
N—H	1.02	C—N	1.47	C—Cl	1.78
O—H	0.96	C—O	1.43	C—Br	1.92
S—H	1.34	C—S	1.82	C—I	2.12
C═C	1.33	C⋯C	1.40	C≡C	1.21

[a] Data from G. W. Wheland, *The Theory of Resonance*, 1944, pp. 99, 286–296; L. Pauling, *Nature of the Chemical Bond*, 1960, pp. 221–223; D. R. Lide, Jr., *Tetrahedron*, **17**, 125 (1962); B. P. Stoicheff, *ibid.*, **17**, 135 (1962).

We are now in a position to calculate the magnitude of rotation to be expected for single conformational units by use of this model. Taking tetrahedral bond angles ($\sin\alpha = \sin\beta = 2\sqrt{2}/3$) and a dihedral angle of 60°:

$$[\Delta\Phi]_D = 251[d_1d_2d_3/(d_1 + d_2 + d_3)^2](\sum \Delta R_D)f(n)$$

Single bond distances (38) are shown in Table I and bond, octet, and group refractions in Table II. The latter values are calculated in the standard way so that the sum of bond refractions for a substance equals the sum of atomic refractions; the refraction data of Vogel (39) are used, in part because they are suitable for use at several wavelengths in the visible. We calculate octet refractions for saturated groups acting as terminal atoms; note the variation in polarizability of the attachment carbon atoms of alkyl groups. Octet values for the carbonyl and olefinic units are strictly for use when the multiple bond is terminal (A–*i* or B–*k*). The refractions of unsaturated and conjugated substituents are lumped into a "group" refraction containing all electrons.

Single helix rotation contributions $[\Delta\Phi]_D/f(n)$ have been computed for the case where atoms A and B are saturated carbon and where *i* and *k* should be reasonably close to cylindrical or spherical symmetry (Table III). (The refractive index or "rotivity" correction would, if applied, make the values of $[\Delta\Phi]_D$ 30–50% larger.) From these values we compute the rotations of the conformation shown at the head of Table IV, again leaving the "rotivity" unspecified. It is seen that these values are of the same order of magnitude as those obtained in the earlier empirical analysis (25) (we use a value of $\sqrt{2}$ for the refractive index to make the data more nearly comparable). Thus the uniform conductor model leads to predictions of rotations generally comparable to those made by use of the empirical "conformational dissymmetry" model (24–29).

Rotation values have been calculated for the case where the two terminal atoms are the same (Table V). These values are used (Table VI) to calculate the factorial equivalent:

$$[k(\mathrm{X} - \mathrm{H})^2 \times k(\mathrm{C} - \mathrm{H})^2/f^2(n)]^{1/2} \sim k(\mathrm{X} - \mathrm{H})(\mathrm{C} - \mathrm{H})/f(n)$$

of the values obtained directly in Table IV. Considering that refractions enter these equations as sums rather than products, it is surprising that the values are in such close agreement. Thus the original assumption that these terms are factorable (25) is shown to be a reasonably good approximation.

TABLE II

Bond, Octet, and Group Refractions

		ΔR values			
Unit	Method for calculation from bond refractions[a,b]	R_C H_α 6563 Å	R_D Na_D 5893 Å	R_F H_β 4861 Å	R_G H_γ 4340 Å
Bonds					
C—H	C/4 + H	1.669	1.676	1.693	1.704
C—C	C/2	1.286	1.296	1.300	1.328
C═C	C + D.B.	4.117	4.166	4.273	4.375
C≡C	3C/2 + T.B.	5.817	5.865	5.961	6.068
$\mathrm{C}\overset{\cdots\cdots}{-}\mathrm{C}$	$[C_6H_6]/6$ – (C—H)	2.691	2.722	2.799	2.862
Octets					
C—CH_3	(C—C) + 3(C—H)	6.293	6.324	6.379	6.400
C—CH_2R	2(C—C) + 2(C—H)	5.910	5.944	5.986	6.064
C—CHR_2	3(C—C) + (C—H)	5.527	5.564	5.593	5.688
C—CR_3	4(C—C)	5.144	5.184	5.200	5.312
C—NH_2	C/4 + [NH_2]	5.057	5.086	5.157	5.234
C—OH	C/4 + [OH]	3.179	3.194	3.220	3.252
C—SH	C/4 + [SH]	9.334	9.405	9.569	9.721
C—F	C/4 + F	1.453	1.458	1.440	1.444
C—Cl	C/4 + Cl	6.464	6.492	6.568	6.637
C—Br	C/4 + Br	9.324	9.389	9.542	9.675
C—I	C/4 + I	14.468	14.602	14.960	15.284
C═O	[C═O] – C/2	3.293	3.305	3.353	3.374
C═CH_2	(C═C) + 2(C—H)	7.455	7.518	7.659	7.783
C═CHR	(C═C) + (C—C) + (C—H)	7.072	7.138	7.266	7.407
C═CR_2	(C═C) + 2(C—C)	6.689	6.758	6.873	7.031
Groups					
C—CN	C/4 + [C≡N]	6.074	6.107	6.163	6.225
C—NO_2	C/4 + [NO_2]	7.305	7.361	7.473	7.582
C—CO_2H	C/4 + [CO_2H]	7.834	7.874	7.958	8.032
C—C_6H_5	C/4 + [C_6H_5]	25.779	26.007	26.556	27.020

[a] Calculated from values of A. I. Vogel (39). Values are atomic refractions or sums of atomic refractions (e.g., [C_6H_6], [C═O]) unless enclosed in parentheses [e.g., (C—C), (C—H)].

[b] D.B. = double bond; T.B. = triple bond.

TABLE III

Single Helix Rotations $[\Delta\Phi]_D/f(n)$

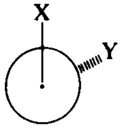

X	Y = H	F	OH	NH_2	CH_3	Cl	SH	Br	I
H	154	159	225	297	347	365	480	483	698
F	159	168	240	319	376	398	528	531	775
OH	225	239	314	395	453	478	609	615	860
NH_2	297	317	395	477	537	566	700	707	957
CH_3	347	374	453	537	598	633	767	777	1037
Cl	365	396	478	566	633	672	813	823	1100
SH	480	525	609	700	767	813	956	971	1125
Br	483	528	615	707	777	823	971	988	1270
I	698	770	860	957	1037	1100	1255	1270	1570

[a] Calculated from: $[\Delta\Phi]_D = 251 \dfrac{d_1 d_2 d_3}{(d_1 + d_2 + d_3)^2} (\sum \Delta R_D) f(n)$

$f(n) = [(n^2 + 2)/3][(n^2 + 2)/3n]$

TABLE IV

Rotations of Full Conformations $\sum [\Delta\Phi]_D/f(n)$

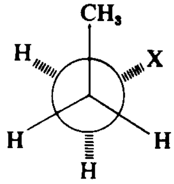

X	$+k CH_3X$	$-k XH$	$-k H$ $(CH_3 - H)$	$\sum [\Delta\Phi]_D/f(n)$	$[\Delta\Phi]_D^a/1.33$
F	374	−159	−193	+22	No data
OH	453	−225		+35	+38
NH_2	537	−297		+47	+41
CH_3	598	−347		+58	+45
Cl	633	−365		+75	+127
SH	767	−480		+94	No data
Br	777	−483		+101	+135
I	1037	−698		+146	+188

[a] Calculated from empirical values (25), using $n = \sqrt{2}$.

TABLE V

Rotations of Full Conformations $\sum [\Delta\Phi]_D/f(n)$

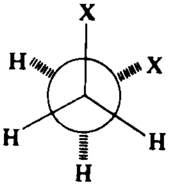

X	$[\Delta\Phi_{XX}]/f(n)^a$	$[\Delta\Phi_{HH}]_D/f(n)^a$	$-2[\Delta\Phi_{XH}]_D/f(n)^a$	$\sum = [\Delta\Phi_{(X-H)^2}]_D/$ $f(n)$
F	168	154	−318	+4
CH	314		−450	+18
NH_2	477		−594	+37
CH_3	598		−694	+58
Cl	672		−730	+96
SH	956		−960	+150
Br	988		−966	+176
I	1570		−1396	+328

[a] Single helix (four atom) values from Table III.

TABLE VI

Factorial Character of Rotatory Effects

X	$(X-H)^2/f(n)^a$	$[(X-H)^2(C-H)^2]^{1/2}/$ $f(n)$	$(C-H)(X-H)^b/$ $f(n)$
F	4	13.2	23
OH	18	32.3	35
NH_2	37	46.3	47
Cl	96	74.7	75
SH	150	93.4	94
Br	176	102	101
I	328	138	146

[a] See Table V.
[b] See Table IV.

We conclude that the uniform helix conductor model can be used wherever the "conformational dissymmetry" model can properly be used. The new model indicates important theoretical limitations on the empirical model and, at least in principle, provides a means of taking those "permolecular dissymmetry" effects which are related to polarizability properties into account.

B. Allenes

van't Hoff's prediction that suitably substituted allenes would be capable of separation into optical antipodes (40) has, after several false starts (41), been fully confirmed by resolution (42–45), by syntheses with dissymmetric catalysts (46,47) and reagents (48,49), and by use of reactions of active compounds containing asymmetric atoms (50–53). A number of natural products, mainly isolated from fungi, owe their molecular dissymmetry wholly (54–60) or in part (59,60–66) to the allene unit. Absolute configurations have been assigned on the basis of reasonable interpretations of reactions giving allenes from compounds with asymmetric carbon atoms (51,67–70) or vice versa (45,71). Configurations based on hypotheses about the role of steric effects in partial asymmetric syntheses (48,49,53) should be accepted with caution unless supported by other evidence (48,49). For our purposes a recent correlation of configurations with long wavelength rotations (72) is especially important, as is an assignment of configuration to 1,3-diphenylallene by analysis of its circular dichroism spectrum (73).

The allene system represents a simple variant of that considered in the preceding section (see Figs. 26 and 27). The central set of double bonds is linear and can be regarded as a "bond" with twice the length and refraction of an olefinic bond (d_2 = 2.68 Å; ΔR_D = 8.332). The bond angles, α and β, are taken as 120° and the dihedral angle, γ, as 90°. The term: LA/D^2 for the unit of structure: A—C=C=C—X then becomes:

$$LA/D^2 = \frac{1}{2}[d_{\text{C-A}}d_{\text{C-X}}2.68/(d_{\text{C-A}} + d_{\text{C-X}} + 2.68)^2]\frac{3}{4}$$

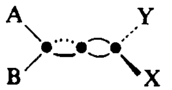

Fig. 26. A dissymmetric allene.

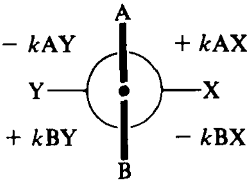

$$[\Phi]_D = kAX - kBX + kBY - kAY$$
$$= k(A - B)(X - Y)$$

Fig. 27. Newman projection of the allene in Figure 26.

or,

$$[\Delta\Phi]_D/f(n)$$
$$= [655.7 d_{C\text{-}A} d_{C\text{-}X}/(d_{C\text{-}A} + d_{C\text{-}X} + 2.68)^2][R_{C\text{-}A} + R_{C\text{-}X} + 8.332]$$

As before (Sect. IV-A) we consider only the octet of a saturated attachment atom but use the entire length and refraction of the conjugated unsaturated portion of a linear substituent. Again, the single helix unit values (Table VII) can be approximated as products of constants characteristic of the terminal groups:

$$[\Delta\Phi_{AX}] \sim [\Delta\Phi_{AA}]^{1/2}[\Delta\Phi_{XX}]^{1/2}$$

TABLE VII

Calculated Molecular Rotatory Contributions of Allenic Single Helix Units: $[\Delta\Phi]_D/f(n)$

A	X = H	CH_3	C_6H_5[c]
$-H$	385	638	1290
$-CH_3$	638	983	1920
$-C{\equiv}CH$[a]	793	1245	
$-(C{\equiv}C)_2H$[b]	1115	1705	
$-C_6H_5$[c]	1290	1920	4120

[a] d_{CA} 2.74 Å; ΔR_D 7.141 (2C + T.B.)

[b] d_{CA} 5.48 Å; ΔR_D 14.282

[c] d_{CA} 4.34 Å; ΔR_D 17.39 $(R_{C_6H_6} - 6R_{CH} + C/2)$

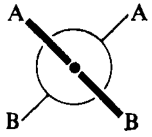

(+) *S*

Fig. 28. A dissymmetric allene with a twofold rotation axis (vertical in the plane of the paper).

Thus, from the values $\Delta\Phi_{HH} = 384$ and $\Delta\Phi_{\Phi\Phi} = 4120$, we obtain $\Delta\Phi_{H\Phi} = 1260$, while the value obtained by the full calculation is 1290 (Table VII). This means that the rotation of an allene can be approximated as the product of two differences (Fig. 27). The use of this expression in predicting the sign of rotation (Na_D) of a particular enantiomer will usually be equivalent to use of Lowe's Rule (72). This states that the allene shown in Figure 26 will be dextrorotatory when A is more polarizable than B and X more polarizable than Y. It is an interesting consequence of this rule that an *S*-allene (74) having a twofold rotation axis (Fig. 28) would be predicted to be dextrorotatory regardless of which group is taken as the more polarizable.

Laballenic acid (58) ($[\Phi]_D$ − 132°, EtOH) has been assigned the linear structure:

$$CH_3(CH_2)_{10}\,CH{=}C{=}CH(CH_2)_3\,CO_2H$$

its rotation is expected to be similar to that estimated for (−)-1,3-dimethylallene (Fig. 29). The predicted configuration (*R*) has been confirmed by asymmetric reduction (60). Concordant configurations have

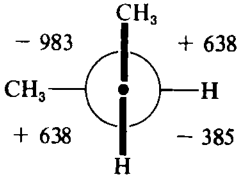

$$\text{Calcd } [\Phi]_D = -92\,f(n)$$
$$= -118 \text{ (EtOH, } n = 1.3624)$$

Fig. 29. (−)-1,3-Dimethylallene (predicted).

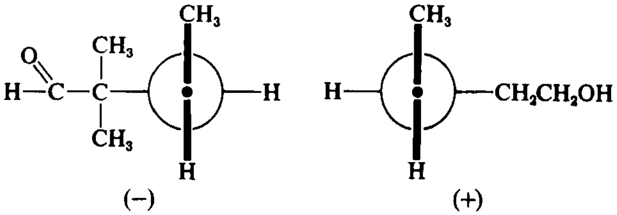

Fig. 30. Absolute configurations of two dialkylallenes.

been assigned to two comparable allenes (Fig. 30) by use of stereospecific rearrangement (48,51) and, in the case of the alcohol, by use of asymmetric hydride reduction (48). We would expect the optically pure forms to show rotations similar to that of laballenic acid (58).

A series of diacetylene allenes has been obtained from fungi (Fig. 32); their rotations are predicted to be similar to those expected for the methyl analog (Fig. 31) for which: $[\Phi]_D + 337f(n)$, $+433$(EtOH), is calculated from values in Table VII.

It is of interest that the octet refraction values given in Table II support Eliel's suggestion that the *t*-butyl group is effectively less polarizable than the methyl (67); this allowed a tentative assignment of configuration to an acetylene alcohol and, thence, the allene formed (50) from it (Fig. 33). The absolute configuration of the alcohol has since been supported by arguments based on the "conformational dissymmetry" model (69) and, more convincingly, by use (68,69) of Prelog's method of asymmetric synthesis (75). It may be noted that this allene follows Lowe's Rule (72), but that the rotation reported (69) ($[\Phi]_D^{20}$ -53.1) is considerably larger than expected from our present model.

An element of ambiguity enters when one attempts to deal with a substituent such as the carboxy group. Is it to be regarded as cylindric-

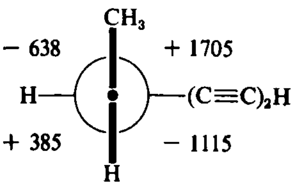

Fig. 31. (+)Octa-2,3-diene-5,7,-diyne (predicted).

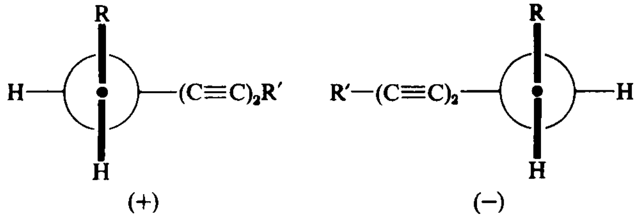

R′	R	$[\Phi]_D$ observed
H	$-CH_2OH$	−448 (ref. 59)
H	$-(CH_2)_2OH$	±507 (refs. 49,56,57,59) (marasin)
H	$-(CH_2)_3OH$	−423 (ref. 59)
H	$-(CH_2)_4OH$	−288 (ref. 59)
H	$-CH_2CO_2CH_3$	+457 (refs. 55,59)
H	$-\overset{\text{OH}}{\overset{\vert}{\text{C}}}\text{H}(\text{CH}_2)_2\text{CO}_2\text{H}$	+723 (refs. 59,61–63,66) (nemotinic acid)
H	$-(CH{=}CH)_2CH_2CO_2H$	−257 (ref. 54) (mycomycin)
CH_3	$-(CH_2)_2OH$	+449 (ref. 59)
CH_3	$-\overset{\text{OH}}{\overset{\vert}{\text{C}}}\text{H}(\text{CH}_2)_2\text{CO}_2\text{H}$	+735 (ref. 59,62,64) (odyssic acid)

Fig. 32. Predicted configurations of some naturally occurring diacetylenic allenes.

ally symmetrical by free rotation or held largely in one plane by conjugation? Does the hydroxy group contribute to the effective refraction? (If not, ΔR_D is 7.874 − 2.546 = 5.328, less than the value for methyl.) Will there be an exaltation contribution? These considerations are not critical for the case of (+)1,3-pentadienoic acid, which has a twofold rotation axis (see Fig. 28), and which has been shown (44,45) to have the *S* configuration (74) (Fig. 34). They do, however,

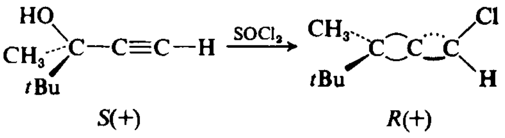

Fig. 33. Correlation of configuration of an allene with a compound containing an assymmetric center.

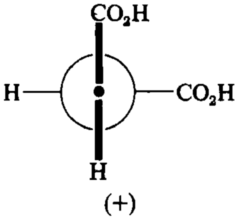

Fig. 34. (+)-1,3-Pentadienoic acid.

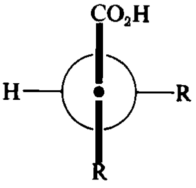

Figure 35

effectively inhibit any confident assignments from rotation to dialkyl allenic acids of the type (43,53) shown in Figure 35.

Mason and Vane (73) have assigned the *S* configuration (74) to (+)-1,3-diphenylallene (47,52,70) (Fig. 37) by use of a form of coupled oscillator theory (Sect. V-B). The substance is taken to consist of two styrene chromophores (Fig. 36) set at right angles. The transition moment for the band near 250 mμ is believed to be long-axis oriented (76) and to lie in the plane of the chromophore at an angle of 28° to the 1,4-axis of the ring (73). Interaction of these two transitions in the allene leads to a splitting of the 40,700-cm^{-1} (246 mμ) styrene band into one of higher intensity at 39,300 cm^{-1} (254 mμ) and one of lower intensity at 43,000 cm^{-1} (233 mμ). It is concluded that the former corresponds to the out-of-phase coupling (Fig. 39), which would be preferred on dipole grounds to the in-phase coupling (Fig. 38). The helicity of each form of coupling can be deduced by noting the components of each moment in the *y* and *z* directions (Figs. 37–39). The in-phase coupling is left helical around the *z* axis (Fig. 38) and should give rise to a negative Cotton effect under the weaker absorption band near 233 mμ. The out-of-phase coupling is right helical about the *y* axis

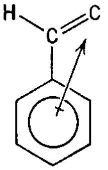

Fig. 36. Transition moment of styrene (250 mμ).

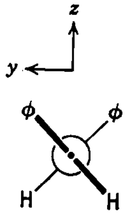

Fig. 37. (+)-1,3-Diphenylallene.

(Fig. 39) and should give a positive Cotton effect, under the stronger absorption band, near 254 mμ. These are observed (73) in the circular dichroism spectrum of the (+) isomer. This same method of approach has also been used by these workers (77,78) in an assignment of configuration to calycanthine. It is to be noted that the simple model we have presented also leads to the conclusion that the out-of-phase coupling shown in Figure 39 would be preferred and would control rotation; it does not provide for the in-phase coupling shown in Figure 38. The circular dichroism spectrum of the diphenylallene (73) shows clearly that such coupling is significant and that, therefore, our model may be oversimplified when it comes to predicting details of circular dichroism spectra.

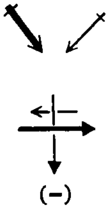

Fig. 38. In-phase coupling of styrene moments in *S*-1,3-diphenylallene.

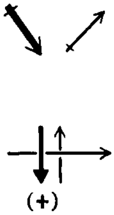

Fig. 39. Out-of-phase coupling of styrene moments in *S*-1,3-diphenylallene.

C. Hexahelicene

Hexahelicene (79,80) (Fig. 40) is the archetype of the inherently dissymmetric chromophore. The large rotation ($[\Phi]_D$ + 12,200, −11,950; $CHCl_3$) illustrates a common characteristic of such chromophores, the transitions of which may have sizeable electric and magnetic dipole moments (14). Fitts and Kirkwood (81) have calculated $[\Phi]_D$ − 9900° for the left-handed helix isomer (enantiomer of Fig. 40) by considering fifteen pairwise interactions of benzene rings. Moscowitz (14,82,83) has shown that the rotatory dispersion curve can be calculated from the absorption spectrum in an important demonstration of the utility of the Kronig-Kramers theorem (14,83). His calculations, based on 169π–π^* transitions (as expected from Hückel theory) indicate that the right-handed enantiomer (Fig. 40) should be levorotatory. The helix model of Tinoco and Woody (3), and our still more primitive model, however, both lead to the prediction that it will be dextrorotatory in agreement with Fitts and Kirkwood (81).

Our calculation is based on a presumed displacement of one unit of charge from one end of the helix to the other (Fig. 41). The two most nearly regular "pathways" for this displacement are the internal (Fig. 42*a*) and peripheral (Fig. 42*b*). In common with the other workers (3, 81–83) we assume a separation of the ends of the helix, L = 3.80 Å, this being the distance between the planes of benzene molecules in the crystal (84). The bond lengths are taken as 1.40 Å, whence the values for D and A can be set up as shown in Figures 42*a* and 42*b*; in the final computation the number 1.40 cancels. A bond refraction value of $R_{\mathrm{C}\doteq\mathrm{C}} = 2.82$ is obtained from the molecular refractions of naphthalene (44.40) (85a) and of phenanthrene (62.08)

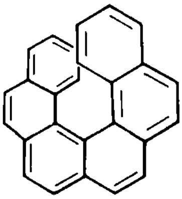

Fig. 40. Hexahelicene (right-handed helix enantiomer).

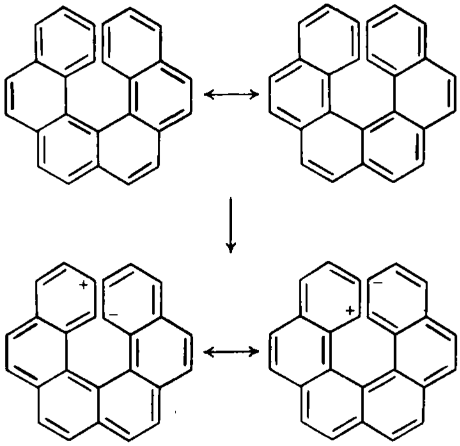

Fig. 41. End-to-end displacement of a charge in hexahelicene.

(85b) by assuming the carbon–hydrogen bond refraction of 1.676 (Table II). The refractive index of the solution is taken as that of pure chloroform ($n_D{}^{20} = 1.4464$). Taking $f(n)$ as $(n^2 + 2)/3 = 1.3640$, the molecular rotation corresponding to "motion" along the inner path is

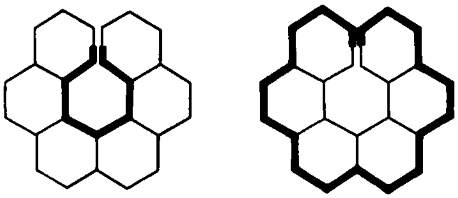

$$L = 3.80\ \text{Å}$$
$$A = \frac{6 \times (1.40)^2(3)^{1/2}}{2 \times 2}\ \text{Å}^2$$
$$D = 7 \times 1.40\ \text{Å}$$
$$\sum \Delta R_D = 7 \times 2.82$$
$$[\Phi]_D = 2595\, f(n)$$

(*a*)

$$L = 3.80\ \text{Å}$$
$$A = \frac{7 \times 6 \times (1.40)^2(3)^{1/2}}{2 \times 2}\ \text{Å}^2$$
$$D = 19 \times 1.40\ \text{Å}$$
$$\sum \Delta R_D = 19 \times 2.82$$
$$[\Phi]_D = 6692\, f(n)$$

(*b*)

Fig. 42. Internal and external "pathways" for charge displacement.

3540, along the outer path 9128. Somewhat smaller values are obtained for $f(n)$ taken as $(n^2 + 2)^2/9n$. There is some evidence indicating that hexahelicene shows a solvent dependence of rotation different (86) from that required by the usual rotivity treatment (18); the significance of the $f(n)$ correction is thus left unclear. Considering the simplicity of the calculation the values obtained here are in reasonable accord with the observed rotation. An independent determination of absolute configuration would be desirable.

D. Proteins

Many proteins have helical conformations when in the native state (87). Denaturation involves the loss of helix structure and the formation of a more open and flexible conformation (88,89), often called the "random coil." This change is accompanied by large shifts in optical rotation (90–92) and it has been suggested (93–94) that the helices as such make large and characteristic contributions to rotatory power. Particular interest attaches to the α helix (95–100) (Fig. 43), which can apparently occur in both right- (101–103) and left-handed (104) forms, and to the poly-L-proline helix (94,105) (Fig. 44), which can only be left-handed and appears to be similar to that found in collagen (106).

The right-handed α helix makes a dextro contribution to the specific rotation, $[\varphi]_D$, of the order of 20–70° (89–92). At shorter wavelengths a levo contribution becomes prominent; this was shown indirectly by use of progressively refined computational methods (112–116) and then by direct observation (117) to be related to a negative Cotton effect at 225 mμ. Deeper penetration into the ultraviolet revealed the first peak of a very strong positive Cotton effect (118,119), probably centered near 190 mμ; it seems likely that this is responsible for the dextro effect at long wavelengths. Random-coil polypeptides do not show either of the Cotton effects mentioned above but instead a small negative one at 204 mμ is found (118). These observations have been confirmed and refined by circular dichroism measurements, which suggest that the small negative Cotton effect at 204 mμ is also given by the helix (120–123).

Native collagen shows a large negative specific rotation ($[\varphi]_D$ ca. $-400°$); denaturation produces a strong dextro shift to $[\varphi]_D$ ca. $-120°$

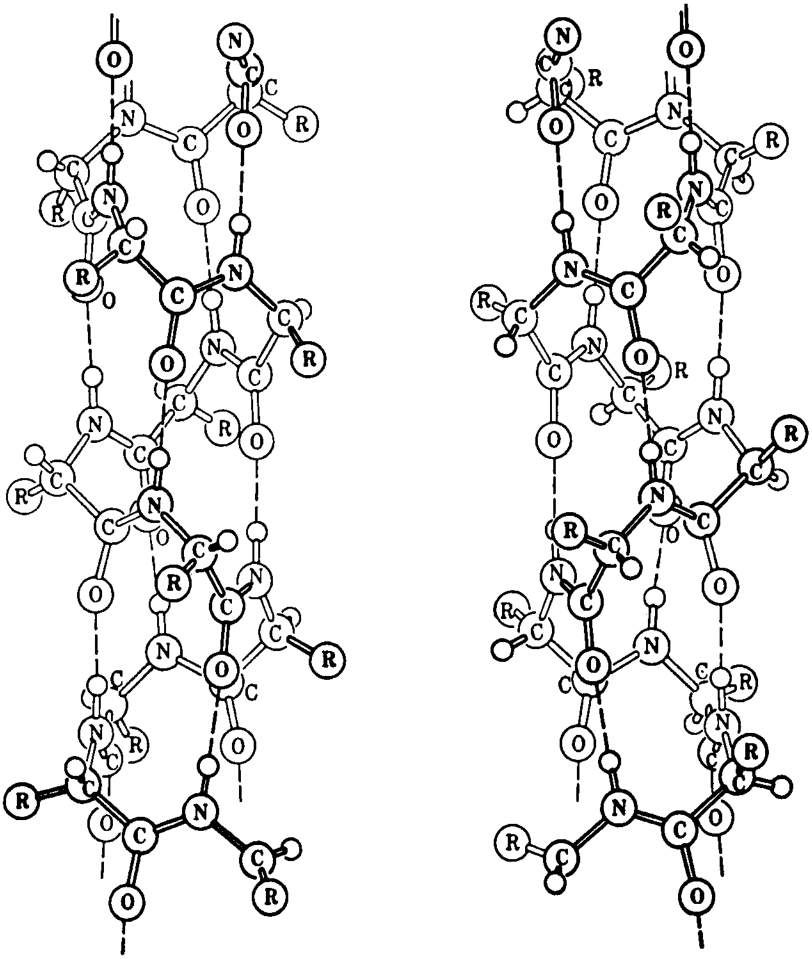

(a)

(b)

Fig. 43. (*a*) Left-handed and (*b*) right-handed forms of the helix conformation of proteins. The amino acid residues are in the *L* or *S* absolute configuration. [After R. B. Corey and L. Pauling, *Rend. Ist. Lombardo Sci.*, P.1, **89**, 10 (1955). Reproduced with permission of the Istituto Lombardo, Milano.

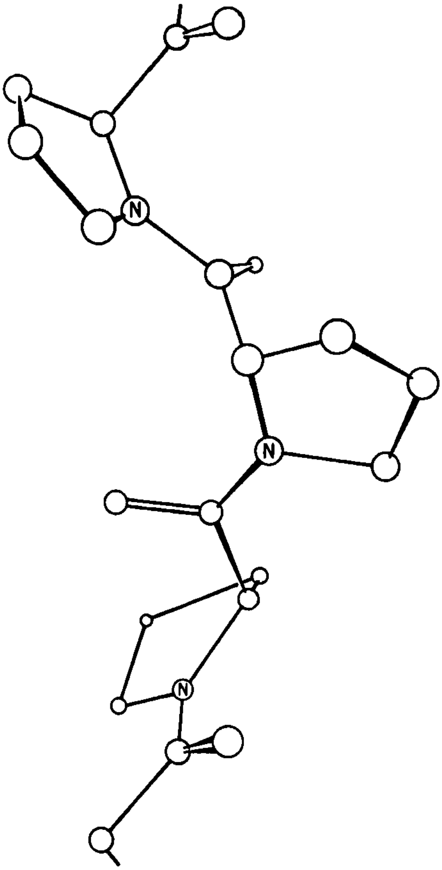

Fig. 44. Poly-L-proline II (94).

(94,124). Poly-L-proline II shows a similar dextro shift, from $[\varphi]_D$ −540° to $[\varphi]_D$ −250° on denaturation with lithium bromide (125). The rotatory dispersion of the native "protein" is simple (126–128) and leads to a strong negative Cotton effect, not at 225 mμ and not at 190 mμ, but at 203 mμ. The two major kinds of helices, thus, show clear qualitative differences in their rotatory properties.

It is of interest that application of the simple helix model to these systems indicates at once that such differences should exist. The α helix

(Fig. 43*b*) (99) has one right-handed helix, formed by the covalent bonds of the protein backbone, and three left-handed helices formed by the hydrogen-bonded amide groups. These helices make opposing contributions, but it is to be expected that the left-handed helices, which contain the whole chromophoric group, will be responsible for the longer wavelength Cotton effect. In contrast, the left-handed helix of poly-L-proline (Fig. 44) (94,105) is not hydrogen bonded so that the backbone contribution (levo) is not counterbalanced. The size of the effect here suggests that each of the counterpoised effects in the α helix must be large.

It is arithmetically simple to estimate the rotatory contributions of these helices by use of our simple model; uncertainties in the choice of refraction values, however, make these calculations doubtful in significance.

The dimensions of the α helix (100) are shown in the legend of Figure 45, which shows an axial projection of four residues in the right helix. The rotatory effect of the backbone helix of X residues is calculated in the following way:

1. Each residue has a rise of 1.48 Å, so that

$$L = X \times 1.48\ \text{Å}$$

2. The sum of the bond distances (Fig. 46) (87) from C^α to C^α is 4.323 Å, so that

$$D = X \times 4.323\ \text{Å}$$

3. The triangular area subtended by each residue (Fig. 45) is $\frac{1}{2}ab \sin C$, so that

$$A = X[(2.28)^2/2] \sin 100^\circ\ \text{Å}^2$$

4. The refractions of the relevant bonds (39) are

$$R_{\text{C—C}} = 1.30$$
$$R_{\text{C—N}} = 1.57$$
$$R_{\text{C=N}} = 3.76$$

whence refractions for the extreme resonance forms are

$$\sum \Delta R = X \times 4.44 \qquad \text{Amide: C—N}$$
$$= X \times 6.63 \qquad \text{Amide: C=N}$$

5. Substituting into

$$[\Phi]_D = 652(LA/D^2) \sum \Delta R_D f(n)$$

we obtain

$$[\Phi]_D/X = 587f(n) \qquad \text{Amide: C—N}$$
$$= 876f(n) \qquad \text{Amide: C}=\text{N}$$

where

$$[\Phi]_D/X = [\varphi]_D\text{MRW}/100$$

(MRW = mean residue weight)

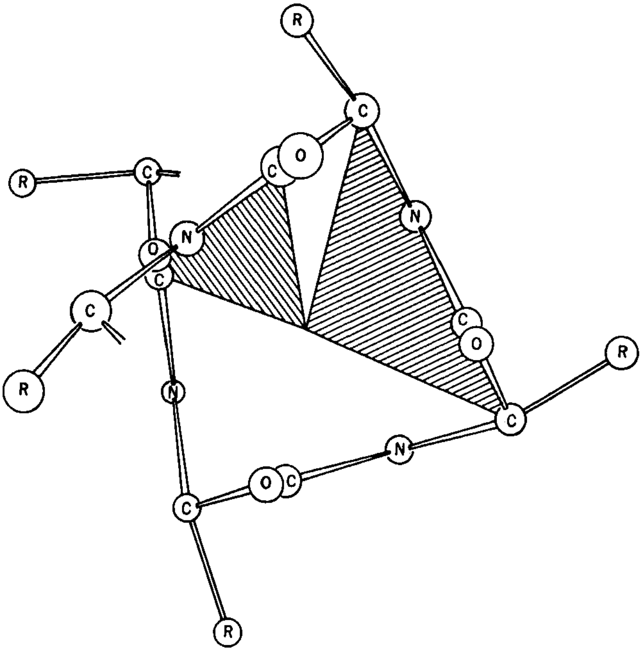

Fig. 45. Right-handed helix.

Atom	Coordinates (100)		
	r, Å	$\phi°$	z, Å
C^α	2.28	0.0	1.48
N	1.57	29.1	0.62
Amide C	1.61	74.6	1.09
O	1.76	83.5	2.29
C^α	2.28	100.0	0.00

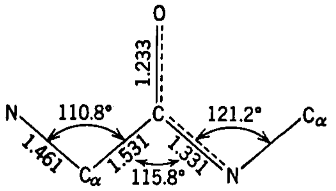

Fig. 46. Dimensions of the peptide unit (87).

For the hydrogen-bonded chains

1. $L = X \times 1.48$ Å

2. The length of the N····H····O system is 2.74 Å, whence, for each helix

$$D = (X/3)5.30 \text{ Å}$$

3. The area subtended by each unit is an equilateral triangle with sides of 1.61 Å, whence, for each helix

$$A = (X/3)[(1.61)^2/2](\sqrt{3}/2) \text{ Å}^2$$

4. The bond refraction values (39) for the extreme forms of the resonance hybrid are shown below:

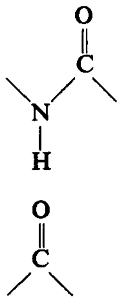

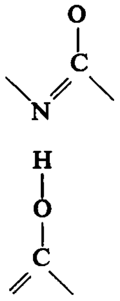

$R_{C=O}$	3.32	R_{C-O}	1.46
R_{N-H}	1.76	R_{O-H}	1.80
R_{C-N}	1.57	$R_{C=N}$	3.76

whence

$\sum \Delta R = 6.65(X/3)$ Amide: 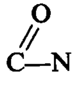
$\overset{O}{\overset{/\!/}{C}}\text{—N}$

$\sum \Delta R = 7.02(X/3)$ Amide: 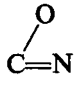
$\overset{O}{\overset{/}{C}}\text{=N}$

5. Calculating for the rotatory effect of all three helices, we obtain:

$[\Phi]_D/X = -769f(n)$ Amide:

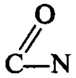

$\mathrm{O{=}C{-}N}$

$-812f(n)$ Amide:

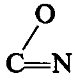

$\mathrm{O{-}C{=}N}$

The average values are $+732f(n)$ and $-790f(n)$. It is of interest that circular dichroism measurements (120) give rotational strengths of $+3.6 \times 10^{-39}$ and -4.1×10^{-39} erg cm^3 rad for the bands at 192 and 220 mμ, respectively. This suggests that the relative contributions of the two helices are approximated by our model.

The case of poly-L-proline II is possibly more significant. An axial projection (Fig. 47) shows that the helix is highly irregular. Two sets of

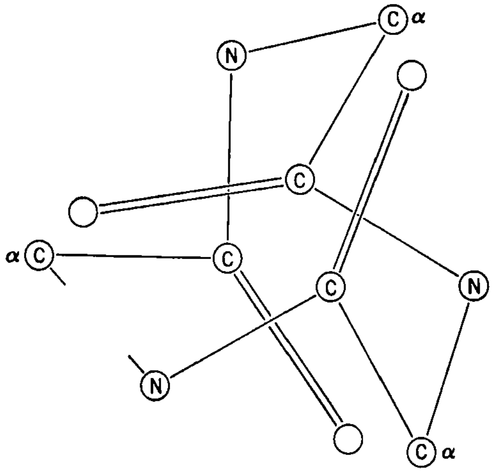

Fig. 47. Coordinates for backbone atoms of poly-L-proline II.

Atom	Cowan and McGavin (94) r, Å	ϕ	z, Å	Sasisekharan (105) r, Å	ϕ	z, Å
C^α	1.30	0°00′	0.00	1.25	0°00′	0.00
C amide	0.32	−12°30′	1.14	0.27	−20°30′	1.16
N	1.01	76°00′	1.95	1.01	75°30′	1.94
C^α	1.30	120°00′	3.12	1.25	120°00′	3.12
Area/unit		0.5725 Å^2				0.5189 Å^2

dimensions are available (94,105). Both agree that there are exactly three residues per turn, with a rise of 3.12 Å per residue.

1. $L = X \times 3.12$ Å

2. $D = X \times 4.323$ Å

3. We average the refraction values for the extreme forms of the resonance hybrid:

$$\sum \Delta R = X \times 5.53$$

4. The area subtended by one repeating unit is obtained by adding and subtracting areas of triangles calculated from the dimensions given in Figure 47. The two sets of data give:

$$A = X \times 0.5725 \text{ Å}^2 \qquad X \times 0.5189 \text{ Å}^2$$

5. From these values we calculate the residue rotation:

$$[\Phi]_D/X = -345f(n) \qquad -313f(n)$$

These values are to be compared with that obtained from the shift in rotation observed (125) (290°) on denaturation of poly-L-proline II.

The first attempt at a theoretical analysis of this problem was that of Fitts and Kirkwood (129), who treated the α-helix backbone (only) as a uniform and regular helix of polarizability. They concluded that the dextrorotatory contribution of the helix at long wavelengths indicated right handedness. The failure of their model to predict the important negative Cotton effect at 225 mμ arises from their neglect of the left-handed hydrogen-bonded helices. In a more sophisticated analysis, Moffitt (112,130,131) suggested that the amide absorption band would be split by coupling to give two transitions at somewhat different wavelengths. One would be polarized along the helix axis with a quasi-symmetric coupling which would tend to reinforce and so have a lower frequency. Given the orientation of the transition moment in the amide group (Fig. 48) (132) it can, perhaps, be seen from Figure 43*b*, that this effect will be levorotatory (Fig. 49). The other band, at higher frequency, will be polarized perpendicular to the axis (along a radius) and be dextrorotatory (Fig. 50). This represented a clear advance for it indicated that the helix would make both a dextro and a levo contribution, that the corresponding Cotton effects would be close together and that the longer wavelength one would be negative. It allowed a correct prediction of the form of the dispersion equation (112). Errors in the original Moffitt treatment (130) were corrected in a collaborative paper with

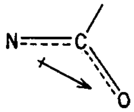

Fig. 48. Transition moment for the amide group.

Fitts and Kirkwood (133). The resultant model was further refined (134). More recently, Tinoco (135) has reconsidered the ORD effects due to interactions among all the groups in a regular helix and suggested that they will give rise to a special type of Cotton effect, characterized in the present instance by a large positive effect with smaller negative wings. The α helix negative Cotton effect at 225 mμ has also been ascribed to an effect of the *n*–π* transition of the amide group (136,137), This, of course, would put an entirely new light on the whole matter.

While the earlier theories were, in a very general way, parallel to the simple model presented above, the more modern treatment has diverged. This appears to be related to greater interest in the details

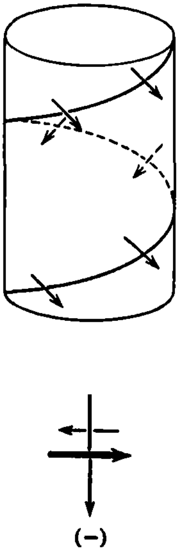

Fig. 49. Amide transition moments polarized parallel to the helix axis.

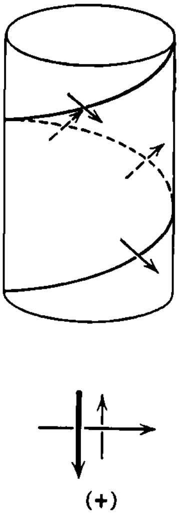

Fig. 50. Amide transition moments polarized perpendicular to the helix axis.

of rotatory properties in absorption bands, an area in which the simple model probably should not be applied.

V. CORRELATIONS WITH OTHER MODELS

Many models of optical activity have been presented over the years. While some are only of historical interest, a number contain ideas that remain useful. Most of the modern models are sophisticated enough that this author is not qualified to summarize them fairly, let alone to criticize them. And yet some useful purpose may be served by the presentation of what one organic chemist sees in them. The barrier to communication between the theoretician and the organic chemist is very high and can hardly be broken until the theoretician can learn what is and what is not getting through. At the same time a broadly based attempt to tie together the theoretical models (as seen through the barrier) may help other organic chemists to find their way over.

Broadly speaking the models can be categorized by their emphasis on either refraction (circular birefringence) or absorption (circular dichroism) properties. Those of the first group require that light set several charges into limited oscillation along different paths so that their joint actions and interactions are dissymmetric. Classical refraction and polarizability theory seems suitable for such models and lends itself to the drawing of analogies with familiar phenomena. It seems fair to say that in most of these models correlation with absorption properties is almost an afterthought, excitation being treated as little more than an exaggerated oscillation. Those of the second group focus attention on one electron at a time and on the dissymmetry of excitation processes. Here a quantum mechanical approach becomes appropriate, with the result that simple analogies become difficult to draw. In this case ordinary rotation, in regions of transparency or due to transitions in inaccessible regions of the spectrum, is relegated to a background role.

Moscowitz (14) has stressed the fact that the Kronig-Kramers theorem indicates a close relationship between absorption and refraction; the two groups of models are not, then, altogether disparate in any fundamental sense. Other reviews (2,138) have emphasized the multiplicity of ways in which the response of optical rotation can be elicited from complex systems. It is our belief that the uniform helix conductor model provides a bridge, at the naive level at which organic chemists must work in this area, among many of these models.

A. Tetrahedral Models

The recognition of the role of the asymmetric atom in producing molecular dissymmetry (40,139,140) and thus, optical activity, and the success of this concept in accounting for numbers of stereoisomers (141,142) led naturally to the view that optical rotatory power was a property of the asymmetric atom as such. Accordingly the early molecular models dealt with tetrahedral systems. Stark (143) proposed a nonmathematical picture based on the concept of independent isotropic oscillations of electrons along the four bonds of the asymmetric atom and showed that this model had the required symmetry properties. Shortly thereafter several workers presented theories in which the key feature was anisotropic polarization of the four substituents and coupling of their oscillations through a field effect (144–146). The principle of coupling, that is, the perturbation of one group as a consequence of the polarization of another, has become a central feature of most

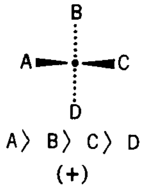

Fig. 51. Atomic asymmetry.

subsequent pictures. The mathematics of these models was refined (8,147,148) and eventually (149) correlated with the quantum mechanical equations of Rosenfeld (150). The more strictly chemical aspects were developed in terms of the polarizabilities (volumes) of the radicals (151,152). Boys' model, the culmination of the latter trend, leads to the conclusion that the enantiomer shown in Figure 51, in which the volume (or polarizability) of the whole radical decreases in the order $A > B > C > D$, will be dextrorotatory.

We have suggested (25) that rotatory effects attributable to the asymmetric atom as such will be significant only when the polarizabilities of the atoms directly attached to the asymmetric center are different (thus clearing the field for consideration of other rotatory effects in compounds having two or more saturated carbon atoms attached to the asymmetric centers). It was found empirically (25) that compounds in which atomic asymmetry effects might be predominant did indeed follow this modification of the Boys rule. However, it has since become clear (28,37) that other effects, probably involving dissymmetric perturbation of aromatic (and possibly carboxyl) chromophores, contribute importantly to the rotations of most of those compounds, drastically undercutting the empirical basis of the rule. Accordingly it becomes uncertain whether the "atomic asymmetry" effect (25) is ever large enough to require that it be taken into account. Molecular orbital calculations (153) indicate that the system shown in Figure 51 will often be dextrorotatory but do not provide a basis for estimating the magnitude of the effect.

For these reasons it is probably only of academic interest that the atomic asymmetry model can be incorporated into the helix model. We assume that the four attachment atoms acquire partial positive charges by an outward deformation of their electron shells and in proportion

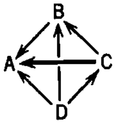

Fig. 52. Right-handed helicity in an asymmetric atom.

to their polarizabilities. These charges, in turn, by direct field effects between attachment atoms, produce additional polarization (from the less polarizable to the more). This produces the pattern shown in Figure 52, in which the line D–C–B–A forms a right-handed helix. We are in no position to evaluate the magnitude of the atomic asymmetry effect (25) but would now suggest that it be neglected until it can be shown to be large enough to require consideration. In the meantime, the origin of the large rotations of compounds cited in support of the "atomic asymmetry model" (25) should be investigated.

B. Paired Oscillator Models

1. *Kuhn's Model*

Kuhn (9,154–160) pointed out that a pair of isotropic oscillators could produce optical rotation if they were coupled dissymmetrically. This represented an important breakaway from the tetrahedral models. Despite the fact that it is classical, rather than quantum mechanical, it is clearly the first of the modern models in terms of the chemical structure concepts employed.

In this model attention is focussed on a pair of groups oriented so that the induced oscillations of their electrons will be neither collinear nor coplanar, as, e.g., in Figure 53. The groups are coupled so that the "symmetric" (Fig. 53*a*) and "antisymmetric" (Fig. 53*b*) oscillations differ in energy. It is clear from the diagrams of circular polarized light (Figs. 6 and 7) that if such a system is placed so that light is propagated to the right along the z axis then Figure 53*a* will interact better with right circular polarized light and so be levorotatory while Figure 53*b* will be dextrorotatory. (The distance d must be shorter than one-half the wavelength of light.) This model leads to the prediction that the

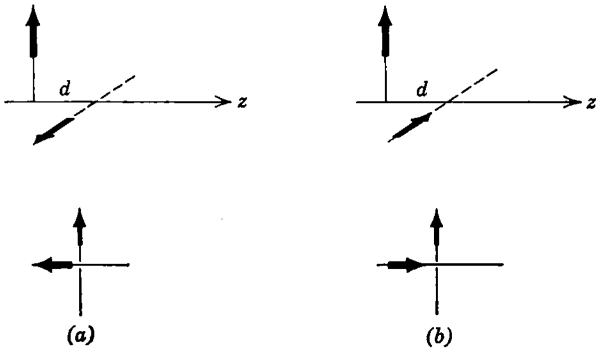

Fig. 53. Coupled oscillators: (*a*) "symmetric," (*b*) "antisymmetric."

system shown in Figure 54, in which coupling can occur along the central bond, would show the following properties:

a. The coupling will produce a splitting of the absorption band of the group X.

b. The long wavelength band, corresponding to the preferred coupling (here, Fig. 53*b*), will have a positive Cotton effect and make a dextrorotatory contribution at long wavelength.

c. The short wavelength band, corresponding to the unfavored coupling (here Fig. 53*a*) will have a negative Cotton effect and make a levorotatory contribution at long wavelengths.

d. At long wavelengths the dextro effect will be dominant, but the two contributions will cancel at very long wavelengths.

e. The two oscillators may be different; in this case we have a mechanism whereby an inherently symmetrical chromophore can be made optically active through the "vicinal effect" of a nearby group.

It is clear that this is a helix model of optical rotation, but that it differs from the one considered here in its full reliance on the electrical field of the circular polarized ray. The principal difficulty arises from

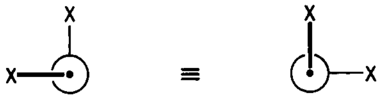

Fig. 54. The skew conformation as a set of coupled oscillators.

the disparity in size of the pitch of the usual molecular helix (a few Ångstroms) and of the ordinary optical helix (λ = 2000–7000 Å). In an effort to take this into account, Kuhn and Bein (156) modified the model so that the two oscillators became almost coplanar. The necessity for this makes it difficult to apply this model in detail to actual stereochemical problems. Nevertheless, it remains true that this model, considered more from the chemical point of view than the optical, is the foundation on which the modern models rest.

2. *Kirkwood's Model*

The Kirkwood polarizability model (161–163) is a culmination of the trends featuring coupling of oscillators (144,154–156) and keying of rotatory effects to polarizability or refraction properties (146,151,152). Basically it is concerned with the magnetic moment produced by electrical displacements along two axes of polarizability that are neither collinear nor coplanar (Fig. 54). In Figure 55*a*, the vertical electrical field E_0 produces electrical displacements, E_i and E_k, the vertical and horizontal components of which (Fig. 55*b*), taken as a whole, have left-hand helix character. In the same way, the horizontal field E_0 of Figure 56*a* produces electrical displacements with horizontal and vertical components (Fig. 56*b*) but now with right-hand helicity. It turns out that the levo (Fig. 55) and dextro (Fig. 56) effects would cancel if the two modes of response to the electrical field were equal in energy. In this model it is considered that the two groups are coupled

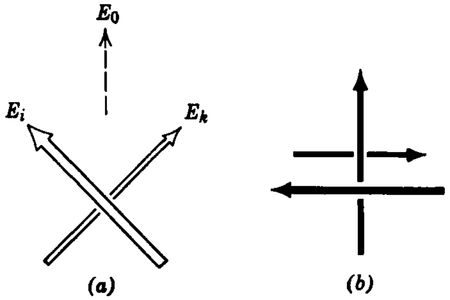

Fig. 55. A left-helical pattern of electrical displacement along two axes of polarizability.

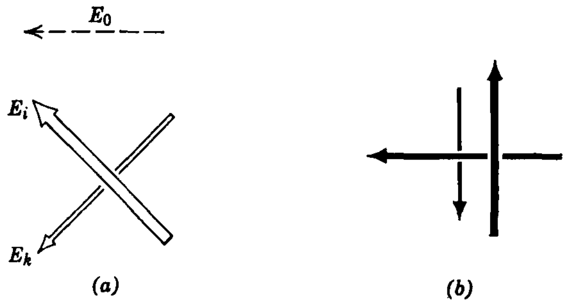

Fig. 56. A right-helical pattern of electrical displacement along two axes of polarizability.

by dipole–dipole interactions so that the second (dextrorotatory) mode of coupling (Fig. 56) is favored for the system shown in Figure 54.

The equations of the Kirkwood model, using the trigonometric formulation of Fitts (163) rather than the original vector formulation and considering an isolated pair of oscillators (*i* and *k*), are:

$$[\Delta\Phi_{ik}]_{\mathrm{D}} = 4930[(n^2 + 2)/3]g_{ik}{}^{(0)}$$
$$g_{ik}{}^{(0)} = 1/6(\alpha_i\beta_i)(\alpha_k\beta_k)G_{ik}R_{ik} \cos \chi_{ik} \sin \theta_{ik}$$
$$G_{ik} = (1/R_{ik}{}^3)(\cos \theta_{ik} - 3 \cos \phi_i \cos \phi_k)$$

The first equation describes molecular rotation at the $\mathrm{Na_D}$ line in terms of a constant, the "Lorentz factor" and a molecular rotatory parameter, $g_{ik}{}^{(0)}$. This latter term is equivalent and, indeed, equal to the term γ of eq. (19). As shown by the second equation, the magnitude of this term is controlled by polarizability properties (α,β), the distance between the groups (R_{ik}) and angular relations (θ,χ,ϕ) between them. The coupling of the two groups (G_{ik}) which is required to make one response (Fig. 56) easier than the other (Fig. 55) is taken as a dipole–dipole interaction of the Keesom type (third equation; see Kauzmann (2), pp. 503–507 for the origin of such expressions).

For deeper insight we turn to a more chemically structured system (Fig. 57). The groups *i* and *k* are attached to the main body of a molecule by the bonds A—*i* and B—*k*, with each group cylindrically symmetrical about the axis of its bond. The sensitivity of each group to the electric field of light and to the induced dipole in the other group is proportional to its mean polarizability α. In this model no optical activity results if

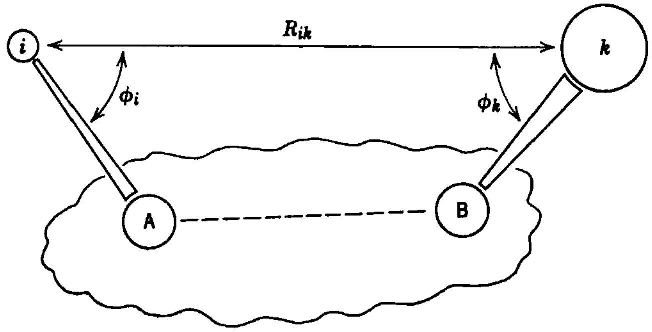

Fig. 57. Long-range interaction of two substituents, *i* and *k*, in the Kirkwood model.

the groups are isotropic (equally polarizable in all directions); the term β is the "anisotropy ratio" which indicates how much more (or, rarely, less) than one-third of the total polarizability can be considered to be directed along the line formed by each bond axis. It is this portion of the polarizability which gives rise to the effects shown in Figures 55 and 56 and so produces the magnetic effect.

The remainder of the terms are best understood by reference to an orientation of the system *i*–A---B–*k* which places the terminal bonds in parallel planes (Figs. 58 and 59). The angle θ_{ik} is seen in Figure 59, where the two planes are parallel to the paper; it is the angle formed by

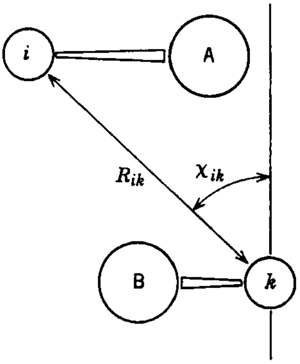

Fig. 58. Distance ($R_{ik} \cos \chi_{ik}$) between parallel planes, one containing the bond A–*i* and the other the bond B–*k*.

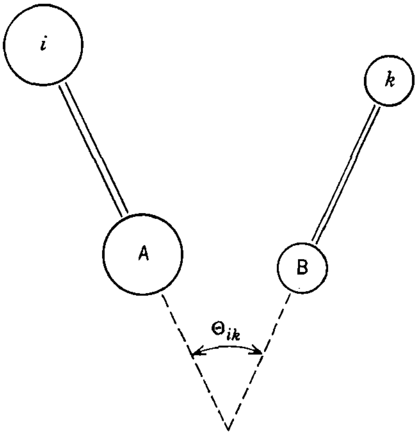

Fig. 59. Projected angle (Θ_{ik}) between bonds A–i and B–k when they lie in parallel planes.

projecting the bonds until they cross. The components of the electrical displacements corresponding to circular motion (see Figs. 55*b*, and 56*b*) are proportional to cos $(\theta/2)$ sin $(\theta/2)$, and thus to sin θ_{ik}. The magnitude of the magnetic moment will also be proportional to the separation of the antiparallel electrical displacements. As seen in Figure 58, this separation is $R_{ik} \cos \chi_{ik}$.

We can generalize from this that the system shown in Figure 57 will be dextrorotatory whether A and B are linked by a single bond or a chain of bonds. This conclusion is broadly the same as that obtained from the helix model (where a coordinated electron displacement: $k \rightarrow \mathrm{B} \rightarrow \mathrm{A} \rightarrow i$ would be used) but there are several significant points of difference.

1. The Kirkwood model does not take into account the electric moment produced by the magnetic field of light. It is therefore not applicable to effects produced by those weak absorption bands which have strong magnetic transition moments.

2. It does not take into account coupling along a bond system by, for example, the inductive mechanism. This model will, therefore, underestimate the contributions of compact systems, as the skew conformation.

3. The model does not take into account the possibility that i and k should be taken as the electron pairs of the bonds A–i and B–k. Were this done it would be necessary to take into account all bonds (as is done in the Conformational Dissymmetry treatment). In the usual applications of the Kirkwood model hydrogen atoms and the bonds to them are ignored.

These comments should not detract from the fact that this is one of the few models directly applicable to a broad range of organic chemical problems. It has been used in the assignment of absolute configuration to a number of aliphatic compounds (161,162) (where it should be particularly reliable). The effects of solvent on conformational dissymmetry and, thus, on optical rotation have been considered in detail for the case of 1,2-dichloropropane (162). The illustration of the details of calculations for the case of *trans*-1,2-dimethylcyclopropane (163) is particularly illuminating; the absolute configuration assigned there has been confirmed chemically (164), though the calculated rotation (16°) is noticeably lower than that actually observed (46°).

Yamana (165), in a lengthy series of papers, has applied a variant of the Kirkwood model ("polarizability multiplying," or PM method) to pyranoses and cyclohexane derivatives. In this model the Kirkwood structural relationships are used to obtain parameters which are then multiplied by factors obtained empirically from known compounds. These factors are large enough to suggest that some of the criticisms offered above need to be taken into account in further uses of this model.

C. One-Electron Models

The idea of "optically active absorption bands" can be traced back at least to Drude (7). When accepted in full it requires that optical activity must eventually be described only in terms of individual dissymmetric excitation processes. This view has been stultifying when adopted as a *sine qua non* because the paucity of data or the complexity of calculations provides excuses for doing nothing. It has, however, been a stimulus to other workers because it suggests that especially significant experimental results could be obtained by optical rotatory dispersion or, better, circular dichroism studies of well-chosen compounds with suitable chromophores. This latter point has been handsomely illustrated in recent years, by the work of Djerassi and his school (11,12,166).

Moscowitz (14) distinguishes two kinds of one-electron system:

1. The inherently symmetrical chromophore in a dissymmetric environment. Commonly this will be a group giving a transition with a weak electric moment; absorption via such transitions is weak, being forbidden by symmetry but becoming allowed by perturbations of that symmetry. If molecular dissymmetry makes the perturbations dissymmetric and if the transition has a magnetic moment an appreciable rotatory effect may result.

2. The inherently dissymmetric chromophore. Here the chromophore extends over a number of atoms that provide a twisted framework in which the transition occurs (as with hexahelicene, Sect. IV-3). Such chromophores may produce enormous rotations because their transitions have strong electric and magnetic moments.

A group which perturbs a chromophore may, in some respects, be regarded as part of a composite chromophore which is inherently dissymmetric (167). There will, then, be a more or less continuous distribution between the extremes given above. A bridge between these models and those considered in Section V-B is provided by the special model of Eyring and Jones (below) wherein is considered the perturbation of the environment by an electronic transition in the chromophore.

1. Inherently Symmetrical Chromophores

The idea that a symmetrical group could be made dissymmetric by its environment was advanced by Lowry (168,169) in an effort to account for the specific rotatory effect of the carbonyl group of camphor and its derivatives (170), as seen first in dispersion constants and then by measurement of the Cotton effect at 290 mμ (171,172). The finding that this absorption band had almost no influence on the refractive index (173) showed that this rotatory effect, at least, could not be controlled by polarizability (174). Although the use of the concept of "asymmetric induction" to account for the stereoselectivity of carbonyl reactions is now known to have been ill advised, the concept was fruitful in leading to the one-electron theory (1,10,83,175–179). It is a typical result of the barrier to communication between theoreticians and organic chemists that it took nearly twenty-five years for the octant rule (180) to appear, even though it is implicit (138,181) in the one-electron treatment of ketonic Cotton effects.

The octant rule (180) has proven of great value in organic stereochemistry (11,12,164) not only because it is a powerful tool for studying configuration and conformation but because it produced a major reorientation of patterns of thought. Some important extensions and

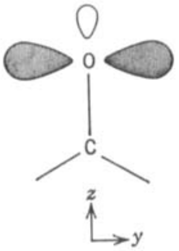

Fig. 60. Carbonyl group: *n* orbital.

refinements merit reference (167,182–186,200) but no review can be attempted here. We would, however, point out that the general helix model of optical activity was developed largely by the authors of the one-electron theory; it provides a simple "explanation" of how substituents can make the carbonyl *n*–π^* transition optically active.

The transition involves the promotion of an electron from the *n* orbital (shaded area in Fig. 60) to the antibonding π orbital (Fig. 61). These orbitals are set at right angles and so do not overlap (Fig. 62); no pathway is available for an electron to go from one orbital to the other. Deformation of the molecular framework or of the orbital system could, however, allow leakage between the orbitals and such effects do allow the transition to occur to some extent; it gives a weak absorption band near 290 mμ. Let us now imagine a modification of the system which produces a selective improvement of transmission and specifically involves the left lobe of the *n* orbital and the upper lobe of the π^* orbital as seen in Figure 63. This will have the effect of promoting what amounts to a clockwise "motion" of negative charge around the *z* axis (as seen in Figs. 62 and 63), coupled with a linear displacement putting increased negative charge on carbon. This "motion" has right-handed

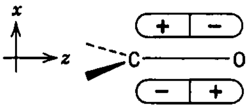

Fig. 61. Carbonyl group: π^* orbital.

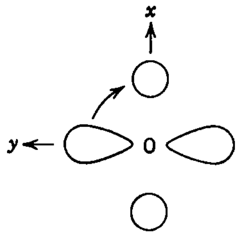

Fig. 62. *n*- and π^* orbitals; O forward.

helicity* and so, from the general helix model, should produce a positive Cotton effect. Positively charged and highly polarizable groups might be expected to have this effect, either by deforming orbitals or by bridging them. Groups having orbitals capable of overlapping those of the carbonyl group could be particularly effective. Such groups do, indeed, give positive Cotton effects and it will be recognized that we have simply restated the octant rule as it applies to the rear octants. We leave open the problem of the front octants (185,186).

It is to be emphasized that the uniform helical conductor model can not be applied in detail to this kind of system because the electron pathway is not delineated by bonds.

2. *Inherently Dissymmetric Chromophores*

A number of the more important inherently dissymmetric chromophores are easily seen to be unsaturated versions of the skew conformation (Sect. IV-A). It is comforting to find that these systems, where the Cotton effect can be observed directly or approached rather

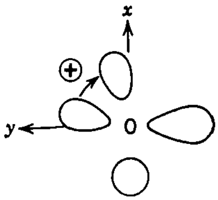

Fig. 63. Distortion of *n* and π^* orbitals.

---

*An analysis in terms of flow of formal positive charge gives the same helicity.

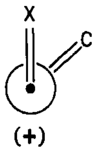

Fig. 64. Dextrorotatory skew conformational unit for cisoid dienes (X = C) and α,β-unsaturated ketones (X = O).

closely, are dextrorotatory when their bonds have right-handed helicity. In particular, cisoid dienes skewed as in Figure 64 (X = C) show strong dextrorotatory trends in visible ORD measurements (187) and positive Cotton effects (188,189) at the π–π* absorption band at 260–280 mμ. Further examples supporting this rule and illustrating its utility are cited by Crabbé (12). Similar effects are to be expected with right-helical *trans* dienes (Fig. 65; X = C). It is likewise to be expected that α,β- unsaturated ketones, twisted in the sense of Figures 64 and 65 (X = O) will show positive Cotton effects at the wavelengths of their π–π* transitions (240–260 mμ) (190). This has been confirmed (190) and is, again, well reviewed by Crabbé (12).

Homoconjugated systems (191–198) also give very large rotations (191) indicating that they are acting as composite inherently dissymmetric chromophores (167,199). It is of interest that these systems produce strong positive Cotton effects when twisted as shown in Figure 66, which shows right-handed helicity when viewed along the end-to-end line (167,199). This subject has been reviewed by Mislow (199) and by Crabbé (12).

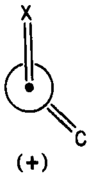

Fig. 65. Dextrorotatory skew conformational unit for transoid dienes (X = C) and α,β-unsaturated ketones (X = O).

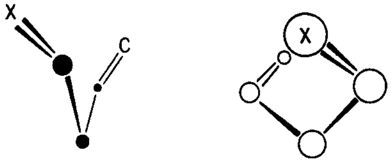

(a) (b)

Fig 66. Right-helix conformation in homoconjugated systems.

D. The Eyring-Jones Model

Eyting and Jones have presented an interesting model (181) which provides a bridge between the one-electron models (Sect. IV-C) and the coupled oscillator models (Sect. IV-B). Here attention is given to perturbation of the environment by an electric dipole moment change in a chromophore; one oscillator is much more effective than the other. The model is easy to apply in principle, but sometimes difficult in practice. With our skewed conformational unit (Fig. 67), for example, we assume a perturbation in group A collinear with the bond axis. Group A is placed at the origin in a right-handed coordinate system with the C—A bond on the negative z axis. The system is swung until the next most polarizable direction (the central C—C bond) is in the yz plane. The group B, which is perturbed by the transition at A is now found in an octant characterized by the coordinates $(+x, +y, -z)$. The sign of rotation is opposite that of the product of coordinates; in this

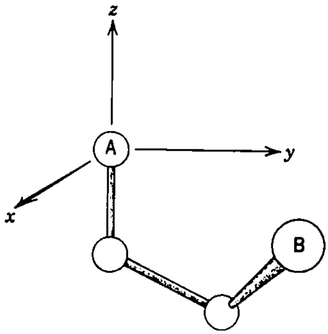

Fig. 67. The skew conformational unit in the Eyring-Jones model.

case the rotation effect is positive. It is easily shown that this model gives predictions of sign comparable to those of the present helix model. It resembles our model more closely than it does the coupled oscillator model in the sense that only the coordinated flow of charge is taken into account. The original papers should be consulted for details of the derivation and application of this model (181).

VI. CONCLUSION

The general rule, that a system in which electrons are constrained to right-handed helical paths will give a positive Cotton effect and dextrorotation at long wavelength, enters, explicitly or implicitly, into all of the major theoretical models of optical activity. An especially simple model, in which the helical path is taken to be analogous to a uniform conductor, gives fairly good predictions of magnitude of rotation for cases where the pathway for electronic motions is delineated by bonds. It does not seem to be appropriate in a quantitative way for transitions such as the n–π^* of ketones, where the pathway does not correspond to a bond system, and should be used cautiously, if at all, in such cases.

Acknowledgment

The author wishes to thank the Abbott Laboratories, North Chicago, Illinois, for a generous grant which provided helpful support during the preparation of this chapter.

References

1. E. U. Condon, *Rev. Mod. Phys.*, **9**, 432 (1937).
2. W. Kauzmann, *Quantum Chemistry*, Academic Press, New York, 1957; (a) pp. 616–636; (b) pp. 703–725.
3. I. Tinoco, Jr. and R. W. Woody, *J. Chem. Phys.*, **40**, 160 (1964).
4. (a) A. Fresnel, *Ann. Chim. Phys.* (2), **28**, 147 (1825); see, J. R. Partington, *Advanced Treatise on Physical Chemistry*, Vol. IV, Longmans Green, London, 1953, pp. 333–340; (b) A. Fresnel, *Mèm. Acad. Sci.*, **7**, 45 (1827); *Oeuvres*, Vol. II, Imprimerie Imperiale, Paris 1868, p. 479; cited by J. R. Partington (above) p. 301.
5. L. Pasteur, "Lectures 1860," *Alembic Club Reprint*, **14**, 24 (1905).
6. J. W. Gibbs, *Am. J. Sci.*, (3), **23**, 460 (1882); *Collected Works*, Vol. II, part 2, Longmans Green, New York, 1928, p. 195.

7. P. Drude, *Göttinger Nachrichten*, **1892**, 366; *Theory of Optics* (trans. by C. R. Mann and R. A. Millikan) (publ. 1900), Dover reprint, 1959, p. 400–407.
8. M. Born, *Ann. Physik* (4), **55**, 177 (1918).
9. W. Kuhn, *Z. Phys. Chem.*, **20B**, 325 (1933).
10. W. J. Kauzmann, J. E. Walter, and H. Eyring, *Chem. Rev.*, **26**, 339 (1940).
11. C. Djerassi, *Optical Rotatory Dispersion*, McGraw-Hill, New York, 1960.
12. P. Crabbé, *Optical Rotatory Dispersion and Circular Dichroism in Organic Chemistry*, Holden-Day, San Francisco, 1965.
13. L. Velluz, M. Legrand, and M. Grosjean, *Optical Circular Dichroism*, Academic Press, New York, 1965.
14. A. Moscowitz, *Tetrahedron*, **13**, 48 (1961).
15. E. von Fleischl, *Wien. Ber.* (II), **90**, 478 (1884); *Ann. Physik*, **24**, 127 (1885).
16. See, C. K. Ingold, *Structure and Mechanism in Organic Chemistry*, Cornell University Press, Ithaca, New York, 1953, pp. 119–137.
17. See ref. 2, p. 603, 620.
18. (a) C. O. Beckmann and K. Cohen, *J. Chem. Phys.*, **4**, 784 (1936); (b) K. Cohen and C. O. Beckmann, *J. Chem. Phys.*, **6**, 163 (1938); (c) C. O. Beckmann and H. C. Marks, *J. Chem. Phys.*, **8**, 827 (1940); (d) H. C. Marks and C. O. Beckmann, *J. Chem. Phys.*, **8**, 831 (1940).
19. T. M. Lowry, *Optical Rotatory Power*, Longmans Green, London, 1935; Dover reprint, New York, 1964; (a) pp. 105–148; pp. 414–423; (b) pp. 149–159, 393–413, 424–456.
20. A. Cotton, *Ann. Chim. Phys.* (7), **8**, 347 (1896).
21. K. F. Lindman, *Ann. Physik* (4), **38**, 523 (1912); **63**, 621 (1920); **69**, 270 (1922); **74**, 541 (1924); **77**, 337 (1925).
22. M. H. Winkler, *J. Phys. Chem.*, **60**, 1656 (1956); **62**, 1342 (1958).
23. I. Tinoco, Jr., and M. P. Freeman, *J. Phys. Chem.*, **61**, 1196 (1957).
24. D. H. Whiffen, *Chem. Ind. (London)*, **1956**, 964.
25. J. H. Brewster, *J. Am. Chem. Soc.*, **81**, 5475 (1959).
26. J. H. Brewster, *J. Am. Chem. Soc.*, **81**, 5483 (1959).
27. J. H. Brewster, *J. Am. Chem. Soc.*, **81**, 5493 (1959).
28. J. H. Brewster, *Tetrahedron Letters*, **1959**, 23.
29. J. H. Brewster, *Tetrahedron*, **13**, 106 (1961).
30. J. A. Berson, J. S. Walia, A. Remanick, S. Suzuki, P. Reynolds-Warnhoff, and D. Willner, *J. Am. Chem. Soc.*, **83**, 3986 (1961).
31. M. Davis and G. H. R. Summers, *J. Chem. Soc.*, **1960**, 4707.
32. J. H. Brewster and W. E. Braden, Jr., *Chem. Ind. (London)*, **1964**, 1759.
33. R. A. Sneen and N. P. Matheny, *J. Am. Chem. Soc.*, **86**, 5503 (1964).
34. H. M. Walborsky, L. Barash, A. E. Young, and F. J. Impastato, *J. Am. Chem. Soc.*, **83**, 2517 (1961).
35. H. M. Walborsky and C. G. Pitt, *J. Am. Chem. Soc.*, **84**, 4831 (1962).
36. J. H. Brewster and J. E. Privett, *J. Am. Chem. Soc.*, **88**, 1419 (1966).
37. J. H. Brewster and J. G. Buta, *J. Am. Chem. Soc.*, **88**, 2233 (1966).
38. G. W. Wheland, *The Theory of Resonance*, Wiley, New York, 1944, pp. 99, 286–296.

39. A. I. Vogel, *J. Chem. Soc.*, **1948**, 1833; A. I. Vogel, W. T. Cresswell, G. H. Jeffrey, and J. Leicester, *J. Chem. Soc.*, **1952**, 514.
40. J. H. van't Hoff, *La Chimie dans l'Espace*, Bazendijk, Rotterdam, 1875, p. 29.
41. See, R. Kuhn in *Stereochemie*, K. Freudenberg, Ed., F. Deuticke, Leipzig, 1933, p. 804.
42. E. P. Kohler, J. T. Walker, and M. Tishler, *J. Am. Chem. Soc.*, **57**, 1743 (1935).
43. J. H. Wotiz and R. J. Palchak, *J. Am. Chem. Soc.*, **73**, 1971 (1951).
44. W. C. Agosta, *J. Am. Chem. Soc.*, **84**, 110 (1962).
45. W. C. Agosta, *J. Am. Chem. Soc.*, **86**, 2638 (1964).
46. P. Maitland and W. H. Mills, *J. Chem. Soc.*, **1936**, 987.
47. T. L. Jacobs and D. Dankner, *J. Org. Chem.*, **22**, 1424 (1957).
48. R. J. D. Evans, S. R. Landor, and J. P. Regan, *Chem. Commun.*, **1965**, 397.
49. S. R. Landor, B. J. Miller, J. P. Regan, and A. R. Tatchell, *Chem. Commun.* **1966**, 585.
50. S. R. Landor and R. Taylor-Smith, *Proc. Chem. Soc.*, **1959**, 154.
51. E. R. H. Jones, J. D. Loder, and M. C. Whiting, *Proc. Chem. Soc.*, **1960**, 180.
52. W. M. Jones, J. W. Wilson, Jr., and F. B. Tutwiler, *J. Am. Chem. Soc.*, **85**, 3309 (1963).
53. I. Tömösközi and H. J. Bestman, *Tetrahedron Letters*, **1964**, 1293.
54. W. D. Celmer and I. A. Solomons, *J. Am. Chem. Soc.*, **74**, 1870, 2245, 3838 (1952); **75**, 1372, 3430 (1953).
55. M. Anchel, *Science*, **126**, 1229 (1957).
56. G. Bendz, *Arkiv. Kemi.*, **14**, 305, 475 (1959); **15**, 131 (1960).
57. R. C. Cambie, A. Hirschberg, E. R. H. Jones, and G. Lowe, *J. Chem. Soc.*, **1963**, 4120.
58. M. O. Bagby, C. R. Smith, Jr., and I. A. Wolff, *Chem. Ind.* (*London*), **1964**, 1861; *J. Org. Chem.*, **30**, 4227 (1965).
59. R. E. Bew, J. R. Chapman, E. R. H. Jones, B. E. Lowe, and G. Lowe, *J. Chem. Soc.* (*C*), **1966**, 129.
60. S. R. Landor and N. Punja, *Tetrahedron Letters*, **1966**, 4905.
61. M. Anchel, J. Polatnick, and F. Kavanagh, *Arch. Biochem.*, **25**, 208 (1950).
62. J. D. Bu'Lock, E. R. H. Jones, and P. R. Leeming, *J. Chem. Soc.*, **1955**, 4270.
63. J. D. Bu'Lock, E. R. H. Jones, P. R. Leeming, and J. M. Thompson, *J. Chem. Soc.*, **1956**, 3767.
64. J. D. Bu'Lock, E. R. H. Jones, and P. R. Leeming, *J. Chem. Soc.*, **1957**, 1097.
65. R. Bonnett, A. A. Spark, J. L. Tee, and B. C. L. Weedon, *Proc. Chem. Soc.*, **1964**, 419.
66. R. E. Bew, R. C. Cambie, E. R. H. Jones, and G. Lowe, *J. Chem. Soc.* (*C*), **1966**, 135.
67. E. L. Eliel, *Tetrahedron Letters*, **1960**, No. 8, 16.
68. R. J. D. Evans and S. R. Landor, *Proc. Chem. Soc.*, **1962**, 182.
69. R. J. D. Evans and S. R. Landor, *J. Chem. Soc.*, **1965**, 2553.
70. W. M. Jones and J. W. Wilson, Jr., *Tetrahedron Letters*, **1965**, 1587.
71. M. H. Gianni, Ph.D. Thesis, University of New Hampshire, 1961; *Dissertation Abstr.*, **21**, 2474 (1961).
72. G. Lowe, *Chem. Commun.* **1965**, 411.

73. S. F. Mason and G. W. Vane, *Tetrahedron Letters*, **1965**, 1593.
74. R. S. Cahn, C. K. Ingold and V. Prelog, *Experientia*, **12**, 81 (1956); *Angew. Chem.* (*Intern. Ed.*), **5**, 385 (1966).
75. V. Prelog, *Helv. Chim. Acta*, **36**, 308 (1953).
76. J. Tanaka, *Bull. Chem. Soc. Japan*, **36**, 833 (1963).
77. S. F. Mason, *Proc. Chem. Soc.*, **1962**, 362.
78. S. F. Mason and G. W. Vane, *J. Chem. Soc.* (*B*), **1966**, 370.
79. M. S. Newman, W. B. Lutz, and D. Lednicer, *J. Am. Chem. Soc.*, **77**, 3420 (1955).
80. M. S. Newman and D. Lednicer, *J. Am. Chem. Soc.*, **78**, 4765 (1956).
81. D. D. Fitts and J. G. Kirkwood, *J. Am. Chem. Soc.*, **77**, 4940 (1955).
82. A. Moscowitz, Ph.D. Thesis, Harvard University, 1957.
83. A. Moscowitz in *Advances in Chemical Physics*, Vol. IV, I. Prigogine, Ed. Interscience, New York, 1962, p. 67.
84. E. G. Cox, *Proc. Roy. Soc.* (*London*), **A135**, 491 (1932).
85. G. Egloff, *Physical Constants of Hydrocarbons*, Vol. IV, Reinhold, New York, 1947. (a) pp. 81, 82; n_D^{100} 1.5821, d_4^{100} 0.9628; (b) p. 193; $n_D^{129.8}$ 1.6502, $d_4^{129.8}$ 1.046.
86. N. C. Kneten, N. J. Krause, T. O. Carmichael, and O. E. Weigang, Jr., *J. Am. Chem. Soc.*, **84**, 1738 (1962).
87. D. R. Davies, *Prog. Biophys. Mol. Biol.*, **15**, 189 (1965).
88. F. W. Putnam, in *The Proteins*, Vol. IB, H. Neurath, Ed., Academic Press, New York, 1953, p. 807.
89. W. Kauzmann, *Advan. Protein Chem.*, **14**, 1 (1959).
90. A. C. Alexander, *J. Exp. Med.*, **1**, 304 (1896).
91. L. K. Christensen, *Compt. Rend. Trav. Lab. Carlsberg*, **28**, 37 (1952).
92. R. B. Simpson and W. Kauzmann, *J. Am. Chem. Soc.*, **75**, 5139 (1953).
93. C. Cohen, *Nature*, **175**, 129 (1955).
94. P. M. Cowan and S. McGavin, *Nature*, **176**, 501 (1955).
95. L. Pauling and R. B. Corey, *J. Am. Chem. Soc.*, **72**, 5349 (1950).
96. L. Pauling, R. B. Corey, and H. R. Branson, *Proc. Natl. Acad. Sci. U.S.*, **37**, 205 (1951).
97. L. Pauling and R. B. Corey, *Proc. Natl. Acad. Sci. U.S.*, **37**, 235 (1951).
98. L. Pauling and R. B. Corey, *Proc. Natl. Acad. Sci. U.S.*, **37**, 241 (1951).
99. R. B. Corey and L. Pauling, *Rend. Ist. Lombardo Sci. Lettere*, **89**, 10 (1955).
100. L. Pauling, R. B. Corey, H. L. Yakel, Jr., and R. E. Marsh, *Acta Cryst.*, **8**, 853 (1955).
101. M. L. Huggins, *J. Am. Chem. Soc.*, **74**, 3963 (1952).
102. A. Elliott and B. R. Malcolm, *Nature*, **178**, 912 (1956).
103. J. C. Kendrew, R. E. Dickerson, B. E. Strandberg, R. G. Hart, and D. R. Davies, *Nature*, **185**, 422 (1960).
104. E. R. Blout, *Tetrahedron*, **13**, 123 (1961).
105. V. Sasisekharan, *Acta Cryst.*, **12**, 897, 903 (1959).
106. W. F. Harrington and P. H. von Hippel, *Advan. Protein Chem.*, **16**, 1 (1961).
107. P. Doty and J. T. Yang, *J. Am. Chem. Soc.*, **78**, 498 (1956).
108. P. Doty and R. D. Lundberg, *Proc. Natl. Acad. Sci. U.S.*, **43**, 213 (1957).
109. C. Cohen and A. G. Szent-Gyorgyi, *J. Am. Chem. Soc.*, **79**, 248 (1957).

110. J. T. Yang and P. Doty, *J. Am. Chem. Soc.*, **47**, 761 (1957).
111. P. J. Urnes, K. Imahori, and P. Doty, *Proc. Natl. Acad. Sci. U.S.*, **47**, 1635 (1961).
112. W. Moffitt and J. T. Yang, *Proc. Natl. Acad. Sci. U.S.*, **42**, 596 (1956).
113. W. J. Leonard, Jr. and J. F. Foster, *J. Mol. Biol.*, **7**, 590 (1963).
114. E. Shechter and E. R. Blout, *Proc. Natl. Acad. Sci. U.S.*, **51**, 695, 794 (1964).
115. E. Shechter, J. P. Carver, and E. R. Blout, *Proc. Natl. Acad. Sci. U.S.*, **51**, 1029 (1964).
116. S. C. Harrison and E. R. Blout, *J. Biol. Chem.*, **240**, 299 (1965).
117. N. S. Simmons, C. Cohen, A. G. Szent-Gyorgyi, D. B. Wetlaufer, and E. R. Blout, *J. Am. Chem. Soc.*, **83**, 4766 (1961).
118. E. R. Blout, I. Schmier, and N. S. Simmons, *J. Am. Chem. Soc.*, **84**, 3193 (1962).
119. J. T. Yang and T. Samejima, *J. Biol. Chem.*, **238**, 3262 (1963).
120. G. Holzwarth, W. B. Gratzer, and P. Doty, *J. Am. Chem. Soc.*, **84**, 3194 (1962).
121. J. Brahms and G. Spach, *Nature*, **200**, 72 (1963).
122. G. Holzwarth and P. Doty, *J. Am. Chem. Soc.*, **87**, 218 (1965).
123. L. Velluz and M. Legrand, *Angew. Chem. (Intern. Ed.)*, **4**, 838 (1965).
124. R. E. Burge and R. D. Hynes, *Nature*, **184**, 1562 (1959).
125. W. F. Harrington, *Nature*, **181**, 997 (1958).
126. G. D. Fasman and E. R. Blout, *Biopolymers*, **1**, 3 (1963).
127. W. D. Gratzer, W. Rhodes, and G. D. Fasman, *Biopolymers*, **1**, 319 (1963).
128. E. R. Blout, J. P. Carver, and J. Gross, *J. Am. Chem. Soc.*, **85**, 644 (1963).
129. D. D. Fitts and J. G. Kirkwood, *Proc. Natl. Acad. Sci. U.S.*, **42**, 33 (1956).
130. W. Moffitt, *J. Chem. Phys.*, **25**, 467 (1956).
131. W. Moffitt, *Proc. Natl. Acad. Sci. U.S.*, **42**, 736 (1956).
132. D. L. Peterson and W. T. Simpson, *J. Am. Chem. Soc.*, **77**, 3929 (1955); **79**, 2375 (1957).
133. W. Moffitt, D. D. Fitts, and J. G. Kirkwood, *Proc. Natl. Acad. Sci. U.S.*, **43**, 723 (1957).
134. D. D. Fitts and J. G. Kirkwood, *Proc. Natl. Acad. Sci. U.S.*, **43**, 1046 (1957).
135. I. Tinoco, Jr., *J. Am. Chem. Soc.*, **86**, 297 (1964).
136. J. A. Schellman and P. Oriel, *J. Chem. Phys.*, **37**, 2114 (1962).
137. B. J. Litman and J. A. Schellman, *J. Phys. Chem.*, **69**, 978 (1965).
138. D. J. Caldwell and H. Eyring, *Rev. Mod. Phys.*, **35**, 577 (1963).
139. J. van't Hoff, *Bull. Soc. Chim. France*, **23**, 295 (1875).
140. A. LeBel, *Bull. Soc. Chim. France*, **22**, 337 (1874).
141. See, R. L. Shriner and R. Adams in *Organic Chemistry, an Advanced Treatise*, Vol. I, 2nd ed., H. Gilman, Ed., Wiley, New York, 1943, pp. 220–240.
142. See, E. L. Eliel, *Stereochemistry of Carbon Compounds*, McGraw-Hill, New York, 1962, pp. 16–30.
143. J. Stark, *Jahrb. Radioakt.*, **11**, 194 (1914).
144. M. Born, *Phys. Z.*, **16**, 251, 437 (1915).
145. C. W. Oseen, *Ann. Physik* (4), **48**, 1 (1915).
146. F. Gray, *Phys. Rev.* (2), **7**, 472 (1916).
147. A. Landè, *Ann. Physik* (4), **56**, 225 (1918).

148. R. Gans, *Z. Physik*, **17**, 353 (1923); **27**, 164 (1924); E. L. Palumbo (with R. Gans), *Ann. Physik* (4), **79**, 533 (1926).
149. M. Born and P. Jordan, *Elementare Quantenmechanik*, Springer, Berlin, 1930, pp. 250–259.
150. L. Rosenfeld, *Z. Physik*, **52**, 161 (1928).
151. R. de Mallemann, *Rev. Gen. Sci.*, **38**, 453 (1927); *Trans. Faraday Soc.*, **26**, 281 (1930).
152. S. F. Boys, *Proc. Roy. Soc. (London)*, **144A**, 655, 675 (1934).
153. A. Julg, *Tetrahedron*, **12**, 146 (1961).
154. W. Kuhn, *Z. Phys. Chem.*, **4B**, 14 (1929).
155. W. Kuhn, in *Stereochemie*, K. Freudenberg, Ed., Deuticke, Leipzig, 1933, pp. 317–434.
156. W. Kuhn and K. Bein, *Z. Phys. Chem.*, **22B**, 406 (1933).
157. W. Kuhn, *Z. Elektrochem.*, **56**, 506 (1952).
158. W. Kuhn, *Angew. Chem.*, **68**, 93 (1956).
159. W. Kuhn, *Ann. Rev. Phys. Chem.*, **9**, 417 (1958).
160. W. Kuhn, *Tetrahedron*, **13**, 1 (1961).
161. J. G. Kirkwood, *J. Chem. Phys.*, **5**, 479 (1937).
162. W. W. Wood, W. Fickett, and J. G. Kirkwood, *J. Chem. Phys.*, **20**, 561 (1952).
163. D. D. Fitts, in *Technique of Organic Chemistry*, Vol. I, Part III, A. Weissberger, Ed., Interscience, New York, 1960, pp. 2165–2180.
164. W. v.E. Doering and W. Kirmse, *Tetrahedron*, **11**, 272 (1960).
165. S. Yamana, *Bull. Chem. Soc. Japan*, **23**, 259 (1950); **30**, 203, 207, 916 (1957); **31**, 558, 564 (1958); **32**, 597 (1959); **33**, 1741 (1960); **34**, 1212, 1414 (1961); **35**, 1269, 1421, 1950 (1962); **36**, 473 (1963). *J. Am. Chem. Soc.*, **86**, 1606 (1964). *Experientia*, **21**, 305 (1965). *Tetrahedron*, **21**, 709 (1965).
166. C. Djerassi, *Proc. Chem. Soc.*, **1964**, 314.
167. A. Moscowitz, K. Mislow, M. A. W. Glass, and C. Djerassi, *J. Am. Chem. Soc.*, **84**, 1945 (1962).
168. T. M. Lowry and E. E. Walker, *Nature*, **113**, 565 (1924).
169. T. M. Lowry, *Nature*, **131**, 566 (1933).
170. T. M. Lowry and J. O. Cutter, *J. Chem. Soc.*, **127**, 604, (1925); J. O. Cutter, H. Burgess, and T. M. Lowry, *ibid.*, **127**, 1260 (1925); E. M. Richards and T. M. Lowry, *ibid.*, **127**, 1503 (1925); T. M. Lowry and G. Owen, *ibid.*, **1926**, 606.
171. W. Kuhn and H. K. Gore, *Z. Phys. Chem.*, **12B**, 389 (1931).
172. T. M. Lowry and H. K. Gore, *Proc. Roy. Soc. (London)*, **135A**, 13 (1932).
173. C. B. Allsopp, *Proc. Roy. Soc. (London)*, **146A**, 300 (1934).
174. T. M. Lowry and C. B. Allsopp, *Proc. Roy. Soc. (London)*, **146A**, 313 (1934).
175. E. U. Condon, W. Altar, and H. Eyring, *J. Chem. Phys.*, **5**, 753 (1937).
176. E. Gorin, J. Walter, and H. Eyring, *J. Chem. Phys.*, **6**, 824 (1938).
177. E. Gorin, W. Kauzmann, and J. Walter, *J. Chem. Phys.*, **7**, 327 (1939).
178. T. Kwoh and H. Eyring, *J. Chem. Phys.*, **18**, 1186 (1950).
179. T. Watanabe and H. Eyring, *J. Chem. Phys.*, **40**, 3411 (1964).
180. W. Moffitt, R. B. Woodward, A. Moscowitz, W. Klyne, and C. Djerassi, *J. Am. Chem. Soc.*, **83**, 4013 (1961).

181. L. L. Jones and H. Eyring, *Tetrahedron*, **13**, 235 (1961); *J. Chem. Educ.*, **38**, 601 (1961).
182. W. Klyne, *Tetrahedron*, **13**, 29 (1961).
183. C. Djerassi and W. Klyne, *Proc. Natl. Acad. Sci. U.S.*, **48**, 1093 (1962).
184. C. Djerassi and W. Klyne, *J. Chem. Soc.*, **1962**, 4929; **1963**, 2390.
185. J. A. Schellman, *J. Chem. Phys.*, **44**, 55 (1966).
186. G. Wagnière, *J. Am. Chem. Soc.*, **88**, 3937 (1966).
187. R. Deen and H. J. C. Jacobs, *Koninkl. Ned. Akad. Wetenschap. Proc., Ser. B (Amsterdam)*, **64**, 313 (1961).
188. A. Moscowitz, E. Charney, U. Weiss, and H. Ziffer, *J. Am. Chem. Soc.*, **83**, 4661 (1961).
189. H. Ziffer and U. Weiss, *J. Org. Chem.*, **27**, 2694 (1961).
190. C. Djerassi, R. Records, E. Bunnenberg, K. Mislow, and A. Moscowitz, *J. Am. Chem. Soc.*, **84**, 870 (1962).
191. R. B. Woodward and E. G. Kovach, *J. Am. Chem. Soc.*, **72**, 1009 (1950).
192. W. D. Kumler, L. A. Strait, and E. L. Alpen, *J. Am. Chem. Soc.*, **72**, 1463 (1950).
193. E. L. Alpen, W. D. Kumler, and L. A. Strait, *J. Am. Chem. Soc.*, **72**, 4558 (1950).
194. M. Simonetta and S. Winstein, *J. Am. Chem. Soc.*, **76**, 18 (1954).
195. R. C. Cookson and N. S. Wariyar, *J. Chem. Soc.*, **1956**, 2302.
196. H. Labhart and G. Wagnière, *Helv. Chim. Acta*, **42**, 2219 (1959).
197. S. Winstein, L. DeVries, and R. Orloski, *J. Am. Chem. Soc.*, **83**, 2020 (1961).
198. S. MacKenzie, S. F. Marsocci, and H. C. Lampe, *J. Org. Chem.*, **30**, 3328 (1965).
199. K. Mislow, *Ann. N.Y. Acad. Sci.*, **93**, 459 (1962).
200. J. C. Tai and N. L. Allinger, *J. Am. Chem. Soc.*, **88**, 2179 (1966).

Topics in Stereochemistry, Volume 2
Edited by Norman L. Allinger, Ernest L. Eliel

Concepts of Polymer Stereochemistry*

MURRAY GOODMAN

*Department of Chemistry, Polytechnic Institute of Brooklyn,
Brooklyn, New York*

I. INTRODUCTION

Fundamental properties of polymers depend upon the stereochemistry of the polymer chain. In this report we will deal only with linear structures composed of monomeric units in a head-to-tail

---

*Contribution from the Department of Chemistry and Polymer Research Institute, Polytechnic Institute of Brooklyn, Brooklyn, New York.

$$-\mathrm{CHR}-\mathrm{CH_2}-\mathrm{CHR}-\mathrm{CH_2}-\mathrm{CHR}-\mathrm{CH_2}-\mathrm{CHR}-\mathrm{CH_2}-\mathrm{CHR}-\mathrm{CH_2}-$$

(*a*)

$$-\mathrm{CH_2}-\mathrm{CHR}-\mathrm{CHR}-\mathrm{CH_2}-\mathrm{CH_2}-\mathrm{CHR}-\mathrm{CHR}-\mathrm{CH_2}-\mathrm{CH_2}-\mathrm{CHR}-$$

(*b*)

Fig. 1. (*a*) Head-to-tail arrangement of monomeric units; (*b*) head-to-head, tail-to-tail arrangement of monomeric units.

arrangement (Fig. 1). It is also possible for the same monomeric units to be arranged in a head-to-head and tail-to-tail fashion (Fig. 1) although these structures are rare. We will omit any discussion of these materials and branched or network polymers.

It was as a result of the discoveries of Ziegler (1) and Natta and his co-workers (2–6) that the era of stereochemistry of linear synthetic polymers achieved maturity. Earlier workers such as Staudinger, Huggins, and Schildknecht discussed and even prepared stereoregular macromolecules. It remained for Natta to provide convenient routes for the preparation of stereoregular polymers.

II. STEREOCHEMISTRY OF A POLYMER CHAIN

A. Tacticity

Natta's work created a whole new area of polymer chemistry (7). In order to define the structures of these new materials, he suggested the terminology which remains basic to the area of polymer stereochemistry (8). Figure 2 shows the designation of stereoregular placements of the monomeric residues in vinyl and related polymers. When all of the relative configurations* at the tertiary carbons are identical, the material is called isotactic; when the relative configurations at these tertiary carbons alternate along the polymer chain, the polymer is called syndiotactic. Random stereochemistry for the tertiary carbon leads to an atactic polymer structure (Fig. 2).

---

*The assignment of "configuration" (D or L) for vinyl stereoregular polymers is open to serious question. Since the vinyl polymers really contain pseudo-asymmetric units (ignoring the end groups) it is definitely not proper to use D and L symbols. Bovey (9) suggested, and this author heartily concurs, that the terms D and L be used with low molecular weight compounds only, or with those polymers such as polypeptides, polypropylene oxide, or others where there is a genuine asymmetry within the polymer chain or side chains.

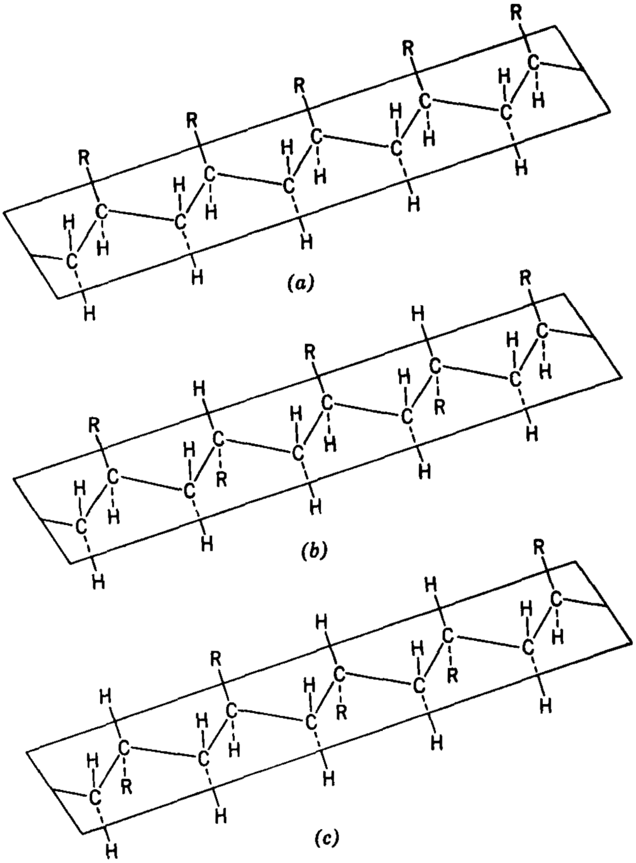

Fig. 2. (*a*) Isotactic placement of polymeric units; (*b*) syndioactic placement of polymeric units; (*c*) atactic placement of polymeric units.

In order to interpret the structure of polymers from 1,2-disubstituted monomers, Natta extended his tacticity designations (10) to include ditacticity assignments (Fig. 3). If the polymer is isotactic with respect to both substituents A and B, two structures are possible: *erythro* or *threo* diisotactic (Fig. 4). The designations *erythro* and *threo* used here are identical with those of traditional organic stereochemistry. In

$$\mathrm{RCH{=}CHR'} \longrightarrow \mathrm{-CHR-CHR'-CHR-CHR'-CHR-CHR'-}$$

Fig. 3. Polymerization of a 1,2-disubstituted monomer.

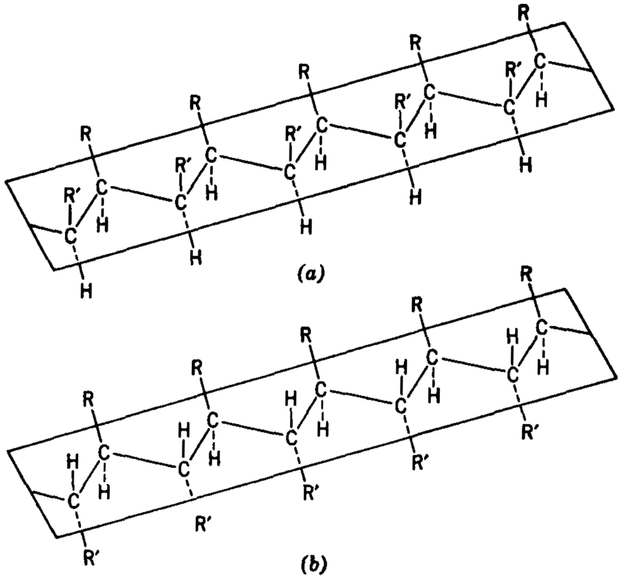

Fig. 4. (*a*) *Threo* diisotactic placement of polymeric units; (*b*) *erythro* diisotactic placement of polymeric units.

addition, it is possible that both A and B are syndiotactic leading to a disyndiotactic structure (Fig. 5). In a disyndiotactic polymer, structural relationships of the A and B substituents require that the polymer be made up of equal amounts of *erythro* and *threo* placements as shown in Figure 5. In these discussions of tacticity we have placed the polymer backbone in a planar *trans* staggered structure. Isotactic polymers

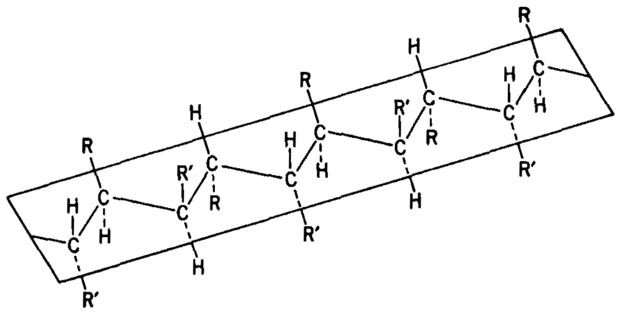

Fig. 5. Disyndiotactic placement of polymeric units.

cannot ordinarily assume this planar form because the substituents located on alternate carbon atoms would sterically interfere with one another. In order to avoid such contacts, the main chain assumes *gauche* placements. This aspect of polymer stereochemistry involves conformational analysis.

Conjugated dienes such as 1,3-butadiene can be polymerized to give isotactic and syndiotactic stereoregular structures (11) (Fig. 6). They can also be converted to polymers which are geometric isomers of each other (Fig. 6). A 1,4-polymerization can yield either a *cis* or *trans* structure for the stereoregular polymer. The dependence of the properties of these polydienes on their geometric form is dramatic. The regular structure of the 1,4-*trans* polymer leads to a brittle powdery material while the *cis* polymer gives a coil-like form making it an excellent elastomer (12).

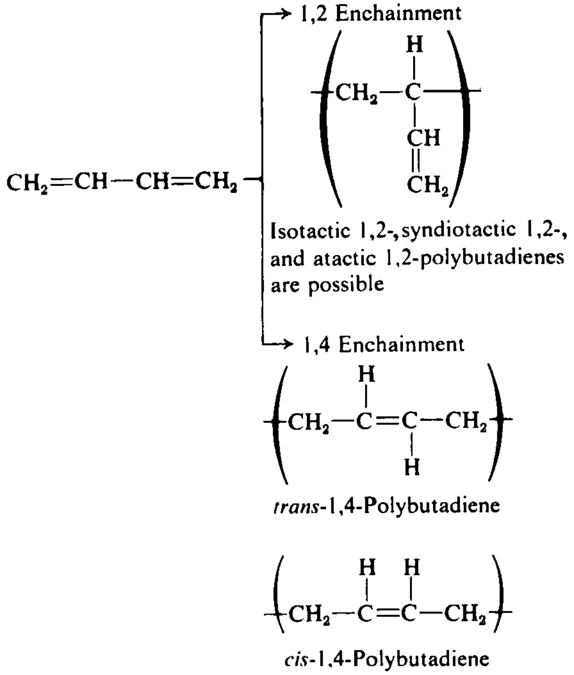

Fig. 6. Possible structures for polybutadiene.

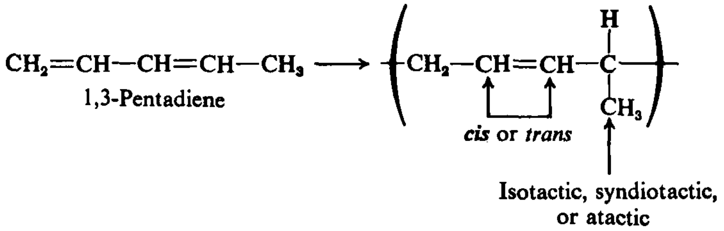

$$CH_2{=}CH{-}CH{=}CH{-}CH_3 \longrightarrow \left(CH_2{-}CH{=}CH{-}\overset{H}{\underset{CH_3}{C}} \right)$$

Fig. 7. Polymerization of 1,3-pentadiene.

The stereoregular polymers discussed to this point cannot be optically active. Both isotactic and syndiotactic vinyl polymers (ignoring end groups) are centrosymmetric with respect to the main chain (13).[*] Polydienes of the 1,4-type derived from butadiene and isoprene must also be optically inactive. Natta, Porri, and Valenti (14) prepared the simplest optically active ditactic homopolymer from the hydrocarbon 1,3-pentadiene and optically active catalysts (Fig. 7). They obtained a crystalline *cis* 1,4-polymer most efficiently by using (−)titanium tetramenthoxide and triethyl aluminum. This polymer contains a fascinating combination of true asymmetry superimposed on a *cis* 1,4-polydiene structure.[†] As proof of preferential configuration and tacticity induced by the catalyst, Natta carried out ozonolysis of the polymer and obtained optically active methylsuccinic acid (14,15) (Fig. 8).

A general consideration of some stereochemical aspects of polypentadiene structure is presented in Figure 9. The isotactic polymers can exhibit optical activity if the polymerization is initiated by an

---

[*] A paradox exists between low molecular weight compounds and high polymers. We can consider that the methylene groups in an isotactic chain are the central units of *meso* dyads, each having the same configuration. In low molecular weight compounds such as the 2,4-disubstituted pentanes, carbons 2 and 4 in a *meso* structure have opposite configurations. The racemic dyads in a syndiotactic chain can be regarded in a polymer system as having opposite configurations at succeeding units. In the analogous pentane, however, carbons 2 and 4 have the same configuration.

[†] It should be pointed out that isotactic and syndiotactic structures have somewhat different meanings for polymers with truly asymmetric centers in the main chain. These centers have nonsuperimposable mirror images (D vs. L or *R* vs. *S*).

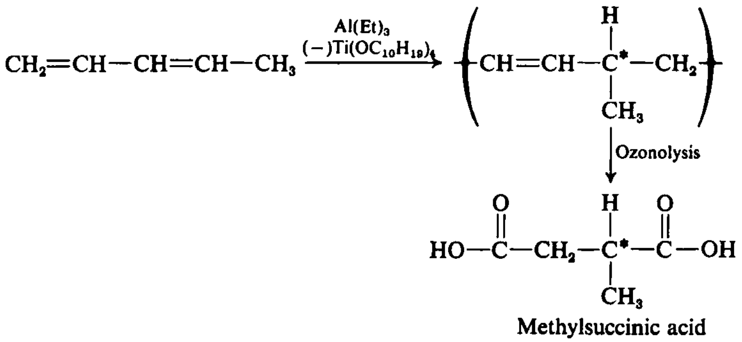

Fig. 8. Asymmetric polymerization of 1,3-pentadiene.

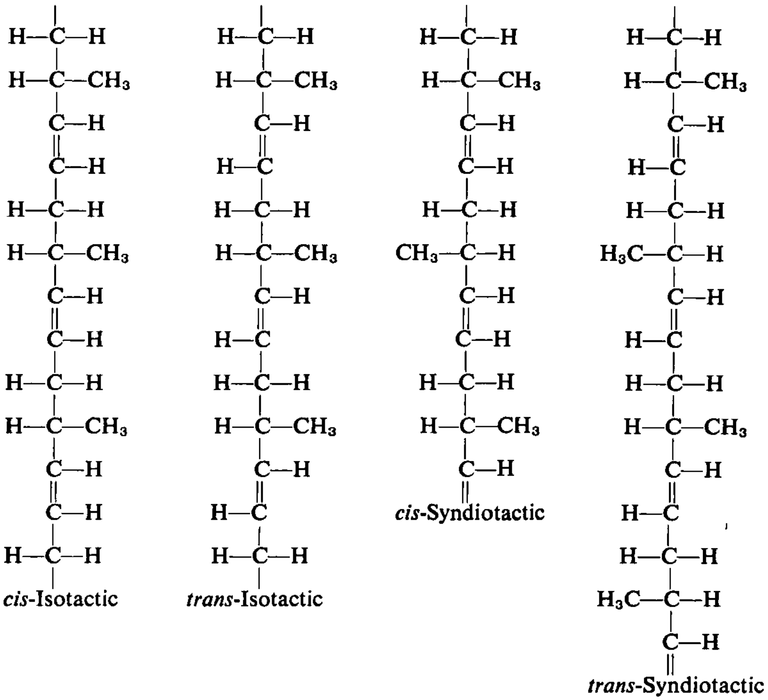
cis-Isotactic
trans-Isotactic
cis-Syndiotactic
trans-Syndiotactic

Fig. 9. Stereochemistry of 1,4-polypentadiene-1,3 [taken primarily from Pino (16)].

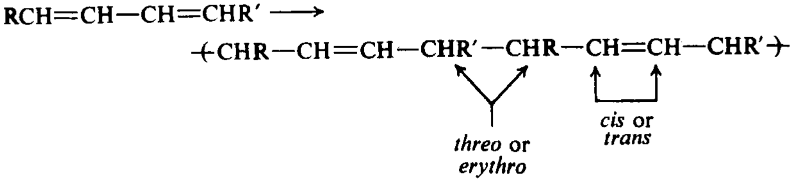

$$\mathrm{RCH{=}CH{-}CH{=}CHR'} \longrightarrow \mathrm{\lnot CHR{-}CH{=}CH{-}CHR'{-}CHR{-}CH{=}CH{-}CHR' \rightarrow}$$

Fig. 10. Polymerization of a 1,4-disubstituted butadiene.

optically active catalyst. Syndiotactic *cis*- or *trans*-1,4-polypentadiene-1,3 must be optically inactive regardless of the optical activity of the catalyst (16).

When R and R′ in a 1,4-disubstituted butadiene are different, tritactic polymers can result from stereoregular polymerization (Fig. 10). Pino (17) analyzed the configurational implications of *cis* and *trans* tritactic polymers. He indicated that *erythro* or *threo* diisotactic polymers (where R does not equal R′) are intrinsically asymmetric.*

Before their work on 1,3-pentadienes, Natta and Farina accomplished the first synthesis of optically active homopolymers from inactive monomers and optically active catalysts (18,19). They polymerized esters of *trans,trans*-sorbic acid and related materials and obtained crystalline tritactic polymers (18,19). Using infrared and x-ray data, they reasoned that the tritactic polymer has a *trans*-1,4-*erythro*-diisotactic structure (Fig. 11).

Natta and his co-workers conclusively demonstrated asymmetric induction in the polymerization of methyl sorbate and methyl β-styrylacrylate by oxidative cleavage to yield methyl- and phenylsuccinic acid,

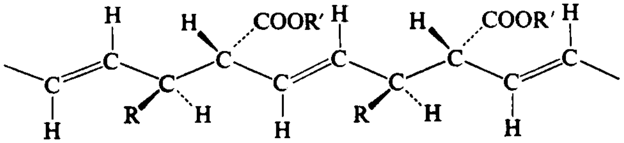

Fig. 11. *Erythro trans*-diisotactic substituted polypentadiene. R ≡ methyl or phenyl and R′ ≡ methyl.

---

*Cf. Section IV for a discussion of asymmetry and dissymmetry.

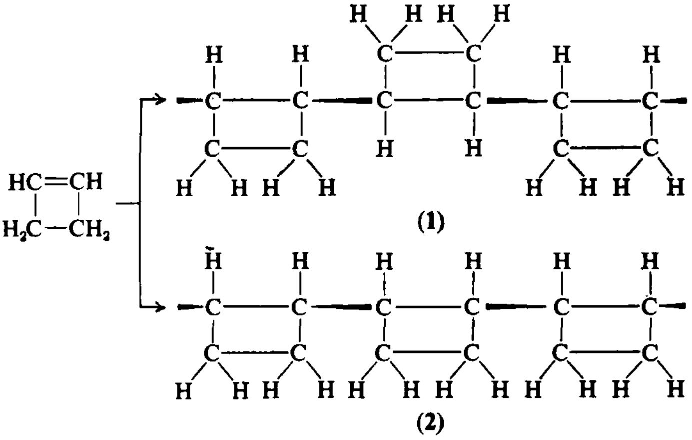

Fig. 12. Polymerization of cyclobutene by opening of the double bond to yield an *erythro* diisotactic structure **1** and an *erythro* disyndiotactic structure **2**.

respectively (19). These dibasic acids showed optical purities of up to 6%, a value consistent with the optical purity of the polymer.

Recently the Natta group has shown (20,21) that monomers such as cyclobutene can polymerize with the aid of vanadium catalysts to yield a new polymer class, the polycyclobutenomers (Fig. 12). Although optically active examples have not been produced to date, their analysis indicates that two forms of the polymer can be obtained; one is probably an *erythro* diisotactic form while the other is an *erythro* disyndiotactic polymer. This type of stereochemical possibility does not exist in the acyclic ditactic polymers since the rings introduce truly asymmetric centers in the chain. A disyndiotactic acyclic structure, as noted above, must have an alternation of *erythro* and *threo* placements as one proceeds along the polymer chain (cf. Fig. 4). In addition to polymerizing to give polycyclobutenomers, the monomer also ring-opens to give poly-1,4-*cis*- and *trans*-butadienes (Fig. 13).

Schuerch (22,23) showed that copolymerization of an optically active monomer such as (*S*)-α-methylbenzyl methacrylate with maleic anhydride gives an optically active alternating copolymer. The resulting copolymer remains optically active after the optically active side chain is removed, because truly asymmetric centers have been induced in the main polymer chain. This process is shown in Figure 14*a*, where it

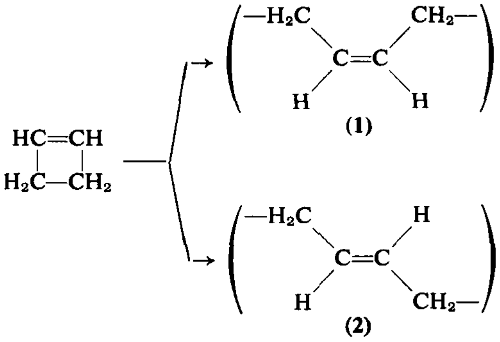

Fig. 13. Polymerization of cyclobutene by ring opening to yield, *cis*-1,4-polybutadiene (**1**) and *trans*-1,4-polybutadiene (**2**).

can be seen that if there is a preference between the diastereomers I and II, the resulting copolymer will be optically active. These experiments (22) were actually the first demonstration of asymmetric synthesis in polymer chemistry. Since these polymerizations were radical initiated, we can conclude that under these conditions asymmetric induction, and not stereoregularity, is the basis for the optical activity in the hydrolyzed copolymer.

The first asymmetric synthesis of a polymer from an optically inactive cyclic monomer was accomplished by Natta and Farina (24,25), who used optically active cationic catalysts with benzofuran. They based their efforts on earlier predictions of Arcus (26) and unsuccessful work by Schuerch (27,28). Since benzofuran polymerizes by double-bond opening and not ring scission, stereoregular tactic polymers were obtained. On the basis of optical activity, Natta and Farina suggested a diisotactic structure for the polymer (Figs. 14*b* and 14*c*). Their most efficient asymmetric catalyst was composed of two $AlCl_3$ molecules and one L-phenylalanine molecule in toluene at $-75°C$.

Ring opening polymerizations* can also give stereoregular inactive and optically active polymers. Price (30,31) polymerized racemic

---

* We will not discuss α-amino acid *N*-carboxyanhydride polymerization in this chapter. An excellent review of this extensive subject was published by Szwarc (29). We will discuss optically active polymers from optically active olefins and related monomers in Section IV.

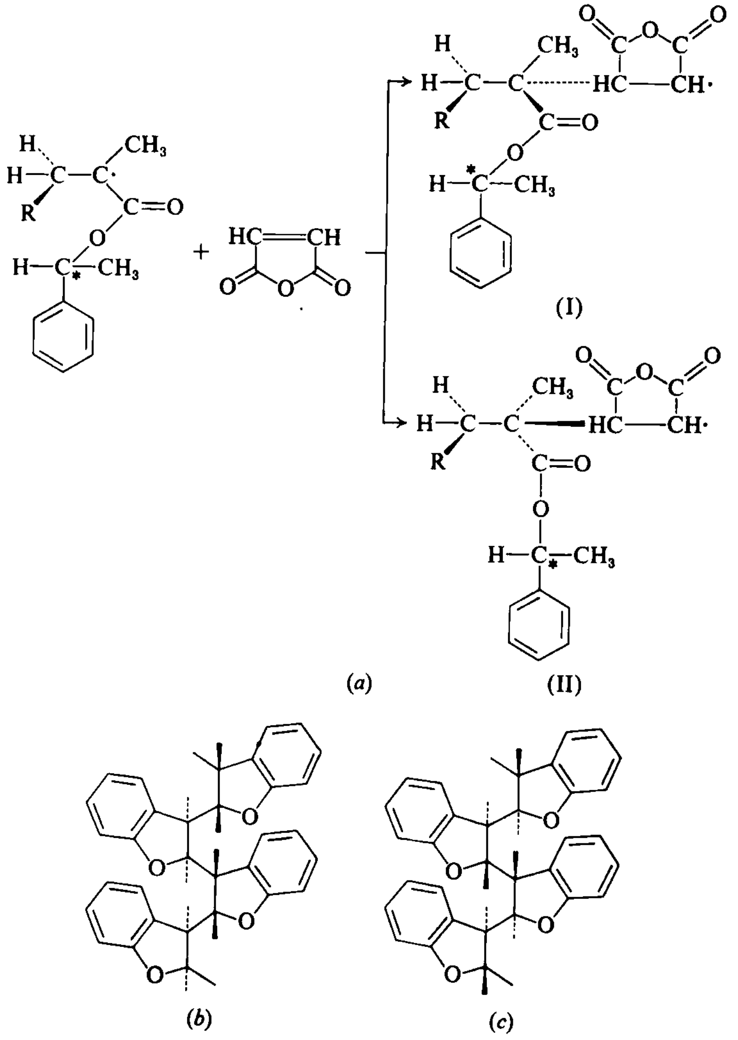

Fig. 14. (*a*) Asymmetric induction during the polymerization of (*S*)-α-methylbenzyl methacrylate and maleic anhydride; (*b*) *erythro*-diisotactic polybenzofuran [taken from Natta (25)]; (*c*) *threo*-diisotactic polybenzofuran [taken from Natta (25)].

propylene oxide to an isotactic polymer and the optically active monomer to optically active isotactic polymer.

In Figure 15, the tacticity relationships of substituted epoxide polymers are presented. If a *trans* staggered structure is assumed for the main chain, the substituents in an isotactic structure are alternately in front and behind the plane of the main chain carbons. For the syndiotactic forms these groups are on the same side. Since there can be true asymmetry in the main chain, it is possible to polymerize an optically active monomer to an optically active isotactic structure. Each of the

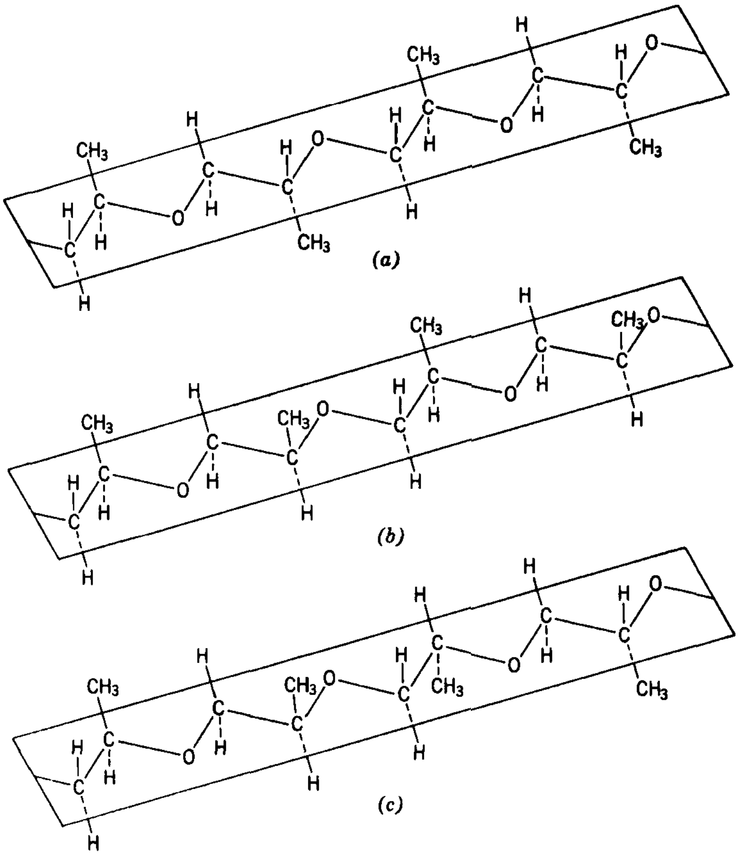

Fig. 15. Polypropylene oxide: (*a*) isotactic; (*b*) syndiotactic; (*c*) atactic.

asymmetric centers in the monomer is preserved during polymerization (32). It is impossible to obtain an optically active syndiotactic polypropylene oxide since the structure requires an alternation of the configuration of successive monomeric units along the chain and thus should exhibit rotatory cancellation. Optically inactive isotactic polypropylene oxide can be viewed as being constructed of sequences of *R* units exactly balanced by sequences of *S* units.

Related in structure to poly-L-propylene oxide is poly-*S*-lactic acid. Kleine and Kleine (33a) were able to convert optically active lactide from lactic acid to highly crystalline isotactic poly-*S*-lactic acid

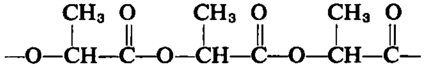

$$-O-\overset{CH_3}{\overset{|}{C}}H-\overset{O}{\overset{\|}{C}}-O-\overset{CH_3}{\overset{|}{C}}H-\overset{O}{\overset{\|}{C}}-O-\overset{CH_3}{\overset{|}{C}}H-\overset{O}{\overset{\|}{C}}-$$

via ring-opening polymerization. They employed weak Friedel-Crafts catalysts at 140°. Specifically, zinc and lead oxides (as catalysts) give essentially no racemization during the polymerization. Trace amounts, however, of the other optical antipode of the lactide cause profound changes in the optical activity of the polymer. This is evidenced by a decrease in crystallinity and melting point noted by Schultz and Schwaab (33b).

We established in our laboratory that the conformation of the polymer is not helical in solution. The configuration of each residue of the polymer chain in solution is identical to that of the model compound, methyl-*S*-lactate (33c). This was confirmed by NMR and optical rotatory dispersion studies.

B. Conformational Aspects of Polymer Structure

It is a well-established concept that a polymer chain can assume a large number of conformations by varying the angles of rotation about the main chain bonds (34). The energetically most stable conformation of an isolated polymer chain can be predicted by locating the deepest minimum in the potential energy as a function of the angles of rotation around these bonds. Moreover, the most probable conformation of a polymer chain in solution can be identical with the conformation in the crystalline state. In solution the steric repulsions cannot by themselves fix the conformations of a polymer because of solvent effects. It is possible that short-range one-dimensional order in solution is similar to the long-range one-dimensional order in the crystalline

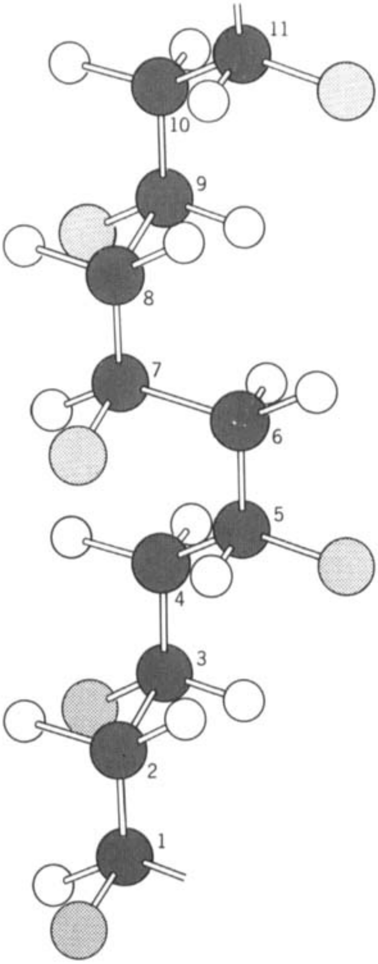

Fig. 16. A poly-α-olefin 3_1-helix showing *trans–gauche* placements along the main chain.

state. This order in a macromolecular chain in solution can be perturbed as a result of both rotational isomerization and torsional oscillation of units about a single equilibrium position (cf. later section).

In an isotactic vinyl polymer structure, the main chain cannot be in a planar zigzag conformation. As a result, if there are rotations about the

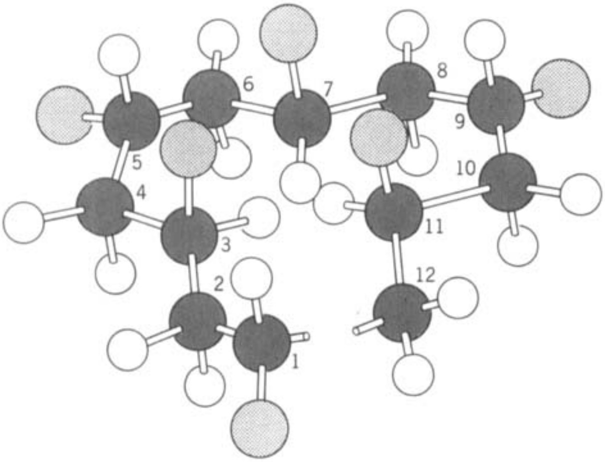

Fig. 17. Conformation of a poly-α-olefin chain showing *trans,trans–gauche, gauche* placements along the chain.

main-chain bonds and only staggered structures are allowed, a helix is generated as shown in Figure 16. The terms *trans* and *gauche* used in conformational analysis for low molecular weight molecules are identical to those used in polymer systems. With respect to the main-chain carbon atoms, the analysis proceeds using butane-like conformational considerations. Thus, it can be seen that the helix in Figure 16 places carbons 1 and 4 *trans* to each other, carbons 2 and 5 *gauche*, carbons 3 and 6 *trans*, carbons 4 and 7 *gauche* to each other, etc. Carbon 7 is a translational repeat of carbon 1. A threefold helix is generated since three monomer residues are necessary for one turn. Such a dissymmetric structure is characterized as a 3_1-helix and the main chain is said to be in the *trans–gauche* conformation.

If the main chain rotation of an isotactic structure is altered to a *trans,trans–gauche,gauche* sequence, the polymer very quickly grows back into itself, as is shown in Figure 17. Considering the possibilities for a syndiotactic vinyl polymer, it is readily apparent that the planar *trans* staggered conformation is stable, since the substituent groups appear alternately on opposite sites of the main chain. This is shown in Figure 2*b*. A syndiotactic polymer can also assume a *trans,trans–gauche, gauche* form. A stable twofold helical structure (Fig. 18) is thereby generated. Thus, the tacticity of a polymer fundamentally affects the

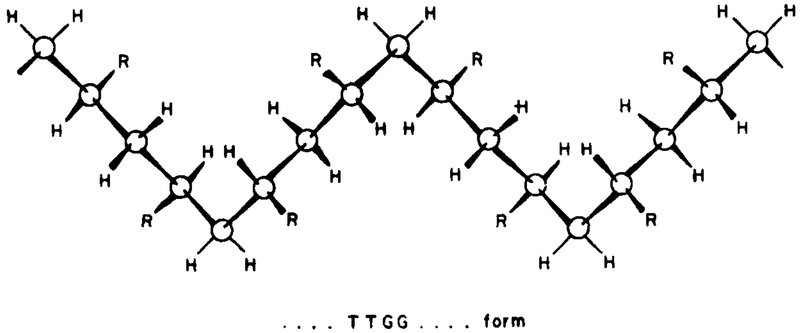

Fig. 18. Conformation of a syndiotactic polymer chain showing *trans,trans–gauche,gauche* placements along the chain.

conformations which the polymer chain can assume. This relationship is certainly one of the most interesting problems in modern day polymer science. The twofold helical conformation noted above has actually been observed for syndiotactic polypropylene (35).

Fordham (36) and Shimanouchi (37) considered the possible conformations of isotactic and syndiotactic polymers on electrostatic and steric grounds. According to them, it can be shown that of the nine different placements of two succeeding units, only two are really possible for each. The others are eliminated by severely interacting arrangements and by overlapping of structures.

Natta and his group (38) used x-ray crystallographic analysis to establish polymer conformation. Their approach is based upon the assumption that in linear crystalline polymers the axis of the macromolecule runs parallel to a crystallographic axis (39). Moreover, in all known structures, the monomeric units have been found to occupy geometrically equivalent positions with regard to this axis. This is known as an "equivalence postulate" (34). A condition which must be met by a crystallizable polymer is that its monomeric units have the configurations required by equivalent positions along an axis. Two monomeric units, whose equivalent atoms have the same z coordinates after a suitable translation of the origin along the chain axis z, are called isoclined; two monomeric units whose equivalent atoms have the same z coordinates after a suitable translation of the origin accompanied by a reversal of direction of the z axis are called anticlined.

Repetition of equivalent monomeric units may be obtained along an axis by:

a. Repetition of isoclined isomorphous equivalent units through the operation of a translation C/p along z, accompanied by a rotation $2\pi(P/p)$ in a plane perpendicular to z. A helix is thus generated which contains p monomeric units and P pitches within the period C (helical-type succession) (Fig. 19).

b. Repetition of isoclined alternately enantiomorphous equivalent units through the operation of a translation $C/2$ accompanied by a reflection in a plane containing the axis of the chain (glide plane-type succession) (Fig. 19).

c. Repetition of isomorphous alternately anticlined equivalent units along a helix associated with twofold axes perpendicular to z (Fig. 19).

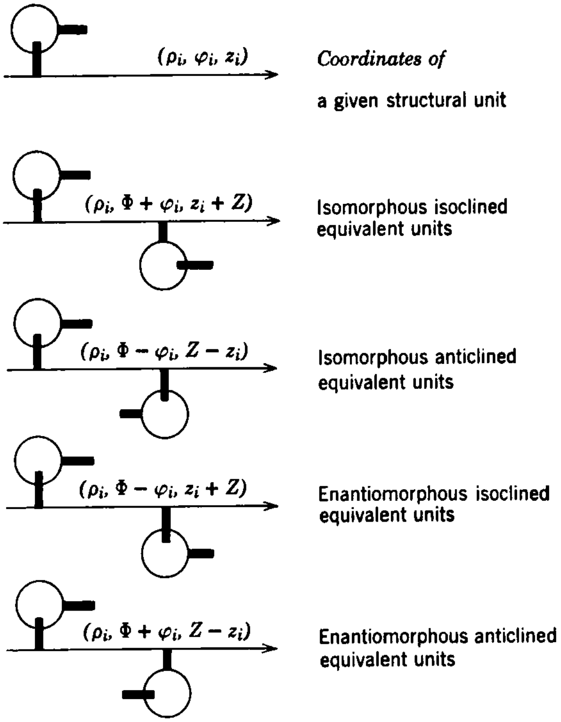

Fig. 19. Coordinates of various structural units [taken from Natta, Corradini, and Ganis (38)].

d. Repetition of enantiomorphous anticlined equivalent units through a translation along *z* associated with a symmetry plane perpendicular to the *z* axis (equivalent to a symmetry center) (Fig. 19).

All of the crystallizable polymers in which the two possible chain directions are intrinsically non-equivalent (for example a polyamide) must be built up in the crystal of isoclined equivalent units. Hence only the helix or glide plane-type structures are possible. In particular, a polypeptide having asymmetric carbon atoms must necessarily have a helical-type chain structure [e.g., the α-helix or a twofold helical β-extended structure (39b)]. We should expect that a polymer chain assumes the conformation which most nearly corresponds to a minimum potential energy for the molecule with the restrictions imposed by the "equivalence postulate."

As with low molecular weight compounds, stable conformations of a chain should in principle satisfy the following conditions: (*1*) bond length; (*2*) bond angle; (*3*) planarity of certain groups of atoms; and (*4*) van der Waals contacts between nonbonded atoms within the chain.

The determination of the most probable shape of a macromolecule involves a reconciliation of the four conditions with the "equivalence postulate" to approach a minimum potential energy. In many instances these four conditions cannot rigorously hold, especially when substituents of large dimensions are present along the chain.

As a consequence of the minimum potential energy postulate, we may expect that while conditions *1* and *3* are always satisfied, bond angles may deform, and van der Waals interactions for some nonbonded atoms in the chain may become greater than normal. Starting from these considerations it has been possible to determine the most probable chain conformations of stereoregular polymers and to compare them with the x-ray fiber data for these polymers.

As noted before, the dimensions of the side-chain groups do not allow an isotactic polymer to be in an all *trans* planar chain conformation. Specifically, suitable accommodations of the methyl groups in isotactic polypropylene may be achieved in a threefold helical structure, imposed by the "equivalence postulate" and in accordance with the four conditions stated above.

This structure may be easily constructed from the planar one, by effecting rotations of 120° around the bonds; thus generating a left- or

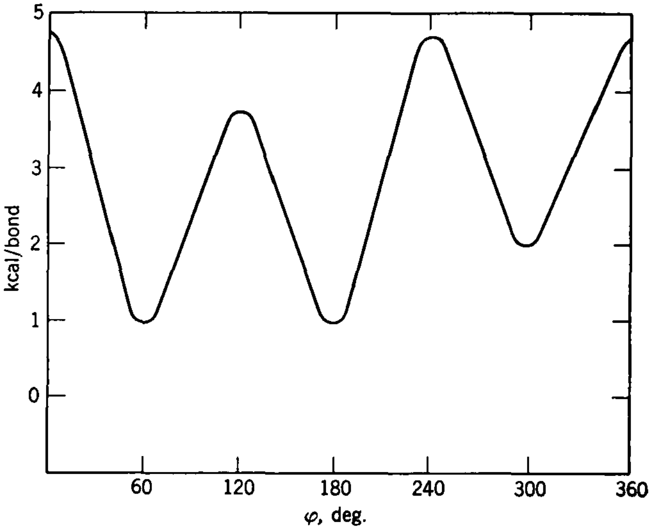

Fig. 20. Graphical representation of the real interaction potential function for vinyl polymers [taken from Natta, Corradini, and Ganis (38)].

a right-handed helix. When built up with normal bond lengths (1.54 Å) and angles (109°28′) the isotactic threefold helix should have an identity period of 6.2 Å; actually for isotactic polypropylene an identity period as large as 6.5 Å has been observed, apparently due to a slight enlargement of the C–C–C angles along the polymer chain. This alteration allows for better van der Waals contacts between the hydrogen atoms of the chain.

Liquori (40a) carried out an approximate calculation of the internal energy of an isolated polymer chain as a function of the internal rotation angles, considering all van der Waals contacts and the barriers opposing free rotation around carbon–carbon bonds. As a first approximation, Natta, Corradini, and Ganis (38) assumed the barriers to be of the same type as those postulated for low molecular weight compounds such as the pentanes.

With reference to Figure 20 we present the real energy of interaction between carbon atoms separated by three bonds. This function has been approximated by the following equation which assumes the

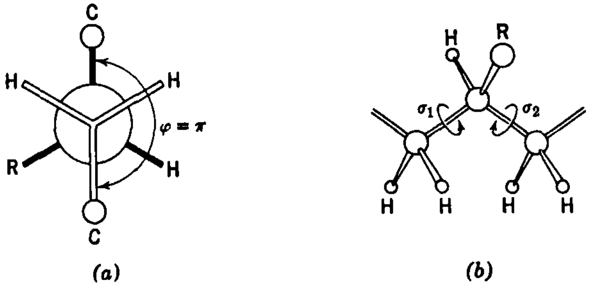

(a) (b)

Fig. 21. Convention for internal rotation angles of poly-α-olefins: (a) the dihedral angle φ, (b) the angles σ_1 and σ_2.

energy difference between a *trans* and a *gauche* conformation to be 1 kcal/bond.

$$V(\varphi) = \frac{3}{2}(1 + \cos 3\varphi) + \frac{2}{3}\left\{2 + \cos\varphi + \cos\left(\varphi + \frac{2\pi}{3}\right)\right\} \text{ (kcal/bond)}$$

where φ represents the dihedral angle shown in Figure 21*a*. A convention has been devised to label the internal rotation angles in terms of σ_1 and σ_2. The angle φ (noted above) can be either σ_1 or σ_2 (Fig. 21*b*).*

From the treatment by Mason and Kreevoy (41), Natta and Corradini (38) assumed that the energy (in kcal/monomer unit) is derived from the van der Waals contacts between carbon atoms separated by three bonds (and between the hydrogen atoms attached to them). They (38) represented the relationship as a function of the carbon–carbon distance as follows:

$$V(r) = 2.390 \times 10^4/r^{7.37} \qquad 2.7 \leq r \leq 3.2\ \text{Å}$$

$$V(r) = 2.739 \times 10^5 \exp(-3.329r) - 2.942 \times 10^3/r^6 \qquad r > 3.2\ \text{Å}$$

In the case of the chain conformation of isotactic crystalline polypropylene only two energy minima are allowed, corresponding, to a

---

*The convention for internal rotation angles:

$$\overset{\wedge}{\overline{L_1L_2}\,\overline{L_2L_3}}$$

of an L_2 bond to L_1 and L_3 is as follows: The internal rotation angle is π for a *trans* conformation, whereas it is less than π, if looking along L_2 from L_3 it is necessary to rotate L_3 by an angle less than π to make it eclipse L_1 (40b).

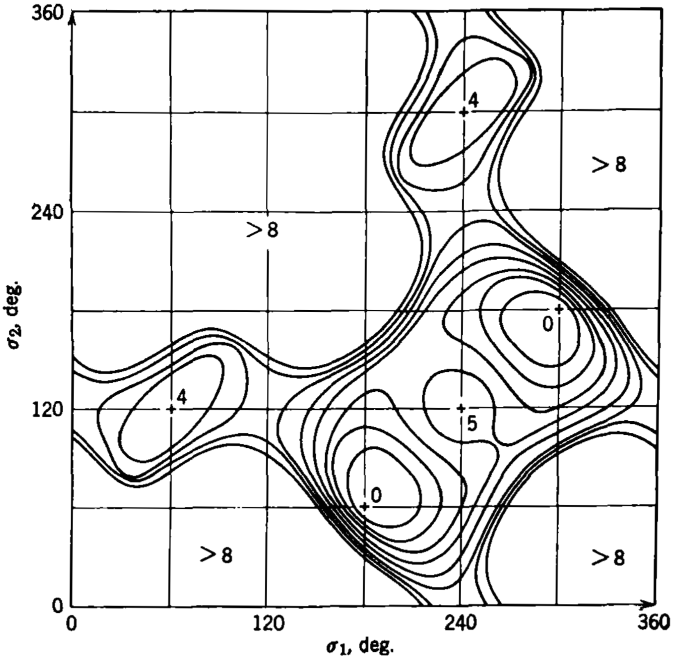

Fig. 22*a*. Internal energy (kcal/monomer unit) of an isotactic polypropylene chain for different helicoidal conformations [taken from Natta (38)].

threefold right- or left-handed helix (Fig. 22*a*), as has been experimentally found by an x-ray determination (35). In the case of syndiotactic polypropylene, three minima are observed (38) (Fig. 22*b*) corresponding to the *trans* staggered and the two forms of the twofold helix (cf. Figs. 2*b* and 18).

In a similar manner, Natta (42) determined the chain conformation for the four different stereoregular polybutadienes, as shown in Figure 23. The isotactic 1,2-polybutadiene forms a threefold helix, while the syndiotactic polymer appears to be *trans* staggered with respect to the main chain. In the cases of the 1,4-*cis* and 1,4-*trans* polymers, the configuration of the double bonds rigidly determines the spatial placement of the atoms of the main chain.

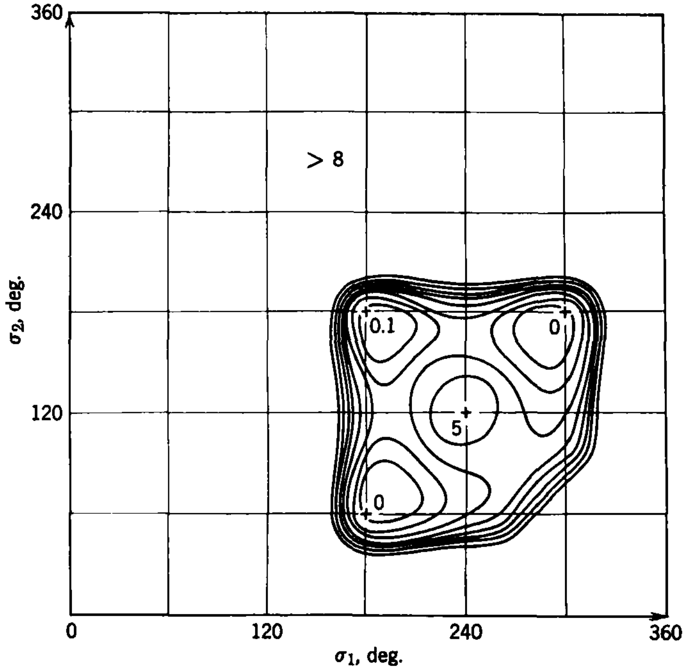

Fig. 22*b*. Internal energy (kcal/monomer unit) of a syndiotactic polypropylene chain for different conformations [taken from Natta, Corradini, and Ganis (38)].

It is a much more difficult task to analyze polymer conformations in solution. Theory tells us that the dimensions and dipole moments of isotactic, syndiotactic, and atactic polymers should differ from each other (43). In most cases studied, the dimensions for isotactic and atactic molecules were found to be identical (44–47). These measurements were carried out in non-ideal solvents where long-range effects are operative. When corrections are made for these long-range effects, the dimensions of isotactic molecules are somewhat larger than those of atactic structures (48). In all experiments to date (49,50), it has been found that the dipole moments of isotactic polymers are larger than those of atactic polymers. Experimentally, syndiotactic polymethacrylates were found to have dipole moments identical to atactic polymethacrylates (51).

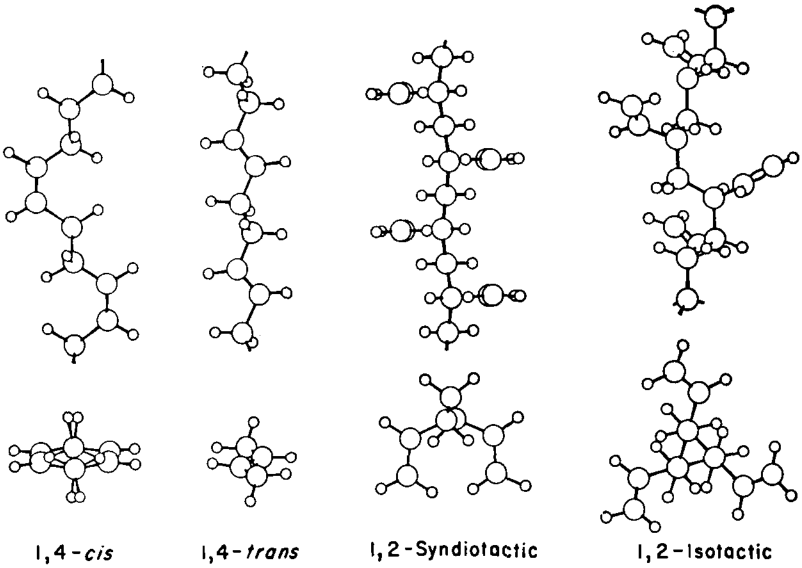

1,4-*cis* 1,4-*trans* 1,2-Syndiotactic 1,2-Isotactic

Fig. 23. Chain conformations in the crystals of the four different stereoisomers of polybutadiene [taken from Natta (42)].

Several models for structural deformations of polymers in solution have been applied to explain the experimental results. The "torsional oscillation" model restricts polymer motions to torsional types about a single equilibrium structure (3_1-helix for isotactic and *trans* staggered for syndiotactic). The experimental values for the root mean square dimensions of typical polymers are between 1.8 and 2.5 times larger than the root mean square dimensions of chains with free rotation. It is possible to calculate the mean dimensions of the polymer as a function of the oscillation of the bonds.

Using this model, oscillations of approximately 60° are necessary to explain the experimental evidence. Similar improbable torsional oscillations are required to obtain the experimentally determined dipole moments. In addition, the oscillations which lead to the correct dipole moments do not give correct dimensions. Thus, the torsional oscillation model does not explain the experimentally observed facts.

A second model is based upon "rotational isomerism." For isotactic polymers the dimensions and dipole moments are dependent upon a parameter p of chain flexibility which is related to the energy ΔE necessary to break the helical structure by:

$$p = \exp(-\Delta E/RT)$$

If we assume that isotactic polypropylene has an identity period of 6.5 Å, the value for $p = 0.35$ gives the correct experimental dimensions and dipole moments. From this we find $\Delta E = 0.6$ kcal/mole. Birshtein (52) carried out a statistical calculation combining rotational isomerism with torsional oscillations. In her calculation she allowed 30° oscillations from the staggered forms of a 3_1-helix and obtained $p = 0.1$–0.2 for the parameter. This leads to a value $\Delta E = 1.0$ kcal/mole, which is close to the value calculated from experimental data. The average number of successive monomer units in helical regions is given by:

$$\nu = (1 + p)/p$$

As p approaches zero, the helical sequence becomes infinite. Thus for $p = 0.35$ the helical segments have average lengths between 3 and 4 units while with $p = 0.1$–0.2 the average length of the helical sequences increases to 6–10 monomer residues.

Allegra, Ganis, and Corradini (53) modified the Birshtein approach. They did not allow oscillations in all bonds but rather assumed a higher steric hindrance for a unit at a junction of helical and random structure. In this manner these authors were able to obtain better agreement with experimental data. All three factors, rotational isomerism, torsional oscillation, and higher steric interactions at junctions, most probably play a significant role in the conformation of a polymer in solution.

A similar treatment can be applied to syndiotactic polymers. It was found that syndiotactic polymers exist in solution in a planar form containing between three and seven monomeric units separated by units in the *gauche* form. Specifically, syndiotactic poly-1,2-butadiene is composed of *trans* staggered sequences containing an average of seven monomeric residues separated by one monomeric unit with a *gauche* structure (54). The chains of syndiotactic polypropylene consist of right- and left-handed twofold helical segments with an average content of about four monomeric units. The junctions between the right- and left-handed helical sequences are, of course, composed of *trans* staggered units (55).

Flory and his co-workers (56,57) have concentrated on determining the temperature coefficient of the change in dimensions of isotactic polymers in solution. They find that they are unable to reconcile the experimental results with theory unless they allow for up to 8% syndiotactic placements in an otherwise isotactic structure (57b). Tacticity imperfections of this magnitude would probably be discernible by high resolution nuclear magnetic spectroscopy.

III. NUCLEAR MAGNETIC RESONANCE

We must now consider the use of high-resolution nuclear magnetic resonance spectroscopy (NMR) and optical activity to measure solution properties of polymers. In the study of microtacticity* NMR has proven to be an invaluable tool.

Bovey and Tiers (58) were among the first to apply NMR to the analysis of polymer structure. They defined a parameter P_m as the probability that addition of a monomer unit to a growing polymer chain would occur so as to produce an isotactic placement of the ultimate unit of the chain (59,60) (the "Bernoulli trial," see below). The

---

* Microtacticity refers to the local sequential spatial arrangements of the pseudoasymmetric centers of a polymeric chain. On this basis "atactic" has no meaning since each placement must be either isotactic or syndiotactic with respect to the previous pseudoasymmetric center. Therefore the following formulas represent the three possible microtacticities of the central unit of the triads (59):

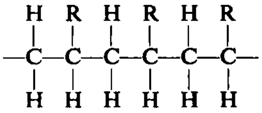

$$-\underset{H}{\overset{H}{C}}-\underset{H}{\overset{R}{C}}-\underset{H}{\overset{H}{C}}-\underset{H}{\overset{R}{C}}-\underset{H}{\overset{H}{C}}-\underset{H}{\overset{R}{C}}-$$

Isotactic triad (i)

(a)

Macrotacticity refers to overall polymer properties (e.g., if a crystalline polymer is mostly isotactic, it can be considered on a macro scale to be all isotactic).

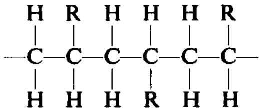

$$-\underset{H}{\overset{H}{C}}-\underset{H}{\overset{R}{C}}-\underset{H}{\overset{H}{C}}-\underset{R}{\overset{H}{C}}-\underset{H}{\overset{H}{C}}-\underset{H}{\overset{R}{C}}-$$

Syndiotactic triad (*s*)

(b)

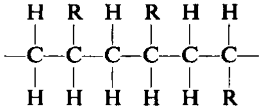

$$-\underset{H}{\overset{H}{C}}-\underset{H}{\overset{R}{C}}-\underset{H}{\overset{H}{C}}-\underset{H}{\overset{R}{C}}-\underset{H}{\overset{H}{C}}-\underset{R}{\overset{H}{C}}-$$

Heterotactic triad (*h*)

(c)

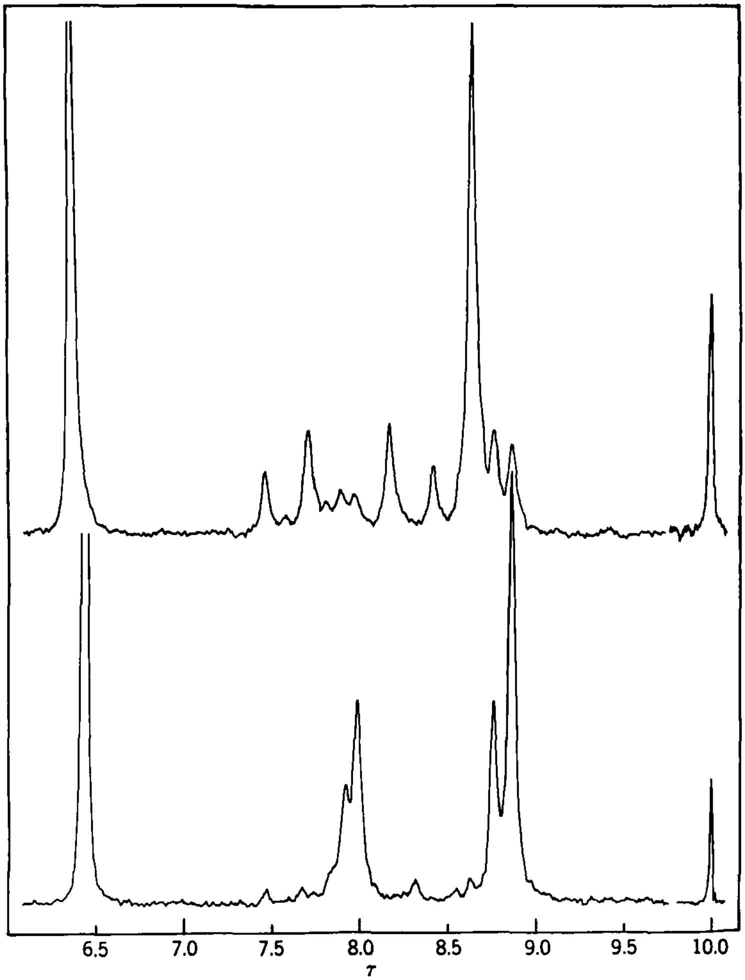

Fig. 24. Nuclear magnetic resonance spectra of poly(methyl methacrylate). Isotactic (top); syndiotactic (bottom) [kindly supplied by F. A. Bovey].

propagation can be described by a single value of P_m.* The dependence of triad frequencies becomes:

$$P_i = P_m^2$$
$$P_s = (1 - P_m)^2$$
$$P_h = 1 - P_i - P_s = 2(P_m - P_m^2)$$

---

*P_m has previously been designated by the terms σ or α.

where P_i, P_s, and P_h represent the probabilities for forming the isotactic, syndiotactic, and heterotactic triads, respectively.

The above relationships were applied to poly(methyl methacrylate) polymerized by free-radical and anionic initiators, some of which give stereoregular polymers (60). Bovey and Tiers applied NMR in these studies since the magnetic environments of the central units of each of the triads should differ. This was readily confirmed, as can be seen in Figure 24. They found that it was necessary to measure polymer NMR spectra at high temperatures ($> 100°$) in order to eliminate the dipolar broadening effect. The predominantly isotactic structure (Fig. 24 top) gives a larger peak at 8.67 τ with two minor peaks at 8.79 and 8.90 τ for residual hetero and syndiotactic placements respectively. The predominantly syndiotactic structure (Fig. 24, bottom) exhibits two peaks, coinciding with the minor bands in the isotactic polymer spectrum. They are attributable to syndiotactic (high-field) and heterotactic (low-field) sequences.

In addition to the triads of pseudoasymmetric centers, Bovey found that the methylene groups* between them are extremely sensitive to tacticity. It is readily apparent that these effects can be seen by examining the methylene region of the NMR spectra contained in Figure 24. For the predominantly syndiotactic polymer (Fig. 24, bottom), the hydrogens of the methylenes are essentially equivalent,

---

*The methylene group between two pseudoasymmetric units can be regarded as racemic or *meso* depending on whether the pseudoasymmetric units are syndiotactic or isotactic with respect to each other.

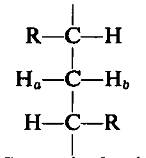

$$\begin{array}{c} | \\ R-C-H \\ | \\ H_a-C-H_b \\ | \\ H-C-R \\ | \end{array}$$

Racemic dyad

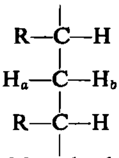

$$\begin{array}{c} | \\ R-C-H \\ | \\ H_a-C-H_b \\ | \\ R-C-H \\ | \end{array}$$

Meso dyad

In these schematics we represent the chains as planar projections though we recognize that this form for the isotactic main chain is impossible. In this treatment we consider only dyads of monomeric units. For a purely syndiotactic structure, H_a and H_b are equivalent and a single peak should be seen for the methylene. Bovey has shown that all conformations for syndiotactic dyads lead to equivalence for H_a and H_b (cf. later discussion on conformational analysis of polymer structure by NMR). For a purely isotactic structure, H_a and H_b are non-equivalent regardless of the conformation selected for the dyad.

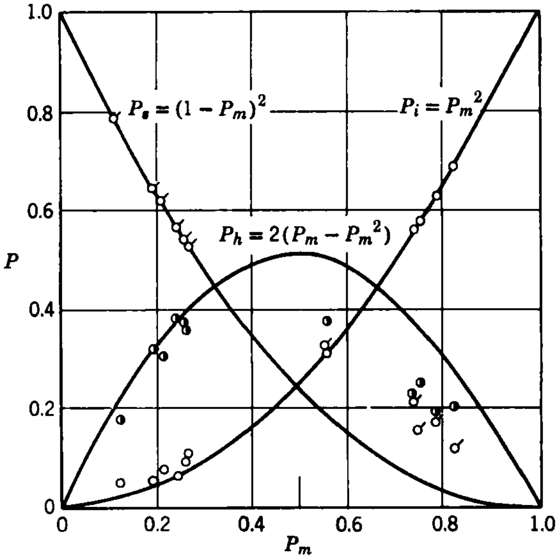

Fig. 25*a*. The probabilities P_i, P_s, and P_h of formation of isotactic, syndiotactic, and heterotactic triads, respectively, as a function of P_m. Experimental points at the left are for methyl methacrylate polymers prepared with free-radical initiators; those at the right for polymers prepared with anionic initiators: (○) *i* peaks; (♂) *s* peaks; and (◑) *h* peaks [taken from Bovey (60)].

showing a large singlet at 7.9 τ and complex smaller bands from the heterotactic placements. In the predominantly isotactic polymer (Fig. 24, top), the hydrogens of the methylenes are non-equivalent, showing the expected AB splitting between 7.3 τ and 8.4 τ ($J = 14.9$).

A plot of the dependence of the probability P on the value of P_m is presented in Figure 25*a*. In this work Bovey showed that in the free radical produced polymers the triad frequencies obey the relationships given above. Therefore a single value of P_m may be chosen to describe the tacticities of each polymer.* For the anionically produced polymers the agreement is poor, particularly in those cases where complexing solvents are used. Deviations from this model can occur if the monomer placement is influenced by the stereochemistry of the chain already formed.

---

* The proportion of heterotactic units is a maximum at $P_m = 0.5$. For a random polymer $i:h:s$ will be 1 : 2 : 1.

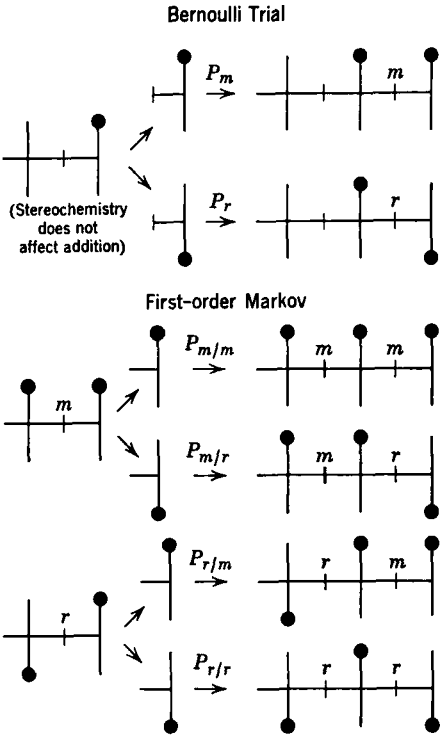

Fig. 25*b*. Statistical models for chain propagation [adapted from Bovey (61)].

Several models have been proposed to extend the simple one-parameter model to take these deviations into account (61,62a–62c). Experimental evidence (61,62d,62e) has shown the utility of applying statistical models to gain an understanding of stereospecific polymerization. The statistical approaches most commonly considered (61) involve the Bernoulli trial and the first-order Markov chain. Figure 25*b* shows the building up of a chain by both models, (where *m* represents a *meso* and *r* a racemic placement with respect to the methylene groups as defined above). In the Bernoulli trial the stereochemistry of the chain end does not affect the incoming monomer unit which therefore can add in two ways with respect to the ultimate unit of the chain as shown. P_m and P_r represent the probabilities of forming a *meso* unit and a racemic unit, respectively. This model describes most free-radical polymerizations.

The first order Markov statistics are generated when the addition of monomer is influenced by the stereochemistry of the growing chain end. The ultimate and penultimate units may be *meso* or racemic with respect to each other. This requires four probabilities to characterize the addition process. (In the diagram the designation $P_{r/m}$ denotes the probability of the monomer adding in *m*-fashion to an *r* chain end.) The four probabilities are actually interrelated, so that there are really only two independent parameters ($P_{r/m}$ and $P_{m/r}$).*

Bovey (61) applied the above models to aid in the elucidation of the mechanism of the 9-fluorenyllithium polymerization of methacrylates in toluene (and also in the presence of small amounts of THF). A partial interpretation of the NMR spectra for these anionically produced polymers indicates that the polymerizations are consistent with first-order Markov statistics.

Many vinyl polymers (9,63) have had their NMR spectra determined and at least partially interpreted. For example, the spectra of polypropylene polymers are quite complex because of complications from spin–spin coupling and the small chemical shift differences between the protons. However, tacticity studies on such polymers are simplified, and the spectra are interpretable if partially deuterated polymers are used. Stehling (64) used this technique to study the tacticities of polypropylene. The spectrum of polypropylene, Figure 26*a*, is extremely complicated. Thus, the spectrum of isotactic polypropylene-2-d_1 may be considered as a superposition of the methylene quartet and a single α-methyl resonance (Fig. 26*b*). On the other hand, the spectrum of the isotactic polypropylene-2,3,3,3-d_4 (Fig. 26*c*) shows a pure AB quartet for the protons on the methylene, which is consistent with the isotactic structure for the dyad.

As instrumentation improves, it becomes possible to examine longer sequences of monomeric units, such as pentads for the study of α substituents and tetrads for the study of the methylene groups. Such considerations have already been applied by Yoshino (65) in his interpretation of the poly(vinyl chloride) NMR spectrum using a 100 Mc/sec instrument.

The use of NMR has been extended to the problem of polymer conformations in solution. Bovey (9), for example, employed model

---

*To test the first order Markov statistics one must have information about tetrad structure. This is the fine structure of the *meso* and racemic dyad sequences.

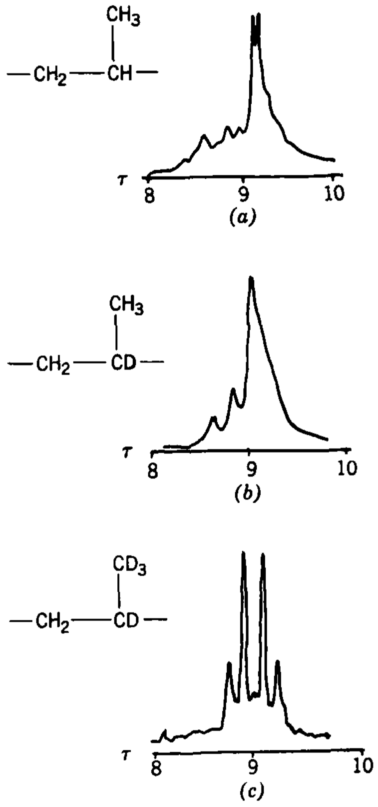

Fig. 26. Proton magnetic spectra for undeuterated and partially deuterated isotactic fractions of polypropylene. (*a*) polypropylene in *p*-dichlorobenzene at 175°; (*b*) polypropylene-2-d_1 in 2-chlorothiophene at 110°; (*c*) polypropylene-2,3,3,3-d_4 in 2-chlorothiophene at 110° [Stehling (64)].

compounds such as *meso* and racemic 2,4-disubstituted pentanes and examined their vicinal and geminal proton couplings (i.e., coupling between methylene and methinyl protons themselves).

There are nine staggered conformers for the *meso*-2,4-disubstituted pentanes (Fig. 27). In conformers **1**,**2**, and **3**, it is obvious that H_a and H_b are non-equivalent. Conformers **4a**,**5a**, and **6a** are mirror images of conformers **4b**,**5b**, and **6b**, respectively. The members of each pair are interconvertible by suitable 120° rotations. In the course of these

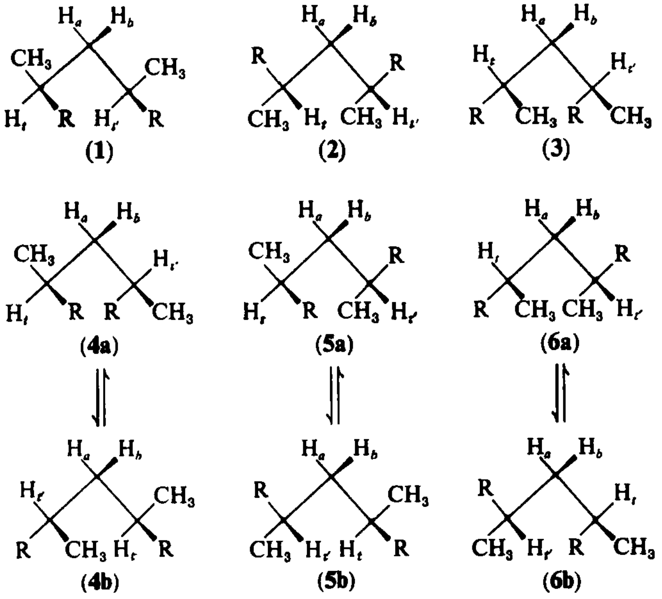

Fig. 27. Conformers for *meso* 2,4-disubstituted pentanes [adapted from Bovey (9)].

interconversions H_a and H_b are not exchanged while the terminal protons H_t and $H_{t'}$ (which represent the methinyl protons on either side of the methylene group, Figs. 27 and 28) are interchanged. Therefore, *meso* disubstituted pentanes are geminally heterosteric* regardless of conformation.

The racemic pentanes also exhibit nine staggered conformations (Fig. 28). In conformers **1**,**2**, and **3**, H_a and H_b are obviously equivalent. Conformers **4**,**5**, and **6** are not converted to mirror images on proper 120° rotations of the carbon–carbon bonds but rather into identical structures (conformers **4′**,**5′**, and **6′**) with H_a and H_b and the terminal

---

*The term "homosteric" refers to methylene groups where the two protons are magnetically equivalent while the term "heterosteric" refers to methylene groups where the two protons are magnetically non-equivalent. The hydrogens on a homosteric methylene have been designated as either equivalent or enantiotopic, while the hydrogens on heterosteric methylenes have been called diastereotopic (65a).

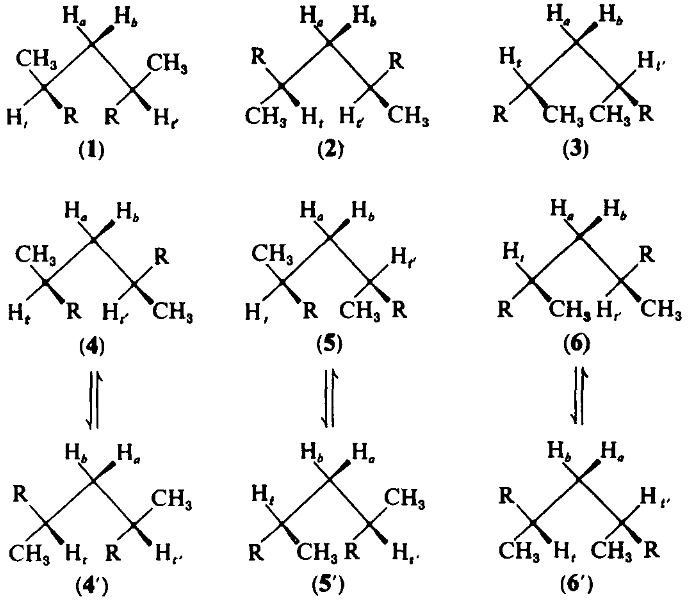

Fig. 28. Conformers for racemic 2,4-disubstituted pentanes [adapted from Bovey (9)].

protons H_t and $H_{t'}$ interchanged. Therefore, racemic disubstituted pentanes are geminally homosteric either by symmetry or by interchange of the environment of the two protons.

Bovey and his colleagues applied these considerations to 2,4-diphenylpentanes (R = phenyl in Figs. 27 and 28) as models of polystyrene conformation. From analysis of the *meso*-diphenylpentane spectra, they concluded that conformer **5a** and its mirror image **5b** are strongly preferred. In these structures the phenyl groups have the same relationship as they have in the 3_1-helical conformation for isotactic polystyrene (66a) (i.e., *trans–gauche*).

Analysis of the racemic diphenylpentane spectra led these authors to conclude that conformer **1** (Fig. 28) (*trans–trans* for the polymer) is probably preferred but that conformer **2** (Fig. 28) (*trans,trans–gauche, gauche* for the polymer) probably contributes substantially to the pentane conformation, and by extrapolation, to the conformation of syndiotactic polystyrene in solution.

IV. SOLUTION STUDIES ON OPTICALLY ACTIVE POLYMERS

We will now turn our attention to the use of optical activity to investigate the conformations of stereoregular polymers in solution.† In most cases, asymmetric and dissymmetric designations have been used interchangeably by polymer stereochemists. The terms, however, have special meanings with regard to characterization of polymer structure by optical activity and nuclear magnetic resonance. Farina (66b), in a review on optically active polymers, has correctly indicated that symmetry properties of polymers are better indicated by line symmetry rather than by point symmetry. The term "asymmetric" refers to polymeric structures that have no symmetry elements, that is, not even rotation or translation. The term "dissymmetric" denotes structures having no mirror symmetry elements although the molecules contain certain rotation and/or translation axes. Stereoregular vinyl and related polymers without asymmetric side chains can exist either as *meso* structures, which are of course nondissymmetric, or they can exist as dissymmetric racemates. In any case one would not expect these polymers to exhibit optical activity. Polymers from the following optically active monomers have been used to study stereochemical effects in solution:

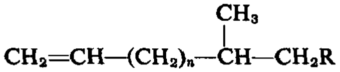

$CH_2{=}CH{-}(CH_2)_n{-}\overset{\overset{CH_3}{|}}{C}H{-}CH_2R$

(*A*)

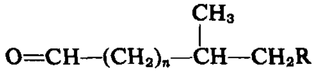

$O{=}CH{-}(CH_2)_n{-}\overset{\overset{CH_3}{|}}{C}H{-}CH_2R$

(*B*)

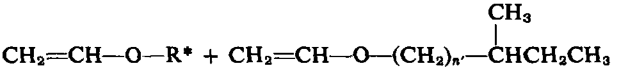

$CH_2{=}CH{-}O{-}R^* + CH_2{=}CH{-}O{-}(CH_2)_{n'}{-}\overset{\overset{CH_3}{|}}{C}HCH_2CH_3$

R*=menthyl or (*S*)α-methylbenzyl.

(*C*)

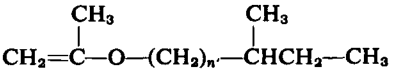

$CH_2{=}\overset{\overset{CH_3}{|}}{C}{-}O{-}(CH_2)_{n'}{-}\overset{\overset{CH_3}{|}}{C}HCH_2{-}CH_3$

(*D*)

Certainly the most definitive work in group *A* has been carried out by Pino (16) and co-workers who employed Ziegler catalysts to obtain isotactic polymers of (*S*)-3-methyl-1-pentene, (*S*)-4-methyl-1-hexene, (*S*)-5-methyl-1-heptene, (*R*)-3,7-dimethyl-1-octene, and (*S*)-6-methyl-

---

† Pino (16) has published an excellent review on this subject. I commend this article to the reader for its comprehensiveness and interpretations.

1-octene. The rotations of the polymers (where $n = 0,1,2$) are much greater than those of low molecular weight model compounds. The enhancement becomes very low for poly[(*S*)-6-methyl-1-octene] (i.e., where $n = 3$).

Further work in this field has been carried out in our laboratory (67–69). We obtained results similar to Pino's for poly[(*R*)(−)-3,7-dimethyl-1-octene] and aldehydes of group *B* containing optically active centers: (*R*)(+)-citronellal, (*R*)(+)-6-methoxy-4-methylhexanal, and (*S*)(+)-2-methylbutanal. As in Pino's cases, the magnitude of the optical activity enhancement depends upon the distance of the asymmetric center from the main chain.

Monomers of group *C* were polymerized by Schuerch (23) who prepared copolymers of vinyl (*S*)-α-methylbenzyl ether with maleic anhydride (noted earlier): by Liquori (70) who worked with vinyl menthyl ether; and by Pino (71,72) who worked with vinyl (*S*)-(2-methyl)-butyl ether and also vinyl (*S*)-2-butyl ether. The optical rotatory properties of these polymers are similar to those encountered with optically active poly-α-olefins and polyaldehydes. The differences between the optical activity of the polymers and their low molecular weight analogs depend on the position of the asymmetric center in the side chains and also on the isotacticity of the polymer. While a great enhancement was observed by Pino for isotactic poly[(*S*)-2-butyl vinyl ether] ($n' = 0$), no significant enhancement of optical activity was noted for isotactic poly[(*S*)-2-methyl-butyl vinyl ether] ($n' = 1$). This latter polymer does exhibit a sizable increase in rotation when complexed in solution with strong Lewis acids (73).

We have carried out work with two polymers from group *D* ($n' = 0$ and 1) (74). These poly(α-methylvinyl alkyl ethers) appear to be highly syndiotactic and exhibit no appreciable optical activity enhancement with or without complexation by Lewis acids.

It is possible to make some generalizations about these optically active polymers. Isotacticity and the location of the asymmetric center in the side chain play important roles in the magnitude of the optical activity enhancement of polymers over low molecular weight analogs. When the optical activity is sufficiently far from the main chain (e.g., groups *A* and *B*, $n = 3$; group *C*, $n' = 1$) there is no enhancement of the rotation, regardless of the stereoregular structure of the main chain. When an enhancement is present, the change of rotation with increasing temperature is much larger than the change encountered for the corresponding model compound. The enhancement of optical activity for poly(2-methylbutyl vinyl ether) on complexation with Lewis acids has been attributed primarily to the increased rigidity and bulkiness of the asymmetric side chains (73). Lastly, it is important to realize that these polymers behave in solution as flexible coils. Therefore, long-range helical order does not appear to be involved.

These generalities can be explained on the basis that the asymmetric side chains induce a preference for one *gauche* placement over the other (left vs. right) for the isotactic main chain. If we assume an asymmetric group of the (*S*) configuration is attached to the main chain, there is an

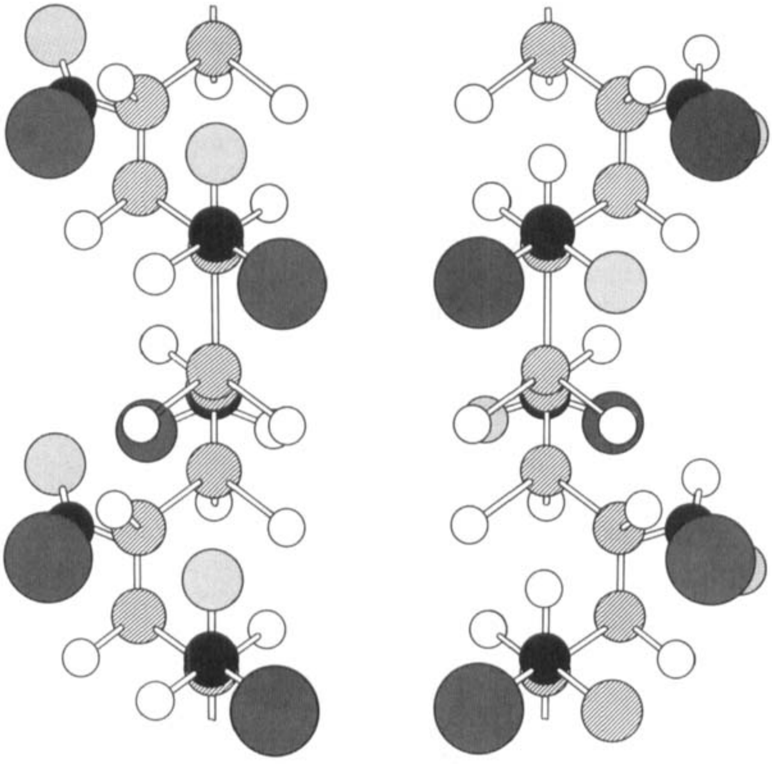

(*a*) (*b*)

Fig. 29. Schematic representation of isotactic left and right 3_1-helices for optically active poly[(*S*)-3-methyl-1-pentene]: (*a*) left-handed; (*b*) right-handed (13).

appreciable steric interaction difference between the left- and right-handed main chain helices (Fig. 29). In Figure 29, the asymmetric side chains are placed in both helical forms so that the largest group is furthest from interaction with main-chain carbon atoms. With this reasonable conformation of the side chain and a right-handed helix, we find that the largest and medium groups are placed so that a carbon of the backbone is staggered between them (Fig. 29). For the left-handed helix and the equivalent conformation of the side chain, we find that a hydrogen from the main chain is staggered between the largest and medium-sized components of the asymmetric center (Fig. 29).

Thus it appears that the (*S*) configuration in the side chain prefers the left-handed helix. If this idealized and oversimplified picture were to hold for the entire isotactic structure, a helix of a single sense would result with a substantial optical activity enhancement. (Recall that these polymers appear to be flexible coils in solution.) It is sufficient, of course, to have even a small preference for one sense over the other in order to observe rotational contributions from the conformation of the main chain (i.e., helical segments of one handedness will predominate). The equilibrium among the various conformations of the main chain depends on temperature. Since the excess of helical segments of one sense over the other will be destroyed as the temperature is raised, a larger temperature coefficient of rotation is observed.

Using the Brewster (75) conformational analysis approach, Pino (76) calculated the conformational structure for poly-α-olefins such as poly[(*S*)-3-methyl-1-pentene] and poly[(*S*)-4-methyl-1-hexene]. Only three conformations are possible for these polymers, two left-handed and one right-handed helices. Pino believes the helical excess to be of the left-handed sense since the experimental optical rotations agree well with the left-handed helical structures. In fact he stated a generalization, based on this approach, that an (*S*) group in the side chain prefers a left-handed helix while an (*R*) group induces a right-handed helical preference. We arrived at a similar deduction based on the analysis of models of these polymers (Fig. 29 and related text).

A stereoselective effect of the asymmetric side chains was demonstrated by Pino and Natta (77). They were able to partially resolve racemic poly(4-methyl-1-hexene) chromatographically using a column prepared from poly[(*S*)-3-methyl-1-pentene]. This shows that a given chain was composed primarily of a single antipode. The driving force for such a structural selectivity must come from the influence of the side chain in choosing the proper enantiomer to add to the growing chain.

Pino (78,79) extended this work to the polymerization of racemic monomers such as (*RS*)-3-methyl-1-pentene, (*RS*)-4-methyl-1-hexene, and (*RS*)-3,7-dimethyl-1-octene with optically active Ziegler-Natta catalysts. Optically active polymers and monomers were obtained for the first and third monomers since the potential asymmetric centers are adjacent to the polymer chain. The second monomer, on the other hand, showed no asymmetric synthetic effect. These results are consistent with the requirements of the explanation used above for the optical activity enhancement. The requirements are much more rigorous for asymmetric synthesis than for an optical activity enhancement. Consequently only in those homopolymer vinyl systems where the asymmetric side chain is attached directly to the isotactic main chain will an effect be observed.

V. MECHANISMS OF STEREOREGULAR POLYMERIZATIONS

To this point, our attention has been focused on the stereochemical aspects of polymer structure. We will now examine the mechanistic factors which contribute to stereoregulation during polymerization.*

A decade ago it was assumed that only heterogeneous catalysts could lead to stereoregular polymerization. Today we know that regardless of whether the polymerization occurs heterogeneously or homogeneously via free-radical, cationic, anionic, or coordination mechanisms, stereoregulation can be obtained under certain well-defined conditions. Thus, independent of the mechanism of polymerization, the principle of stereoregulation involves control of each monomer addition to the end of the growing chain. The entering monomeric unit must be oriented and directed before it is chemically bonded to the growing chain. The catalyst must be able to interact with both monomer and growing chain. The growing chain must have a structure such that the adding monomer prefers to enter the polymer chain by one specific

---

*Two review articles have appeared on this subject, by Bawn and Ledwith (80), and Goodman, Brandrup, and Mark (81). It is with special thanks that I acknowledge the help of Dr. Bawn and Dr. Ledwith. Much of the mechanistic presentation is based on their outstanding review article.

approach over all others. We can, therefore, divide the forces of stereoregulation into the effect of orientation and/or complexation of the entering monomer; the nature of the double bond-opening process (*cis* vs. *trans*); and also the stereoelectronic interactions among monomer, catalyst, and growing chain during initiation and propagation.

A. Ziegler-Natta Polymerization (82,83)*

Coordination-catalyzed polymerization was announced in 1955 by Ziegler (1), who reported the low pressure polymerization of ethylene. This was accomplished using his new catalyst formed by mixing solutions of triethylaluminum and titanium tetrachloride. Natta and his co-workers (84–89) demonstrated that modified Ziegler-type catalysts could polymerize α-olefins such as propylene, styrene, and 1-butene to highly crystalline linear products. These polymers exhibit low solubilities, high densities, and high melting points as compared with corresponding amorphous analogs. Previously, crystalline synthetic polymers were rarely encountered. These types of structures were limited to polyethylene and polymers derived from symmetrical vinylidene monomers.

Natta showed that the crystallinity of poly-α-olefins prepared with the new coordination catalysts is a direct consequence of the stereoregular structure of the polymer. As noted in Section II, two stereoregular structures were possible for a head-to-tail vinyl polymer (namely, isotactic and syndiotactic).

1. *Structure of Ziegler-Natta Catalysts*

A Ziegler-Natta catalyst is defined as an active initiator prepared by combining a transition metal halide (e.g., titanium chlorides) with a reducing agent (e.g., aluminum alkyls) in an inert atmosphere. In addition, there are numerous examples of modified Ziegler-Natta catalysts where vanadium halides are substituted for titanium halides; or where titanium alkyl halides and/or aluminum alkyl halides are used;

---

*Two review articles have appeared in *Macromolecular Reviews* on the mechanisms of Ziegler polymerization, by H. W. Coover (82) and by John Boor, Jr. (83). I wish to thank these authors for allowing me to quote from their manuscripts prior to publication. Specifically, Dr. Boor presents a complete and critical discussion of heterogeneous catalysis, mechanism and structure using Ziegler-Natta systems.

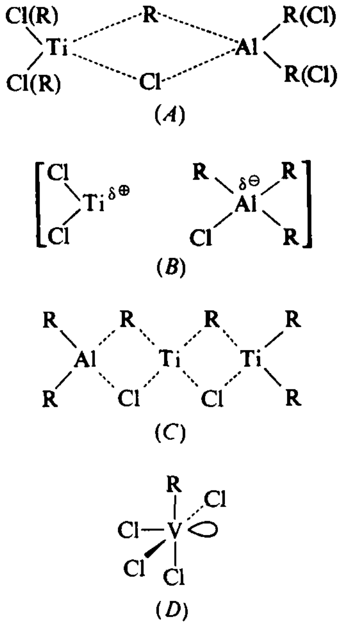

Fig. 30. Suggested structures for active Ziegler-Natta catalysts.

or where hydride reducing agents are employed; or where complexing agents such as acetylacetonates are added (82,83). To cover all these variations and possibilities represents a task far beyond the scope of this work. Numerous references can be found to catalysts and mechanisms of stereoregular polymerization in other articles (90–95). It will suffice for us to examine the standard Ziegler-Natta systems (using $TiCl_3$ or VCl_4 with AlR_3) and deduce general mechanistic considerations from them.

Many structures have been suggested for active Ziegler-Natta catalysts. Several proposals are noted in Figure 30. With the exception of structures *B* and *D* in this figure, bridged bonds are involved to describe the facile bond making and breaking in the region of complexation with monomer. Structure *B* relies on ionic and polarization effects to achieve activity while structure *D* uses a vacant orbital in the proximity of an organometallic bond.

The preorientation of the monomeric unit can be achieved in a number of different ways. It has been found that α-olefins can be

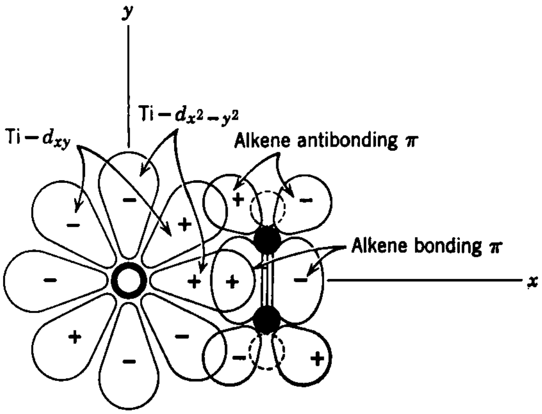

Fig. 31. The π-bond between titanium and an alkene. (○) titanium; (●) carbon; (○) hydrogen [adapted from Bawn and Ledwith (80)].

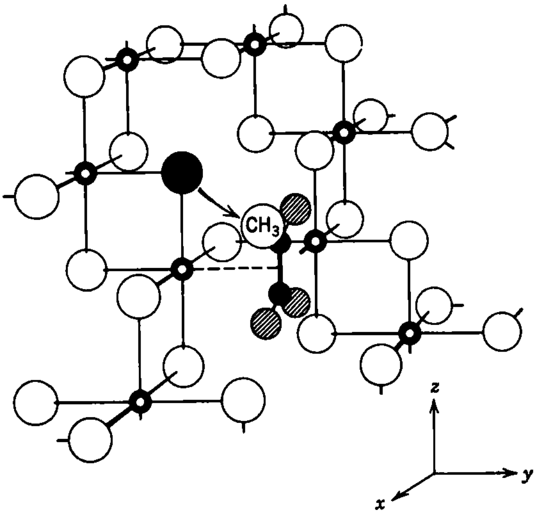

Fig. 32. Schematic model of the titanium trichloride lattice, showing an "active center" with a monomer propylene molecule in the orbital vacancy. (No crystal dimensions are intended.) Small circles, titanium; large open circle, chlorine; large filled-in circles, alkyl; shaded circles, hydrogens on monomer [adapted from Bawn and Ledwith (80)].

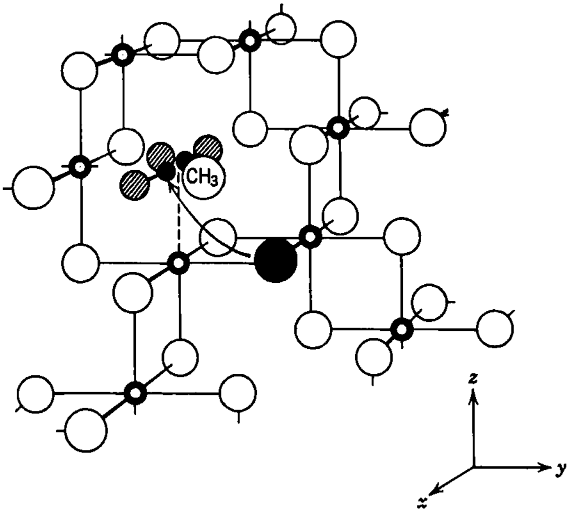

Fig. 33. The situation after migration of the alkyl group according to the reaction path indicated by the arrow in Figure 32. The next propylene monomer is placed in the new vacancy. Propagation according to this stereoselective route leads to syndiotactic polypropylene (cf. Fig. 38 and related text). The reaction path of the second alkyl group is indicated by the arrow. (No crystal dimensions are intended.) Small circles, titanium; large open circles, chlorine; large filled-in circles, alkyl; shaded circles, hydrogens on monomer [adapted from Bawn and Ledwith (80)].

adsorbed on the surface of nickel metal or titanium salts forming a complex between the π electrons of the double bond and the vacant *d* orbitals of the metal by opening the double bond (Fig. 31) (80). The adsorption and complexing of the monomer in this manner can be used to explain syndiotactic polymerization (Figs. 32 and 33). Specifically, the π electrons of the monomer must overlap with a vacant *d* orbital of the titanium at the same time that another *d* orbital from the metal overlaps with the antibonding orbitals of the monomer. This leads, as explained by Cossee (96), Bawn and Ledwith (80) and Boor (83), to a lowering of the energy gap between the highest filled and the empty *d* orbitals of the metal. The π complex between monomer and transition metal halide should destabilize the metal–carbon bond sufficiently for insertion of the monomer between existing organometallic bonds. If the energy of a metal 3*d* orbital lies between the energies of the bonding and antibonding orbitals of the monomer, an active catalyst is generated.

This molecular orbital examination of the interaction between monomer and active site (Fig. 31) explains why the environment of an active site in a heterogeneous crystalline lattice requires extremely rigid spatial approaches for the monomer (Figs. 32 and 33). Bawn and Ledwith, using Cossee's mechanistic considerations, schematically described how a propylene monomer fits into a titanium chloride lattice. It is readily seen that the direction of the methyl group in the monomer is quite important to the energy of π complexation. Arlman and Cossee (97) have recently modified these views. They now believe that the isotactic polypropylene chain grows on the edge of a crystal plate.

2. *Polymerization Mechanisms*

Several variations of a bimetallic mechanism have been suggested. In 1960 Natta (42) proposed that the bridged bond structure of the catalyst (cf. Fig. 30) can be applied mechanistically. Although Natta did not specifically say so, we can regard the monomer as coordinated in a manner similar to the Cossee structure (described above). According to Natta, the olefin is simply inserted between the existing titanium–carbon bond through the polarization mechanism in Figure 34. The bridged bond opens, producing an electron-deficient metal which attracts the π electrons from the monomer into a σ-type bond. At the

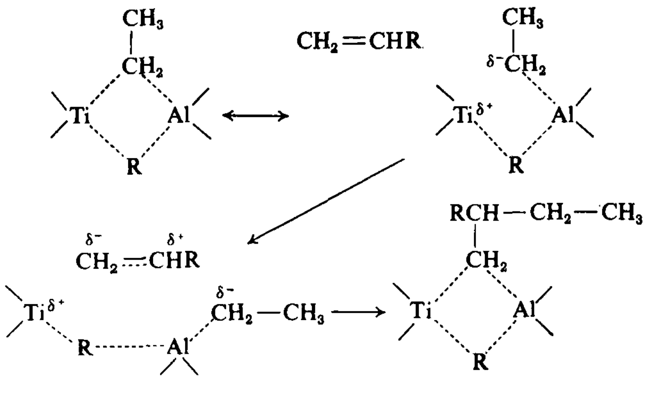

Fig. 34. Bimetallic mechanism proposed by Natta (42).

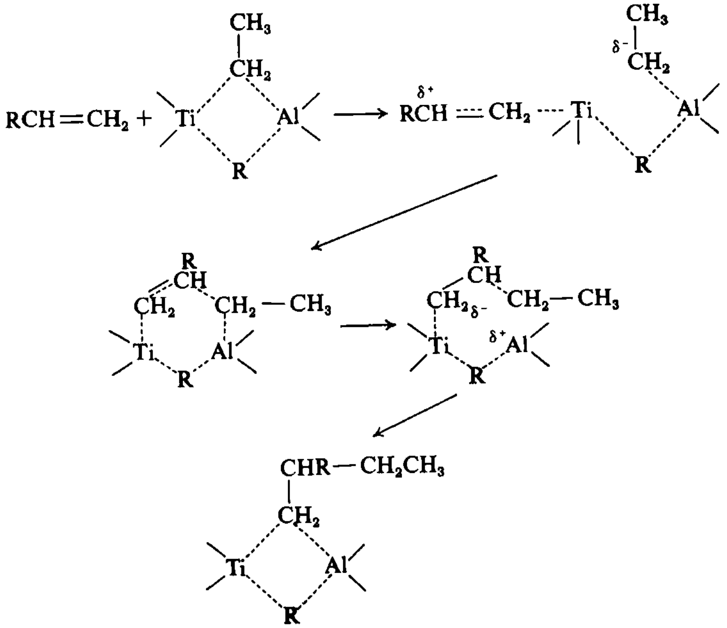

Fig. 35. Bimetallic mechanism proposed by Patat and Sinn (98).

same time, the carbanion produced attacks the electron-deficient center in the monomer. When this occurs, a new bridged bond structure is generated which includes the formerly complexed monomer. Earlier, a related mechanism was proposed by Patat and Sinn (98). In their approach the olefin becomes partially bonded between the titanium and the methylene of the ultimate group of the polymer chain (Fig. 35), which in turn is partially bonded to aluminum. When the bond between the olefin and this methylene forms, the titanium carbon bridged bond is reestablished to the terminal carbon, including the monomer as described in Figure 35.

These bimetallic mechanisms are attractive in that they provide for an active site which can complex an approaching monomer and maintain the terminal group of the polymer chain in a position suitable for reaction. Naturally the bimetallic structure need not be made up of titanium and aluminum. It is possible to devise a mechanism similar to those proposed by Natta (42) and Patat (98) by utilizing two titanium atoms in the active site (cf. Fig. 30*C*).

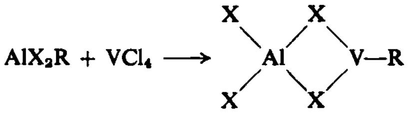

Fig. 36. Carrick mechanism for Ziegler-Natta polymerization of α-olefins (99). X = halogen, alkyl, or aryl and R = alkyl or aryl (valence of *V* = 2).

The preponderance of evidence indicates that growth of the polymer chain in Ziegler-Natta catalysis involves participation of the transition-metal centers. Why, therefore, is it necessary to construct a mechanism using two metal sites? As a result of this question several monometallic mechanisms have been proposed.

Carrick (99) suggested a mechanism (shown in Fig. 36) in which vanadium tetrahalides are used as the transition-metal compounds and the particular function of the aluminum is to reduce the vanadium to the +2 valence state. Complexation and insertion occur solely on vanadium. This catalyst system is rather special since it is active for ethylene only and therefore cannot be applied to our general consideration of α-olefin polymerization.

Cossee (96) proposed a monometallic mechanism involving an active site in which the transition metal has an octahedral configuration. Figure 30, structure *D*, shows Cossee's proposed model for the active site with one position vacant because of a missing ligand.*

The Cossee isotactic propagation mechanism is shown in Figure 37. A monomer is complexed to the vacant orbital of the transition metal and then is inserted between the metal and the alkyl group as indicated. This leads to the regeneration of a vacant orbital with a different orientation. It is necessary for the polymer chain containing the added monomer to migrate to its original site so that the original vacant orbital can be regenerated. If one carries out the propagation utilizing monomer complexes with the vacant orbital generated after the initial reaction, syndiotactic polymers will be produced, as explained by Youngman and Boor (100) (Fig. 38).

At present it is not possible to distinguish between the mono- and bimetallic mechanisms. The bimetallic mechanisms appear attractive since they do not involve growing-chain migration for isotactic propagations. They also provide a method for introduction of an optically

---

*The factors involved in our discussion of the structure of the catalyst were drawn primarily from the Cossee analysis.

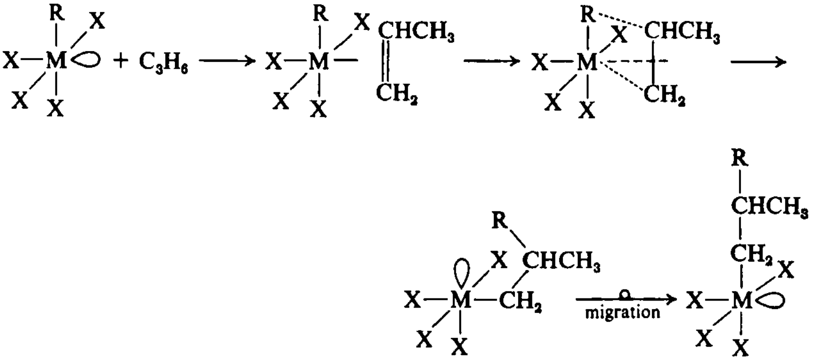

Fig. 37. Sequence of steps by which olefin polymerization takes place (Cossee). The growing polymer chain is represented by R and the vacant octahedral position by the loop (96).

active monomer selecting the same approach and monomer conformation at all times. On the other hand, the monometallic suggestions involve a significant simplicity over the bimetallic mechanisms. It is difficult to require two complicated metal sites to participate in the myriad of catalytic situations which exist under Ziegler-Natta conditions. In addition, Boor (83) believes that the geometry of the monometallic

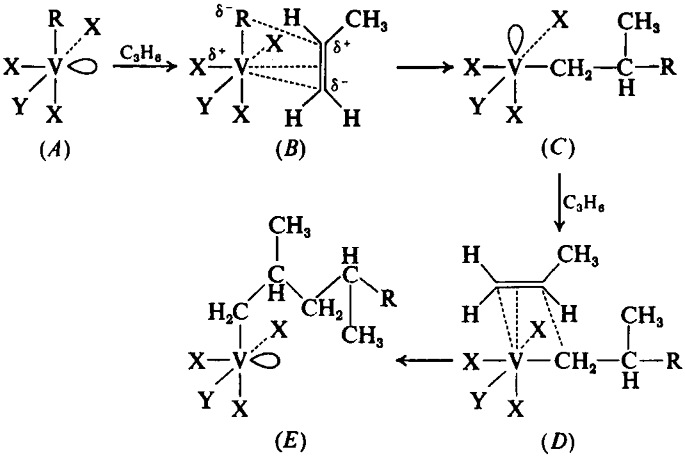

Fig. 38. Suggested model for syndiotactic propagation. In structures *B* and *D* the monomer enters so as to avoid methyl-methyl steric interactions. [Taken from Youngman and Boor (100).]

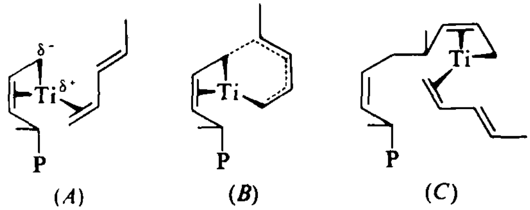

Fig. 39. Suggested scheme for the isotactic propagation of 1,3-pentadiene. Structure *C* is identical to structure *A*. Hence, the newly coordinated monomer of *C* will give, after insertion into the Ti—C bond, a monomeric unit isotactic with respect to the preceding one [taken from Natta and Porri (101)].

active site does not present a serious problem for the migration. He also suggests that insertion of the monomer without complexation could lead to propagation without change of orbitals even with a monometallic mechanism (83). Lastly, Boor claims that the Cossee octahedral structure for the active site leads to diastereomeric centers after reaction with monomer. Thus any given site preferentially complexes with one antipode rather than the other. This can explain Pino's racemic α-olefin polymerization (cf. Sect. IV) and his asymmetric synthesis using the same monomers (cf. Sect. IV). Although these ideas are quite attractive, this writer suggests that it is not consistent to do away with complexation in one case (i.e., to avoid the migration) and to use it for diastereomeric selectivity in another (i.e., optically active polymers).

In an extension of the stereoregular mechanistic considerations in α-olefin polymerization, Natta and Porri (101) undertook to explain the origin of stereoregulation using 1,3-pentadiene as a monomer. Figures 39 and 40 and related text contain a mechanistic description for these

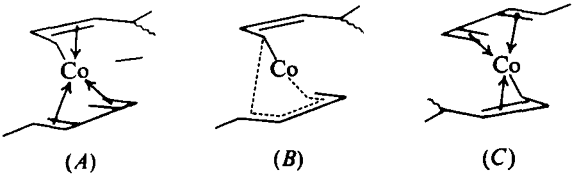

Fig. 40. Suggested scheme for the syndiotactic propagation of 1,3-pentadiene. Structures *C* and *A* are enantiomers. Hence, the newly coordinated monomer of *C* will give, after insertion into the Co—C bond, a monomeric unit syndiotactic with respect to the preceding one [taken from Natta and Porri (101)].

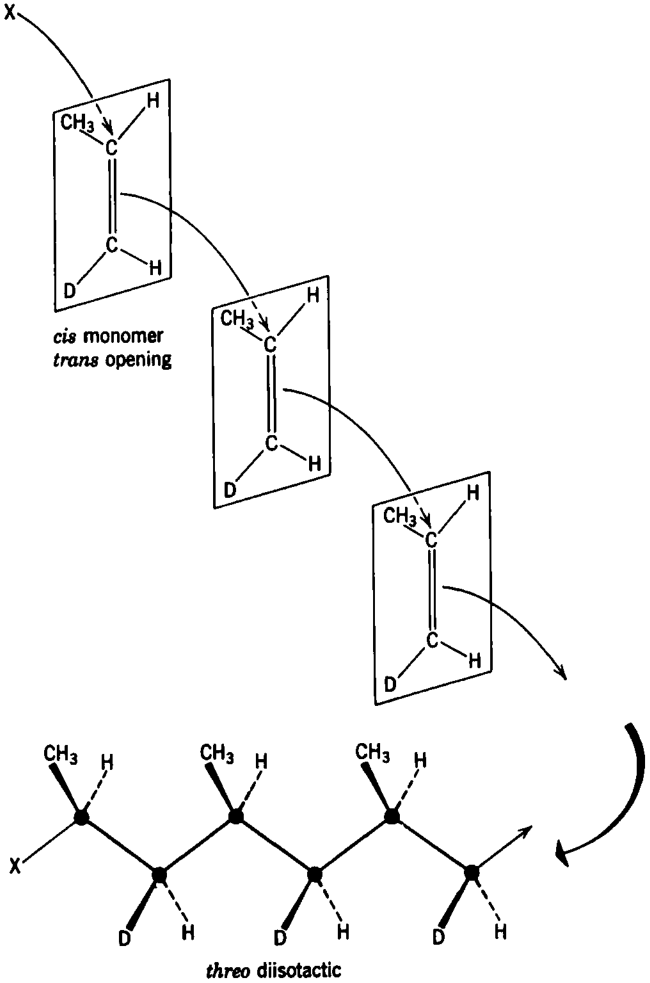

(a)

Fig. 41. Presentations and *trans* double bond opening for *cis*

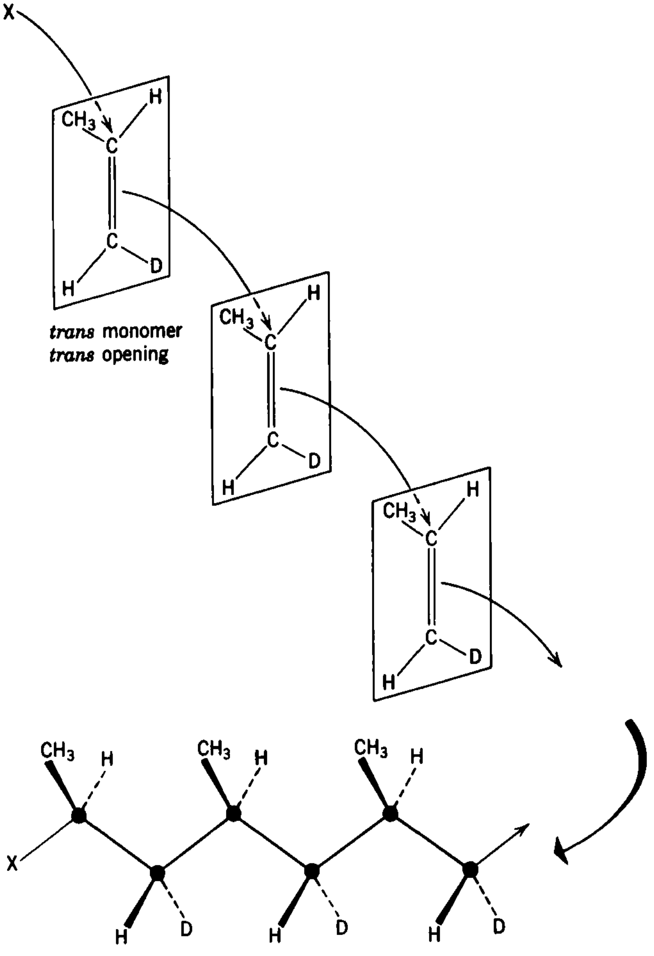

(*b*)

and *trans* 1-deuteropropylenes to yield diisotactic polymers.

stereoregular polymerizations. To explain the formation of the isotactic 1,4-pentadiene using titanium catalysts, these authors invoke the cyclic transition state shown in Figure 39 involving a titanium complexed to an incoming monomer and to the terminal residue of the polymer chain. This leads to an isotactic *trans*-1,4 polymer structure. In a like manner, Figure 40 shows the cobalt complexed to the terminal residue of the polymer chain and also complexed to the two double bonds of the monomer. The result of this type of propagation is that the polymer will have a syndiotactic *cis*-1,4 structure.

B. The Dependence of Stereoregularity on Monomer Approach and Double Bond Opening

Before leaving the area of Ziegler-Natta polymerization, we must examine the question of monomer approach and the opening of the double bond. The ditacticity of polymers derived from the monomers shown in Figure 3 depends on the structure of the monomer (*cis* or *trans*), the orientation of the monomer with respect to the growing chain, and the opening of the double bond (*cis* or *trans*). Natta (89) showed that *cis*-1-deuteropropylene gives *erythro* diisotactic structures while the *trans* isomer gives *threo* diisotactic structures.

In most alkene addition reactions (102), *trans* opening of the double bond prevails. If this were so with the deuterated propylenes, the *cis* monomer would have yielded *threo* polymer while the *trans* monomer would have led to the *erythro* product through the stereochemical sequences shown in Figure 41. Natta, therefore, proposed the *cis* opening of the double bond shown in Figure 42.

For the proper stereochemical products to be obtained, the monomer must be uniformly oriented toward the growing chain. An alternation in the presentation of monomer leads to the disyndiotactic structure as shown in Figure 43. In these diagrams, all reacting polymer structures are written in the planar form for clarity. The reader must bear in mind that polymer chains rotate to assume favorable conformations (cf. Fig. 44). Nevertheless, it is obvious that the *cis* opening involves more steric hindrance than the *trans* since each monomer addition places a carbon in a 1,2 eclipsed structure. We therefore propose to modify the stereochemical mechanism by allowing rotation of the carbon–carbon bond in the monomer unit after addition takes place in order for the ultimate unit to avoid the fully eclipsed 1,2 interactions, as shown in

Figure 44. This in effect converts a *cis* into a *trans* monomer (and vice versa) and allows *trans* addition to take place. By this route, the *cis* and *trans* monomers yield the correct products. In addition, this route is completely consistent with the Ziegler-Natta mechanisms discussed earlier since the deuteromethylene group is attached to the transition-metal site and can therefore rotate easily.

C. Polymerization of Dienes by Alkali Metals and Organoalkali Compounds (103)*

Dienes may be polymerized by alkali metals such as lithium, sodium, and potassium and by organoalkalies such as butyllithium, benzyl potassium, and phenyl sodium. Essentially identical structures are observed if the polymerization is carried out in bulk or in hydrocarbon solution. Lithium metal and alkyllithium have high stereoregulating effects giving in the polymerization of isoprene a 93% *cis*-1,4 structure. The lithium-based catalysts exhibit no change in structure with a change in the organic group. It has been found that lithium, *n*-butyllithium, *n*-amyllithium, and isoamyllithium produce polyisoprene of the same structure when carried out in tetrahydrofuran (THF). The temperature appears to have little effect on the microstructure produced. In the course of phenyllithium polymerization in THF, only a few per cent difference in structural composition is observed between −78 and +100°.

While little change in microstructure is found in going from bulk polymerization to polymerization in a hydrocarbon solvent, drastic effects on the structure of the polyisoprene are found when a lithium-based initiator is used in a nonhydrocarbon solvent. This effect is lessened in the case of sodium and potassium. Table I summarizes some of the data (103).

Any mechanism proposed to explain these experimental observations must account for the two most salient features. The first is that lithium and lithium alkyls must have high stereoselectivity to produce such a high degree of stereospecificity. The second is the fact that polar solvents have a drastic effect on the structure of polydienes produced from lithium and lithium alkyls causing a loss in the *cis*-1,4 stereospecificity.

---

* A comprehensive review of this field has appeared by Overberger, Mulvaney, and Schiller (103).

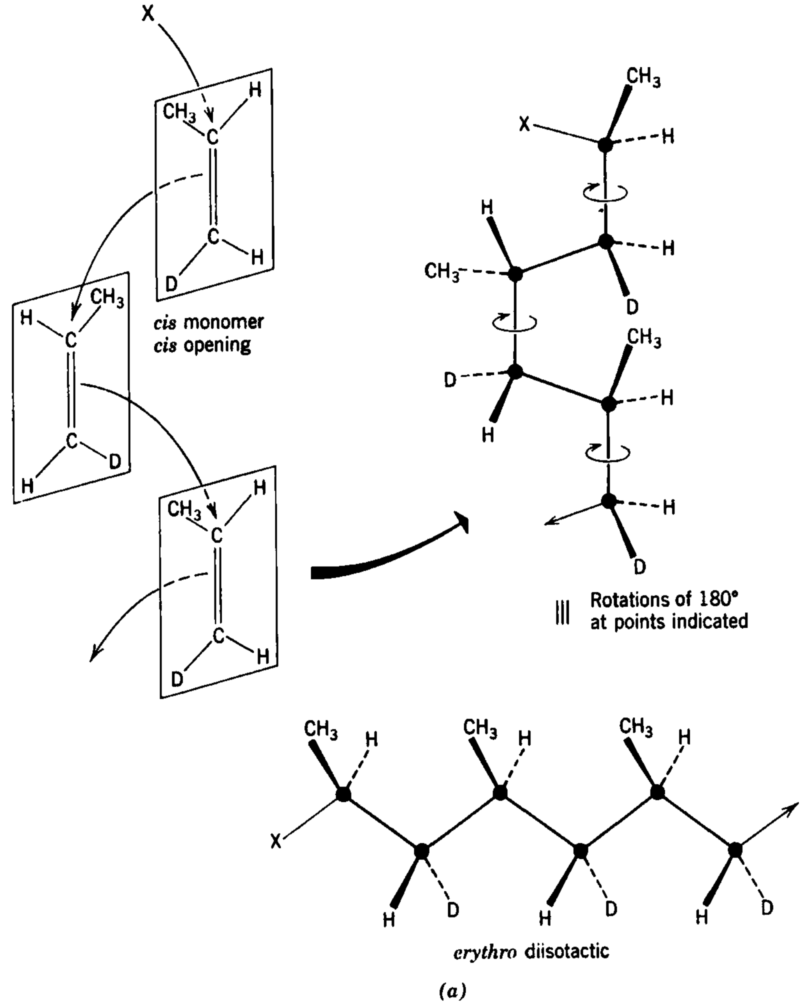

Fig. 42. Presentations and *cis* double bond opening for *cis*

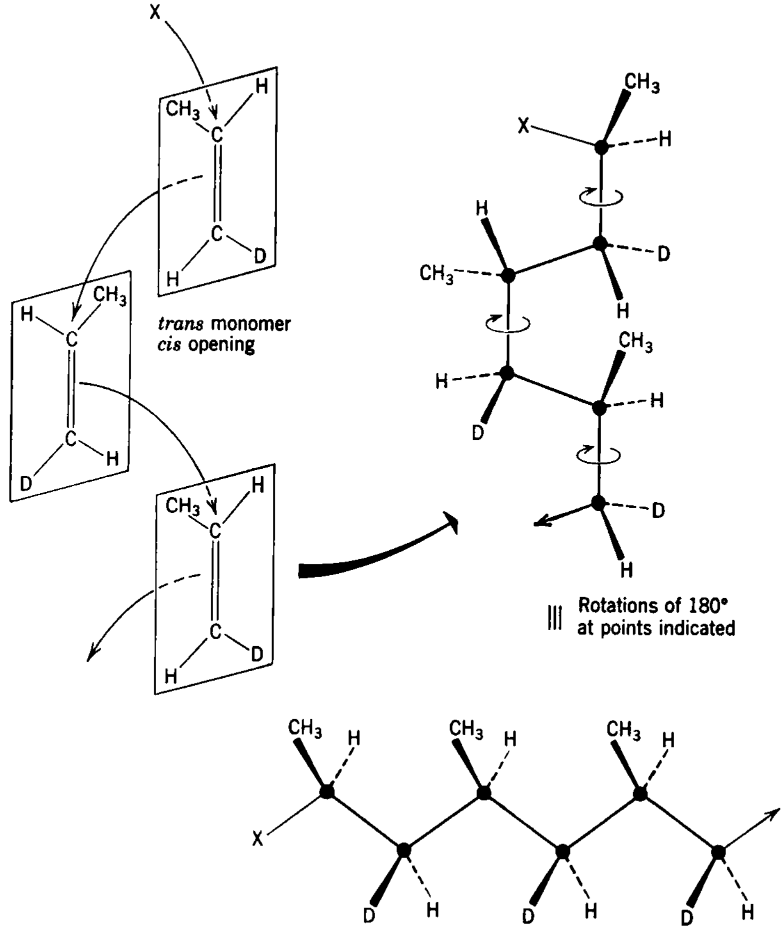

threo diisotactic

(b)

and *trans* 1-deuteropropylenes to yield diisotactic polymers.

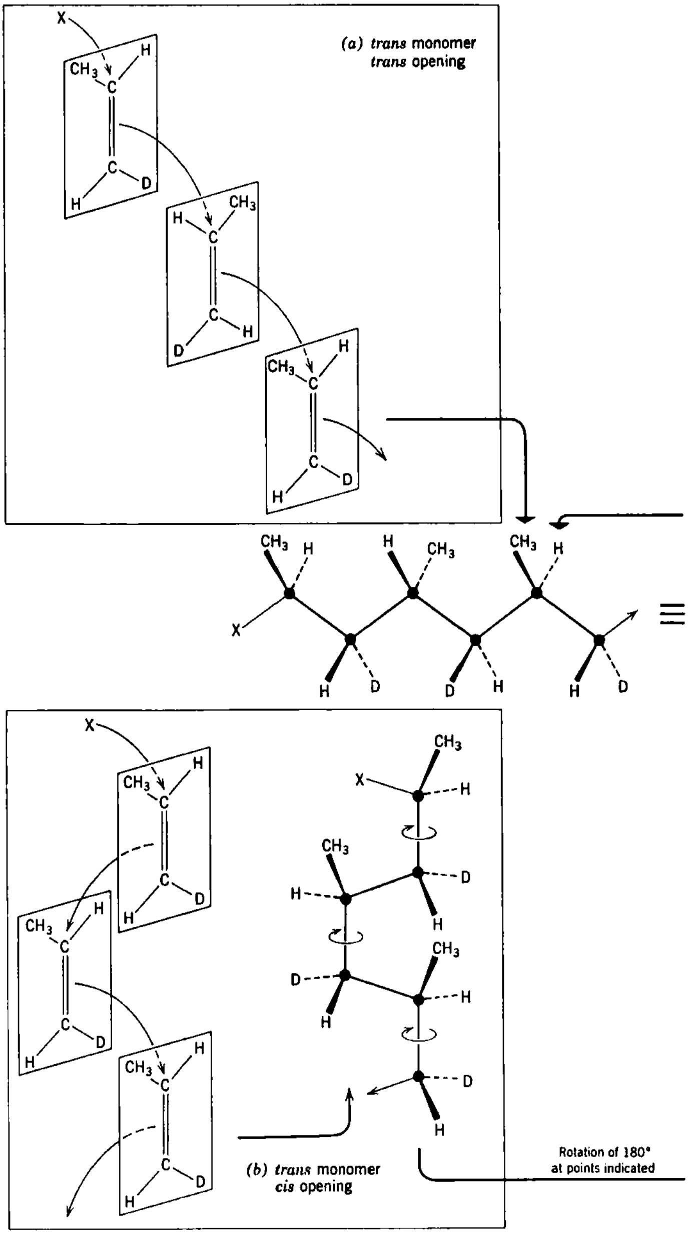

Fig. 43. Presentations for *cis* and *trans* 1-deut-

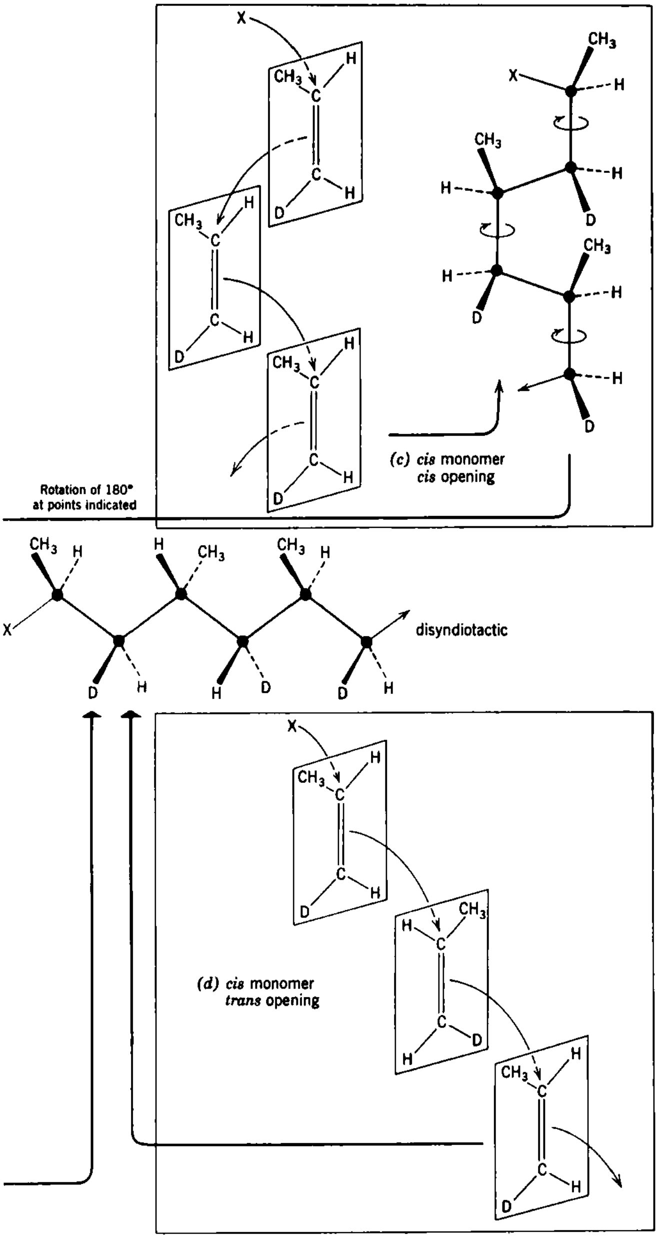

eropropylenes to yield disyndiotactic polymers.

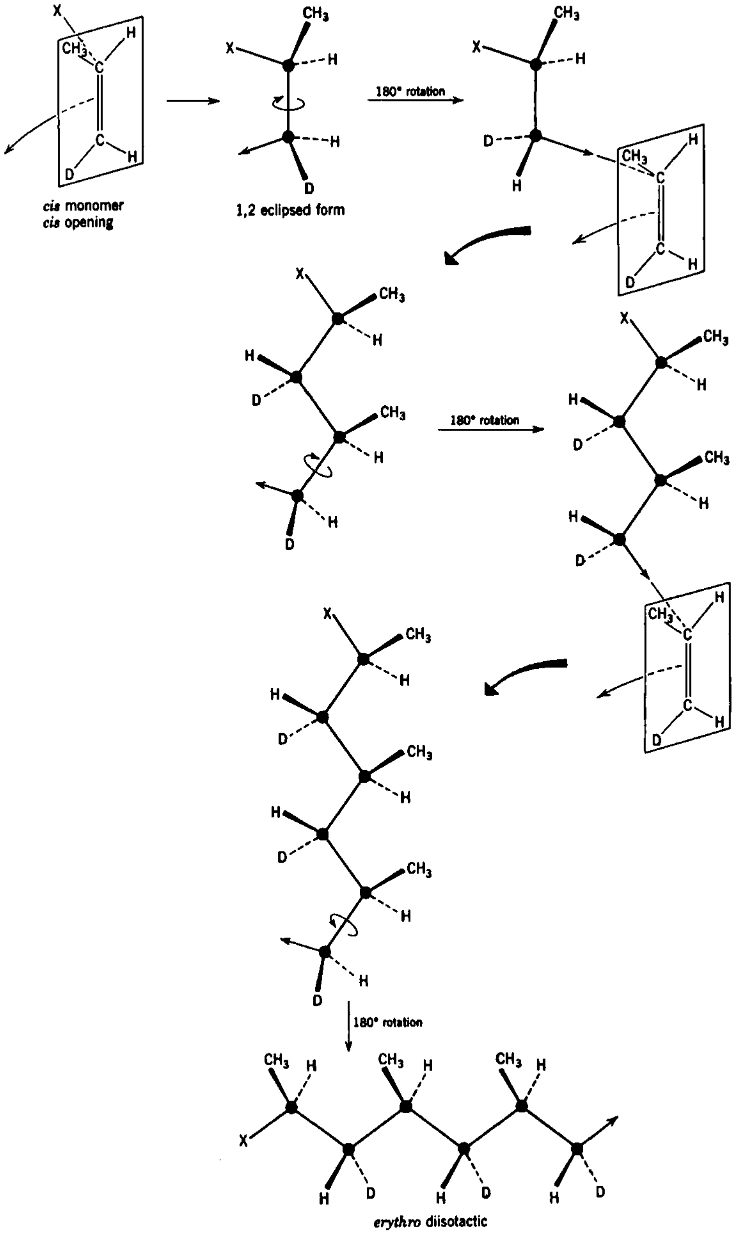

Fig. 44. Presentations for *cis* and *trans* 1-deuteropropylenes conformations (these sequences

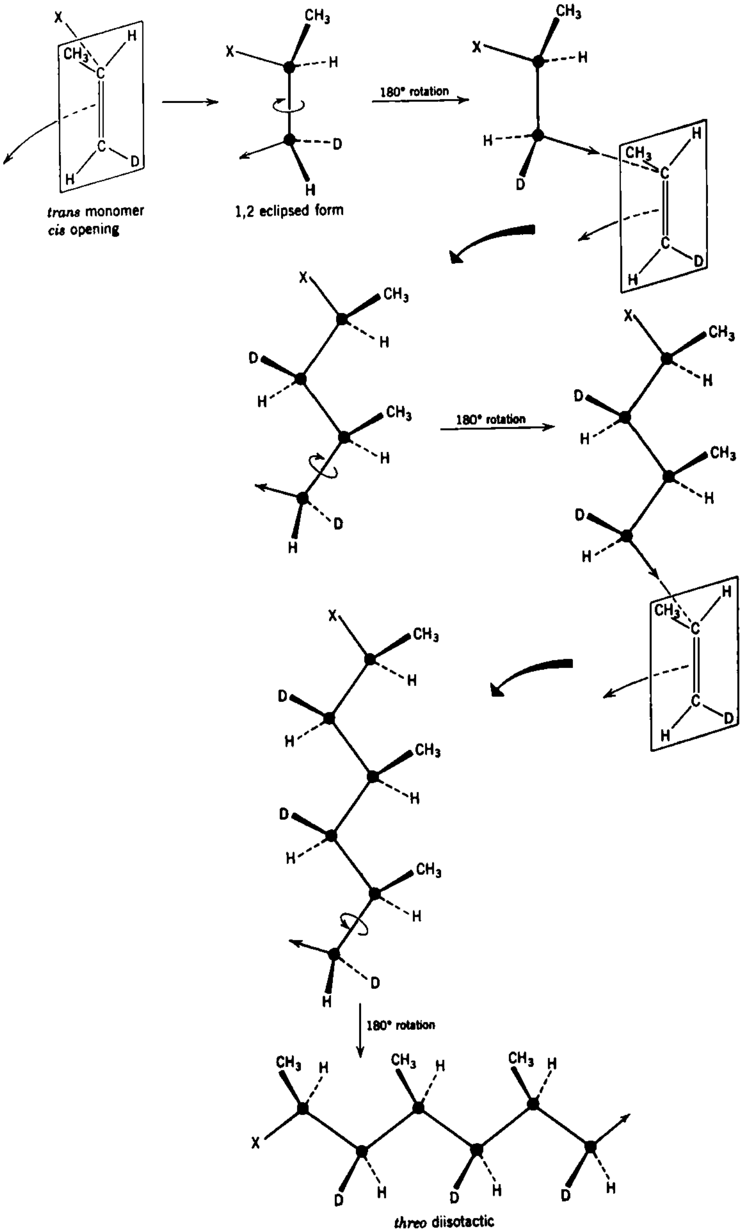

involving rotation following *cis* addition to avoid 1,2 eclipsed lead to "effective *trans* addition").

TABLE I

Dependence of Structure on Polymerization Conditions for Polyisoprene

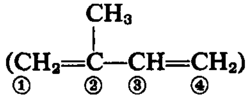

$$(CH_2{=}\overset{CH_3}{\overset{|}{C}}{-}CH{=}CH_2)$$

Solvent	Propagative cation	1,2	3,4	*cis*-1,4	*trans*-1,4
Bulk	Li	0	7	93	0
Heptane	Li	0	7	93	0
Benzene, toluene	Li	0	7	93	0
Ether	Li	5	46	0	49
THF	Li	16	51	0	33
Heptane	Na	9	45	0	46
Ether	Na	12	55	0	33
THF	Na	13	54	0	33
Heptane	K	9	33	0	58
Ether	K	10	39	0	51
THF	K	16	36	0	48

The above experimental results may be reasonably explained by a general mechanism as shown in Figure 45. That only lithium gives almost entirely a *cis* structure can be seen from structure *B*. The small unsolvated lithium is able to fit into such a structure while the larger alkali metals cannot. In this manner the lithium ion is able to complex the adding monomer in a 1,4-*cis* form while it remains attached to the carbanionic end of the growing chain.

Compound *A* is called a Schlenk adduct; its existence has been demonstrated by indirect means. For example, with 2,3-dimethylbutadiene, Ziegler (104) demonstrated the existence of the following molecules.

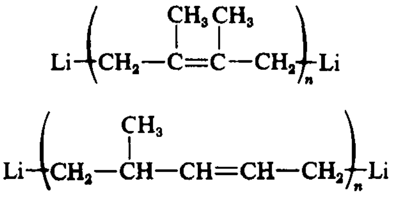

$$Li{-}\left(CH_2{-}\overset{CH_3}{\overset{|}{C}}{=}\overset{CH_3}{\overset{|}{C}}{-}CH_2\right)_n{-}Li$$

$$Li{-}\left(CH_2{-}\overset{CH_3}{\overset{|}{CH}}{-}CH{=}CH{-}CH_2\right)_n{-}Li$$

n = 1,2,3,4,5, or 6

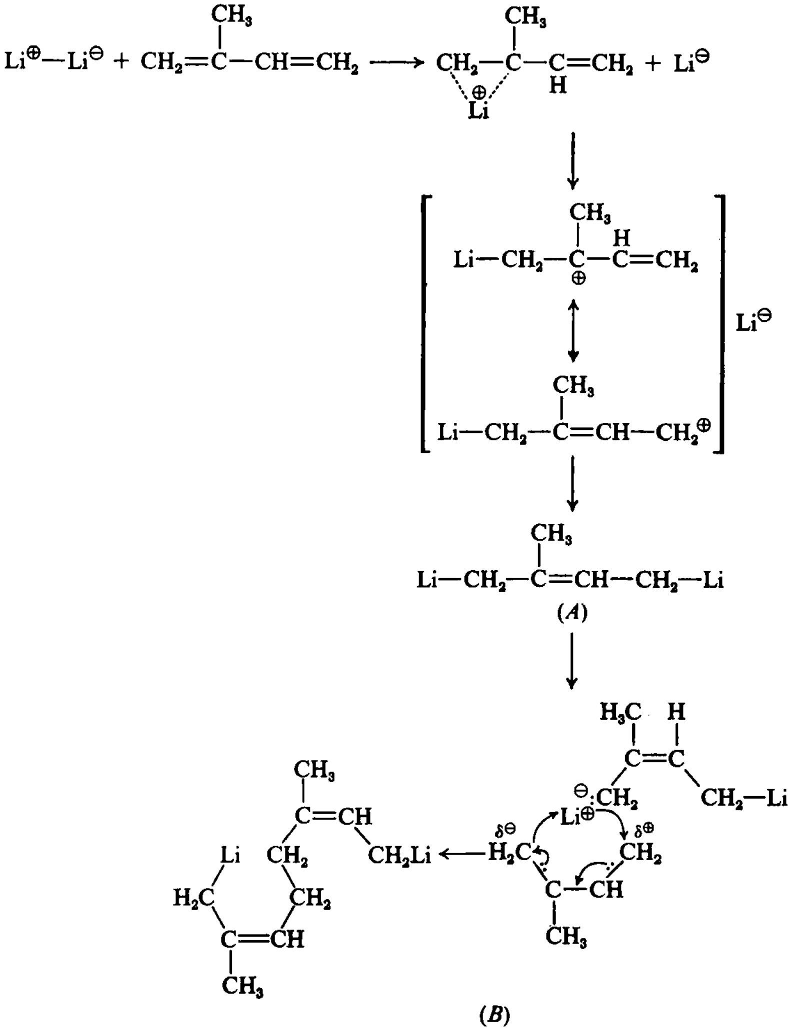

Fig. 45. Mechanism of polymerization of isoprene by lithium.

The existence of the Schlenk adduct in the sodium polymerization of butadiene was shown indirectly by the addition of *N*-methylaniline to the system sodium–butadiene. It was found that 2 moles of sodium methylanilide were obtained for every mole of butadiene consumed.

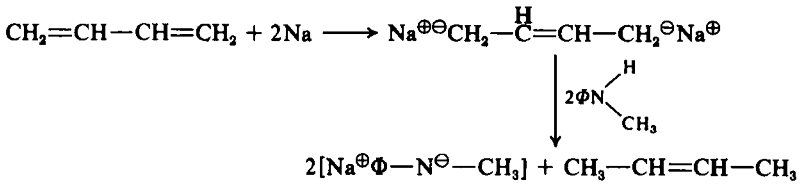

Fig. 46. Reaction of a Schlenk adduct with *N*-methylaniline.

(*N*-Methylaniline does not react with sodium.) The most reasonable explanation for this is described in Figure 46 where reaction occurs only through the intermediacy of the Schlenk adduct.

The above mechanism appears to explain the stereospecific polymerization of isoprene by lithium. Further details on the mechanism of a similar system may be found in reference 103. The butyllithium-initiated polymerization of isoprene can be viewed as proceeding through a route very similar to that in the case of lithium metal. The major difference, of course, is obviously the mode of initiation. A Schlenk adduct is unnecessary. The mechanism is shown in Figure 47. In the first step, the isoprene forms a π complex with the lithium cation. Then the electronic redistribution propagates the chain. Lastly the Li$^{\oplus}$ forms an ion pair with the anion end of the chain.

The disruption of the stereospecificity by solvents such as THF or ether (or any Lewis base) can be seen as arising from a competition for the Li$^{\oplus}$ ion in the manner shown in Figure 48. The ether causes a shift

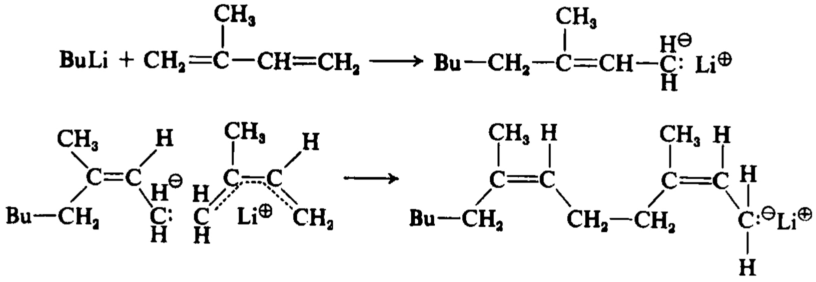

Fig. 47. Mechanism of polymerization of isoprene by butyllithium.

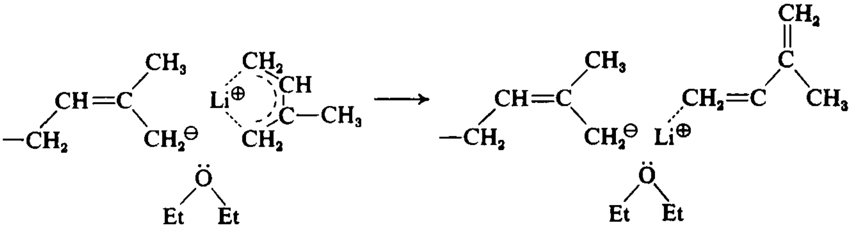

Fig. 48. Disruption of stereospecificity of isoprene polymerization by added ether.

of electron pairs, thus partially destroying the stereospecific complex and allowing the isoprene to enter into the chain in a more random fashion.

VI. STEREOREGULAR POLYMERIZATION OF POLAR MONOMERS

In general, Ziegler-Natta type catalysts are inactivated in the presence of polar monomers. Further investigations in the field of stereospecific polymerization have shown that stereoregular products can be obtained using ionic and free-radical initiators. This has led to the synthesis of a great variety of stereoregular polymers. Free-radical polymerizations at low temperatures yield syndiotactic polymers of isopropyl acrylate (105), cyclohexyl acrylate (105), and methyl methacrylate (106). Similar polymerization of vinyl chloride gives a polymer, portions of which may have a random structure (108).

Anionic catalysts polymerize acrylate and methacrylate monomers to stereoregular products (105–123). The nature of the polymer obtained in the polymerization of methyl methacrylate with 9-fluorenyllithium depends upon solvent. Polymerization in toluene or 1,2-dimethoxyethane yields isotactic or syndiotactic polymers, respectively.

Table II contains a representative series of other stereoregular polymers and the conditions for their preparation.

Watanabe et al. (124) observed that a 1:1 precipitate forms when isotactic and syndiotactic poly(methyl methacrylate) are mixed. Later, Liquori and co-workers (125) reported the formation of a 2:1 complex of isotactic and syndiotactic poly(methyl methacrylate) in polar solvents. This structure was called a "stereocomplex." These workers believe

TABLE II

Stereoregular Polar Polymers

Polymer	Catalyst	Structure	Reference
Methyl methacrylate	Fluorenyllithium in toluene at −78°	Isotactic	106,107
	Fluorenyllithium in THF at −78°	Syndiotactic	107
	Butyllithium in heptane at −78°	Isotactic	107
	Grignard reagent at −78°	Isotactic	109
	Fluorenyllithium in dimethoxyethane at −60°	Syndiotactic	106,107
	Fluorenyllithium in toluene–ether at −78°	Stereoblock	106
Menthyl methacrylate	*n*-Butyllithium in toluene at −78°	Isotactic	110
α-Methylbenzyl methacrylate	*n*-Butyllithium in toluene at ~ −70°	Isotactic	111
	n-Butyllithium in THF at ~ −70°	Syndiotactic	111
Isopropyl acrylate	Photosensitized or Co^{60} free-radical initiation in bulk or toluene at < −70°	Syndiotactic	105
	Grignard reagent in toluene at −78°	Isotactic	105
Cyclohexyl acrylate	Photosensitized or Co^{60} free-radical initiation in bulk or toluene at < −70°	Syndiotactic	105
	Grignard reagent in toluene at −78°	Isotactic	105
tert-Butyl acrylate	Li dispersion in monomer or hexane at RT	Isotactic	112,113
N,*N*-Disubstituted acrylamides	Organometallics of groups I and II of the periodic table	Isotactic	114,115

(continued)

TABLE II (*continued*)

Polymer	Catalyst	Structure	Reference
Acetaldehyde, propionaldehyde	$Al(C_2H_5)_3$, $Zn(C_4H_9)_2$	Isotactic	116,117
Iso- and *n*-butyraldehyde	$Al(C_2H_5)_2Cl$	Isotactic	116,117
Isobutylvinyl ether	BF_3 etherate	Isotactic	118,119
tert-Butylvinyl ether	$BF_2C_4H_9$	Isotactic	120
tert-Butylvinyl ether	BF_3 etherate	Isotactic	121
α-Methylvinyl methyl ether	$FeCl_3$, $Al(C_4H_9)Cl_2$, I_2, $Al(C_4H_9)_2Cl$, BF_3 etherate	Syndiotactic	122,123
Isopropyl, isobutyl, neopentyl, vinyl ethers	$Al(C_2H_5)_2Cl$, $Al(C_2H_5)Cl_2$	Isotactic	42

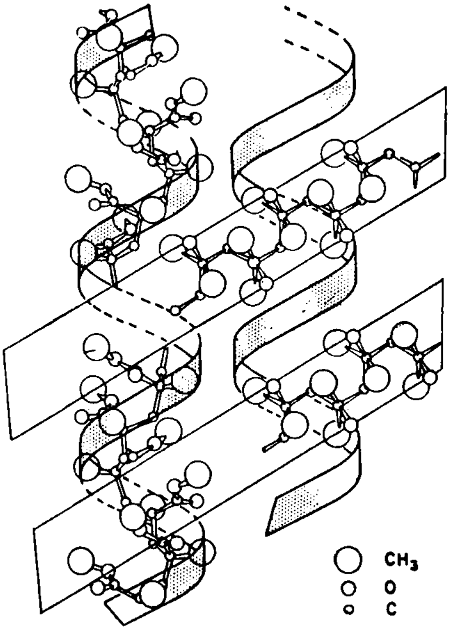

Fig. 49. Schematic drawing of the structure of the stereocomplex showing the arrangement of syndiotactic and isotactic chains [taken from Liquori et al (125)].

that the stereoblock copolymer described by Hughes (106) is in reality a stereocomplex. Figure 49 shows their suggested structure for the stereocomplex.

A. Poly(methyl Methacrylate) (80)

Alkyllithium catalysts have been extensively employed in the preparation of stereoregular methacrylates. Initial complexes between monomer and catalyst can involve a π complex between the alkene and the lithium ion or a delocalized complex where the alkene, carbonyl, and lithium ion interact with each other. These structures are shown in Figure 50. From considerations such as these, we can devise several mechanisms to explain the stereochemistry of various methacrylate anionic polymerizations. For example, the lithium ion can be considered coordinated with the ultimate and penultimate units of the chain as shown in Figure 51. Since it is the carbonyl oxygen of the penultimate unit which is coordinated with the lithium ion, an isotactic propagation occurs because the ester groups that become the prepenultimate and penultimate units of the growing chain have the same tacticity (cf. ester carbons 4 and 8 in addition to the pseudoasymmetric centers 5 and 7 in the product).

The lithium ion is intramolecularly solvated by the electron pairs of the delocalized complex and the carbonyl from the penultimate residue. The incoming monomer always presents itself with the same orientation toward the end of the growing chain.

Cram and Kopecky (126,127) suggested an alternate mechanism which involves a six-membered ring stabilization as shown in Figure 52.

Stereoregulation in this mechanism arises from the coordination of the lithium ion with the oxygen atoms as shown in Figure 52. It is perhaps too restrictive to assume that a six-membered ring must be

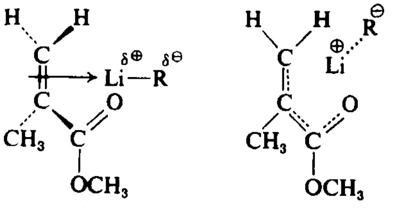

(*A*) (*B*)

Fig. 50. Initial complex between an alkyllithium catalyst and methyl methacrylate: (*A*) π complex; (*B*) delocalized complex.

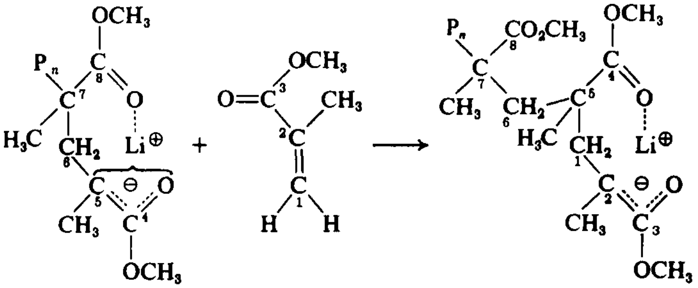

Fig. 51. Mechanism of stereospecific anionic polymerization of methyl methacrylate, via lithium alkyl initiation.

formed prior to addition of each monomer unit. If we merely require penultimate residue effects, both mechanisms become extremely similar.

It is clear that addition of Lewis bases will strongly affect the intramolecular solvation of the lithium ion. If the intramolecular forces are destroyed by agents or solvents such as THF, stereoregularity is strongly altered changing from isotactic to syndiotactic (107) propagation. [Recall that poly(methyl methacrylate) (PMMA) produced by free-radical initiation is highly syndiotactic.]

Since lithium alkyls are highly associated in nonpolar organic solvents (80), we shall expect various species to exist in solution from the covalently bonded ions, through ion pairs, to free ions as the polarity of the solvent increases. Glusker (128) undertook to study the kinetics and molecular weight distributions for the polymerization of methyl methacrylate with 9-fluorenyllithium as the initiator in hydrocarbon solution at temperatures below −60°. They established that the

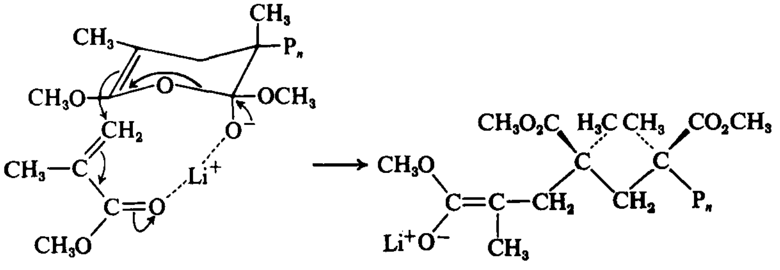

Isotactic polymer

Fig. 52. Reestablishment of six-membered ring by attack of the penultimate carbonyl by the alkoxide anion (80).

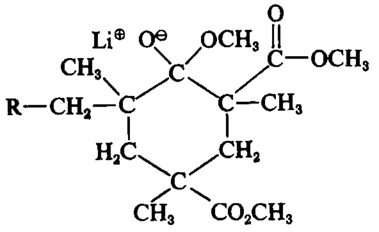

Fig. 53. Pseudoterminated poly(methyl methacrylate).

initiator rapidly disappears. A slow stage in the polymerization ensues until a $\overline{DP} \sim 8$ is reached. From this point, a rapid stage commences leading to a highly isotactic polymer of high molecular weight. Glusker obtained a binodal molecular weight distribution which is consistent with the kinetic findings above. He explained these findings by indicating that most of the initiator goes to a cyclic pseudotermination structure during the early stages of polymerization as shown in Figure 53. This cyclic trimer can propagate slowly. A small fraction of the growing polymer chains reach a stage where the cyclic pseudotermination structures give way to the complexes discussed earlier in our survey of the polymerization mechanism (Figs. 50–52). As the polarity of the solvent increases, or as Lewis bases are added, these intramolecular forces are broken up and a conventional anionic polymerization system is obtained. No longer does one observe high isotacticity or the slow and fast stages or a binodal molecular weight distribution.

B. Monomer Approach and Double Bond Opening with Acrylates and Methacrylates

In an independent series of experiments related to those reported earlier by Natta on deuteropropylenes, Bovey, Schuerch, and their co-workers (129), and Yoshino and his associates (130–134), prepared deuteroacrylates such as:

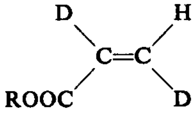

where R = isopropyl or methyl

This structure is *cis*, since the ester and β-deuterium are on the same side. Perhaps it is clearer to view the assignment from the standpoint of the α-deuterium and the proton. If the α-deuterium were changed to a proton, the compound would be obviously *cis*, yet no change in the geometric character of the molecule would have occurred.

Standard radical initiations of acrylates lead to random head-to-tail polymers with regard to the ester group and the β-proton. Because of the α and β substituents in the monomer, ditacticity must be considered. Phenylmagnesium bromide anionic initiation of the polymerization of isopropyl *cis*-β-dideuteroacrylate in toluene solution (with a small amount of ether present) at −78° leads to highly diisotactic polymer with an equal contribution from *erythro* and *threo* β-proton structures. If an excess of diethyl ether is added (10:1 mole ratio to the Grignard), a completely *threo* diisotactic polymer results. When all ether is rigorously excluded, an *erythro* diisotactic polyacrylate is obtained. Figure 54 shows these relationships. Lithium aluminium hydride (in toluene and ether) leads to a mixture of *erythro* and *threo* diisotactic structures and also some syndiotactic structures with the *threo* predominating. With fluorenyllithium, the *erythro* diisotactic content increases with increasing THF.

The structural assignments are based on NMR spectra of the radical-initiated polymer and on model compounds. The *erythro* diisotactic peak is located at 7.86 τ while the *threo* diisotactic peak is centered at 8.32 τ. Syndiotactic placements are found at 8.20 τ. This deuteromethylene resonance, of course, results from a racemic dyad.

Bovey and Schuerch extended their work to include β-monodeuterated methyl and ethyl methacrylates, using fluorenyllithium as an initiator. They found once again that *threo* predominates in the absence of THF. Increasing the amounts of THF added shifts the β-proton to an *erythro* position. If the ether added is in large excess, a primarily syndiotactic structure for the polymer is encountered.

When *erythro* and *threo* placements occur simultaneously, a question arises as to whether these structures arise randomly or in long blocks. In the extreme it can be asked if a given site generates *threo* or *erythro* only. Yoshino and Kuno employed isopropyl *trans*-mono-β-deuteroacrylate and studied the coupling patterns. They concluded that *threo* units appear to have only *threo* units as neighbors while *erythro* units have

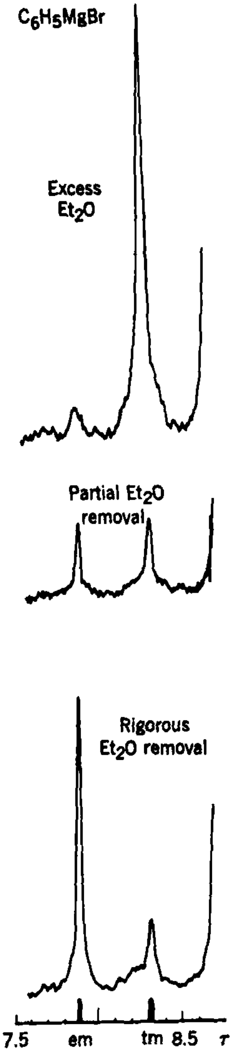

Fig. 54. Polyisopropyl *cis*-d_2-acrylate Grignard intiation [adapted from Bovey (61)].

neighboring *erythro* units. Thus it is probable that a given site is stereoselective for one ditactic placement.

Before going to the mechanistic interpretations, I would like to discuss recent conformational findings from model compounds. Bovey (135), Doskocilova (136,137), Tincher (138), and Shimanouchi (139) examined the conformational preferences of 2,4-disubstituted pentanes (cf. Figs. 27 and 28 and associated text). For the 2,4-diphenylpentanes (discussed earlier) and the other model compounds, evidence seemed to be that the *trans, gauche* (*tg*) conformation is favored by the *meso* compound while the all *trans* (*tt*) or the *gauche, gauche* (*gg*) forms are favored by the racemic compounds.

Doskocilova and her co-workers (140) recently found that 2,4-dicarboxymethylpentanes and 2,4,6-tricarboxymethylheptanes [models for poly(methyl acrylates)] do not follow these rules completely. For the racemic pentane compound, there appears to be no energetic difference between the all *trans* (*tt*) and the *gauche, gauche* (*gg*) form in agreement with Bovey's results on 2,4-diphenylpentane (135) and in contrast to Tincher's findings with 2,4-dichloropentane (138) and Shimanouchi's work on the acetates of 2,4-pentanediols (139). For the *meso*-pentane compound, Doskocilova (140) found that the *trans, gauche* (*tg*) forms are favored, but she also indicated the presence of a considerable amount of *gauche,trans–trans,gauche* (*gttg*) structure in the appropriate heptane model compound which corresponds to the transition point between a left- and a right-handed helical sense in the analogous polymeric structure.

In order to explain the products obtained with these deuterated acrylates and methacrylates, Bovey (61) proposed the mechanisms shown in Figure 55, where the monomer presents itself to the growing chain in an isotactic (*a*) or syndiotactic (*b*) fashion. A simple *trans* opening of the double bond in the former case leads to the *threo* diisotactic polymer. In the latter, a rotation is necessary to maintain the diisotacticity (i.e., to avoid syndiotactic placements) and obtain an *erythro* diisotactic structure.

We can consider the driving force for a preferred isotactic stereochemistry as coming from the chelating nature of the metallic gegenion. This is fully consistent with the proposed mechanisms for anionic acrylate and methacrylate stereoregular polymerizations (Figs. 50–53 and text). In hydrocarbon solvents, the chelating effect of the gegenion is at a maximum. This restricts the entering monomer to an isotactic

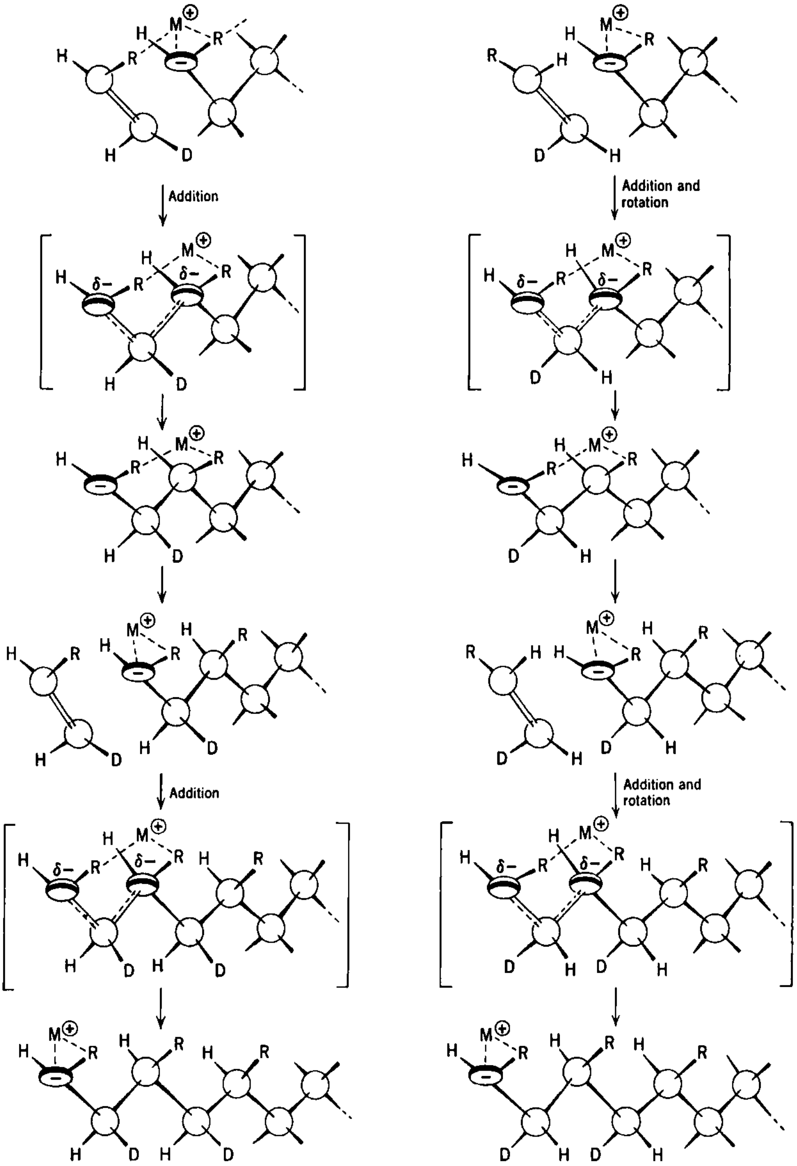

threo diisotactic
(*a*)

erythro diisotactic
(*b*)

Fig. 55. Presentation and *trans* double bond opening for 1-deuteroacrylates leading to diisotactic polymers [adapted from Bovey (61)].

presentation, which explains why under these conditions only *threo* diisotactic polymer is obtained. With small additions of a Lewis base (THF) this guiding influence is diminished and syndiotactic presentation becomes possible. However, the chelating effect remains strong enough to insure diisotacticity by rotation of the chain end. As a result the polymer becomes primarily, but not exclusively *erythro* diisotactic. Naturally, any time monomer presentation is isotactic, *threo* diisotactic polymer is produced. When the additions of Lewis base become substantial, the control of presentation and chelation are lost and the polymer becomes disyndiotactic.

At this stage it is important to compare these mechanistic interpretations with those presented earlier for the deuteropropylene polymerizations. The growing chain in a Ziegler-Natta polymerization has a transition metal–methylene bond (Figs. 33–37). This is opposite to the acrylate or methacrylate cases where the terminal carbon of the chain attached to the metal contains the ester group. In Ziegler-Natta systems the monomer is complexed in a *cis* form (Fig. 31) and presentation is rigorously controlled (Fig. 32). Following monomer insertion (via bimetallic or monometallic mechanism) it is reasonable to postulate rotations about the deuteromethylene end group (shown in Fig. 44) even in these highly nonpolar media. Certainly rotation about a deuteromethylene is more facile than rotation about the substituted carbon of the chain. The driving force can be considered to be the avoidance of 1,2 eclipsed forms. In this manner we can explain why in hydrocarbon solvents the products of polymerization of *cis*-1-deuteropropylene are *erythro* diisotactic while the products from *cis*-β-deuteroacrylates are *threo* diisotactic in nature.

C. Poly(vinyl Ether)s

Although he did not fully extend his findings, C. E. Schildknecht (141) provided the first synthesis of an isotactic stereoregular polymer. He polymerized isobutyl vinyl ether at −70° using $BF_3:OEt_2$ and obtained a crystalline polymer. Since that time many investigations have been carried out on stereoregular polymerizations of alkyl vinyl ethers. Two mechanistic suggestions appear to be most reasonable. In fact, they represent cationic analogs of the intramolecular intermediates used for the poly(methyl methacrylate) polymerization mechanism.

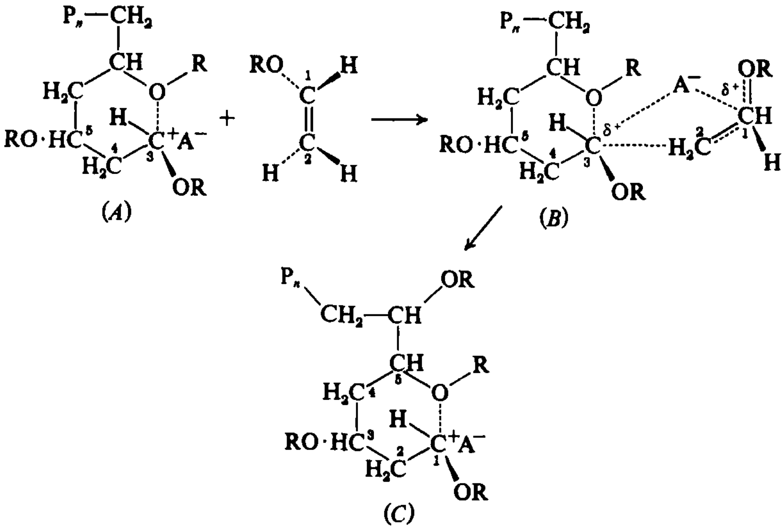

Fig. 56. Bawn and Ledwith's mechanism for vinyl ether polymerization to yield an isotactic polymer (80).

Bawn and Ledwith (80) postulated that the growing cation can be stabilized through an intramolecular effect utilizing the prepenultimate unit in the chain (as shown in Fig. 56) to form an oxonium ion which

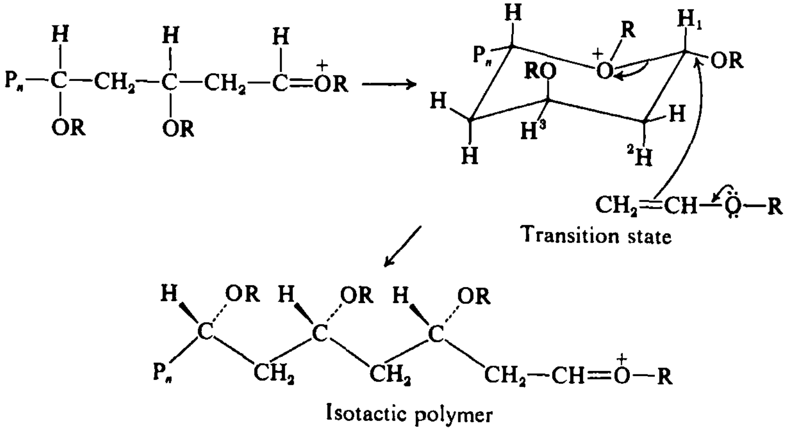

Fig. 57a. (a) Cram and Kopecky's mechanism for vinyl ether polymerization to yield an isotactic polymer (126).

stabilizes the carbonium ion end group. They then indicated a complex involving carbonium ion, gegenion, and monomer that possesses the specific geometric form *B* (Fig. 56). Attack by the electrons of the approaching monomer (carbons 1 and 2) displace the existing oxonium ion form, the oxygen attached to carbon 7, forming a new oxonium ion from the oxygen attached to carbon 5. In the process, the monomer unit is added to the chain end.

The other mechanism, proposed earlier by Cram and Kopecky (126), is quite similar to the route described above except that the driving force for stereochemical control derives from the axial versus equatorial placements in a fairly rigid six-membered oxonium ring transition state (Fig. 57*a*).

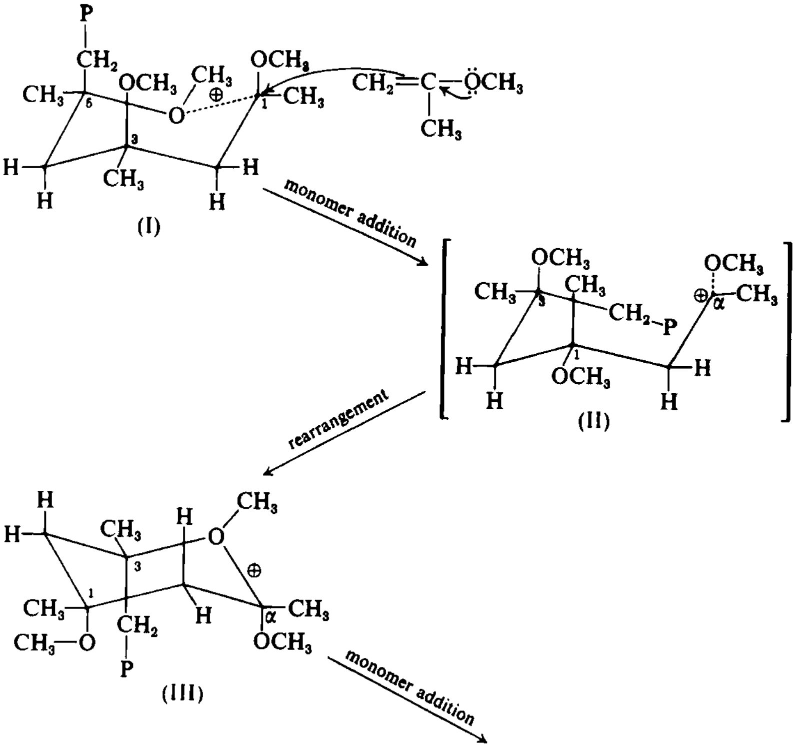

Fig. 57*b*. Stereochemistry of the poly(α-methylvinyl methyl ether) growing chain, leading to the formation of a syndiotactic polymer (122).

The alkoxyl group at position 1 assumes the equatorial placement in the six-membered ring. Inversion at each addition step by the attack of the monomer's electron pair insures that when carbon 3 becomes part of the prepenultimate unit and carbon 1 becomes part of the penultimate unit they will have the same configurations. Thus isotactic structures result. Although this mechanism has great merit, it does not explain why changing the alkyl group of a vinyl ether can change the stereoregularity of a polymer made under conditions which give isotacticity for vinyl isobutyl ether.

In spite of this shortcoming, we have found the Cram and Kopecky approach very useful in explaining why a syndiotactic polymer is obtained from α-methylvinyl methyl ether (122,123).

We invoked a similar six-membered ring transition state (Fig. 57*b*). Using the same logic as Cram and Kopecky, we assigned the methoxyl groups axial and the methyl groups equatorial placements at C_1 and C_3 of the pseudo six-membered ring. Inversion at carbon 1 by monomer attack makes carbons 1 and 3 assume opposite configurations when they become prepenultimate and penultimate units in the chain. Rotation about the last three units of the chain reestablishes the six-membered ring which is ready for another monomer addition. In this way we explain why poly-(α-methylvinyl methyl ether) is highly syndiotactic when polymerized at low temperatures with typical cationic catalysts.

It is important to point out that six-membered ring transition states are more satisfactory for explaining the cationic polymerization of vinyl ethers than for interpreting the anionic polymerization of methyl methacrylate. In the former, there is simply an interaction between the oxygen on the prepenultimate residue and the carbonium ion at the end of the chain controlling the stereochemistry. In the latter, it is necessary to involve extremely special kinds of interactions among the six-membered ring anionic structure, the monomer, and the gegenion in order to restrict the attack on monomer to a specific stereochemical route.

D. Polypropylene Oxide

Of all the cyclic ethers polymerized, only propylene oxide has been extensively studied from the stereochemical standpoint. Price and Osgan (30,31) following the discovery of Pruitt and Baggett (142)

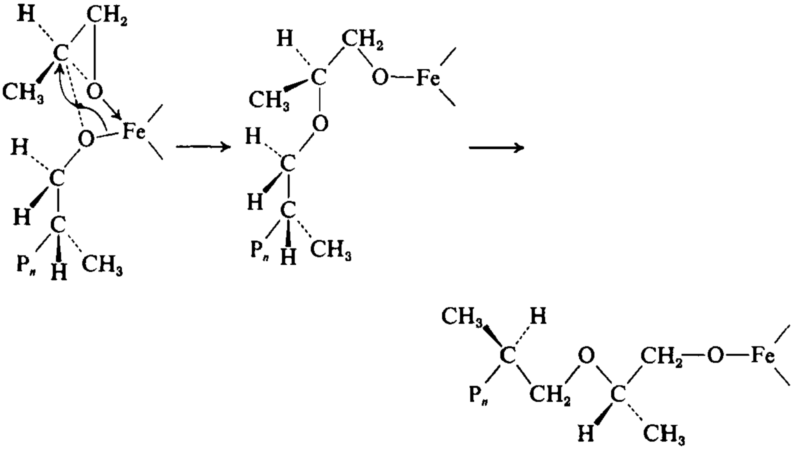

Fig. 58. Mechanism of stereoregular polymerization of propylene oxide.

studied the stereoregular polymerization of propylene oxide using solid KOH or $FeCl_3$ as a catalyst. If they employed the optically active form of the monomer, the asymmetry was conserved during polymerization. Furukawa, Tsuruta, and their co-workers (143–146) also studied the stereoregular polymerization of propylene oxide using, among others, dialkyl zinc (ZnR_2) as a catalyst. A mechanism as shown in Figure 58 has been proposed to account for the structure of the polymer. These polymerizations most probably involve a surface. For $FeCl_3$-initiated systems it is best to use a primer prepared from $FeCl_3$ and a small amount of propylene oxide. With this and additional monomer all goes well. The steric repulsion between the methyl groups on the complexed monomer and the terminal residue on the chain (attached to the catalyst) insures that the methyl groups are *trans* to each other in the planar zigzag form of the main chain. Such a propagation leads to an isotactic structure. Although this is the most attractive mechanism, the maintenance of the asymmetric center is difficult to explain. In Figure 58, if bond breaking for the epoxide precedes the attack of the oxygen attached to the metal, extensive racemization should result. In addition, the configuration of the asymmetric centers in the polymer should be opposite that in the monomer [i.e., (*R*) monomer produces polymer with (*S*) units]. Price and Osgan (30,31) suggested that the

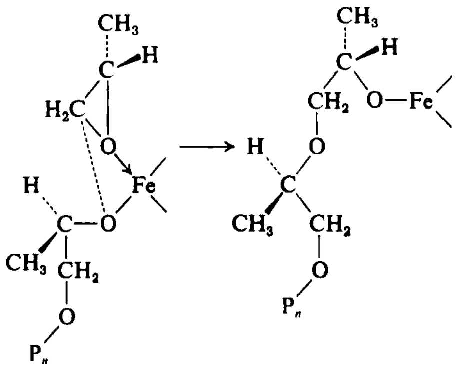

Fig. 59. Mechanism of stereoregular polymerization of propylene oxide as modified by Price and Osgan (30,31).

mechanism shown in Figure 58 could be modified as shown in Figure 59.

A mechanism of this type does not affect the asymmetric center and may be somewhat better in explaining the fact that optically active ferric alkoxides induce asymmetry into the propagating polymer chain. However, it is more difficult to explain the tacticity results, since the steric interactions between the methyl groups on the complexed monomer and the ultimate unit of the chain are mostly absent. One must resort to the orienting force of the heterogeneous catalyst to explain the stereoregulating effect. Gee and his associates (147) isolated adducts of propylene oxide and $FeCl_3$ and found that they have structures consistent with ring opening of the type shown in Figure 58.

Furukawa, Tsuruta, and their co-workers (148,149) extended the work in this area to the use of asymmetric catalysts such as diethylzinc with optically active alcohols (menthols, borneols, 1-methoxypropan-2-ol, and even low molecular weight poly(D-propylene oxide) with hydroxyl end groups), and obtained asymmetric syntheses of the polymers. The latest results (149) demonstrate that the mechanism involves an inversion at each asymmetric center during the insertion of the complexed monomer (Fig. 58).

They demonstrated that the poly(D-propylene oxide)–diethylzinc catalyst picked up the L-propylene oxide from solutions of racemic monomer. Partial racemization and amorphous polymer should therefore be highly probable during these polymerizations since the effect of inversion can never be complete.

VII. SUMMARY AND CONCLUDING REMARKS

This report seeks to outline some fundamentals of polymer stereochemistry. We covered the concepts of tacticity originated over a decade ago by Professor Natta, and extended the presentation to include areas of more complicated order such as di- and tritacticity. Geometric forms for polydienes were also analyzed.

Stereoregular polymers of the vinyl type regardless of tacticity cannot be optically active. However, in the cases where asymmetric centers are included in the side chains of stereoregular vinyl and related polymers, optical activity can be used to deduce very important structural information. It is possible to prepare optically active polymers from suitably substituted 1,3-dienes using optically active initiators. These polymers combine *erythro* and *threo* asymmetry tacticity and the 1,4 geometric forms of poly-1,3-dienes.

Our survey of the types of stereoregular structures included the polybenzofurans and the polybutenomers. These materials prepared by Professor Natta and his associates are in themselves rather special stereoregular materials since they can contain a *cis* or *trans* organization of rings about the main chain.

We then proceeded to examine the consequences of tacticity on the conformational structure of the polymer.

A *trans,gauche* arrangement for an isotactic structure leads to a threefold helix with all staggered bonds. A *trans,trans–gauche,gauche* repeating sequence for an isotactic polymer very quickly forces the polymer to grow back into itself. Therefore one cannot expect an isotactic structure to adopt conformations of this sort. On the other hand, syndiotactic materials can adopt the planar zigzag all *trans* structure or a twofold helical arrangement which is a consequence of *trans,trans–gauche,gauche* repetitions.

Conformational order for stereoregular polymers was also briefly examined using some elements of symmetry. This approach combined with x-ray diffraction results led Professor Natta and his associates to characterize the solid-state conformation of many stereoregular vinyl polymers. Natta and Liquori extended this approach by calculating the energy of steric interactions as a function of rotations about specific main chain bonds. They showed that left- and right-handed 3_1-helices are preferred for isotactic polypropylene while the syndiotactic polypropylene can assume a fully *trans* conformation or the left- or right-handed twofold helices.

These findings are related to the calculation and measurements of dimensions and dipole moments of polymer chains in solution which are discussed as a function of stereoregularity.

Our report continued with a description of the application of nuclear magnetic resonance to the analysis of the tacticity of polymers in solution. Nuclear magnetic resonance provides an absolute measurement of the contributing tactic forms and therefore represents an extremely valuable addition to the x-ray crystallographic technique.

We then attempted to explain the effect of an asymmetric side-chain group on the optical activity of a polymer. It was our postulate that the consequence of asymmetric centers close to the main chain is to limit conformational choices for the main chain. Thus a given configuration in the side chain induces a special conformation for the main chain. A left-handed 3_1-helix may become more preferred than a right-handed 3_1-helix, which leads to enhanced optical activity.

This review also deals with mechanisms of stereoregular polymerizations including α-olefin (Ziegler-Natta type), dienes and polar systems. Concepts of presentation and double bond openings for monomers were extensively considered. In this context, we presented a rather complete analysis for the 1-deuteropropylene polymerization. We were able to explain why an *erythro* diisotactic polydeuteropropylene is obtained from the *cis* monomer while a *threo* diisotactic polymer is obtained from the *trans* monomer. The anionic polymerization of acrylates and methacrylates (monodeuterated in the β carbon) can be examined in a manner similar to the stereochemical analysis of poly-1-deuteropropylene. Although the formalism is similar, the consequences of the mechanism lead to opposite products. A *cis*-acrylate or methacrylate monomer in a hydrocarbon solvent is polymerized to a *threo* diisotactic structure.

It must be emphasized that our approach is fully consistent with modern organic stereochemistry, with the additional restrictions imposed by the chain nature of the molecules. We have concentrated on the implications of structure on mechanism and the consequences of stereoregulation on such properties as optical activity, dipole moment, and NMR spectra. It is this author's hope that the coverage of these aspects of modern synthetic polymer stereochemistry will be useful to the organic and polymer chemist. If successful, it should demonstrate to all interested chemists that the fundamental rules of stereochemistry followed by low molecular weight molecules are also obeyed in polymer systems. The study of the conformations of low molecular weight compounds is in reality one basic support upon which polymer stereochemistry rests.

With the development of new, sophisticated tools, I believe that more detailed microstructural analysis of polymer systems will be possible. High resolution nuclear magnetic resonance instruments with 220 Mc/sec magnets are now being developed. It will be possible through these to see long sequences of the polymer chain. It will prove feasible to analyze many polymer conformations by nuclear magnetic resonance using proper model compounds. Development of highly sensitive dipole moment instrumentation will also be extremely useful to characterize polymers in solution.

In summary, it is my belief that the subject matter covered actually provides the bridge between the work of the low molecular weight organic stereochemist with his rigorous approach and well defined systems, and the biophysicist who deals with complicated biopolymer structures.

Acknowledgment

The author would like to express his deep appreciation for the efforts of Mr. Joseph Falcetta who carefully read and criticized the manuscript, helped design many figures, and checked the references for the chapter.

References

1. K. Ziegler, E. Holzkamp, H. Breil, and H. Martin, *Angew. Chem.*, **67**, 541 (1955).
2. G. Natta, P. Pino, P. Corradini, F. Danusso, E. Mantica, G. Mazzanti, and G. Moraglio, *J. Am. Chem. Soc.*, **77**, 1708 (1955).
3. G. Natta, *Makromol. Chem.*, **16**, 213 (1955).
4. G. Natta, *J. Polymer Sci.*, **16**, 143 (1955).
5. G. Natta and F. Danusso, *J. Polymer Sci.*, **34**, 3 (1959).
6. G. Natta, *Makromol. Chem.*, **35**, 94 (1960).
7. N. G. Gaylord and H. F. Mark, *Linear and Stereoregular Addition Polymers*, Interscience, New York, 1959.

8. M. L. Huggins, G. Natta, V. Desreux, and H. F. Mark, *J. Polymer Sci.*, **56**, 153 (1962).
9. F. A. Bovey, paper presented at Symposium on Macromolecular Chemistry, Prague, 1965; *J. Polymer Sci. C*, in press.
10. G. Natta, M. Peraldo, M. Farina, and G. Bressan, *Makromol. Chem.*, **55**, 139 (1962).
11. B. L. Johnson and M. Goodman, Eds., *Advan. Chem. Ser.*, **52** (1966).
12. F. W. Stavely et al., *Ind. Eng. Chem.*, **48**, 778 (1956).
13. M. Goodman, A. Abe, and Y.-L. Fan, in *Macromolecular Reviews*, Vol. 1, A. Peterlin, S. Okamura, M. Goodman, B. Zimm, and H. Mark, Eds., Interscience, New York, 1966, p. 1.
14. G. Natta, L. Porri, and S. Valenti, *Makromol. Chem.*, **65**, 106 (1963).
15. G. Natta, L. Porri, A. Carbonaro, and G. Lugli, *Chim. Ind.* (*Milan*), **43**, 529 (1961).
16. P. Pino, *Fortschr. Hochpolymer. Forsch.*, **4**, 399 (1966).
17. Reference 16, pp. 400–401.
18. G. Natta, M. Farina, P. Corradini, M. Peraldo, M. Donati, and P. Ganis, *Chim. Ind.* (*Milan*), **42**, 1361 (1960).
19. G. Natta, M. Farina, M. Donati, and M. Peraldo, *Chim. Ind.* (*Milan*), **42**, 1363 (1960).
20. G. Dall'Asta, G. Mazzanti, G. Natta, and L. Porri, *Makromol. Chem.*, **56**, 224 (1962).
21. G. Natta, G. Dall'Asta, G. Mazzanti, and G. Motroni, *Makromol. Chem.*, **69**, 163 (1963).
22. N. Beredjick and C. Schuerch, *J. Am. Chem. Soc.*, **80**, 1933 (1958).
23. G. J. Schmitt and C. Schuerch, *J. Polymer Sci.*, **45**, 313 (1960).
24. G. Natta, M. Farina, M. Peraldo, and G. Bressan, *Chim. Ind.* (*Milan*), **43**, 161 (1961).
25. G. Natta, *Makromol. Chem.*, **43**, 68 (1961).
26. C. L. Arcus, *J. Chem. Soc.* (*London*), **1955**, 2801.
27. C. Schuerch, *J. Polymer Sci.*, **40**, 533 (1959).
28. G. J. Schmitt and C. Schuerch, *J. Polymer Sci.*, **49**, 287 (1961).
29. M. Szwarc, *Fortschr. Hochpolymer. Forsch.*, **4**, 1 (1965).
30. C. C. Price and M. Osgan, *J. Am. Chem. Soc.*, **78**, 4787 (1956).
31. M. Osgan and C. C. Price, *J. Polymer Sci.*, **34**, 153 (1959).
32. J. Furukawa and T. Saegusa, *Polymerization of Aldehydes and Oxides*, Interscience, New York, 1963, p. 196.
33. (a) J. Kleine and H. Kleine, *Makromol. Chem.*, **30**, 23 (1959); (b) R. C. Schultz, and J. Schwaab, *ibid.*, **87**, 90 (1965); (c) M. Goodman and M. D'Alagni, *J. Polymer Sci. B.*, **5**, 515 (1967), in press.
34. L. Pauling and R. B. Corey, *Proc. Natl. Acad. Sci. U.S.*, **37**, 235, 241 (1951).
35. G. Natta et al., *Atti Accad. Nazl. Lincei Rend. Classe Sci. Fis. Mat. Nat.*, **28**, 539 (1960).
36. J. W. L. Fordham, *J. Polymer Sci.*, **39**, 321 (1959).
37. T. S. Shimanouchi and M. Tasumi, *Bull. Chem. Soc. Japan*, **34**, 359 (1961).
38. G. Natta, P. Corradini, and P. Ganis, *J. Polymer Sci.*, **58**, 1191 (1962).

39. (a) W. Cochran, F. H. C. Crick, and V. Vand, *Acta Cryst.*, **5**, 581 (1952); (b) C. W. Bunn and D. R. Holmes, *Discussions Faraday Soc.*, **25**, 95 (1958).
40. (a) P. DeSantis, E. Giglio, A. M. Liquori, and A. Ripamonti, *J. Polymer Sci. A.*, **1**, 1383 (1963); (b) E. B. Wilson, Jr., J. C. Decins, and P. C. Cross, *Molecular Vibrations*, McGraw-Hill, New York, 1955, p. 60.
41. M. M. Kreevoy and E. A. Mason, *J. Am. Chem. Soc.*, **79**, 4851 (1957).
42. G. Natta, *J. Polymer Sci.*, **48**, 219 (1960).
43. T. M. Birshtein and O. B. Ptitsyn (Trans. by S. N. Timasheff and M. J. Timasheff), *Conformations of Macromolecules*, Interscience, New York, 1966.
44. G. Natta, F. Danusso, and G. Moraglio, *Makromol. Chem.*, **20**, 37 (1956).
45. F. Danusso and G. Moraglio, *J. Polymer Sci.*, **24**, 161 (1957).
46. W. R. Krigbaum, D. K. Carpenter, and S. Newman, *J. Phys. Chem.*, **62**, 1586 (1958).
47. L. Trossarelli, E. Campi, and G. Saini, *J. Polymer Sci.*, **35**, 205 (1959).
48. W. R. Krigbaum, J. E. Kurz, and P. Smith, *J. Phys. Chem.*, **65**, 1984 (1961).
49. W. R. Krigbaum and A. Roig, *J. Chem. Phys.*, **31**, 544 (1959).
50. R. Salovey, *J. Polymer Sci.*, **50**, S7 (1961).
51. T. L. Borisova, L. L. Burshtein, and G. P. Mikhailov, *Vysokomolekul. Soedin.*, **4**, 1479 (1962).
52. T. M. Birshtein, *Vysokomolekul. Soedin.*, **5**, 1675 (1963).
53. G. Allegra, P. Ganis, and P. Corradini, *Makromol. Chem.*, **61**, 225 (1963).
54. N. P. Borisova and T. M. Birshtein, *Vysokomolekul. Soedin.*, **6**, 1234 (1964).
55. T. M. Birshtein and O. B. Ptitsyn, *Vysokomolekul. Soedin.*, **2**, 628 (1960).
56. P. J. Flory, V. Crescenzi, and J. E. Mark, *J. Am. Chem. Soc.*, **86**, 146 (1964).
57. (a) P. J. Flory, J. E. Mark, and A. Abe, *J. Am. Chem. Soc.*, **88**, 639 (1966); (b) P. J. Flory and J. D. Baldeschwieler, *ibid.*, **88**, 2873 (1966).
58. F. A. Bovey and G. V. D. Tiers, *J. Polymer Sci.*, **44**, 173 (1960).
59. F. A. Bovey, G. V. D. Tiers, and G. Filipovich, *J. Polymer Sci.*, **38**, 73 (1959).
60. F. A. Bovey and G. V. D. Tiers, *Fortschr. Hochpolymer. Forsch.*, **3**, 139 (1963).
61. F. A. Bovey, International Symposium on Macromolecular Chemistry, Kyoto, Japan, 1966.
62. (a) B. D. Coleman, and T. G Fox, *J. Polymer Sci. A*, **2**, 3183 (1963); (b) R. L. Miller, *J. Polymer Sci.*, **56**, 375 (1962); (c) F. P. Price, *J. Chem. Phys.*, **38**, 1065 (1963); (d) Y. Ohsumi, T. Higashimura, and S. Okamura, *J. Polymer Sci. A*, **3**, 3729 (1965); (e) T. Tsuruta, T. Makimoto, and H. Kanoi, *J. Macromol. Chem.*, **1**, 31 (1966).
63. F. A. Bovey, in *Polymer Handbook*, J. Brandrup and E. H. Immergut, Eds., Interscience, New York, 1965, p. v–27.
64. F. C. Stehling, *J. Polymer Sci. A*, **2**, 1815 (1964).
65. (a) T. Yoshino and J. Komiyama, *J. Polymer Sci. B*, **3**, 311 (1965); (b) K. Mislow and M. Raban, in *Topics in Stereochemistry*, Vol. 1, N. L. Allinger and E. L. Eliel, Eds., Interscience, New York, 1967, p. 1.

66. (a) G. Natta, P. Corradini, I. W. Bassi, and L. Porri, *Atti Accad. Nazl. Lincei, Rend., Classe Sci. Fis. Mat. Nat.*, **24**, 121 (1958); (b) M. Farina and G. Bressan, we wish to thank Dr. Farina for sending us a preprint of his paper which will appear in an edited volume on polymer chemistry.
67. M. Goodman and A. Abe, *J. Polymer Sci.*, **59**, S37 (1962).
68. A. Abe and M. Goodman, *J. Polymer Sci. A*, **1**, 2193 (1963).
69. M. Goodman, K. G. Clarke, M. A. Stake, and A. Abe, *Makromol. Chem.*, **72**, 131 (1964).
70. D. Basagni, A. M. Liquori, and B. Pispisa, *J. Polymer Sci. B*, **2**, 241 (1964).
71. G. P. Lorenzi, E. Benedetti, and E. Chiellini, *Chim. Ind.* (*Milan*), **46**, 1474 (1964).
72. P. Pino and G. P. Lorenzi, *Makromol. Chem.*, **47**, 242 (1961).
73. P. Pino, G. P. Lorenzi, and E. Chiellini, *International Symposium on Macromolecular Chemistry Prague 1965* (*J. Polymer Sci. C*, **16**), O. Wichterle and B. Sedláček, Chairmen, Interscience, New York, 1967, p. 455.
74. M. Goodman and Y.-L. Fan, *J. Polymer Sci.*, in press.
75. J. H. Brewster, *J. Am. Chem. Soc.*, **81**, 5475 (1959).
76. Reference 16, p. 445–447.
77. P. Pino, F. Ciardelli, G. P. Lorenzi, and G. Natta, *J. Am. Chem. Soc.*, **84**, 1487 (1962).
78. P. Pino, F. Ciardelli, and G. P. Lorenzi, *J. Am. Chem. Soc.*, **85**, 3888 (1963).
79. P. Pino, F. Ciardelli, and G. P. Lorenzi, *Makromol. Chem.*, **70**, 182 (1964).
80. C. F. H. Bawn and A. Ledwith, *Quart. Rev.* (*London*), **16**, 361 (1962).
81. M. Goodman, J. Brandrup, and H. F. Mark, in *Crystalline Olefin Polymers*, Part I, R. A. V. Raff and K. W. Doak, Eds., Interscience, New York, 1965, Chap. 4.
82. H. W. Coover, R. L. McConnell, and F. B. Joyner, *Macromolecular Reviews*, Vol. 1, Interscience, New York, 1966, p. 91.
83. J. Boor, Jr., *Macromolecular Reviews*, Vol. 2, A. Peterlin, S. Okamura, M. Goodman, B. Zimm, and H. Mark, Eds., Interscience, New York, 1967, p. 115.
84. G. Natta, *Soc. Petrol. Engrs.*, **3**, 99 (1963).
85. Montecatini Societa Generale per L'Industria Mineraria e Chimica, Brit. Pat. 916,643 (1963).
86. G. Natta, I. Pasquon, and A. Zambelli, *J. Am. Chem. Soc.*, **84**, 1488 (1962).
87. A. Zambelli, G. Natta, and I. Pasquon, in *International Symposium on Macromolecular Chemistry, Paris, 1963*, Part I, M. Magat, Ed. (*J. Polymer Sci. C*, **4**), Interscience, New York, 1964, p. 411.
88. G. Natta, *Experientia*, **19**, 609 (1963).
89. G. Natta, *Science*, **147**, 261 (1965).
90. F. W. Breuer, L. E. Geipel, and A. B. Loebel, in *Crystalline Olefin Polymers*, Part I, R. A. V. Raff and K. W. Doak, Eds., Interscience, New York, 1965, Chap. 3.
91. H. N. Friedlander, in *Crystalline Olefin Polymers*, Part I, R. A. V. Raff and K. W. Doak, Eds., Interscience, New York, 1965, Chap. 6.
92. C. A. Luckach and H. M. Spurlin, in *Copolymerization*, G. E. Ham, Ed., Interscience, New York, 1964, Chap. IVA, p. 115.

93. G. Bier and G. Lehmann, in *Copolymerization*, G. E. Ham, Ed., Interscience, New York, 1964, Chap. IVB p. 149.
94. G. Crespi, A. Valvassori, and G. Sartori, in *Copolymerization*, G. E. Ham, Ed., Interscience, New York, 1964, Chap. IVD, p. 275.
95. K. W. Doak and A. Schrage, in *Crystalline Olefin Polymers*, Part I, R. A. V. Raff and K. W. Doak, Eds., Interscience, New York, 1965, Chap. 8.
96. P. Cossee, *Trans. Faraday Soc.*, **58**, 1226 (1962).
97. E. J. Arlman and P. Cossee, *J. Catalysis*, **3**, 99 (1964).
98. F. Pattat and H. Sinn, *Angew. Chem.*, **70**, 496 (1958).
99. W. L. Carrick, *J. Am. Chem. Soc.*, **80**, 6455 (1958).
100. E. Youngman, and J. Boor, Jr., in *Macromolecular Reviews*, Vol. 2, A. Peterlin, S. Okamura, M. Goodman, B. Zimm, and H. Mark, Eds., Interscience, New York, 1967, p. 33.
101. G. Natta and L. Porri, *Advan. Chem. Ser.*, **52**, 24 (1966).
102. S. Patai, Ed., *The Chemistry of Alkenes*, Interscience, New York, 1964, Chaps. 8 and 9.
103. C. G. Overberger, J. E. Mulvaney, and A. M. Schiller, in *Encyclopedia of Polymer Science and Technology*, Vol. II, H. F. Mark, N. G. Gaylord, and N. M. Bikelas, Eds., Interscience, New York, 1965, p. 95.
104. K. Ziegler, L. Jakob, H. Wollthau, and A. Wenz, *Ann. Chem.*, **511**, 64 (1934).
105. B. S. Garrett et al., *J. Am. Chem. Soc.*, **81**, 1007 (1959).
106. T. G Fox et al., *J. Am. Chem. Soc.*, **80**, 1768 (1958).
107. W. E. Goode, F. H. Owens, R. P. Fellman, W. H. Snyder, and J. E. Moore, *J. Polymer Sci.*, **46**, 317 (1960).
108. (a) J. W. L. Fordham, *J. Polymer Sci.*, **41**, 73 (1959); (b) F. A. Bovey and G. V. D. Tiers, *Chem. Ind.* (*London*), **1962**, 1826.
109. R. G. J. Miller, B. Mills, P. A. Small, A. Turner-Jones, and D. G. M. Wood, *Chem. Ind.* (*London*), **1958**, 1323.
110. H. Sobue, K. Matsuzaki, and S. Nakano, *J. Polymer Sci. A*, **2**, 3339 (1964).
111. K. Liu, J. S. Lignowski, and R. Ullman, *Polymer Preprints*, **6**, No. 2, 904 (1965).
112. M. L. Miller and C. E. Rauhut, *J. Am. Chem. Soc.*, **80**, 4115 (1958).
113. M. L. Miller and C. E. Rauhut, *J. Polymer Sci.*, **38**, 63 (1959).
114. D. J. Attfield, K. Butler, A. T. Radcliffe, P. R. Thomas, R. A. Thompson, and G. J. Tyler, *Chem. Ind.* (*London*), **1960**, 263.
115. K. Butler, P. R. Thomas, and G. J. Tyler, *J. Polymer Sci.*, **48**, 357 (1960).
116. G. Natta, G. Mazzanti, P. Corradini, and I. W. Bassi, *Makromol. Chem.*, **37**, 156 (1960).
117. G. Natta, P. Corradini, and I. W. Bassi, *J. Polymer Sci.*, **51**, 505 (1961).
118. C. E. Schildknecht, S. T. Gross, H. R. Davidson, J. M. Lambert, and A. O. Zoss, *Ind. Eng. Chem.*, **40**, 2104 (1948).
119. G. Natta, I. W. Bassi, and P. Corradini, *Makromol. Chem.*, **18**, 455 (1955).
120. I. W. Bassi, G. Dall'Asta, U. Campigli, and E. Strepparola, *Makromol. Chem.*, **60**, 202 (1963).
121. S. Okamura, T. Kodama, and T. Hiyashimura, *Makromol. Chem.*, **53**, 180 (1962).
122. M. Goodman and Y.-L. Fan, *J. Am. Chem. Soc.*, **86**, 4922 (1964).

123. M. Goodman and Y.-L. Fan, *J. Am. Chem. Soc.*, **86**, 5712 (1964).
124. W. H. Watanabe, C. F. Ryan, P. C. Fleisher, Jr., and B. S. Garrett, *J. Phys. Chem.*, **65**, 896 (1961).
125. A. M. Liquori, G. Anzuino, V. M. Coiro, M. D'Alagni, P. DeSantis, and M. Savino, *Nature*, **206**, 358 (1965).
126. D. J. Cram and K. R. Kopecky, *J. Am. Chem. Soc.*, **81**, 2748 (1959).
127. D. J. Cram, *J. Chem. Educ.*, **37**, 317 (1960).
128. (a) D. L. Glusker, E. Stiles, and B. Yoncoskie, *J. Polymer Sci.*, **49**, 297 (1961); (b) D. L. Glusker, I. Lysloff, and E. Stiles, *J. Polymer Sci.*, **49**, 315 (1961).
129. C. Schuerch, W. Fowells, A. Yamada, F. A. Bovey, F. P. Hood, III, and E. W. Anderson, *J. Am. Chem. Soc.*, **86**, 4481 (1964).
130. T. Yoshino, J. Komiyama, and M. Shinomiya, *J. Am. Chem. Soc.*, **86**, 4482 (1962).
131. T. Yoshino, M. Shinomiya, and J. Komiyama, *J. Am. Chem. Soc.*, **87**, 387 (1965).
132. T. Yoshino and K. Kuno, *J. Am. Chem. Soc.*, **87**, 4404 (1965).
133. T. Yoshino and J. Komiyama, *J. Am. Chem. Soc.*, **88**, 176 (1966).
134. T. Yoshino, Y. Kikuchi, and J. Komiyama, *J. Phys. Chem.*, **70**, 1059 (1966).
135. F. A. Bovey, F. P. Hood, III, E. W. Anderson, and L. C. Snyder, *J. Chem. Phys.*, **42**, 3900 (1965).
136. D. Doskocilova, *J. Polymer Sci. B*, **2**, 421 (1964).
137. D. Doskocilova and B. Schneider, *Collection Czech. Chem. Commun.*, **29**, 2290 (1964).
138. P. E. McMahon and W. C. Tincher, *J. Mol. Spectr.*, **15**, 1800 (1965).
139. T. Shimanouchi, paper presented at Main Lecture, International Symposium on Macromolecular Chemistry, IUPAC, Prague, 1965.
140. D. Doskocilova, S. Sykora, H. Pivcova, B. Obereigner, and D. Lim, Preprints of Scientific Papers, International Symposium on Macromolecular Chemistry, Kyoto, Japan, 1966, Paper 2-5-07.
141. C. E. Schildknecht, A. O. Zoss, and C. McKinley, *Ind. Eng. Chem.*, **39**, 180 (1947).
142. M. E. Pruitt and J. M. Baggett, U.S. Pat. 2,706,181 (1955).
143. J. Furukawa, S. Akutsu, and T. Saegusa, *Makromol. Chem.*, **94**, 68 (1966).
144. S. Inoue, T. Tsuruta, and J. Furukawa, *Makromol. Chem.*, **53**, 215 (1962).
145. T. Tsuruta, S. Inoue, N. Yoshida, and J. Furukawa, *Makromol. Chem.*, **55**, 230 (1962).
146. T. Tsuruta, S. Inoue, M. Ishimori, and N. Yoshida, *J. Polymer Sci. C*, **4**, 267 (1963).
147. R. O. Colclough, G. Gee, W. C. E. Higginson, J. B. Jackson, and M. Litt, *J. Polymer Sci.*, **34**, 171 (1959).
148. S. Inoue, Y. Yokota, N. Yoshida, and T. Tsuruta, *Makromol. Chem.*, **90**, 131 (1966).
149. J. Furukawa, T. Saegusa, S. Yasui, and S. Akutsu, *Makromol. Chem.*, **94**, 74 (1966).

Topics in Stereochemistry, Volume 2
Edited by Norman L. Allinger, Ernest L. Eliel

Steric Course of the Kinetic 1,2 Addition of Anions to Conjugated Cyclohexenones

EDMOND TOROMANOFF

Centre de Recherches Roussel-Uclaf,
Romainville, France

I. THE KINETIC 1,2 ADDITION OF ANIONS TO CONJUGATED CYCLOHEXENONES (1)

A. Introduction

The prospect of understanding and thus being able to predict the steric course of 1,2 anion additions to conjugated cyclohexenones is very attractive to any organic chemist involved in synthetic work, since the resulting allylic alcohols are compounds of choice for carrying out stereospecific reactions (2).

In the reduction of cyclohexenones by complex hydrides, the major reaction products can often be predicted by Barton's rule (3), which suggests that reduction with sodium borohydride and with lithium aluminum hydride, in general, affords the equatorial epimer if the ketone is unhindered, and the axial epimer if it is hindered or very hindered. This rule usually gives better predictions with conjugated cyclohexenones than with the corresponding saturated cyclohexanones for which, apparently, it was primarily designed; however, in a few cases where the rule fails, the experimental results in the corresponding saturated and unsaturated series are nearly the opposite (Table I). It was felt that the difference in behavior between the cyclohexenones and the corresponding saturated compounds had to be connected with the peculiar properties of the unsaturated ring, since the introduction of an ethylenic bond into a cyclohexanone alters the chair geometry of the ring (4,5), and imparts special electronic demands on any reaction

TABLE I

Lithium Aluminum Hydride Reduction of Some Steroidal Ketones (5α Series)

Steroid	Major alcohol of reduction	Refs.
Cholestane-1-one	1α-OH (≃65%)	6
Δ^2-Cholestene-1-one	1β-OH (>70%)	7
Cholestane-4-one	4β-OH (>85%)	8
Δ^5-Cholestene-4-one	4α-OH (>95%)	5,8
Cholestane-6-one	6β-OH (>90%)	9
Δ^4-Cholestene-6-one	6α-OH (>90%)	5,8

affecting either the ketone or the conjugated olefinic bond. Hence with respect to cyclohexanones, the reduction or, more generally, the addition of anions to cyclohexenones, should evince some special features as evidenced by the comparison of the results in Table I.

It is therefore our purpose to give here an interpretation of the experimental results concerning the kinetic 1,2 addition of anions to α,β-unsaturated cyclic ketones, based on a few simple hypotheses about the role of steric and electronic factors. We do not intend to give an exhaustive review of the subject but rather to give the principles which can be used to interpret or predict the results of hydride ion or carbanion 1,2 addition to any conjugated cyclohexenone.

First it is necessary to start with an inventory of what is taken for granted and what is really known about the factors involved in the 1,2 addition of anions to α,β-unsaturated cyclohexenones.

B. Shapes of Molecules and Factors Involved in the Reaction

1. Steps of the Reaction

The 1,2 addition of anions to unsaturated ketones can be depicted as proceeding through the steps of Figure 1 in which only the probable conformations of the starting ketone and the final product are known with some degree of accuracy.

In agreement with general principles of stereochemistry (4,10) we admit the existence of the starting unsaturated ketone either in its most stable conformation if there is only one, or as a mixture of conformers in equilibrium if several stable conformations are allowed.

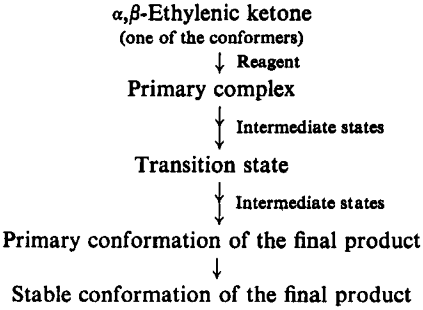

Fig. 1. 1,2 Addition of anions to unsaturated ketones.

In the same way one can guess what the stable conformation of the final product looks like, but at this point we are only interested in the primary conformation of the final product as it results from the 1,2 addition of the reagent to the starting ketone. Although not necessarily the stable one, this primary conformation of the final product has an obvious bearing on the energy level of the transition state, since the latter can be connected with the ease of going from a conformation of the starting ketone to the corresponding primary product of reaction.

To arrive at an understanding of the course of the reaction we have to reach a more precise idea of the primary conformation of the final product; as will be shown later, this necessarily involves a hypothesis about the direction of steric approach of the reagent with regard to the ketone.

Insufficient as all this may seem, we know even less about the geometry or the stereoelectronic requirements of the primary complex of the ketone with the reagent. This lack of information makes more difficult any quantitative evaluation of the energy level of the transition state, and makes unlikely for the time being a computed prediction of the steric course of the kinetic addition of an anion to a conjugated cyclohexenone.

2. *Stable Conformations of Cyclohexenones*

X-ray analysis of the crystal structures of various natural products [5-bromogriseofulvin (11), cedrelone iodoacetate (12), ecdysone (13), etc.] containing cyclohexenone systems is a very valuable source of information about the stable conformations of cyclohexenones in the solid state.

The conformations of cyclohexenones dissolved in organic solvents are not so well known (14,15). There are few experimental results whose reliability cannot be questioned. Thus, although numerous physical studies show unequivocally that in most cases the ketone and the conjugated olefinic bond do not lie in the same plane (16,17), there has been no precise method available up to the present for the determination of the angular twist between the planes of the two chromophores (cf. the approximations made in the evaluation of the angular skewness of Δ^4-cholestene-6-one in ref. 18). Nor does it seem possible to connect with certainty the extent of angular twist measured from Dreiding models, with the real value which could eventually be calculated from the appropriate physical measurements of circular dichroism, optical rotatory dispersion, nuclear magnetic resonance, etc. However, it has to be said that the frequent existence of several conformers in solution does not simplify the problem.

We assume that the most stable conformations of cyclohexenones are analogous to those of the corresponding cyclohexene derivatives, taking into account a further flattening of the cyclohexene ring under the influence of the additional trigonal carbon. Concerning the conformations of cyclohexene, it was first noted by Bucourt and Hainaut (19) that only the half-chair form corresponds to an energy minimum, while the other forms correspond to pseudo-rotational motions but not to energy minima. When the cyclohexene is fused to another ring, there are ordinarily found two energy minima which correspond to the half-chair and the 1,2 diplanar forms. Although frequently mentioned in the literature, the boat (usually called half-boat) is the least stable form in almost all cases, because it is not located at an energy minimum but occurs on the side of the pseudorotational potential curve. In the following we adopt for the conformers of equatorially substituted cyclohexenones, the order of decreasing stabilities that was given by Bucourt and Hainaut (19) for the various conformations of the unsubstituted cyclohexene (Table II), namely:

$$\begin{array}{c}\text{monoplanar}\\ \text{(half-chair)}\end{array} > \begin{array}{c}\text{1,2 diplanar}\\ \text{(also called envelope, sofa)}\end{array} > \text{1,3 diplanar} > \text{1,4 diplanar (boat)}$$

For example, in the case of 3-keto-Δ^4-unsaturated steroids the conformational equilibrium in solution will involve (Fig. 3, Sect. II-B-2) a population of half-chair (major component) and 1,2 diplanar form (minor component) and only minute amounts, if any, of either 1,3 diplanar or boat forms. Because of their high energetic content (19) the 1,3 diplanar form and especially the boat can be neglected, especially in our simplified treatment (20). From a practical standpoint, the 1,2 diplanar form (which will be called diplanar for short) in which carbons 1,10 and 4,5 of the double bond are coplanar, can easily be differentiated from the half-chair, where the dihedral angle (1,10–4,5) is around 15°, with the help of Dreiding models.

While the above order of stability of cyclohexenone conformers appears qualitatively valid in most cases, it should be kept in mind that the nature of the solvent and the choice of experimental conditions (temperature, concentration, etc.) are able to induce a more or less

TABLE II

Conformations of Cyclohexene (19)

Name	Structure	Features
Monoplanar (half-chair)	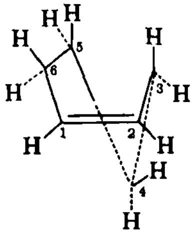	Carbons 6,1,2,3, coplanar; carbon 4 and carbon 5 below and above this plane, respectively (or the reverse)
1,2 Diplanar (envelope, sofa)	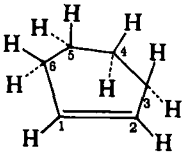	Carbons 6,1,2,3 and 1,2,3,4 in the same plane; carbon 5 above (or below) this plane; five consecutive carbons (6,1,2,3,4) coplanar
1,3 Diplanar	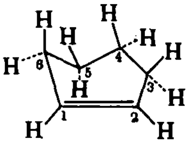	Carbons 6,1,2,3 and 2,3,4,5 in two different planes; two sets of four consecutive carbons coplanar with two common consecutive carbons
1,4 Diplanar (boat, usually called half-boat in the literature)	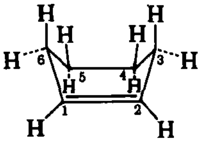	Carbons 6,1,2,3 and 3,4,5,6 in two different planes; both carbons 3 and 6 above (or below) the 1,2,4,5 plane; two sets of four consecutive carbons coplanar with two common carbons at their ends

pronounced shift in the equilibrium of conformers. Besides, the size of the reagent (tri-*t*-butoxyaluminohydride vs. lithium aluminum hydride for instance) also plays a noticeable but not dominant part.

3. *Steric Direction of Anionic Approach to the Ketone*

The reaction takes place only if the reagent is able to come within bonding distance of the ketone. Moreover, if we want to define the shape of the primary complex and the shape of the primary conformation of the final product, we have to advance a hypothesis about the direction of steric approach of the reagent to the ketone, or more specifically, to the plane of the substituents of the ketone. With respect to the latter plane, the reagent can come from either direction, provided there is no steric hindrance to its approach. We will assume then, that there is a preferential approach of the anionic part of the reagent to the ketone along an axis passing through the trigonal carbon of the ketonic group and perpendicular to the plane of the substituents of the ketone (21). This assumed perpendicular addition of the anion to the ketone allows us to qualitatively appreciate the steric factors which can hinder or even prevent the formation of the primary complex in any part of the space. In the following, we identify the bulk of the reagent with that of the corresponding anion; this is only a rough approximation whose validity will be gauged in due course.

4. Stereoelectronic Requirements of Intermediate and Transition States

Following the progress of the reaction (Fig. 1) there is, first, a perpendicular approach of the anionic part of the reagent towards the trigonal carbon of the ketone to form the primary complex in which, as we see it, there are only weak deformations of the valency angles of the ring in comparison with those of the starting unsaturated ketone. Then, through an infinity of intermediate states this primary complex reaches an energy maximum represented by the transition state. Again through an infinity of intermediate states, the transition state gives way to the primary conformation of the final product. During the whole evolution of the primary complex, the olefinic bond imposes two requirements. The first requirement is steric: the double bond maintains the coplanarity of this part of the molecule. The second requirement is electronic in nature: the orbital of the anion should maximally overlap with the orbitals of the double bond (22–25, ref. 22 gives an early application of this concept).

We are thus led to make the following postulate: the perpendicular addition of the anion to the trigonal carbon of the ketone will take place selectively on the conformation of lowest energy among all those of the various authorized transition states allowing a maximum, unbroken overlap of the anionic orbital with the orbitals of the ethylenic bond.

This assumption leads us to a simple prediction of the major product of reaction for it allows us to establish a relationship between the energy of the allowed transition state and the energies of the conformations, on the one hand, of the starting ketone and, on the other hand, of the primary final product, both of which we can qualitatively estimate (26, 27).

In the next section we shall examine the *kinetic* 1,2 addition of hydride anion, and in a later section the addition of carbanions from organometallics to α,β-unsaturated six-membered cyclic ketones.

II. THE KINETIC REDUCTION OF CONJUGATED CYCLOHEXENONES BY COMPLEX HYDRIDES

A. Introduction

To interpret or predict the results of the reduction of any α,β-unsaturated cyclohexenone by lithium aluminum hydride and related hydrides (such as lithium alkoxyaluminohydrides in various solvents) or by alkaline borohydrides in anhydrous or aqueous alcohols, one has to evaluate, at least qualitatively, the respective importance of the steric and electronic factors involved in the reaction. An estimation of the relative value of these factors can be reached conveniently through an analysis of the reduction of unhindered and hindered ketones which we shall examine separately and successively. Since the notion of a hindered ketone is hardly a clear one, let us begin by defining it. We refer to a hindered ketone with respect to a reagent when the progression of the perpendicular approach of this reagent to within bonding distance of the ketone in one of its conformations is delayed or stopped because of severe non-bonded interactions between individual atoms of the reagent and atoms of the unsaturated compound, in the vicinity of the ketone. The steric compression, resulting from nonbonded interactions, can show up in two ways. (*1*) Either the primary complex cannot be formed at all, because of strong interactions of the 1,3-diaxial type for instance, or (*2*) the formation of the complex actually takes place, but the latter does not progress further, for the energy of the corresponding transition state is too high. Although it will be detailed later (Sects. II-C and III) it is necessary to insist first on the idea that the hindrance is only relative to a given reagent and, second, that it generally varies with the various conformers of a cyclohexenone; this is rather obvious if conformationally mobile cyclohexenones are envisioned (cf. Sect. II-D).

B. Reduction of Unhindered Unsaturated Ketones

For unhindered conjugated cyclohexenones for which the perpendicular approach of the hydride ion to the ketone is free of nonbonded interactions, a simple correlation can be drawn between the energy levels of the conformations of the initial and primary final states on the one hand, and of the conformation of the transition state on the other hand. This can be stated as the following rule. Whenever possible, the reduction of unhindered cyclohexenones occurs through a pre-half-chair intermediate (28) or, for lack of it, through a pre-diplanar intermediate (28).* In other words, the major product of the kinetic reduction of a conjugated cyclohexenone corresponds to the addition of hydride ion to the conformation of the starting unsaturated ketone of lowest energy, and from the same side as the axial hydrogen of the saturated carbon of the ring β to the ketone.

The practical application of this general rule, whose justification will be given in Section II-B-2, must take into account whether the unsaturated ring is able to adopt either a single or several preferred conformations of low energy.

1. Single Conformation

If the ketonic ring can have only one conformation of low energy such as a half-chair or a diplanar form (the other possible form being, then, a boat of much higher energy), the kinetic addition of hydride ion will take place mainly, if not exclusively, on the energetically preferred conformation and from the same side as the β axial hydrogen. A few typical examples are given in Figure 2.

---

*The words pre-half-chair and pre-diplanar (short for pre-1,2 diplanar) are used here in complete analogy with the words pre-chair and pre-boat as defined in ref. 28. In other words, when speaking of a pre-half-chair or pre-diplanar intermediate, we mean the transition state corresponding to the formation of this primary conformation of the final product.

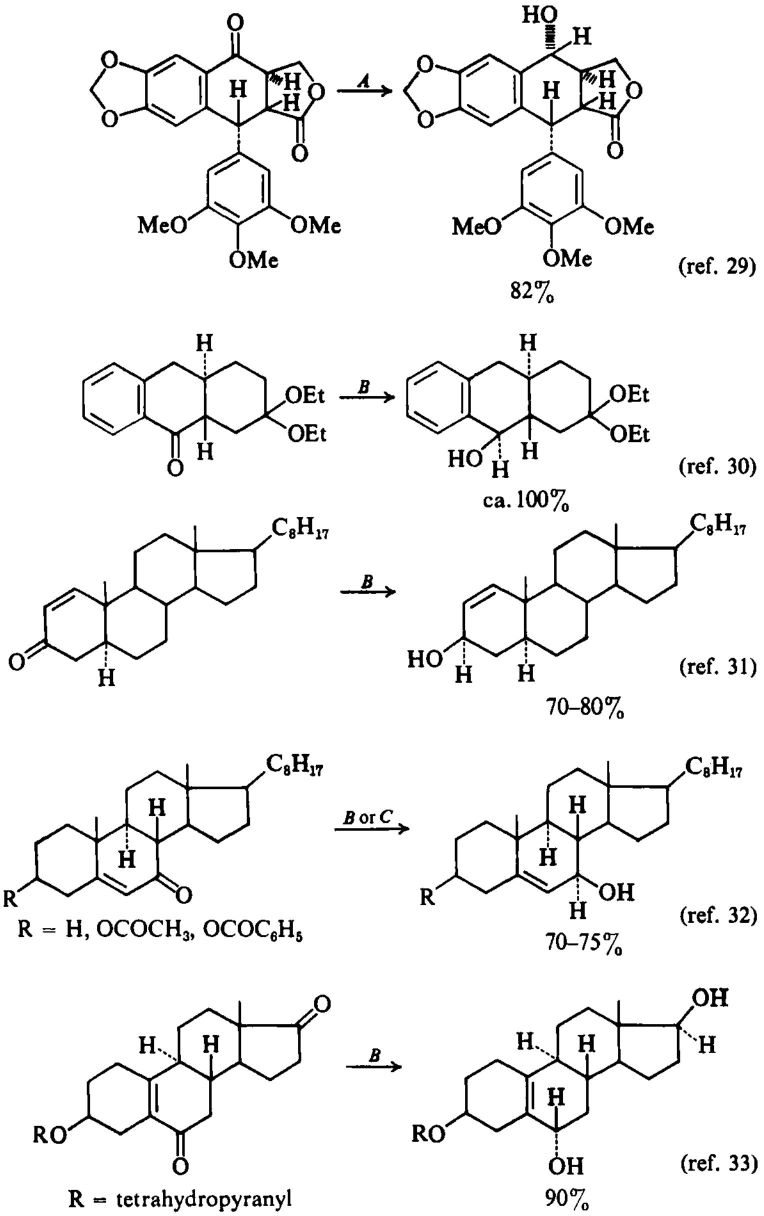

Fig. 2. Reduction of unhindered unsaturated ketones. Reagents: *A*, $(BH_4)_2Zn$; *B*, $LiAlH_4$; *C*, BH_4Na.

2. *Several Conformations*

If the ring is able to adopt several conformations of comparable energies, an equilibrium exists between the various conformers. In such cases one can expect from the reduction of the unsaturated ketone a mixture of epimeric allylic alcohols whose relative proportions will depend only to a minor degree on the experimental conditions (solvent, temperature, size of the hydride donor etc.). This fairly frequent case will be examined in detail, selecting as a typical example the reduction of 3-keto-Δ^4-steroids (Fig. 3).

a. Analysis of the Hydride Reduction of 3-Keto-Δ^4-Steroids. As shown in Figure 3, besides its two conformations of low energy (the half-chair I and the diplanar form II), ring A of 3-keto-Δ^4-steroids may also exist in the boat conformation III of much higher energy, which can therefore be neglected to a first approximation.* Each conformer (I or II) could give rise to the formation of two primary complexes, one on the α side and the other on the β side of the molecule. However, with the previously advanced hypotheses, which assumed in particular a maximum overlapping of the hydride orbital with those of the ethylenic bond from the formation of the complex up to the final primary product, there is only one allowed transition state for each conformer, namely T_1 for conformer I and T_2 for conformer II.

Transition state T'_2 is not allowed since it gives way to the primary conformation of the final product with an axial 3β-hydroxyl; this implies a breaking of the orbital overlap at some moment and thus it is in contradiction with our initial postulate. In this connection, the formation of the primary complexes leading to not-allowed T'_1 or T'_2 states would correspond to intermediates of very high energy, as can be recognized if one tries with Dreiding models to introduce in position 3 of the steroid a tetrahedral carbon whose C—H bond remains roughly parallel to the orbitals of the ethylenic bond, while maintaining the initial conformation of the starting ketones.

Under these conditions only the allowed transition states pre-half-chair T_1 or pre-diplanar T_2 have to be taken into account. Since conformer I has a lower energy content than II and the same relationship holds true for the corresponding primary product of reduction, we assume that the energy of transition state T_1 is below the energy of

---

* To simplify the discussion, the 1,3 diplanar form has been omitted. Since its energy is close to that of the boat it does not significantly alter our conclusions.

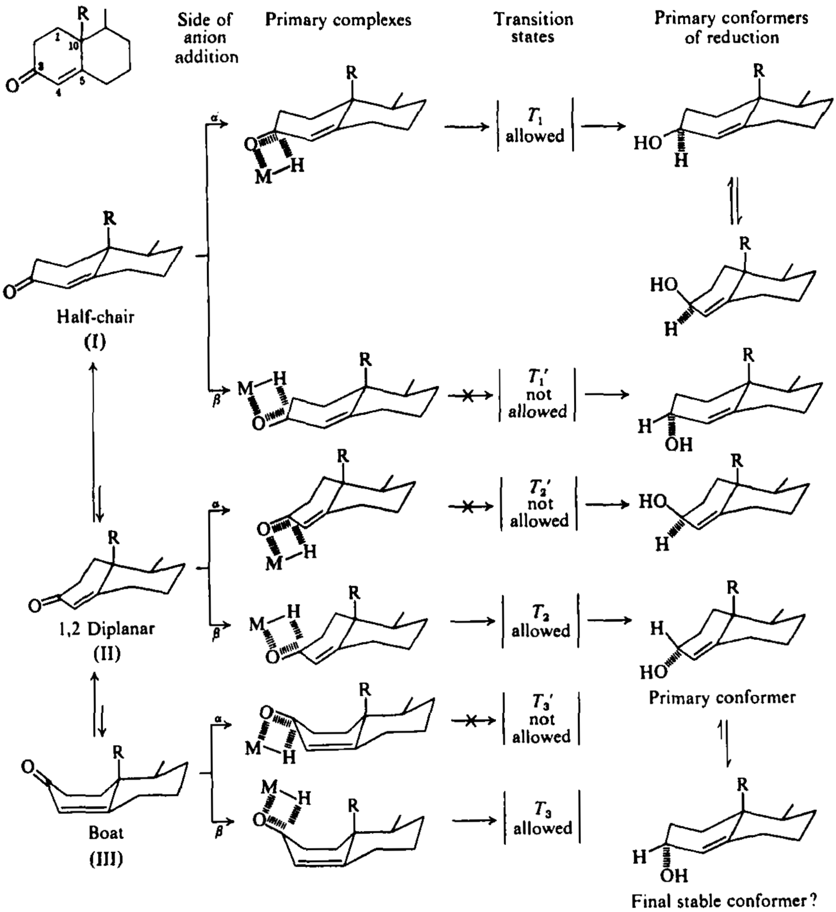

Figure 3

transition state T_2 (for a similar mode of analysis in connection with the stereochemistry of the Michael addition reaction see 34). Therefore, the major product of reduction should correspond to T_1, which is in good agreement with the experimental results; the allylic 3β-hydroxyl represents 70–90% of the mixture of isomers (35).

At this point it is important to focus attention on the fact that passage of I to its primary product of reduction through T_1 and of II to the corresponding primary product of reduction through T_2 takes place with the minimum extent of deformation with respect to the dihedral angles of the starting conformers of the α,β-unsaturated ketone. The whole sequence thus appears very favorable from an energetic point of view (36,37). Ref. 37 gives another application of the principle of minimum deformation to the reduction of cyclic six-membered imines and immonium salts with complex hydrides.

b. Factors that Influence the Conformational Equilibrium of 3-Keto-Δ^4-Steroids. Several conclusions can be drawn from the interpretation given for the reduction of 3-keto-Δ^4-steroids, which appear to be generally applicable to the reduction of all unhindered conjugated cyclohexenones, including the conformationally mobile cyclohexenones treated in Section II-D.

Since the most stable primary conformer of the final product corresponds, through the most favorable transition state, to the most stable conformation of the starting unsaturated ketone, it can be said that the reduction of unhindered, unsaturated, cyclic ketones reflects the equilibrium of the starting conformers. Therefore it seems worthwhile to critically examine the various factors which are able to induce a shift of this equilibrium. While briefly reviewing these factors for the case of 3-keto-Δ^4-steroids we shall endeavor to link the empirical results with existing physical data.

(1) Influence of Substituents of Ring A. A 2α substituent should stabilize the half-chair while destabilizing the diplanar form; conversely a 2β substituent should destabilize the half-chair but stabilize the diplanar conformer (38). (We believe that the so-called "twist" form attributed in ref. 38 to the A ring of 2β-methyl-19-nortestosterone is identical to our 1,2 diplanar form.) The bulkier the substituent, the more pronounced will be the stabilizing effect on the conformation: a phenyl more than a methyl, a methyl more than a hydroxyl. However, even a hydroxyl, an acetoxyl, or a halogen at position 2 of a 3-keto-Δ^4-steroid appears to yield a stabilizing influence on the half-chair or diplanar conformer of ring A. Indeed, it has been noted several times (39–43) that with respect to the unsubstituted parent compounds or to the 2α-hydroxy, 2α-acetoxy, or 2α-halogeno substituted compounds, where ring A very likely exists in the half-chair conformation, the 2β-hydroxy, 2β-acetoxy or 2β-halogeno-3-keto-Δ^4-unsaturated steroids exhibited a special spectral behavior which was ascribed to a conformational change of ring A. We believe this change actually takes

place, ring A no longer being in the half-chair, but rather in its diplanar conformation. In this event, the hydride reduction of a 2β-substituted 3-keto-Δ^4-steroid should lead mainly to a 3α-oriented allylic hydroxyl, and the bulkier the substituent, the more pronounced the effect. Admittedly chemical evidence for this latter point is lacking, while as expected, the *trans*-2α,3β-diol appears to be the major product of hydride reduction of a 2α-acetoxy-3-keto-Δ^4-unsaturated steroid (44); the course of hydride addition is the same as that of the unsubstituted parent compound.

In the absence of steric interference with the 11α-hydrogen, it is expected that a substituent at position 1, a methyl for example, would induce shifts of the conformational equilibrium exactly opposite to those induced by a 2-methyl of the same orientation. In fact from the models, and in agreement with the interpretation of physical data (45,46), it would appear that to avoid any severe nonbonded interaction with the 11α-hydrogen, a methyl at position 1 generally stays axial either in the β orientation on a diplanar form, or in the α orientation on a half-chair. Since we are dealing now with conformations of hindered ketones, we can no longer apply the former rules to predict the major product of reduction.

However, insofar as the 1-methyl remains axial on the half-chair or diplanar conformation, it can be predicted on steric grounds which will be detailed in Section II-C, that the main reduction products of epimeric 1-methyl-3-keto-Δ^4-steroids will be the 3α-allylic hydroxyl for the α-isomer, and the epimeric 3β-allylic hydroxyl for the β-isomer. A quantitative study of the products of reduction of epimeric 1-methyl 3-keto-Δ^4-steroids would enable us to assess the relative importance of steric and conformational factors.

(2) Correlation with Physical Data. The former predictions concerning the course of the kinetic reduction of 3-keto-Δ^4-steroids substituted on the A ring are qualitatively in agreement with the physical data of the literature which have been widely interpreted (43,47–50) as indicating the existence of a conformational equilibrium and the shift of such an equilibrium under the influence of a suitably oriented substituent at positions 1, 2, or 6.

However, these sometimes contradictory indications stem from more or less valid interpretations of physical measurements where steric and conformational effects often have not been cleanly separated from electronic effects. Due to the existence in solution of several conformers with different optical contributions, a slight shift of the equilibrium changing the population of a conformer with an important contribution, can make it appear that the ring has undergone a complete conformational change, while actually this may be only a change in the conformational equilibrium. In this respect the results of the reduction of 3-keto-Δ^4-steroids by complex hydrides can be presented as a piece of evidence for the existence of a conformational equilibrium and for the shift of equilibrium under the influence of substituents in the A ring. Furthermore, through an analysis of the experimental results of the reduction of substituted, unhindered cyclohexenones with hydrides, it should be possible to separate the purely conformational effects from electronic and other (solvents, etc.) effects. An even more detailed analysis could be reached by a knowledge of the relative rates of reduction of the various conformers. This could be determined by kinetic measurements on conjugated cyclohexenones maintained in fairly rigid conformations. In this respect the use of bulky hydride donors could insure a greater selectivity of the kinetic reduction and might allow differentiation of the various conformers from one another—the half-chair from the diplanar form, the half-chair from the boat and perhaps the diplanar form from the boat.

Indeed, variations in the rate of reduction of different conformers are probably responsible for the greater selectivity of reduction observed experimentally, when using tri-*t*-butoxyaluminohydride or other bulky hydride donors instead of lithium aluminum hydride in the reduction of 3-keto-Δ^4-steroids (35d,51–53) and other unhindered conjugated cyclohexenones (54).

(*3*) *Influence of Substituents and Size of Ring B.* The conclusions attained by analyzing the reduction of 3-keto-Δ^4-steroids are essentially independent of the presence and nature of rings C and D and of the presence of the angular 19-methyl. Therefore the reduction of bicyclic and tricyclic compounds corresponding, respectively, to AB and ABC rings of 3-keto-Δ^4-steroids should yield epimeric alcohols in proportions comparable to those obtained with the 3-keto-Δ^4-unsaturated system; this conclusion is borne out by the experimental results (**1** and **2**). In the major product of reduction the hydroxyl group is *cis* to the angular hydrogen (**1a**,**2**) or angular methyl (**1b**) of the ring containing the unsaturated ketone.

In connection with substitution in ring B, it is interesting to note that the reduction of a 3-keto group in 3-keto-$\Delta^{4,6}$-steroidal dienes proceeds quite similarly to that of the corresponding steroidal Δ^4-ene-3-one, in both cases the allylic 3β-hydroxyl is the predominant product of reduction (54a,58).

We turn now to the much-discussed question of the influence of a 6β-substituent of a 3-keto-Δ^4-steroid on the conformation of ring A (42,43,47,49,59). Let us recall that at position 6 of a 3-keto-Δ^4-steroid a bulky β-oriented substituent (methyl, bromo, etc.) reverses the chirality of the conjugated ketone from what it is in the unsubstituted parent compound or in the corresponding 6α-isomer. In the latter compound ring A exists mainly as the usual half-chair conformer, as evidenced by the predominant formation of the allylic 3β-hydroxyl on reduction of 6α-methyl-Δ^4-cholestene-3-one with lithium tri-*t*-butoxyaluminohydride (53,60). Regarding, for instance, the 6β-methyl derivative, we feel that the corresponding physical data can be accommodated without resorting to a conformational inversion of ring A. If one pushes apart the *syn*-diaxial methyls in a Dreiding model, one notes that the repulsion between them decreases and the chirality also decreases and eventually inverts. While the exact position of the energy minimum cannot be immediately deduced from an examination of the models, it is clear that the diplanar form where the 6β-methyl appears to be even closer to the angular methyl cannot be a main optical contributor. In our interpretation, a change in the skewness of the α,β-ethylenic ketone has taken place as a result of the 6β substitution, but we believe that we are still dealing with a slightly deformed half-chair of ring A. In any event, a test of the conformational change can be found in the reduction of the 6β-methyl-3-keto-Δ^4-unsaturated derivative by complex hydride. If a deformed half-chair is still the main conformer of the equilibrium mixture, the major product of reduction should be the 3β-oriented allylic hydroxyl, whereas if a boat is the main component, the diplanar form being excluded, the reduction should yield mainly the isomeric 3α-hydroxyl.

Another interesting case of assumed conformational inversion of ring A with respect to unsubstituted 3-keto-Δ^4-unsaturated steroids arises when instead of being six-membered, ring B becomes five-membered as in B-nor-3-keto-Δ^4-steroids (48,61). Looking at a model, it is clear that the presence of a B-nor ring causes the 3-keto-Δ^4-unsaturated system to be nearly planar, and it forces ring A to adopt a very flattened half-chair conformation close to the diplanar form. Therefore, if the model is of any value, it is believed that the optical contribution of the unsaturated ketonic system ceases to be strongly dominant and that the main contribution arises from the neighboring asymmetry. Again this interpretation can be tested with lithium aluminum hydride reduction of B-nor-3-keto-Δ^4-unsaturated steroids. If ring A exists in the low-energy, flattened half-chair conformation, we can expect the allylic 3β-hydroxyl to be the major product of reduction, whereas a predominant boat form of ring A would, of course, yield chiefly the epimeric 3α-hydroxyl. The few available results (62,63) seem to support a flattened half chair as the main conformer of ring A, but we feel that more evidence is needed to settle this question.

(4) Influence of the Angular 19-Methyl. We have still to consider the influence of the angular 19-methyl (Fig. 3) on the formation of primary complexes leading to allowed transition states T_2 and T_3. Since any important contribution from T_3 has been dismissed, we have only to examine whether the 19-methyl has any influence on the formation of T_2, where the approach of the anion takes place on the side of the angular methyl. The model of the diplanar conformer shows that the angular methyl is quasi-axial, therefore during complex formation the steric compression between the incoming anion and the angular substituent probably remains low, but may not be entirely negligible. The importance of this steric compression can be judged by comparison of the experimental results of the reduction of testosterone-17-acetate (64,65) with those of the corresponding 19-nor analog (66) (**3**). Clearly the absence of an angular methyl lowers the energetic differences between the preferred conformations and makes the intervention of 1,3 diplanar or boat forms more likely. Taking all these factors into account, the results in the literature (which are not strictly comparable since the experimental conditions used by different workers are not identical) show that the half-chair conformer still remains the most favored one, although the other conformations cannot be ignored. Thus, although it does not play a decisive role, the angular methyl cannot be neglected. With the bi- or tricyclic compounds (**1**,**2**) one is led to the same conclusions.

c. Kinetic Character of the Reduction by Complex Hydrides. The reduction with complex hydrides (lithium aluminum hydride or sodium borohydride) of a hindered ketone located 3- to an axial methyl usually yields the least stable axial alcohol (see Sect. II-C-2) resulting from a kinetically controlled reaction.

The reduction of unhindered, conjugated cyclohexenones by complex hydrides is also a kinetically controlled reaction in the sense that the

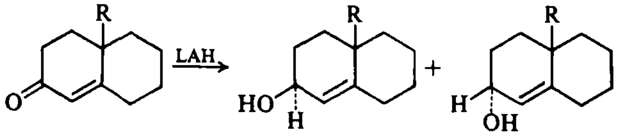

(1a) R = H
(1b) R = CH_3

3β-OH:3α-OH
4:1
9:1

(ref. 55)

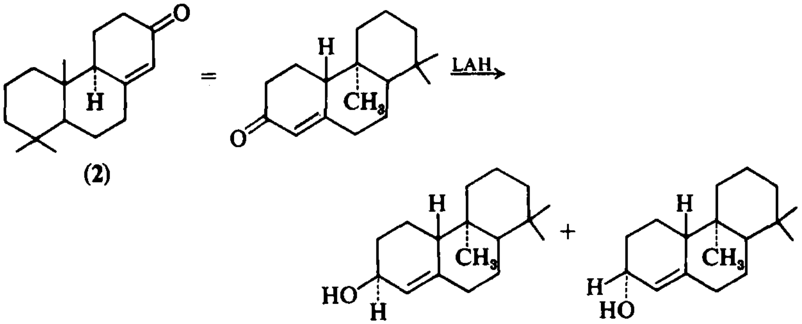

(2)

76%

20%

(ref. 56)
(ref. 57)

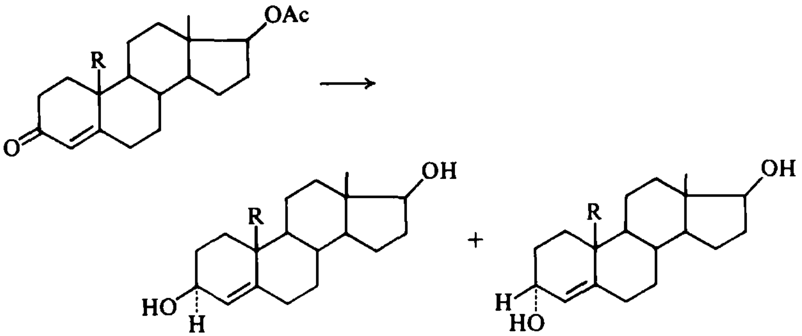

(3a) R = H $\xrightarrow{\text{LAH}}$
(3b) R = CH_3 $\xrightarrow{\text{BH}_4\text{Na}}$

3β-OH:3α-OH
3:1
7:1

(ref. 66)
(ref. 64,65)

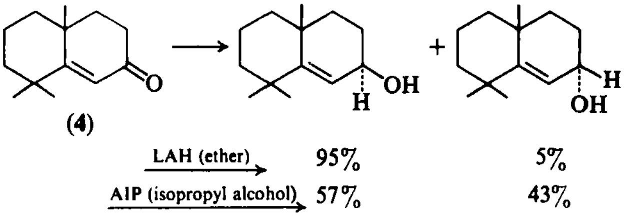

(ref. 67)

composition of epimeric allylic alcohols obtained in this manner does not appear to reflect the composition at equilibrium. This is especially obvious once it is admitted that protracted reduction with aluminum isopropoxide in isopropyl alcohol usually occurs under equilibrating conditions.

A comparison of the reduction of a conjugated cyclohexenone (**4**) with the various reagents demonstrates unequivocally that reduction with complex hydrides yields a proportion of epimers different from that from reduction with aluminum isopropoxide (AIP). This difference cannot be ascribed to some special effect of the solvent since sodium borohydride usually gives a better selectivity than lithium aluminum hydride (51), and moreover, performing the reduction with sodium borohydride in isopropyl alcohol would still improve the selectivity with respect to methyl alcohol as solvent (68). The kinetic character of the reduction of ketones by complex hydrides, supported by numerous examples (35e, see also Table IV, Sect. II-D) appears quite general. It is understandable if, as previously assumed, the primary product of reduction is not necessarily the most thermodynamically stable. Conformational changes (from a diplanar to a half-chair form, see Fig. 3) and formation of intra- or intermolecular hydrogen bonds are probably among the factors to be reckoned with for the shifting of the kinetic mixture to the thermodynamic equilibrium, where admittedly the relative percentages of epimers may depend to a small degree on the nature of the equilibrating system.

C. Reduction of Hindered Unsaturated Ketones

With respect to the addition of hydride ion, the hindered unsaturated ketones may be classified into two groups. In the first group steric and electronic factors concur to yield, with a high selectivity, the final product (1-keto-Δ^2-5α-steroids, 3-keto-Δ^1-5β-steroids, etc.); in the second group, steric and electronic factors are in opposition and the evaluation of their respective importance is required to be able to interpret or to predict the outcome of the reduction. For the clarity of exposition we have preferred to present successively the reduction of ketones *ortho* or *meta* to an angular methyl* which is the main cause of hindrance to the approach of the reagent. Moreover, to simplify the discussion we have purposely chosen examples where the conformations are relatively rigid; the reduction of conformationally mobile cyclohexenones will be deferred to Section II-D.

1. Reduction of Unsaturated Ketones Whose Ketonic Group is ortho to an Angular Methyl

It has already been mentioned that the reduction of 5α-cholestane-1-one yields mainly the saturated alcohol whose hydroxyl is *trans* to the adjacent 19-angular methyl, while the corresponding Δ^2-unsaturated steroidal 1-ketone of the same 5α-series is reduced mainly to the alcohol *cis* with respect to the 19-methyl (Sect. I, Table I). This last result could have been confidently predicted, since electronic and steric factors concur here to favor the addition of hydride ion on the opposite side from the angular methyl, thus securing the high selectivity of the reaction (69). In agreement with expectations, the preponderant formation of the alcohol *cis* to the angular methyl is also observed experimentally in the reduction of other conjugated cyclohexenones whose ketonic group is *ortho* to an angular methyl, and with a *trans* junction of the rings sharing the angular methyl [12-keto-$\Delta^{9,11}$-steroids (70,71), bicyclic compounds **5** (72) and **6** (73)]. It is noteworthy that the dominant steric course of the reduction is the same whether the conjugated ethylenic bond is extranuclear (**5**) or intranuclear (**6**). Furthermore, it can be safely predicted that, like its corresponding 19-methyl homolog, a 19-nor-1-keto-Δ^2-unsaturated 5α-steroid will give chiefly the allylic 1β-hydroxyl on reduction with complex hydrides.

The conjunction of electronic and steric factors should also allow the hydride ion to add on the β side of 1-keto-Δ^2-steroids of the 5β series, since the equatorial orientation with respect to ring A of the

---

*We use this unofficial but unequivocal nomenclature in order to avoid, in the steroid series, any confusion between the positions (α or β) of the carbon with respect to the angular methyl and the orientations (α or β) of the carbon substituents.

19-methyl does not hinder the approach of the anion, and since the folding of the AB rings hinders the backside α approach. While the former case does not appear in the literature, we can note the stereoselective addition of hydride ion on the side of the angular hydrogens in the case of 7 (74).

2. *Reduction of Unsaturated Ketones Whose Ketonic Group is meta to an Angular Methyl*

We shall discuss the kinetic reduction by complex hydrides of unsaturated ketones *meta* to an angular methyl with a few examples selected from the steroid series (Table III).

Table III

Reduction of Hindered Unsaturated Ketones *meta* to an Angular Methyl

Unsaturated ketone	Series	Reagent	Major product of reduction, %	Refs.
4-Keto-Δ^5		LAH	4α-OH, >90	75,76
6-Keto-Δ^4		LAH	6α-OH, >90	75,76
3β-Acetoxy 6-keto-Δ^4		LAH	6α-OH, 75	77
3β-Acetoxy 6-keto-Δ^7	5α	BH_4Na	6β-OH, sole isomer	78
3β-Acetoxy 11-keto-Δ^8	5α	LAH	11β-OH, sole isomer	35c

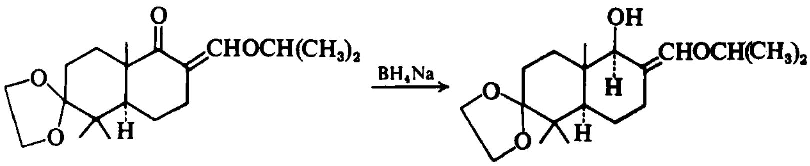

(5)

70% (ref. 72)

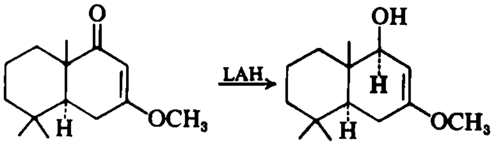

(6)

(main product) (ref. 73)

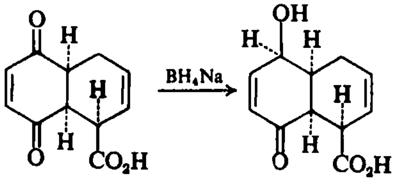

(7) (ref. 74)

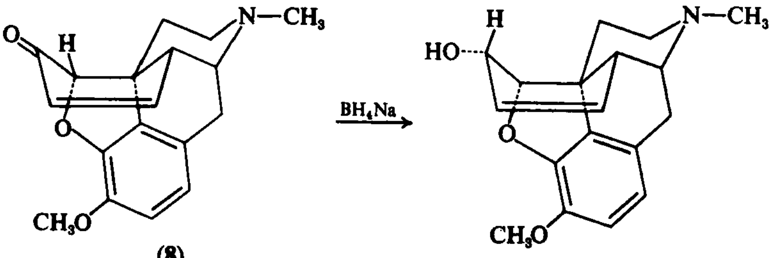

(8) (ref. 79)

As is apparent from Table III the reduction of 4-keto-Δ^5- and 6-keto-Δ^4-unsaturated steroids by lithium aluminum hydride yields almost exclusively the α-oriented, equatorial alcohol; this means that the hydride ion has come from the same side as the 19-methyl. On the contrary, the main product of reduction of 6-keto-Δ^7 and 11-keto-Δ^8 unsaturated steroids by the same reagent is the β-oriented axial allylic alcohol. In the latter case the introduction of hydride ion has taken place from the α side, opposite to the side of the angular methyl, and has involved a pre-boat or pre-diplanar intermediate rather than pre-half-chair or pre-diplanar intermediates as formerly.

We propose the following interpretation of these experimental results. The steric effect arising from the presence of an angular methyl in the position *meta* to the ketone, and which shows up by an interaction between the hydride ion and the hydrogens of the angular methyl, raises the energy of the transition state corresponding to a pre-half-chair or a pre-diplanar intermediate to a higher level than the one which corresponds to the pre-boat intermediate. Whether this is due to the difficulty of anionic approach to the ketone so that the formation of the primary complex does not even occur, or to the absence of progress in the primary complex once formed because of the high energy of the corresponding transition state, cannot be determined easily. However, it should be noted in this connection that the addition of hydride ion (or others anions) to the ketonic group of a cyclohexenone maintained in a boat conformation is not unusual (8).

The evaluation of the steric interaction between the hydride ion and the angular methyl can theoretically be studied by following the changes in bond distances and angles from the point of approach of the reagent to the ketone in its starting conformation up to the primary conformation of the final product. This will probably be realized some day with the help of electronic computers. Meanwhile one can empirically estimate the steric interaction of the hydride ion with the angular methyl, either on the conformation of the starting unsaturated ketone, which corresponds to a hindrance to the formation of the primary complex, or on the primary conformation of the reduced product, which, to a certain extent, corresponds to the difficulty of reaching the transition state. The latter estimation is conveniently effected by replacing the trigonal carbon of the ketonic group by a tetrahedral carbon on a Dreiding model and to measuring the shortest distance between one hydrogen of the angular methyl and the axial hydrogen corresponding to the pre-half-chair or pre-diplanar intermediate.

Performing these measurements in all preceding cases one notices that for 11-keto-Δ^8- and 6-keto-Δ^7-unsaturated steroids the above mentioned distance is less than 1.9 Å, while for the 4-keto-Δ^5 and-6-keto-Δ^4 derivatives, this distance is more than 2.1 Å. (In the case of the 6-keto-Δ^4-unsaturated compound there are two low-energy conformers of ring A.) It can then be concluded that when the shortest distance between the hydride ion and one hydrogen of the angular methyl is less than 2 Å there is a strong steric compression in the corresponding transition state, which thus appears energetically less favored than the one which corresponds to the pre-boat intermediate. Also, it can be predicted on the same grounds that the kinetic addition of hydride ion to the ketone on the side of the angular methyl will take place only if the distance of approach of the hydride to any hydrogen of the angular methyl is not below a (provisionally estimated) value of 2 Å.* This value seems to correspond to the steric requirement of complex formation and of the progress to a transition state of the pre-half-chair or pre-diplanar type.

---

* We evaluate the precision of these measures to be around 10% due to the capacity for deformation of the models.

The experimental results of the reduction of 4-keto-Δ^5- and 6-keto-Δ^4-unsaturated steroids (Table III) are in good agreement with the predictions that could have been drawn taking into account the influence of a double bond exocyclic to a ring on the value of the dihedral angles of that ring and of its steric implications (80). Indeed, comparing the shortest distance between any hydrogen of the axial methyl to any *syn*-axial hydrogen of the ring of a cyclohexane with the corresponding distances in the unsaturated cyclohexenones, one is led to the following observations. Any Δ^5 or Δ^4 ethylenic bond exocyclic, to rings A and B respectively, widens the distance of any hydrogen of the angular 19-methyl to the 4β and 6β hydrogens, respectively, as compared to the corresponding value of the chair mentioned above. This lengthening of the distances could explain why complex formation is allowed on the β side of the molecule of 4-keto-Δ^5- and 6-keto-Δ^4-unsaturated steroids. Concerning the latter unsaturated system, it is quite apparent from the models that the distance (ca. 2.2 Å) between the 6β-H and a hydrogen of the 19-methyl is greater when ring A is in the half-chair conformation than when it is in the diplanar form (ca. 2 Å), and therefore the preferred half-chair conformer appears to favor β addition of hydride ion more than does the other conformer.

On the other hand, the Δ^7 and Δ^8 ethylenic bonds endocyclic to rings B and C, respectively, carrying the ketonic group do not yield any such widening distance effect, but rather they keep these distances fairly close to what they are in the corresponding saturated cyclohexane.

Analyzing the reduction of hindered cyclohexenones further, we can detect a difference between the reduction of 6-keto-Δ^7- and 11-keto-Δ^8-unsaturated steroids. The latter system exists, from the models, in the diplanar conformation with carbons 14,8,9,12 coplanar. On the β side, complex formation leading to a transition state of very high energy is prevented by a very strong interaction with the angular 18-methyl; on the α side where the addition is not sterically hindered, the formation of a pre-boat intermediate, which does not raise a strong steric compression, appears favorable. Therefore hydride addition occurs exclusively on that side, and the theoretical interpretation is in good agreement with the experimental result. By contrast, the reduction of 6-keto-Δ^7-unsaturated steroids appears more complex; hydride addition on the β side is prevented so that complex formation does not take place, but on the α side hydride addition, while not sterically prevented, should involve a pre-diplanarlike transition state whose energy also seems fairly high. In this case the experimental results may receive several interpretations. Either the steric factor is still strongly dominant, or the reduction of this unsaturated ketone does not follow the general rule. In the latter event the presence of the conjugated olefinic bond would not appreciably contribute, via a pre-diplanarlike intermediate, to the decrease in the energy of the transition state compared to the one which would correspond to the unconjugated parent ketone, and therefore the reduction would be equivalent to the reduction of the unconjugated ketone. Such an explanation cannot be ruled out at this moment.

Needless to say the interpretation of the reduction of hindered ketones is not limited to cyclohexenones of steroids but appears quite general.

D. Reduction of Conformationally Mobile Unsaturated Ketones

Up to now we have only examined the simple cases of cyclohexenones incorporated in relatively rigid bi- or polycyclic systems. If we turn to such conformationally mobile systems as monocyclic cyclohexenones or derivatives of *cis* octalones, the distinction between hindered and unhindered ketones does not have much meaning. In such cases the prediction or interpretation of the steric course of the reduction has to take into account the various possible conformers and their allowed transition states. In this way we shall analyze the steric course of the kinetic reduction of monocyclic 2-cyclohexen-1-ones bearing only one substituent on a saturated carbon of the ring in the *meta*, *ortho*, or *para* position of the ketone.

1. Reduction of 5-Substituted Δ^2*-Cyclohexen-1-ones*

The lithium aluminum hydride reduction of 5-substituted 2-cyclohexenones (Table IV) yields chiefly the *cis* isomer as can be predicted by the following interpretation (Fig. 4).

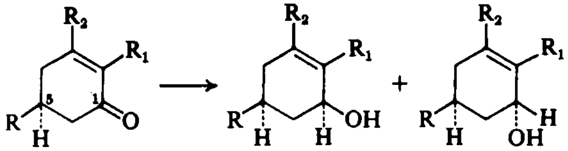

TABLE IV

Reduction of 5-Substituted Δ^2-Cyclohexen-1-ones Under Kinetic and Equilibrating Conditions

Substituted cyclohexenone	Hydride donor (a)	% *cis*	% *trans*	Reference
$R = CH_3$, $R_1 = R_2 = H$	LAH	93	7	81
	AIP	60	40	
$R = CH_3$, $R_1 = H$, $R_2 = CH_3$	LAH	90,5	9,5	82
	AIP	64	36	
$R = HC(CH_3)_2$, $R_1 = CH_3$,		Major	Minor	
$R_2 = H$	LAH	product	product	35c
	AIP			
$R = (CH_3)C{=}CH_2$, $R_1 = CH_3$,				
$R_2 = H$	LAH	91	9	83,84
	AIP	40	55	

[a] LAH = lithium aluminum hydride, AIP = aluminum isopropoxide.

To the four possible conformers, namely half-chairs I, II, and boats III, IV (Fig. 4) correspond four allowed transition states T_1, T_2, T_3, T_4. Of these we can already exclude T_2 where complex formation is sterically hindered because of a 1,3-diaxial type interaction between the hydride and the axial alkyl group. Therefore only T_1, T_3, and T_4 contribute to give the products of kinetic reduction. Now, the energies of transition states T_3 and T_4 are probably much higher than that of T_1 since conformers III and IV, whose populations are probably negligible, are already of a higher energy than I, and the same is true for the corresponding primary conformations of the final product. Therefore, the only significant contribution should come from T_1, and the major product of reduction should correspond to T_1 in conformity with the experimental results of Table IV.

A look at Table IV shows that the experimental results of the kinetic reduction of 5-substituted 2-cyclohexenones are in complete agreement; the additional presence of a substituent on one of the trigonal carbons of the olefinic bond is without apparent influence on the results. In contrast, the results of reduction under equilibrating conditions differ markedly from the kinetic results and thus yield evidence of the influence

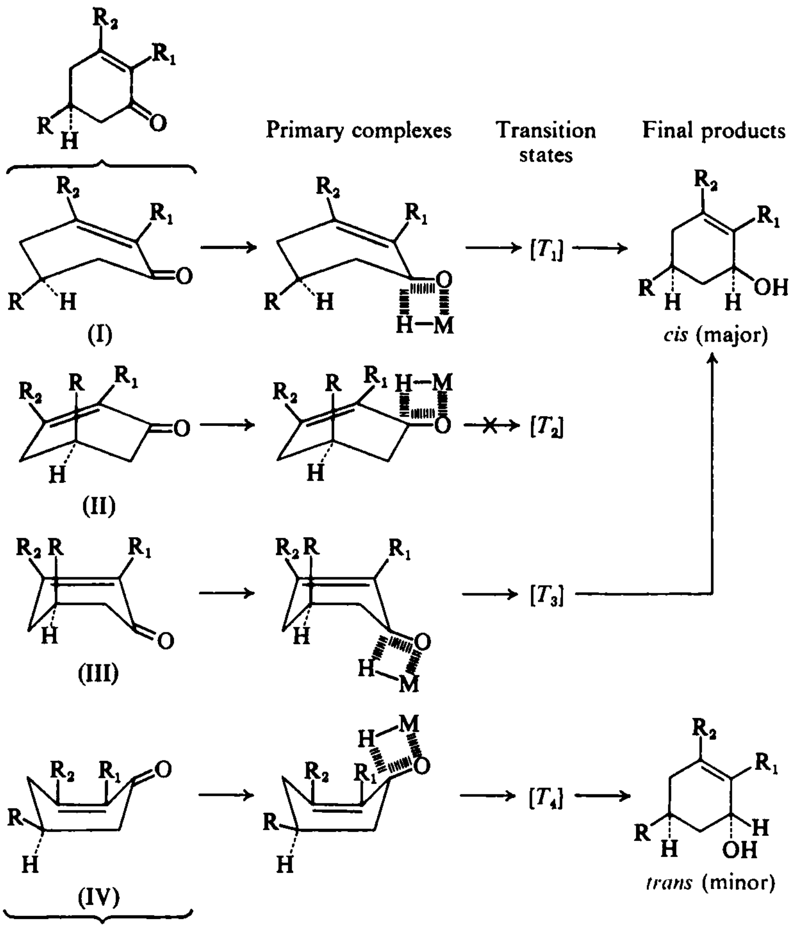

Figure 4

of the nature and size of the substituent on the thermodynamic equilibrium. It is noteworthy that the main product of the kinetic reduction of carvone (Table IV last entry) is *cis*-carveol, while *trans*-carveol appears as the stable product of aluminum isopropoxide reduction of carvone. This again confirms that the steric course of the reduction of conjugated cyclohexenones by complex hydrides is not determined only by the relative thermodynamic stabilities of the final product of reduction.

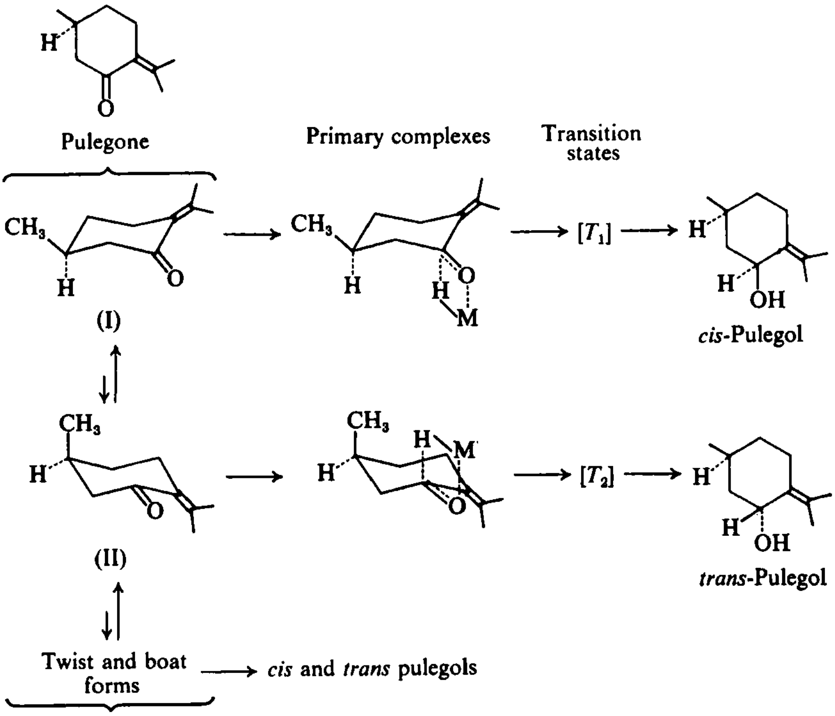

Figure 5

Once again for the reduction of pulegone (Fig. 5) we can focus attention on the different influences of an exo- versus an endo-cyclic double bond in the reduction of a conjugated cyclohexenone. According to Macbeth and Shannon (85), lithium aluminum hydride reduction of pulegone (Fig. 5) yields both *cis*- and *trans*-epimeric pulegols in fair proportions. Using the same interpretation as in the case of the endocyclic isomer, one has to conclude that here the allowed transition state corresponding to T_2 will contribute significantly to the final product, but less than T_1 which corresponds to the main conformer and, very likely, to the transition state of lowest energy. A detailed analysis of the reduction of pulegone with complex hydrides should involve an evaluation of the energetic contents of the various twist and boat forms, which does not allow for a simple interpretation.

2. *Reduction of 6-Substituted Δ^2-Cyclohexen-1-ones*

The kinetic reduction of a 6-substituted-2-cyclohexen-1-one such as piperitone (Fig. 6, entry 1) gives, besides the *trans*-epimer as the main product of reaction, a fair amount of the *cis* isomer (86). According to our usual interpretation (Fig. 6) the concentration of conformer II (half-chair with axial isopropyl) has to be appreciable, which agrees with recent suggestions in the literature (87,88). The results of the reduction of piperitone allow us to assign the *trans* configuration to the more abundant of the isomers obtained from the hydride reduction of 6-(Δ^3-butenyl)-Δ^2-cyclohexenone (89) and its 3-methyl homolog (90) (Fig. 6, entries 2 and 3).

3. *Reduction of 4-Substituted Δ^2-Cyclohexen-1-ones*

The kinetic reduction of cryptone (**9**), a typical 4-substituted 2-cyclohexen-1-one, also gives mainly the *trans* isomer and an amount of *cis* epimer smaller than in the case of piperitone (86). The interpretation of these results is quite similar to the one given in Fig. 6 for piperitone and similarly substituted cyclohexenones.

Again by analogy with the reduction of cryptone, we can assign to the mixture of epimers obtained by lithium aluminum hydride reduction of 4-(Δ^3-butenyl)-3-methyl-2-cyclohexen-1-one (**10**) (90) the configurations shown.

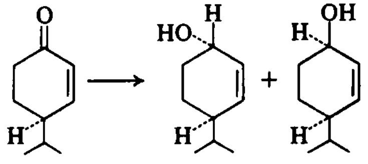

(**9**) 75% *trans* 25% *cis* (ref. 86)

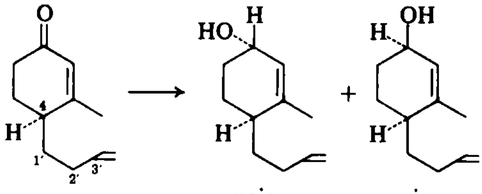

(**10**) major minor (ref. 90)

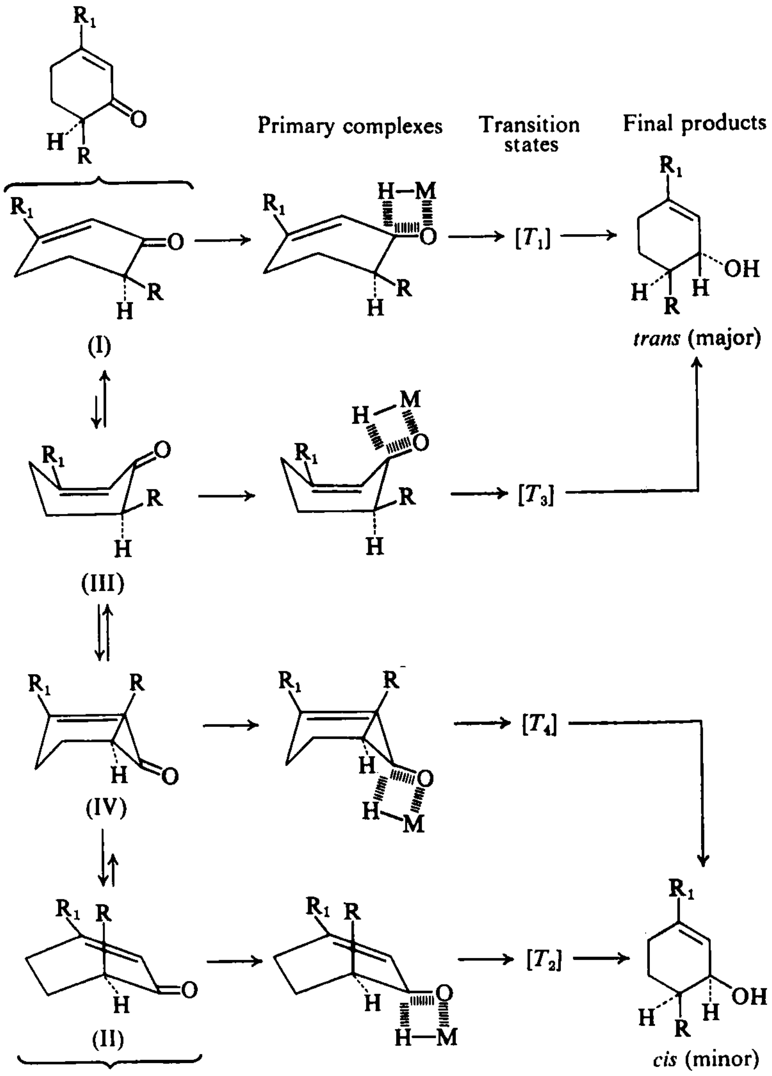

1. $R_1 = CH_3$, $R = CH(CH_3)_2$[64% *trans*, 36% *cis* (86)]
2. $R_1 = H$, $R = CH_2—CH_2—CH=CH_2$ (89)
3. $R_1 = CH_3$, $R = CH_2—CH_2—CH=CH_2$ (90)

Figure 6

a. Summary of the Hydride Reduction of Conjugated Cyclohexenones. In the case of conjugated unhindered cyclohexenones, the steric addition of hydride ion to the conformation of lowest energy is unequivocally fixed by the previously advanced hypothesis of continuous overlap of the anion orbital with the orbitals of the double bond.

In the case of hindered conjugated cyclohexenones, when steric and electronic factors do not concur to yield the final product, it is necessary to evaluate the respective importance of these factors in order to be able to predict the major product of the reduction.

III. 1,2 ADDITION OF CARBANIONS TO CONJUGATED CYCLOHEXENONES

A. Importance of the Bulk of the Reagent

The rules which govern the steric course of the 1,2 addition of hydride ion to conjugated cyclohexenones apply also to the 1,2 addition of carbanions from organometallic derivatives (organolithium or magnesium compounds, salts of acetylenic derivatives etc.). Since a carbanion is generally of a much larger size than a hydride ion, the bulk of the carbanion involved in the addition becomes one of the main factors responsible for the steric course of the reaction. In most reductions with complex hydrides the bulk of the hydride ion could be neglected, since nonbonded hydride–hydrogen 1–2 or 1–3 interactions were weak and could therefore be ignored. Contrariwise in the 1,2 addition of carbanions to ketones, the bulk of the reagent cannot be underestimated since it plays a major part in complex formation or in raising the energy of the transition state because of crowding resulting from nonbonded steric interactions. Once the importance of this steric factor has been recognized it is possible to show the validity of the rules previously given for the 1,2 kinetic addition of anions. The discussion of the carbanion 1,2 addition to conjugated cyclohexenones follows the same order of presentation as the reduction of cyclohexenones.

B. Carbanion Addition to Unhindered Ketones

When the approach of the carbanion to the trigonal carbon of the ketone is not hindered the steric course of the addition still corresponds to the preferential formation of a pre-half-chair or a pre-diplanar intermediate. In other words, the carbanion is introduced on the conformation of lowest energy of the starting unsaturated ketone, from the side of the axial hydrogen *meta* to the ketone. Two principal cases will be considered.

1. The Unsaturated Ring Exists Mainly in One Conformation of Low Energy

If the unsaturated ketonic ring can adopt only one conformation of low energy (half-chair or diplanar) the 1,2 addition of a carbanion gives the major product according to the preceding rule. For instance, the addition of methyl carbanion (from methyl lithium or methyl magnesium iodide) to a 3β-acetoxy 7-keto-Δ^5-unsaturated steroid takes place, as expected, from the α side of the molecule (**11**).

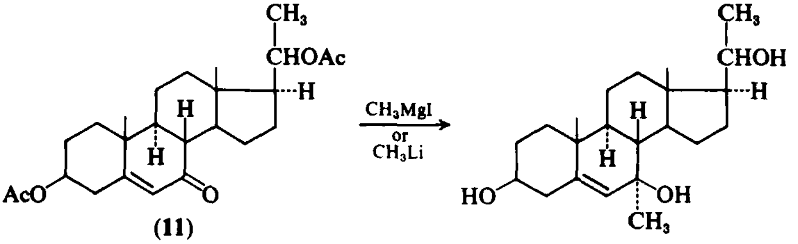

(**11**)

69% (ref. 91)

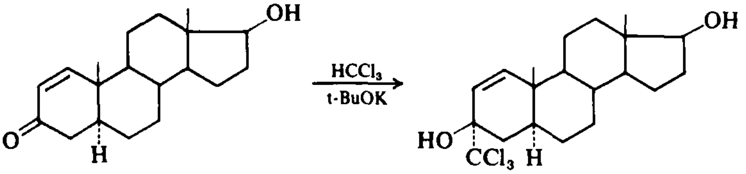

(**12**)

77% (ref. 92)*

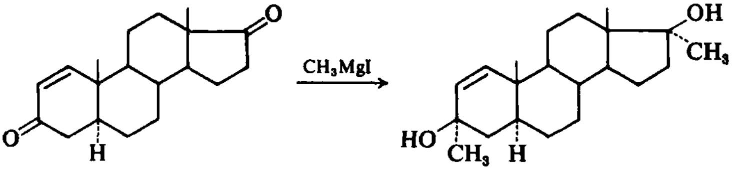

(**13**)

+ other products (ref. 93)*

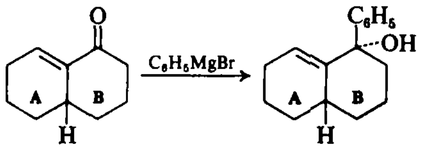

(14) 57% (ref. 94)*

Using the same rule we can tentatively assign to structures obtained from **12–14** the indicated configurations which are not given in the literature (92–94).

In **14**, ring B is a chair regardless of which conformation may be taken by ring A, which can adopt the diplanar or preferably the half-chair conformation. In this latter form the double bond exocyclic to ring B strongly favors the addition of the phenyl anion to the ketone on the same side as the angular hydrogen.

2. *The Unsaturated Ring Can Take Several Conformations of Low Energy*

The ability of the ketonic ring to adopt two conformations whose energies do not differ much (half-chair and diplanar for example) has to be taken into account for the prediction or interpretation of the addition. Thus the 1,2 addition of methyl carbanions to 3-keto-Δ^4-steroids might lead theoretically to two isomers, since the addition can take place through the corresponding allowed transition states (see Fig. 3) on either one of the low energy conformers of ring A. If, as in the case of hydride addition, the results reflect roughly the relative thermodynamic stabilities of the starting conformers, the reaction should yield mainly the 3β-hydroxy-3α-methyl derivative. While suggesting the

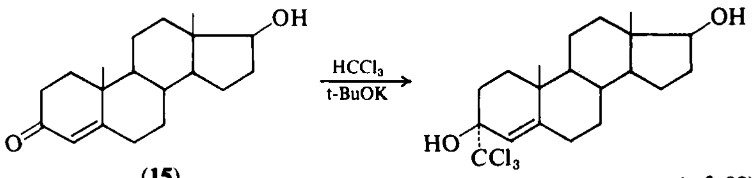

(15) 95% (ref. 92)*

*The indicated configurations of the products of addition are tentatively suggested: they are not given by the authors.

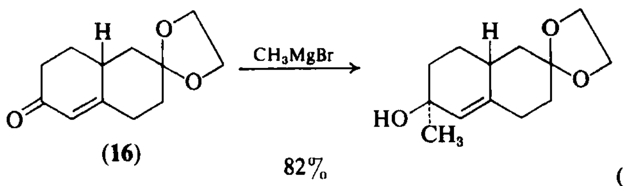

(16)

82%

(ref. 98)*

formation of two isomers during the 1,2 addition of methyl magnesium halides to Δ^4-cholestene-3-one, the experimental results (95–97) do not give much information concerning the respective proportions of isomers and their configurations.

Probably because of its bulk, the addition of trichloromethyl anion to Δ^4-androsten-17β-ol-3-one apparently yields only one isomer (92), presumably with the configuration indicated in **15**.

Again, in the case of the bicyclic analog of a 3-keto-Δ^4-19-norsteroid (**16**), the preferential addition of the methyl carbanion from the opposite side of the angular hydrogen can be predicted.

C. Carbanion Addition to Hindered Ketones

When steric and electronic factors concur to direct the addition of the carbanion to the same side of a molecule, the reaction proceeds with a high stereoselectivity as in the addition of methyl lithium to a 12-keto-$\Delta^{9,11}$-unsaturated derivative of hecogenin (99) (cf. **17**).

In most cases, however, the opposite directive influences of steric and electronic factors do not allow a simple prediction of the major product of addition. Therefore, in order to interpret the steric course of carbanion addition to hindered conjugated cyclohexenones, we have to separately evaluate two factors, namely the steric hindrance to the perpendicular approach of the carbanion to the ketone, and the conformational factor. In **18** the addition of methyl magnesium iodide to the Δ^2-unsaturated 4-ketone (100) can take place only from the α side because of considerable steric interferences between the methyl anion and the 19-methyl at the time of primary complex formation.

The replacement of the angular 19-methyl by hydrogen renders the steric factor less important than in the preceding example and allows the formation of the primary complex on either side of the molecule

---

* The indicated configurations of the products of addition are tentatively suggested; they are not given by the authors.

(101) (**19**). The experimental results reflect the subtle balance between conformational and steric factors since, in this case, a mixture of isomers is obtained in which apparently the main addition product still corresponds to the approach of the anion from the α side. Obviously primary complex formation on the β side is still impeded by nonbonded interactions of the 6β- and 10β-hydrogens with the methyl anion.

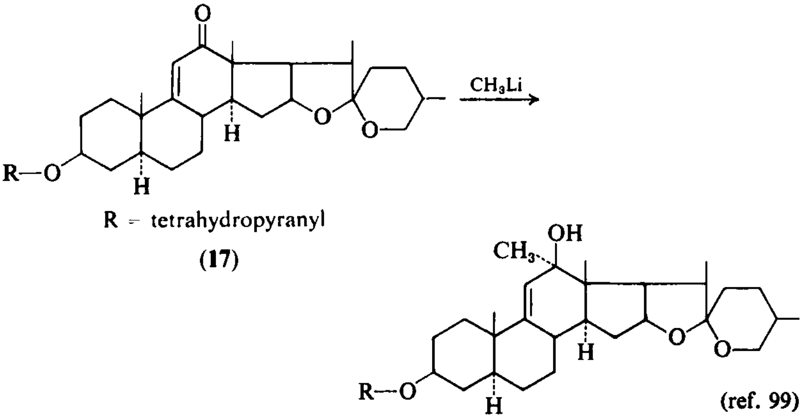

(**17**)

(ref. 99)

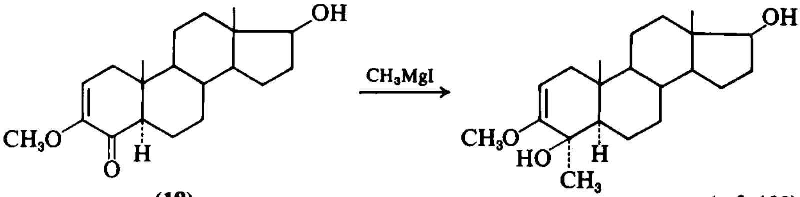

(**18**)

(ref. 100)

From a practical standpoint, differences concerning the steric course of 1,2 anion additions to unsaturated, hindered ketones are to be expected, depending on the bulk of the carbanion, the position of the conjugated double bond with reference to the ring carrying the ketonic group, and the substitution in the neighborhood of the ketone.

As far as the position of the olefinic bond conjugated to the ketone is concerned, two main cases are to be envisioned. If the ethylenic bond is exocyclic to the ketonic ring, the ensuing flattening of a part of the ring should favor the perpendicular addition of the anion to the ketone via a pre-chair-type transition state, provided that the size of the adding carbanion is not too big (acetylenic derivatives would seem to be suitable reagents). On the other hand, if the ethylenic bond is endo to

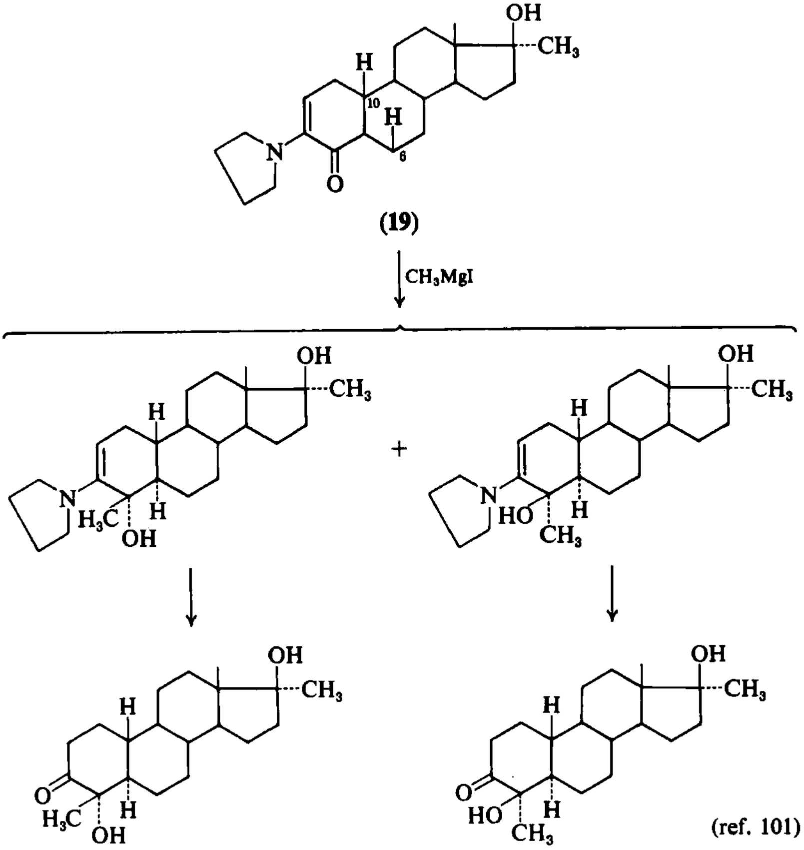

(19)

(ref. 101)

the ketonic ring (ring A of 1-keto-Δ^2-unsaturated steroids of the 5α series, for instance) the addition of the carbanion should take place solely from the side opposite to the dominant steric factor (that is to say an angular methyl etc.), almost independently of the size of the anion.

A more detailed analysis of the experimental results, which is beyond the scope of this chapter, could have allowed delineation in a more quantitative way of the steric and electronic factors responsible for the steric course of the addition.

D. Carbanion Addition to Conformationally Mobile Ketones

In any interpretation or prediction of the steric course of carbanion addition to conformationally mobile conjugated cyclohexenones, the

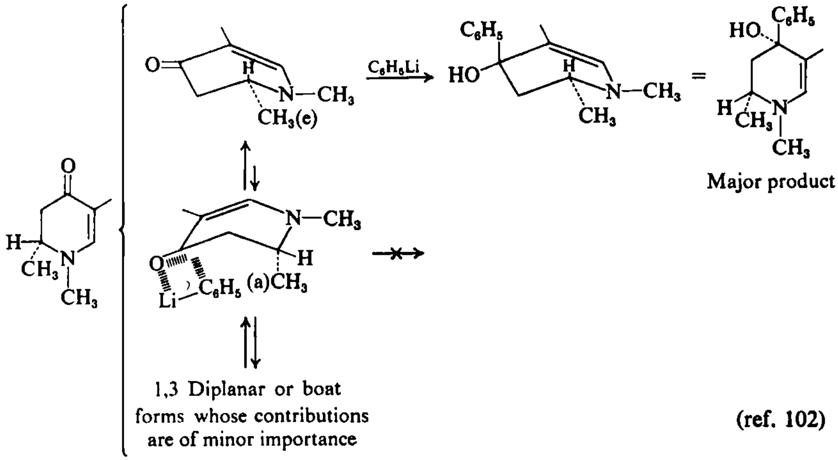

(ref. 102)

Figure 7

various conformers on which the perpendicular addition of the carbanion may take place have to be scrutinized. It may happen that one of the conformations of low energy cannot give rise to an allowed transition state because of steric interactions between an axial alkyl group and the carbanion engaged in primary complex formation with the ketone. Thus, as shown in Figure 7, the conformer with an axial methyl should not contribute much to the final product of phenyllithium addition to the heterocyclic unsaturated ketone, accepting that the replacement of a tetrahedral carbon by a trisubstituted nitrogen does not appreciably change the usual equilibrium between low energy conformers.

Quite similar interpretations allow us to tentatively assign to the main 1,2 addition products of acetylene and vinyl carbanions to the various cyclohexenones (**20**–**22**), the indicated configurations which were not given in the literature.

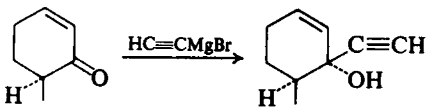

(20)

(ref. 103)

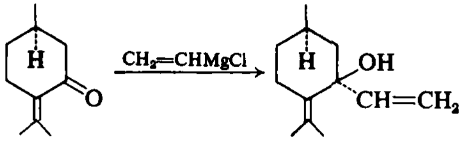

(21)

(ref. 104)

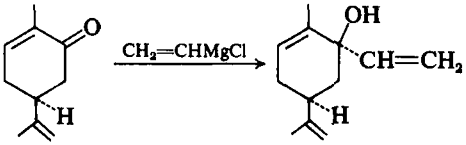

(22)

(ref. 104)

Acknowledgments

The author wishes to thank Professor L. Velluz, Director of Research at Roussel-Uclaf, for permission to publish this work. Constructive criticism of the manuscript by Dr. J. Mathieu and Dr. J. Valls is gratefully acknowledged.

General References

Conformations and Optical Properties of Cyclohexenones

E. L. Eliel, N. L. Allinger, S. J. Angyal, and G. A. Morrison, *Conformational Analysis*, Interscience, New York, 1965.

L. F. Fieser and M. Fieser, *Steroids*, Reinhold, New York, 1959.

C. Djerassi, *Optical Rotatory Dispersion, Applications to Organic Chemistry*, McGraw-Hill, New York, 1960, pp. 60, 83, 101.

W. Klyne, in *Advances in Organic Chemistry*, Vol. I, R. A. Raphael, E. C. Taylor, and H. Wynberg, Ed., Interscience, New York, 1960, p. 323.

L. Velluz, M. Legrand, and M. Grosjean, *Optical Circular Dichroism*, Verlag Chemie, Weinheim/Bergstr., Academic Press, New York, 1965, p. 126.

P. Crabbé, *Optical Rotatory Dispersion and Circular Dichroism in Organic Chemistry*, Holden Day, San Francisco, 1965, p. 191.

Reduction of Unsaturated Ketones with Complex Hydrides

N. G. Gaylord, *Reduction with Complex Metal Hydrides*, Interscience, New York, 1956.

Natrium Boranat in der Chemie der Steroide und Naturstoffe, Bayer-Leverkusen, 1964.

L. F. Fieser and M. Fieser, *Steroids*, Reinhold, New York, 1959.

O. H. Wheeler, "Reduction of Carbonyl Groups," in *The Chemistry of the Carbonyl Group*, S. Patai, Ed., Interscience, London, New York, 1966, p. 507.

Addition of Organometallic Derivatives to Unsaturated Ketones

M. S. Kharasch and O. Reinmuth, *Grignard Reactions of Non-metallic Substances*, Prentice-Hall, New York, 1954.

T. Eicher, "Reactions of Carbonyl Groups with Organometallic Compounds," in *The Chemistry of the Carbonyl Group*, S. Patai, Ed., Interscience, New York, 1966, p. 621.

References

1. E. Toromanoff, *Bull. Soc. Chim. France*, **1966**, 1445.
2. A. W. Burgstahler and I. C. Nordin, *J. Am. Chem. Soc.*, **83**, 198 (1961).
3. D. H. R. Barton, *J. Chem. Soc.*, **1953**, 1027.
4. D. H. R. Barton and R. C. Cookson, *Quart. Rev. London*, **10**, 44 (1956); **10**, 78 (1956).
5. E. J. Becker and E. S. Wallis, *J. Org. Chem.*, **20**, 353 (1955).
6. H. B. Henbest and R. A. L. Wilson, *J. Chem. Soc.*, **1956**, 3289.
7. C. Tamm and R. Albrecht, *Helv. Chim. Acta*, **42**, 2177 (1959).
8. D. N. Jones, J. R. Lewis, C. W. Shoppee, and G. H. R. Summers, *J. Chem. Soc.*, **1955**, 2876.
9. C. W. Shoppee and G. H. R. Summers, *J. Chem. Soc.*, **1952**, 3361.
10. D. H. R. Barton, *Experientia*, **6**, 316 (1950).
11. W. A. C. Brown and G. A. Sim, *J. Chem. Soc.*, **1963**, 1050.
12. I. J. Grant, J. A. Hamilton, T. A. Hamor, J. Monteath Robertson, and G. A. Sim, *J. Chem. Soc.*, **1963**, 2506.
13. R. Huber and W. Hoppe, *Chem. Ber.*, **98**, 2403 (1965).
14. J. B. Bentley, K. B. Everard, R. J. B. Marsden and L. E. Sutton, *J. Chem. Soc.*, **1949**, 2957.
15. D. Izsak and R. J. W. Le Fèvre, *J. Chem. Soc.* (*B*), **1966**, 251.
16. W. B. Whalley, *Chem. Ind.* (*London*), **1962**, 1024.
17. C. Djerassi, R. Records, E. Bunnenberg, K. Mislow, and A. Moscowitz, *J. Am. Chem. Soc.*, **84**, 870 (1962).
18. K. Morita, *Bull. Chem. Soc. Japan*, **32**, 414 (1959).
19. R. Bucourt and D. Hainaut, *Bull. Soc. Chim. France*, **1965**, 1366.
20. A more detailed treatment should take into account some recent work by R. Bucourt (to be published), concerning the conformations of cyclohexenones.
21. E. Toromanoff, *Bull. Soc. Chim. France*, **1962**, 1190.
22. G. Stork in *The Alkaloids*, Vol. VI, R. H. F. Manske, Ed., Academic Press, New York, 1960, p. 222; G. Stork and S. D. Darling, *J. Am. Chem. Soc.*, **82**, 1512 (1960).
23. E. J. Corey and R. A. Sneen, *J. Am. Chem. Soc.*, **78**, 6269 (1956).
24. H. E. Zimmerman, L. Singer, and B. S. Thyagarajan, *J. Am. Chem. Soc.*, **81**, 108 (1959); H. E. Zimmerman and L. Ahramjian, **81**, 2086 (1959); H. E. Zimmerman and L. Ahramjian, **82**, 5459 (1960).
25. E. Toromanoff, *Bull. Soc. Chim. France*, **1962**, 708.

26. M. G. Evans and M. Polanyi, *Trans. Faraday Soc.*, **34**, 11 (1938). The method of these authors seems more relevant here than the Curtin-Hammett principle (27).
27. E. L. Eliel, N. L. Allinger, S. J. Angyal, and G. A. Morrison, *Conformational Analysis*, Interscience, New York, 1965, p. 28 for a discussion of the Curtin-Hammett principle.
28. J. Valls and E. Toromanoff, *Bull. Soc. Chim. France*, **1961**, 758.
29. W. J. Gensler, F. Johnson and A. D. B. Sloan, *J. Am. Chem. Soc.*, **82**, 6074 (1960).
30. I. G. Bolesov, M. N. Kolosov, and M. M. Shemyakin, *Izv. Akad. Nauk SSSR, Ser. Khim.*, **1965**, 1039; *Chem. Abstr.*, **63**, 8284f (1965). Though not given by the authors, we confidently assign the indicated configuration.
31. P. A. Plattner, A. Fürst, and H. Els, *Helv. Chim. Acta*, **37**, 1399 (1954); W. Bergmann, M. Kita, and D. J. Giancola, *J. Am. Chem. Soc.*, **76**, 4974 (1954); H. B. Henbest and R. A. L. Wilson, *J. Chem. Soc.*, **1956**, 3289; R. Albrecht and C. Tamm, *Helv. Chim. Acta*, **40**, 2216 (1957); F. J. Scott, Univ. Microfilms (Ann Arbor, Mich.), Order no. 65–8094, p. 49 (1965).
32. R = OAc. L. F. Fieser, M. Fieser, and R. N. Chakravarti, *J. Am. Chem. Soc.*, **71**, 2226 (1949); R = $OCOC_6H_5$. W. Bergmann and M. B. Meyers, *Ann.*, **620**, 46 (1959); E. J. Corey and G. A. Gregoriou, *J. Am. Chem. Soc.*, **81**, 3127 (1959); R = H. A. Nickon and J. F. Bagli, *J. Am. Chem. Soc.*, **83**, 1498 (1961), discuss the reduction.
33. R. Ginsig and A. D. Cross, *J. Org. Chem.*, **31**, 1761 (1966).
34. N. L. Allinger and C. K. Riew, *Tetrahedron Letters*, **1966**, 1269.
35. (a) P. A. Plattner, H. Heusser, and A. B. Kulkarni, *Helv. Chim. Acta*, **32**, 265 (1949); (b) W. G. Dauben, R. A. Micheli, and J. F. Eastham, *J. Am. Chem. Soc.*, **74**, 3852 (1952); (c) A. S. Hallsworth, H. B. Henbest, and T. I. Wrigley, *J. Chem. Soc.*, **1957**, 1969; (d) A. W. Burgstahler and I. C. Nordin, *J. Am. Chem. Soc.*, **83**, 198 (1961); (e) A. Nickon and W. L. Mendelson, *Can. J. Chem.*, **43**, 1419 (1965).
36. J. Hine, *J. Org. Chem.*, **31**, 1236 (1966).
37. E. Toromanoff, *Bull. Soc. Chim. France*, **1966**, 3357.
38. Y. Yamato and H. Kaneko, *Tetrahedron*, **21**, 2501 (1965).
39. K. Kuriyama, E. Kondo, and K. Tori, *Tetrahedron Letters*, **1963**, 1485.
40. S. L. Patashnik, H. L. Kimball, and S. Burstein, *Steroids*, **2**, 19 (1963).
41. P. Crabbé, *Tetrahedron*, **20**, 1211 (1964).
42. Y. Kondo, K. Kondo, T. Takemoto, K. Yasuda, and G. Snatzke, *Tetrahedron*, **21**, 1191 (1965).
43. G. Snatzke, *Tetrahedron*, **21**, 421 (1965).
44. C. W. Shoppee, D. N. Jones, and G. H. R. Summers, *J. Chem. Soc.*, **1957**, 3100.
45. D. Bertin and J. Perronnet, *Bull. Soc. Chim. France*, **1964**, 2782.
46. W. J. Wechter, G. Slomp, F. A. MacKellar, R. Wiechert, and U. Kerb, *Tetrahedron*, **21**, 1625 (1965).
47. C. Djerassi, O. Halpern, V. Halpern, and B. Riniker, *J. Am. Chem. Soc.*, **80**, 4001 (1958).

48. C. Djerassi, R. Records, E. Bunnenberg, K. Mislow, and A. Moscowitz, *J. Am. Chem. Soc.*, **84**, 870 (1962).
49. W. B. Whalley, *Chem. Ind.* (*London*), **1962**, 1024.
50. G. Snatzke, *Tetrahedron*, **21**, 413, 439 (1965).
51. O. H. Wheeler and J. L. Mateos, *Can. J. Chem.*, **36**, 1431 (1958).
52. O. H. Wheeler and O. Rosado-Lojo, *Rev. Col. Quim. Puerto Rico*, **20**, 24 (1962); *Chem. Abstr.* **58**, 11430h (1963).
53. S. Julia and B. Decouvelaere, *Bull. Soc. Chim. France*, **1963**, 2476.
54. (a) J. S. Baran, *J. Med. Chem.*, **6**, 329 (1963); (b) M. Torigoe and J. Fishman, *Tetrahedron Letters*, **1963**, 1251.
55. J. A. Marshall and W. I. Fanta, *J. Org. Chem.*, **29**, 2501 (1964).
56. H. B. Henbest and J. McEntee, *J. Chem. Soc.*, **1961**, 4478.
57. R. F. Church, R. E. Ireland, and J. A. Marshall, *Tetrahedron Letters*, **1960** No. 17, 1.
58. J. Schmutz, H. Schaltegger, and M. Sanz, *Helv. Chim. Acta*, **34**, 1111 (1951).
59. D. J. Collins, J. J. Hobbs, and S. Sternhell, *Tetrahedron Letters*, **1963**, 197.
60. D. J. Collins, J. J. Hobbs, and S. Sternhell, *Australian J. Chem.*, **16**, 1030 (1963); *Chem. Abstr.*, **60**, 4210e (1964).
61. C. Djerassi, R. Riniker, and B. Riniker, *J. Am. Chem. Soc.*, **78**, 6377 (1956).
62. Y. M. Y. Haddad, W. T. Pike, G. H. R. Summers, and W. Klyne, *J. Chem. Soc.*, **1965**, 6117 (see the experimental part p. 6124).
63. C. B. C. Boyce and J. S. Whitehurst, *J. Chem. Soc.*, **1960**, 4547.
64. F. Ungar, M. Gut, and R. I. Dorfman, *J. Biol. Chem.*, **224**, 191 (1957).
65. N. Kundu, A. A. Sandberg, and W. R. Slaunwhite, Jr., *Steroids*, **6**, 543 (1965).
66. J. A. Hartman, *J. Am. Chem. Soc.*, **77**, 5151 (1955).
67. W. G. Dauben and A. C. Ashcraft, *J. Am. Chem. Soc.*, **85**, 3673 (1963).
68. O. H. Wheeler and J. L. Mateos, *Can. J. Chem.*, **36**, 1049 (1958).
69. C. Tamm and R. Albrecht, *Helv. Chim. Acta*, **42**, 2177 (1959).
70. C. Djerassi, H. Martinez, and G. Rosenkranz, *J. Org. Chem.*, **16**, 1278 (1951).
71. A. Bowers, E. Denot, M. B. Sanchez, F. Neumann, and C. Djerassi, *J. Chem. Soc.*, **1961**, 1859.
72. R. F. Church, R. E. Ireland, and J. A. Marshall, *J. Org. Chem.*, **27**, 1118 (1962).
73. E. Wenkert and D. P. Strike, *J. Am. Chem. Soc.*, **86**, 2044 (1964).
74. R. B. Woodward, F. E. Bader, H. Bickel, A. J. Frey, and R. W. Kierstead, *Tetrahedron*, **2**, 1 (1958).
75. D. N. Jones, J. R. Lewis, C. W. Shoppee, and G. H. R. Summers, *J. Chem. Soc.*, **1955**, 2876.
76. E. J. Becker and E. S. Wallis, *J. Org. Chem.*, **20**, 353 (1955).
77. Y. Urushibara and K. Mori quoted by K. Morita, *Bull. Chem. Soc. Japan*, **32**, 414 (1959).
78. M. Slaytor and K. Bloch, *J. Biol. Chem.*, **240**, 4598 (1965).
79. M. Gates, *J. Am. Chem. Soc.*, **75**, 4340 (1953).
80. R. Bucourt, *Bull. Soc. Chim. France*, **1963**, 1262.
81. H. L. Goering and J. P. Blanchard, *J. Am. Chem. Soc.*, **76**, 5405 (1954).

82. G. Asato, Univ. Microfilms, Inc. (Ann. Arbor, Mich.) Order No. 61.5692 (1961); Dissertation Abstr., **22**, 2186 (1962).
83. R. H. Reitsema, *J. Am. Chem. Soc.*, **75**, 1996 (1953).
84. G. O. Schenck, K. Gollnick, G. Buchwald, S. Schroeter, and G. Ohloff, *Ann.*, **674**, 93 (1964).
85. A. K. Macbeth and J. S. Shannon, *J. Chem. Soc.*, **1952**, 4748.
86. A. K. Macbeth and J. S. Shannon, *J. Chem. Soc.*, **1952**, 2852.
87. F. Johnson and S. K. Malhotra, *J. Am. Chem. Soc.*, **87**, 5492 (1965).
88. S. K. Malhotra and F. Johnson, *J. Am. Chem. Soc.*, **87**, 5493 (1965).
89. W. S. Johnson, W. H. Lunn, and K. Fitzi, *J. Am. Chem. Soc.*, **86**, 1972 (1964).
90. W. S. Johnson, P. J. Neustaedter, and K. K. Schmiegel, *J. Am. Chem. Soc.*, **87**, 5148 (1965).
91. C. H. Robinson, O. Gnoj, W. Charney, M. L. Gilmore, and E. P. Oliveto, *J. Am. Chem. Soc.*, **81**, 408 (1959).
92. E. Kaspar and R. Wiechert, *Chem. Ber.*, **91**, 2664 (1958).
93. B. Pelc, *Collection Czech. Chem. Commun.*, **29**, 3089 (1964).
94. H. O. House and H. W. Thompson, *J. Org. Chem.*, **28**, 360 (1963).
95. O. C. Musgrave, *J. Chem. Soc.*, **1951**, 3121.
96. N. F. Kucherova and M. I. Ushakov, *Zh. Obshch. Khim.*, **23**, 315 (1953); *Chem. Abstr.*, **48**, 2744g (1954).
97. C. W. Shoppee, T. E. Bellas, and R. Lack, *J. Chem. Soc.*, **1965**, 6450.
98. R. F. Church, R. E. Ireland, and D. R. Shridhar, *J. Org. Chem.*, **27**, 707 (1962).
99. P. Bladon and W. McMeekin, *J. Chem. Soc.*, **1960**, 2191.
100. B. Camerino, B. Patelli, and R. Sciaky, *Gazz. Chim. Ital.*, **92**, 709 (1962).
101. R. Sciaky, *Gazz. Chim. Ital.*, **92**, 561 (1962).
102. N. I. Shvetsov and V. F. Kucherov, *Dokl. Akad. Nauk SSSR*, **126**, 1017 (1959); *Chem. Abstr.*, **53**, 21946b (1959) quoted by N. S. Prostakov and N. N. Mikheeva, *Russ. Chem. Rev.* (Engl. Transl. of *Uspekhi Khimii*), **31**, 565 (1962).
103. E. A. Braude, M. U. S. Sultanbawa, and A. A. Webb, *J. Chem. Soc.*, **1958**, 3336.
104. K. Suga, S. Watanabe, and M. Suematsu, *Yuki Gosei Kagaku Kyokai Shi*, **24**, 213 (1966); *Chem. Abstr.*, **64**, 14226d (1966).

Topics in Stereochemistry, Volume 2
Edited by Norman L. Allinger, Ernest L. Eliel

Modern Methods for the Determination of Optical Purity

MORTON RABAN and KURT MISLOW

Department of Chemistry, Princeton University,
Princeton, New Jersey

I. OPTICAL AND ENANTIOMERIC PURITY

Optical purity, p, is defined as the specific rotation, $[\alpha]$, of a substance, divided by the specific rotation, $[A]$, of the pure enantiomer (i.e., the absolute rotation*) [eq. (1)]:

$$p = [\alpha]/[A] \tag{1}$$

The value of the optical purity is equal to the value of the *enantiomeric purity*, which is a measure of the excess of one enantiomer over the other [eqs. (2) and (3)]:

$$\text{Enantiomeric purity} = (F_+ - F_-)/(F_+ + F_-) \tag{2}$$

$$= 2F_+ - 1 \tag{3}$$

where F_+ and F_- are the mole fractions of the enantiomers; F_+ is taken as that of the predominant isomer for convenience.†

---

*The term "absolute rotation" is a convenient expression for and synonymous with "rotation of the pure enantiomer"; cf., e.g., R. F. Farmer and J. Hamer, *J. Org. Chem.*, **31**, 2418 (1966).

†This expression could more accurately be referred to as "net enantiomeric purity." It has been pointed out to us by Professor A. Horeau that the term "enantiomeric purity" could alternatively be used to describe the fraction of one enantiomer in the mixture, i.e., $F_+/(F_+ + F_-)$ or $F_-/(F_+ + F_-)$.

It is seen that optical purity relates to experimental properties, i.e. the magnitudes of the specific rotations [α] and [*A*], whereas enantiomeric purity describes the composition of a substance and is defined without recourse to any physical measurement. The present chapter is concerned with methods for the determination of the more fundamental quantity, enantiomeric purity. Nevertheless, since both quantities are equal or related, and since the term "optical purity" has been far more frequently used, even in cases where no reference to optical properties is made and "enantiomeric purity" is the more directly relevant expression, we shall use optical purity as if it were synonymous with enantiomeric purity. The magnitude of the optical purity may range from zero, in which case the substance is said to be racemic, to 100%, in which case the substance is said to be optically pure.

Several criteria of optical purity have long enjoyed general acceptance, but, as has recently been pointed out by Eliel (1), none is completely reliable. Specifically, resolutions have often been regarded as complete or "total" when the crystalline enantiomer or precursor diastereomer is unchanged in melting point or rotation upon further crystallization, and/or when the two enantiomers are obtained in states of equal optical purity, i.e., with equal specific rotations. Although these criteria have more often than not led to correct estimates of the optical purity, there are many instances where they have failed to yield the desired information and have given estimates which have fallen far off the mark (for some recent examples see ref. 2). The present discussion is concerned with more recently developed methods for establishing the optical purity or absolute rotation* of a substance which do not suffer from the ambiguity and the lack of reliability of the classical criteria listed above. The unambiguous determination of optical purity is of some importance. Thus, knowledge of the absolute rotation is clearly necessary for any discussion involving the relationship between rotatory power, or rotational strength, and molecular structure. The retention or partial loss of optical purity in the course of a reaction can often give valuable information concerning the reaction mechanism, provided the optical purities of the starting material and the product are known. Accurate knowledge of optical purities is especially important in the area of polypeptide synthesis. Here a small amount of optical impurity in the monomeric starting material can lead to a polymeric product of low homogeneity (3).

* As expressed by eq. (1), knowledge of any two of the three quantities (optical purity, specific rotation, and absolute rotation) allows calculation of the third.

We discern four general approaches to the determination of the optical purity of a mixture of enantiomers, B_+ and B_-. The determination may or may not involve a separation of B_+ and B_-. Furthermore, the determination may be performed on the enantiomers themselves, or the enantiomers may be transformed into a pair of diastereomers B_+C_+ and B_-C_+ to facilitate the determination. Thus, it follows that the determination may be carried out on enantiomers with separation, on enantiomers without separation, on diastereomers with separation, and on diastereomers without separation. Each of these four general approaches has been utilized in one or more of the methods that have been devised and that will be discussed in this chapter.

The methods that involve separation of enantiomers or diastereomers are very closely related to methods for resolution. In fact, each of these methods is based on a separation technique which is also used in conventional resolution. The separation methods have employed crystallization, chromatography, and stereospecific reactions to effect a separation of the enantiomers or diastereomers, as will be discussed in detail below. These separation methods are among the most sensitive in the arsenal of the modern organic chemist. Other separation methods may be applied in the future, in special cases or when high sensitivity can be obtained with an as yet undeveloped separation technique.

The methods that do not involve separation require simultaneous analysis of the stereoisomeric components and involve techniques including polarimetry, NMR spectroscopy, and, in a recent application, differential microcalorimetry. Other techniques almost certainly will be developed in the future.

If the pure enantiomer can be obtained, the optical purity of a mixture of enantiomers can be easily calculated by polarimetry, using eq. (1). Also, in a case where the value of the absolute rotation can be calculated from structural considerations (4), the optical purity can be determined by polarimetry. It should be noted, however, that such semiempirical calculations at present have limited applicability.

For these reasons, optical purities have most often been determined by polarimetry, following a "total resolution." However, the polarimetric method rests on certain criteria which may not always be entirely reliable, as has been pointed out above.

One chief criterion indicates that a substance is racemic, namely, the observation of an optical rotation of zero. However, enantiomerically pure compounds which exhibit no measurable rotation (5) are occasionally encountered.

When the optically pure antipode can not be obtained, it is sometimes possible to relate the unknown optical purity of the substance to that of another substance whose optical purity is known (chemical correlation). The optical purity is then known relative to the reference substance. If, for example, A can be converted into B of, let us say, 85% optical purity, it follows that A must be at least 85% optically pure, provided that no optical fractionation has occurred. The optical purity of A may be higher if some racemization occurs in the conversion reaction to B. If no bonds to an asymmetric atom are broken and it can be shown that neither the starting material nor the product is optically labile under the conditions of the reaction, it is reasonable to assume that the optical purities of B and A are the same. Care must be taken to assure that no optical fractionation occurs when correlations of this sort are made. If, for example, A of 85% optical purity is converted into B, and the product is then recrystallized to constant melting point, it is possible that the optical purity of product B may be higher or lower than 85%.

II. THE ISOTOPE DILUTION METHOD

Radioactively labeled compounds are frequently used as an aid in the quantitative analysis of materials in biological sources. If a quantity of radioactively labeled compound is added and the compound is reisolated, the amount of that compound in the biological material can be determined by the dilution of the tracer independent of the yield obtained in the isolation. In 1940 Graff, Rittenberg, and Foster described a method whereby both L- and D-amino acids could be determined in biological materials by an isotope dilution technique (6). The implication that isotope dilution techniques were applicable to the determination of optical purities was not recognized for over fifteen years until Berson and Ben-Efraim developed a simple technique for the determination of optical purities, using isotope dilution (7).

Consider the consequence of adding a quantity (m grams) of labeled racemic A ($A_\pm$) with specific activity S_0 to a test sample of unlabeled optically active A (n grams), and reisolating the racemic A. If the unlabeled test sample is racemic, the specific activity of the reisolated $A_\pm$ will be $S_0[m/(m + n)]$. If the unlabeled test sample is optically pure A_+ (and thus contains no A_-) then the dilution of the label will be less, for only the label of the A_+ molecules but not the label of the A_-

molecules will be diluted. In this case, the specific activity of the A_+ molecules will be $S_0[m/(m + 2n)]$, and that of the A_- molecules will remain the same as that of the labeled racemate, namely S_0; the observed specific activity of the reisolated $A_\pm$ will be the average of the activities of the A_+ and A_- portions, $S_0[(m + n)/(m + 2n)]$.

The specific activity of the reisolated racemic A is thus related to the optical purity of the initial sample of A. Since the specific activities of the A_+ and A_- do not change in the reisolation of the racemic $A_\pm$, the specific activity $S_\pm$ of the reisolated $A_\pm$ can be expressed as the average of the specific activities of the A_+ and A_-:

$$S_\pm = \tfrac{1}{2}S_0[m/(m + 2a)] + \tfrac{1}{2}S_0[m/(m + 2\bar{a})] \tag{4}$$

where a and $\bar{a}$ are the amounts (weights) of A_+ and A_- in the test sample whose optical purity is to be determined, and where:

$$a = \tfrac{1}{2}n(p + 1) = n - \tfrac{1}{2}B \tag{5}$$

and

$$\bar{a} = \tfrac{1}{2}n(1 - p) = \tfrac{1}{2}B \tag{6}$$

where p is the optical purity of the test sample, B is the weight of racemate in the test sample, and n is the weight of the test sample.

Substitution of eqs. (5) and (6) into eq. (4) gives eq. (7) or (8):

$$S_\pm = \frac{S_0m(m + n)}{(m + n)^2 - n^2p^2} \quad \text{or} \quad p^2 = \frac{S_\pm(m + n)^2 - S_0m(m + n)}{n^2S_\pm} \tag{7}$$

$$S_\pm = \frac{S_0m(m + n)}{(m + 2n - B)(m + B)} \tag{8}$$

where B is related to the optical purity of the test sample by:

$$p = (n - B)/n \tag{9}$$

The reisolated material need not be the racemate, but need only be different in optical purity from the material obtained when the labeled racemic $A_\pm$ is added to the test sample. In the general case the absolute rotation of A can be calculated from eq. (10):

$$[A]^2 = \frac{S_tn^2[\alpha]^2 - S_0mn[\alpha][\alpha_t]}{S_t(m + n)^2 - S_0m(m + n)} \tag{10}$$

where $[A]$ is the absolute rotation of A, n is the weight of test sample in grams, m and S_0 are the weight and specific activity, respectively, of the labeled racemate added to the test sample, S_t is the specific activity of the reisolated sample, and $[\alpha]$ and $[\alpha_t]$ are the rotations of the test sample and of the reisolated sample, respectively. If the reisolated sample is racemic, $[\alpha_t]$ is zero and eq. (10) reduces to:

$$[A]^2 = \frac{S_t n^2[\alpha]^2}{S_t(m + n)^2 - S_0 m(m + n)} \tag{11}$$

which is equivalent to eq. (7).*

Goering and his co-workers (8) have used the isotope dilution method to establish optical purity in the following way. A sample of A (a carboxylic acid) is resolved using an alkaloid, e.g., brucine. The labeled racemic $A_{\pm}$ is added and the acid is resolved again. If the original optically active A and the doubly resolved A have the same rotation, eq. (10) becomes:

$$[A]^2 = [\alpha]^2[S_t n^2 - S_0 mn]/[S_t(m + n)^2 - S_0 m(m + n)] \tag{12}$$

---

* Equation 10 is simply derived as follows. In the general case where the reisolated material need not be racemic, the specific activity of the reisolated material (S_t) is given by:

$$S_t = [(p_t + 1)/2]S_+ + [(1 - p_t)/2]S_-$$

where p_t is the optical purity of the reisolated material and S_+ and S_- are the specific activities of the two enantiomers and are given by:

$$S_+ = mS_0/[m + n\,(p_0 + 1)] \quad \text{and} \quad S_- = mS_0\,[m + n\,(1 - p_0)]$$

where m and S_0 are the weight and specific activity of the labeled racemate, n and p_0 are the weight and the optical purity of the original test sample. Combining and simplifying, we obtain:

$$S_t = mS_0 \frac{m + n - p_t p_0 n}{(m + n)^2 - n^2 p_0{}^2}$$

Since p_t and p_0 are given by:

$$p_t = [\alpha_t]/[A] \quad \text{and} \quad p_0 = [\alpha]/[A]$$

where $[\alpha_t]$ and $[\alpha]$ are the specific rotations of the reisolated sample and the original sample and $[A]$ is the absolute rotation, substitution gives:

$$S_t = mS_0 \frac{[A]^2(m + n) - n\,[\alpha][\alpha_t]}{[A]^2(m + n)^2 - n^2[\alpha]^2}$$

Solving for $[A]^2$ gives eq. (10).

An alternative form of eq. (10) has been used by Gerlach (9) and is given by eq. (13):

$$[A]^2 = (Q[\alpha_1][\alpha_i] - [\alpha_1]^2)/(Q - 1) \tag{13}$$

Here $[A]$ and $[\alpha_i]$ are again the absolute rotation and specific rotation of the reisolated sample, respectively; $[\alpha_1]$ is the specific rotation of the test sample after the labeled racemate has been added but before the sample has been resolved or recrystallized again, and is given by eq. (14); Q is the specific activity of the test sample after the labeled racemate has been added, divided by the specific activity of the reisolated sample [eq. (15)].

$$[\alpha_1] = [\alpha][n/(n + m)] \tag{14}$$

$$Q = S_1/S_i = S_0 m/[S_i(m + n)] \tag{15}$$

A radioactive or nonradioactive isotope may be used; deuterium was used by Gerlach (9) as the label in the determination of the absolute rotation of *N*-benzyl-4-phenyloxazolidine-2-thione (BPOT) which is described below as an example of the manner in which the determination of optical purity may be carried out in practice.

A sample of monodeuterated racemic BPOT, (m = 193.6 mg, S_0 = 0.935 g-atom D per mole) was added to the test sample of optically active BPOT (n = 407.3 mg, $[\alpha]_{546}$ + 170°).

The mixture ($[\alpha_1]_{546}$ + 115°, S_1 = 0.31 g-atom D per mole) was recrystallized from 15 ml of cyclohexane and gave 296 mg of BPOT ($[\alpha_i]_{546}$ + 170.5°, S_i = 0.179 ± 0.005 g atom D per mole).

Using eq. (12) we have:

$$[A]^2_{546} = (170°)^2 \frac{0.179(407.3)^2 - 0.935(407.3)(193.6)}{0.179(193.6 + 407.3)^2 - 0.935(193.6)(193.6 + 407.3)}$$

$$[A]_{546} = 170°$$

or using eq. (15) and (13) we have:

$$Q = S_1/S_i = 0.301/0.179 = 1.68$$

$$[A]^2_{546} = [1.68(115°)(170.5°) - (115°)^2]/(1.68 - 1)$$

$$[A]_{546} = 170°$$

The isotope dilution technique has been used to determine the absolute rotations and optical purities of the compounds listed in Table I. In all of the compounds except the last three the radioactive

Table I

Absolute Rotations Determined by Isotope Dilution

Compound[a]	Isotope	Reference
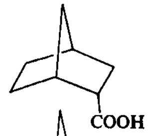	^{14}C	7
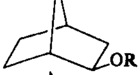	^{14}C	10
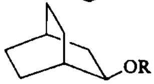	^{14}C	2a
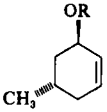	^{14}C	8
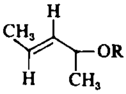	^{14}C	11
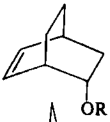	^{14}C	12
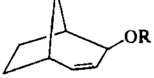	^{14}C	12
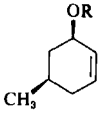	^{14}C	13
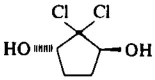	^{36}Cl	14
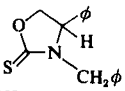	^{2}H	9
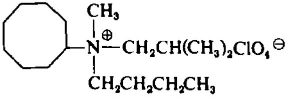	^{15}N	15

[a] R = 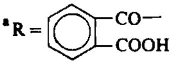

label ^{14}C was used; in the last two examples, the nonradioactive labels used were ^{2}H and ^{15}N, respectively.

III. METHODS OF KINETIC RESOLUTION

Kinetic resolution methods depend on the differences in rates of reaction of enantiomers with chiral (optically active) reagents; the ratio of rates reflects the differences in free energies of activation of the diastereomeric transition states (16). In reactions of enzymes with racemic substrates, the reaction often proceeds with virtually complete stereospecificity, i.e., the ratio of rate constants is of the order of at least 10^4.

The elegant "double resolution" method of Horeau (17) is based on a kinetic resolution. In contrast to the enzymatic methods where the resolution must be total, the method of double resolution involves only a partial kinetic resolution: the stereospecificity of the reaction is not known, and the additional data which are required are derived from the second partial resolution.

When a mixture of enantiomers ($A_+ + A_-$) is allowed to react with another mixture of enantiomers ($B_+ + B_-$), four different reactions (which proceed via stereoisomeric transition states) occur.

$$A_+ + B_+ \xrightarrow{k_1} A_+B_+ \qquad \text{(a)}$$

$$A_+ + B_- \xrightarrow{k_2} A_+B_- \qquad \text{(b)}$$

$$A_- + B_+ \xrightarrow{k_3} A_-B_+ \qquad \text{(c)}$$

$$A_- + B_- \xrightarrow{k_4} A_-B_- \qquad \text{(d)}$$

Reactions (a) and (d) are enantiomeric and proceed through enantiomeric transition states with the same energy content (energy of activation). In achiral media they will, therefore, proceed with the same rate constant, i.e., $k_1 = k_4$. For the same reason $k_2 = k_3$. On the other hand, in general $k_1 \neq k_2$ and $k_3 \neq k_4$ since reactions (a) and (b), as well as (c) and (d) proceed via diastereomeric transitions states with different energies of activation.*

*Strictly speaking, reactions (a) and (d) will be enantiomeric only when the conditions of the reactions are the same, including the requirement that the ratio of reactants in (a), A_+/B_+, equals the ratio of reactants in (d), A_-/B_-. However, we may suppose that the rate constants will be equal for practical purposes even when conditions are such that the symmetry is not maintained, as will be the case if the reaction of A_+ with racemic $B_\pm$ is compared to the reaction of B_- with $A_\pm$.

If racemic $\mathrm{A}_\pm$ is allowed to react with an insufficient quantity of B_+, reactions (a) and (c) will take place at different rates and the products $\mathrm{A}_+\mathrm{B}_+$ and $\mathrm{A}_-\mathrm{B}_+$, will be formed in a ratio determined by the ratio of rate constants k_1/k_3. Since $\mathrm{A}_+\mathrm{B}_+$ and $\mathrm{A}_-\mathrm{B}_+$ are formed at different rates, the residual mixture of unreacted A_+ and A_- will be enriched in one of the enantiomers.

If the amount of B_+ is n and the amount of racemic ($\mathrm{A}_\pm$) is $2N$, the amounts of product are as indicated in reaction (e), where a represents that fraction of B_+ which reacts with A_+.

$$n\mathrm{B}_+ + 2N\mathrm{A}_\pm \dashrightarrow an\mathrm{A}_+\mathrm{B}_+ + n(1-a)\mathrm{A}_-\mathrm{B}_+ + (N-na)\mathrm{A}_+ + (N-n+na)\mathrm{A}_- \qquad \text{(e)}$$

The optical purity of the residual A_- is represented by

$$\text{optical purity of } \mathrm{A}_- = \frac{\mathrm{A}_- - \mathrm{A}_+}{\mathrm{A}_- + \mathrm{A}_+} = \frac{N-n+na-N+na}{N-n+na+N-na} = \frac{2a-1}{(2N/n)-1} \qquad (16)$$

We can set this quantity equal to the ratio $[\alpha_\mathrm{A}]/[A_1]$, where $[A_1]$ is the absolute rotation of A and $[\alpha_\mathrm{A}]$ is the specific rotation of A isolated in the resolution; the ratio expresses the optical purity of A_-. If the reaction does not proceed quantitatively we must then replace the amount of B_+, viz. n, by the amount of B_+ that actually reacts, viz. nr, where r is the yield of the reaction. Finally, if the starting material B is not optically pure, the optical purity of A_- will not be as great as indicated by eq. (16) but will be in proportion to the optical purity of B, viz. $[\alpha_\mathrm{B}]/[A_2]$, where $[A_2]$ is the absolute rotation of B and $[\alpha_\mathrm{B}]$ is the specific rotation of the resolving agent B. These considerations lead to the modification of eq. (16):

$$\frac{[\alpha_\mathrm{A}]}{[A_1]} = \frac{2a-1}{(2N/nr)-1}\,\frac{[\alpha_\mathrm{B}]}{[A_2]} \qquad (17)$$

Equation (17) contains two quantities to be determined in the experiment ($[\alpha_\mathrm{A}]$ and r), three quantities which are known (N, n, and $[A_2]$), and two which are unknown (a and $[A_1]$).

In a second resolution racemic $\mathrm{B}_\pm$ is reacted with an insufficient quantity of A, the optically active material whose optical purity is to be determined. Equation (17) also applies to this resolution.

$$\frac{[\alpha_\mathrm{B}']}{[A_2]} = \frac{2a'-1}{(2N'/r'n')-1}\,\frac{[\alpha_\mathrm{A}']}{[A_1]} \qquad (18)$$

Here $[\alpha_B']$ and $[\alpha_A']$ refer to the specific rotations of B isolated and of the resolving agent A; $2N'$ and n' are the amounts of racemic B and of optically active A, respectively; and a' and r' have the same significance for the second resolution as their unprimed counterparts do for the first. Because of the symmetry of the reactions discussed above we can set $a = a'$, to give eq. (19):

$$\frac{[\alpha_B']}{[A_2]} = \frac{2a - 1}{(2N'/r'n') - 1} \frac{[\alpha_A']}{[A_1]} \tag{19}$$

Equation (19) also contains two unknown quantities $[A_1]$ and a, the same unknowns as in eq. (17). The two equations can be solved simultaneously to give $[A_1]$, the absolute rotation of A, from which the optical purity can be calculated using eq. (1) in Section I.

The final equation is:

$$[A_1] = \sqrt{\frac{[\alpha_A][\alpha_A'][A_2]^2[(2N/nr) - 1]}{[\alpha_B][\alpha_B'][(2N'/n'r') - 1]}}$$

The method of double resolution is a relative method in that it correlates an unknown optical purity or absolute rotation of a substance, A, with that of another substance, B, whose absolute rotation is known. In practice application of this method has been limited to acids and alcohols using a partial asymmetric esterification as the reaction required for the kinetic resolutions. Undoubtedly it can be extended to other systems, but it is necessary that both the rotations of the A and B isolated in the resolutions be large enough to give accurate estimates. This requires that the difference between the rate constants k_1 and k_2 be fairly large in order to get an optical yield that is well outside the range of experimental error. Clearly, if the optical purity of the A used is not large the optical yield will not be high; the optical purity of the resolved B can be no higher than that of the A used even if the reaction is completely stereospecific. Further, since the optical yield undoubtedly depends largely on steric factors in the diastereomeric transition states, if the optical activity is due to a dissymmetric grouping which is far removed from the site of reaction, the optical yield is likely to be low.

Representative results obtained by means of the double resolution technique using α-phenylbutyric anhydride are (17): phenyl-*n*-propylcarbinol, $[A]_D$ 29.6°, lit. 29.3°; amphetamine, $[A]_D$ 35.3°, lit. 35.6°, phenylisopropylcarbinol, $[A]_D$ 24.1°, lit. 24.6°.

The method of double resolutions is clearly inapplicable to the determination of the optical purity of compounds which owe their dissymmetry to deuterium substitution. The partial resolution of α-phenylbutyric anhydride with optically active α-deuterated primary alcohols does lead to residual α-phenylbutyric acid whose optical activity is large enough to be measured; the specific rotation obtained with optically pure alcohol is near 0.5°. On the other hand, since the optical rotations of such α-deuterated primary alcohols are on the order of 10^{-2} times that of α-phenylbutyric acid, the rotation of optically active α-deuterated primary alcohols produced by partial kinetic resolution would be too small to be measured with sufficient accuracy for calculation of optical purities. However, Horeau and Nouaille (18) have suggested that the second resolution of the alcohol by the anhydride is unnecessary in this special case. They argue that:

> . . . it is logical to assume that the ratio of the rates at which an α-deuterated primary alcohol RCHDOH reacts with the dextrorotatory and levorotatory enantiomers of α-phenylbutyric anhydride does not depend, or depends only slightly, on the identity of the radical R (always the most bulky); it depends essentially on the difference in "bulk" of the protium and deuterium atoms, so that the optical yield should be essentially the same for all of the optically pure α-deuterated alcohols.

On the basis of this assumption, it was concluded (18) that the optical yield of α-phenylbutyric acid obtained with a partially optically pure sample of alcohol is related to the optical purity of that sample.

Using neopentyl alcohol-1-*d* and benzyl alcohol-1-*d* obtained by fermentation of the corresponding deuterioaldehydes RCOD, assumed to be optically pure,* Horeau and Nouaille (18) found the same induction in the residual α-phenylbutyric acid, $[\alpha]_D$ 0.55° ± 0.07° and $[\alpha]_D$ 0.55° ± 0.015°, respectively. For two optically impure samples of 1-hexanol-1-*d*, they found optical purities of 24 ± 6% and 53 ± 6%, in excellent agreement with the optical purities determined enzymatically, 30 and 57%, respectively.

Kinetic resolution methods employing enzymic systems ("enzymic methods") depend on the availability of an enzyme which will react quantitatively with one enantiomer in the presence of a large excess of the other enantiomer, which is inert. Hog kidney D-amino acid oxidase, for example, will oxidize many D-amino acids but it is inactive toward

---

* For a demonstration of the optical purity of neopentyl alcohol-1-*d* prepared by fermentation of the deuteroaldehyde, see ref. 49.

their enantiomers, the corresponding L-amino acids (3). This enzyme may be used to test for the presence of very small amounts of D-amino acid in samples of L-amino acids. The method involves the volumetric determination of the oxygen consumed or the carbon dioxide evolved when the amino acid to be tested is incubated with the enzyme system in a Warburg apparatus. The optical purity of D-amino acids may be determined using snake venom L-amino acid oxidase which will catalyze the oxidation of any impurity of the L-enantiomer but is inactive with respect to the D-enantiomer (3).

When these determinations are carefully performed it is said (3) that optical purities can be routinely determined with an accuracy of 0.1%, i.e., 0.1% of optical impurity may be detected. The criteria of optical purity for L-amino acids determined enzymatically require that no more than 1 microatom of oxygen be consumed when 1 millimole of the amino acid is incubated with the D-amino acid oxidase, and that when 2 μmoles of racemic amino acid or 1 μmole of D-amino acid is added, an increment of 1 microatom of consumed oxygen is observed. When these criteria are met the amino acid is judged to be at least 99.9% optically pure.

Enzymic stereospecificity may also be exploited as a tool for the determination of optical purity in compounds which owe their chirality to dissymmetric deuterium substitution. As an example (19), consider the enzymatic oxidation of ethanol to acetaldehyde where only a particular one of the enantiotopic methylene hydrogens is oxidatively removed: it follows that, although both enantiomers of ethanol-1-*d* are oxidized, the (*S*) isomer is converted to acetaldehyde-1-*d*, whereas the (*R*) isomer gives rise to undeuterated acetaldehyde. Consequently the ratio of enantiomers of ethanol-1-*d* is uniquely related to the isotopic composition of the product acetaldehyde.

IV. METHODS OF TOTAL RESOLUTION—GAS-LIQUID CHROMATOGRAPHIC METHODS

The finding (20–24) that diastereomers can frequently be separated by analytical gas-liquid chromatography (GLC) provided the basis for another method for the determination of optical purity, independently developed by several groups (25–28). This method has received considerable attention in recent months and has been extended to new systems (25–41).

The usual approach involves either the conversion of a mixture of enantiomers A_+ and A_- into a mixture of diastereomers A_+B_+ and A_-B_+ by reaction with a chiral reagent B_+ which is optically pure (Scheme 1), or, conversely, the conversion of a mixture of diastereomers into a mixture of enantiomers by the removal of a chiral moiety B_+ (Scheme 2). Conditions are chosen so that the ratio of enantiomers A_-/A_+ is equal to the ratio of the precursor or product diastereomers A_-B_+/A_+B_+ [eq. (21)]. The optical purity can be easily calculated from this ratio [eq. (22)].

Scheme 1: $A_+ + A_- \xrightarrow{+B_+} A_+B_+ + A_-B_+$

Scheme 2: $A_+B_+ + A_-B_+ \xrightarrow{-B_+} A_+ + A_-$

$$A_-/A_+ = A_-B_+/A_+B_+ = R \tag{21}$$

$$\text{Optical purity of A} = (R - 1)/(R + 1) \tag{22}$$

Several conditions are necessary to satisfy eq. (1). The chiral reagent B_+ must be optically pure. There must be no kinetic resolution or racemization in the reaction which transforms the mixture of enantiomers into diastereomers according to Scheme 1 or in the reaction which transforms the mixture of diastereomers into enantiomers according to Scheme 2. In general, a reaction will be chosen that does not involve bond breaking at an asymmetric atom, although reactions that do involve such bond breaking are acceptable in cases where the reaction concerned occurs with complete stereospecificity, whether with inversion or retention of configuration.

The choice of a B reagent is clearly crucial. However, it is easy to screen a series of reagents using small amounts of the test mixture of enantiomers of A or even racemic A. No additional materials are required, other than a suitable B reagent and a column and substrate capable of separating the diastereomers conveniently.

Application of the method requires that the mixture of enantiomers be quantitatively convertible into, or produced from, a pair of diastereomers. In practice this requires a "handle" in the compound whose optical purity one wishes to determine, through which the B reagent may be attached. Further, it is likely that the separation will be considerably less efficient if the dissymmetric moiety of the test compound A is not disposed fairly closely to that of the B reagent in the precursor or product diastereomers A_+B_+ and A_-B_+. The method clearly cannot be employed if the mixture of diastereomers is not chemically and stereochemically stable under the conditions necessary for GLC. Although no extensive systematic studies have yet been carried out, it is clear that difference in retention times will be related to the structural differences between the two diastereomers. Thus, for example, it seems likely that diastereomeric esters of *p*-tolylphenylcarbinol will have far closer retention times than esters of methylphenylcarbinol.

Finally, it should be pointed out that the GLC method, like the double resolution method and unlike the isotope dilution method, is relative in the sense that a standard is required whose optical purity is known, i.e., the B reagent. If the optical purity of the B reagent is significantly less than 100%, a considerable error will be introduced in the determination.

Whereas chromatographic methods other than GLC have not been used to separate diastereomers for the purpose of determining optical purities, this method should be extendable to other systems such as paper or thin-layer chromatography. Like GLC, paper and thin-layer chromatography are capable of separating substances which are structurally similar. Other methods for the separation of diastereomers such as counter-current distribution, fractional distillation or electrophoresis, while clearly applicable in principle, would not be expected to provide the necessary efficiency in separation. The quantitative determination of the diastereomers separated by thin-layer or paper chromatography would be facilitated by the incorporation of a radioactive label into the B reagent before the diastereomeric mixture is prepared. Excision of the spots followed by counting in a scintillation counter would enable an accurate determination of the ratio of the diastereomers. Halpern et al. (36) have suggested a modification suitable to the determination of extremely small quantities of diastereomers (nanogram to submicrogram amounts) using a connected gas chromatograph–mass spectrometer system.

Guetté and Horeau (28) have developed a related method which allows the calculation of the absolute rotation of a substance using a racemic mixture of the substance and an optically pure B reagent. The racemic mixture of A_+ and A_- is reacted with an insufficient amount of an optically pure reagent B_+. Since the formation of A_+B_+ and A_-B_+ will proceed via diastereomeric transition states, the rates of formation will be different, and the amounts of A_+B_+ and A_-B_+ will differ.

The residual A will consequently be enriched in A_+ or A_- (kinetic resolution). This optical enrichment will be related to the difference in the amounts of the two diastereomers A_+B_+ and A_-B_+ which are formed. If the amount of added B_+ is exactly enough to react with half of the racemic mixture of A_+ and A_-, then the ratio of unreacted enantiomers A_-/A_+ will equal the ratio of product diastereomers A_+B_+/A_-B_+.

$$2nA_\pm + nB_+ \dashrightarrow (n - m)A_+B_+ + mA_-B_+ + n - (n - m)A_+ + (n - m)A_-$$

where n is the amount of B_+ in moles, and m is the amount of A_-B_+ produced, in moles.

$$A_+B_+/A_-B_+ = (n - m)/m$$

$$A_+/A_- = m/(n - m) = R$$

The absolute rotation of A, $[A]$, can then be calculated from the specific rotation of the partially resolved A, $[\alpha]$.

$$[A] = [\alpha](R + 1)/(R - 1) \qquad (23)$$

In the general case (28):

$$[A] = [\alpha][(2N/nr) - 1][(R + 1)/(R - 1)] \qquad (24)$$

where N is the number of moles of A, r is the yield of the mixture of A_+B_+ and A_-B_+ from B_+ and R is the ratio of diastereomers.

Most of the recent papers concerning the determination of optical purity and the separation of diastereomers by gas chromatography have dealt with the separation of derivatives of amino acids (23,26,27, 29–39). These have included *N*-trifluoroacetylamino acid esters of (−)-menthol (26,33) and of several *n*-alkan-2-ols (29–32), as well as derivatives in which the B radical, an α-chloroisovaleryl (27) or α-chloropropionyl (37) residue, was attached at the amino function. Dipeptide derivatives have also been studied (23,35,38). In addition, esters of *n*-alkan-2-ols (29–32), and (−)-menthol (28), and the *N*-trifluoroacetyl-L-prolyl derivatives of a series of amines (34), have been examined. This method has been used to determine the absolute rotations of 2,2-dimethylcyclopentane-1-carboxylic acid (28) and 1-phenyl-2,2,2-trifluoroethanol (40) which were previously unknown. The separations have generally been performed on capillary columns although packed columns have also been effective in some cases. For an illustration of the results which may be obtained using the GLC method, see Table II.

TABLE II

Quantitative Analysis of Mixtures of Diastereomeric α-Acetoxy-L-Propionates[a,b]

Compound	Optical rotation $[\alpha]_D$	Optical purity by GLC p	Absolute rotation Calcd.[c]	Absolute rotation Repd.[d]
(−)-2-Butanol	−4.0	33.4	12.0	11.7
(−)-2-Pentanol	−4.6	24.4	18.8	13.7
(−)-2-Hexanol	−7.5	58.6	12.7	12.7
(−)-2-Heptanol	−10.7	72.2	14.8	13.7
(−)-2-Octanol	−9.9	89.6	11.0	9.9
(−)-2-Nonanol	−4.28	36.0	11.9	11.9
(−)-2-Decanol	−3.45	31.6	10.9	11.46
(−)-2-Undecanol	−5.33	50.8	10.5	10.29

[a] Ref. 32a.

[b] Capillary column, 150 ft × 0.01 in., polypropylene glycol coating, temperatures up to 140°. Relative retention times of the two diastereomers ranged from 1.04 to 1.08.

[c] On the basis of the optical purity found by GLC.

[d] Highest optical rotation measured on presumably completely resolved material.

A more direct approach to the determination of the optical purity of a mixture of enantiomers by chromatographic methods is the chromatography of enantiomers on optically active substrates, without prior conversion to diastereomers. Here one deals with diastereomeric interactions, rather than with diastereomeric compounds. The separation of enantiomers by gas chromatography on optically active columns had been claimed by Karagounis and co-workers (42), but their conclusions now appear to have been in error (43). Gil-Av et al. (44) have recently reported the separations of some derivatives of amino acids on capillary columns coated with *N*-trifluoroacetyl-L-isoleucine lauryl ester. Although simpler in principle, separation of enantiomers by GLC on optically active substrates is less convenient in practice than prior conversion to diastereomers and subsequent separation on conventional achiral substrates. Since racemic amino acids are separable by paper chromatography (i.e., chromatography on an optically active substrate, cellulose)

(45), the optical purity of amino acids may in principle be estimated by this direct approach.

V. NUCLEAR MAGNETIC RESONANCE METHODS

As has been noted above, the determination of optical purities may be achieved either by measurement of ratios of precursor or product diastereomers A_+B_+ and A_-B_+, or by measurement of the ratios of enantiomers A_+ and A_-, without physical separation of the diastereomers or enantiomers.

In principle, such a determination requires the measurement of two associated parameters. One corresponds to a structure-dependent intensive property and must give distinguishable values for the two stereoisomers. The other is an extensive parameter which must be structure independent and which must provide a measure of the relative quantities of the two stereoisomers. Nuclear magnetic resonance chemical shifts and integrated intensities suggest themselves as two convenient parameters (41), since nuclei in diastereomeric environments are anisochronous whether reference is made to diastereotopic groups in molecules placed in achiral solvents, or to enantiotopic groups in molecules placed in chiral solvents (see K. Mislow and M. Raban, *Topics in Stereochemistry*, Vol. 1, p. 1); this is the structure-dependent parameter. Furthermore, the integrated intensities are independent of structure, i.e., of the chemical environments of the nuclei in question, in contrast to the intensities of absorption (extinction coefficients) in electronic and vibrational absorption spectra (i.e., UV, IR, Raman, etc.).

The corresponding groups in enantiomeric molecules, for example the two methyl groups in (*S*)- and (*R*)-1-phenylethyl amine (**1a** and **1b**, respectively), reside in enantiomeric environments. Such groups are enantiotopic by external comparison and must be isochronous when in achiral solvents, since they will be equally screened by their environments. When *dl*-1-phenylethyl amine (**1a** and **1b**) is converted into the *O*-methylmandelamide by reaction of the amine with *dl*-*O*-methylmandelyl chloride (**1c** and **1d**) in the presence of pyridine, two diastereomeric *dl*-pairs are possible (**1e** and **1f**, and **1g** and **1h**). The environments of the two methyl groups in the amine portion in the enantiomers of

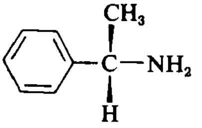

(1a)

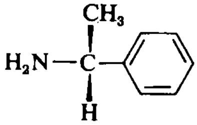

(1b)

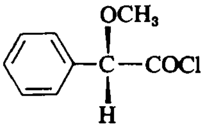

(1c)

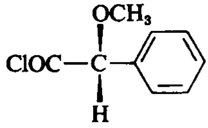

(1d)

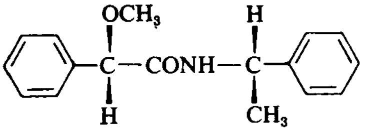

(1e)

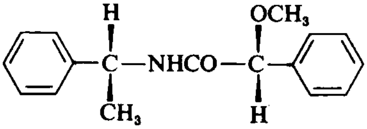

(1f)

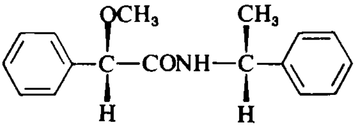

(1g)

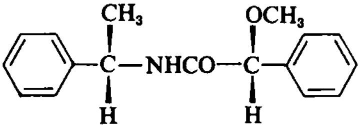

(1h)

either *dl*-pair (e.g., **1e** and **1f**) are enantiomeric. Such methyl groups are enantiotopic and must be isochronous. Thus, the chemical shifts of the C-methyl groups in **1e** and **1f** will be the same; similarly the C-methyl groups in **1g** and **1h** must be isochronous. However, the C-methyl groups in **1e** and **1g** are in diastereomeric environments; they are diastereotopic by external comparison and in principle must be anisochronous. The same applies to the methoxyl and methine hydrogens in the *O*-methylmandelyl moiety. Therefore, the NMR spectrum of a mixture of all four stereoisomers **1e**–**1h** in an achiral solvent should exhibit two different resonances for the C-methyl groups, one due to **1e** and **1f** and one due to **1g** and **1h**. If the difference in chemical shift between the diastereotopic methyl, methoxyl or methine groups is large enough, the proportions of the two diastereomers may be determined from the NMR spectrum by integration of the respective signals.

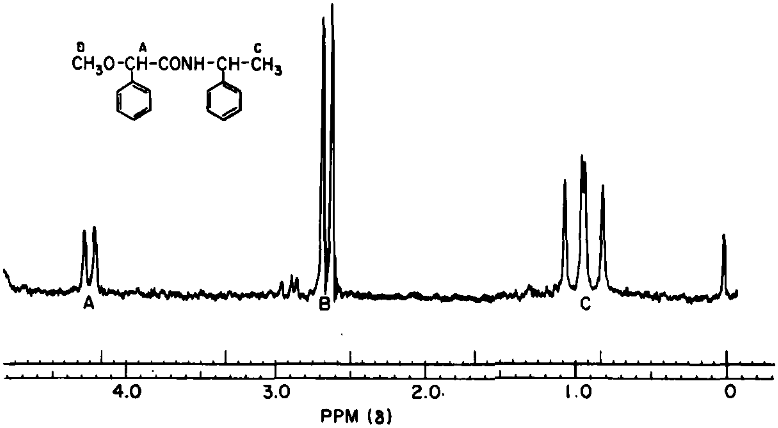

Figure 1

Figure 1 shows the NMR spectrum of a 7% solution in benzene of a sample of amide prepared from racemic acid chloride and racemic amine, and which contains nearly equal amounts of the two *dl*-pairs (**1e** and **1f**, and **1g** and **1h**). The two distinct methoxyl resonances are clearly visible as singlets at δ 2.67 and 2.62 ppm. Two methine signals at δ 4.28 and 4.21 ppm are also observed since the environments of the methine hydrogens are different in the two diastereomers. Similarly, the C-methyl groups give rise to two doublets at δ 0.99 and 0.86 ppm (46a).

When an excess of the acid chloride of optically pure (*R*)-*O*-methylmandelic acid is reacted with a sample of partially resolved 1-phenylethyl amine, $[\alpha]_D = +22.6°$ (*c* 8.6, methanol), only two of the four possible stereoisomers are formed, namely **1f** and **1h**, and the ratio of diastereomers **1f**/**1h** is equal to the ratio of enantiomers **1b**/**1a** in the starting 1-phenylethyl amine. The NMR spectrum again shows two methoxyl signals, as well as two methine singlets and two C-methyl doublets, but here the integrated amplitudes of the peaks are not equal since the amounts of **1f** and **1h** are unequal. Integrated intensities of the *O*-methyl peaks from 50 cycle sweep width scans indicate a diastereomeric ratio of 90/10 corresponding to an optical purity of 80% of the starting amine. The calculated (46a) absolute rotation of 1-phenylethyl amine is 28.3°, lit. 28.5° (46b).

Application of the NMR method to the determination of optical purities necessarily requires measurable chemical shift nonequivalence for a set of signals due to corresponding groups in the two diastereomers. It is desirable that these signals be singlets or doublets and that they not overlap with signals due to other parts of the molecule. The atom or group of atoms which give rise to the signals may be in either the *A* or the *B* portion of the molecules; that is, it may reside either in the portion of the molecule (*A*) which originates in the material whose optical purity is to be determined or in the optically pure derivatizing reagent (*B*) which is used. However, as a general approach, it seems most desirable to incorporate a suitable group or groups in a prospective *B* reagent since in many cases the *A* portion may not contain a group which will give rise to a suitable signal.

O-Methylmandelic acid is an attractive general reagent for the NMR determination of optical purity since it is readily obtainable in optically pure form and contains two groups, the *O*-methyl and the methine hydrogen, which give rise to singlet resonance signals; a specific application was illustrated by the example of the amide in Figure 1. Further, a highly magnetically anisotropic group, here the phenyl group, increases the probability that the chemical shift nonequivalence is large enough to permit the convenient integration of the two signals due to the *AB* diastereomers. To test the utility of *O*-methylmandelic acid as a general reagent for the determination of the optical purities of simple alcohols and amines, it was converted through its acid chloride into diastereomeric mixtures of a variety of esters and amides (46a). Table III lists the chemical shift differences observed for the diastereotopic methoxyl groups and methine hydrogens, and for C-methyl groups when they were present. The table indicates the variability of the magnitude of the chemical shift nonequivalence. Although the factors which determine the magnitude of the nonequivalence are many and complex and a detailed analysis is not possible, the data in the table do reflect some of the factors which seem to be involved. Two factors which are clearly implicated are the "conformer population" distribution (47) and the effect of highly anisotropic groupings. Although it is not possible to analyze in detail the conformational distributions of the compounds listed, it seems likely that, *ceteris paribus*, the greater the conformational restriction due to bulky groups, the greater the nonequivalence of the diastereotopic groups. The large nonequivalences observed for the menthyl and pinacolyl ester mixtures compared with the 2-butyl ester mixture seem to reflect the effect of conformational restriction. Further, it seems that the presence of an aromatic ring in the amine portion tends to make the nonequivalence larger. This is especially marked in the naphthyl derivative described. Solvent effects are also in evidence.

TABLE III

Chemical Shift Nonequivalence of Diastereotopic Hydrogens in Some Derivatives of *O*-Methylmandelic Acid[a]

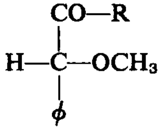

$$\mathrm{H{-}\overset{\displaystyle CO{-}R}{\underset{\displaystyle \phi}{C}}{-}OCH_3}$$

R	$-OCH_3$		$CH_3OC{-}H$		$C{-}CH_3$	
	Benzene	Chloroform	Benzene	Chloroform	Benzene	Chloroform
$OCH(CH_3)CH_2CH_3$	—	—	1.8	—		
$NHCH(CH_3)CH_2CH_3$	0.8	0.7	0.6	—		
$OC_{10}H_{19}$ (menthyl)	0.5	0.4	4.2	2.5		
$NHCH(CH_3)\phi$	3.5	2.3	4.2	2.5	6.8	4.0
$NHCH(CH_3)CH_2\phi$	1.3	2.3	1.9	0.8	5.3	4.1
$NHCH(CH_3)$ $C_{10}H_7$(α-naphthyl)	4.1	3.7	3.1	2.8	10.5	6.5
$OCH(CH_3)\phi$	0.7	0.6	—	—	5.0	7.4
$OCH(CH_3)C(CH_3)_3$[b]	<0.6	0.8	4.0	1.9	6.4	9.5

[a] Chemical shift differences are given in Hz for 60 MHz spectra of approximately 10% solutions.

[b] COOCH, benzene, 1.5, chloroform, 2.3; $C(CH_3)_3$, benzene, 5.6, chloroform, 10.3.

Because of the appreciable chemical shift nonequivalence of the methine protons in the diastereomeric (−)-menthyl esters (Table III), (−)-menthol is a suitable reagent for the determination of the optical purity of the general derivatizing agent, (*R*)-*O*-methylmandelic acid.

For this reason and to ascertain that no appreciable epimerization or racemization occurs in the preparation of the acid chloride or in the subsequent esterification reaction, the (−)-menthyl ester of the (*R*)-acid was prepared and it was found that, although the signals due to the diastereotopic methine protons in the diastereomeric esters are appreciably shifted (Table III), only one resonance (corresponding to the diastereomer which gives the upfield resonance) was detectable. Hence the starting acid was essentially optically pure and no racemization or epimerization had occurred in the formation or reaction of the acid chloride.

Since no physical separation of the diastereomers in the (A_+B_+ + A_-B_+) mixture is required, the NMR method is applicable to the determination of optical purities of compounds which owe their chirality to deuterium substitution. The optical purities of such compounds cannot be determined by the isotope dilution method or by the gas chromatographic method because the physical properties of such enantiomers or diastereomers are too similar to permit separation by physical methods. Even polarimetry frequently does not give accurate values for optical purities because of the very low specific rotations that these compounds exhibit. The low specific rotations also preclude the application of the double partial resolution method, although, as mentioned earlier, a method based on partial resolution has been devised for the limited case of α-deuterated primary alcohols (18). As discussed above, enzymatic methods have also been applied to the determination of the optical purities of α-deuterated primary alcohols, although this requires the assumption of complete enzyme stereospecificity. The validity of this assumption has been demonstrated for ethanol-1-*d*, which is the natural substrate (48). The finding (49) that the neopentyl alcohol-1-*d* produced by fermentation of pivaldehyde-1-*d* is essentially optically pure provides further support for this conclusion. An application of the NMR method for the determination of the optical purity of such compounds is described below (49).

The two methyl groups in isopropyl alcohol are enantiotopic and are isochronous in achiral solvents. An analogous situation is encountered in racemic propan-2-ol-1,1,1-d_3 in which the methyl groups in the two enantiomers are enantiotopic by external comparison, and must also show chemical shift equivalence.

When isopropyl alcohol is esterified with a chiral reagent, such as the acid chloride from (*R*)-*O*-methylmandelic acid, the two isopropyl methyl groups are diastereotopic by internal comparison and are anisochronous, giving rise to two doublets (J_a = 6.2 Hz, J_b = 6.3 Hz) which are chemically shifted by 0.085 ppm.

The chemical shifts of the diastereotopic methyl groups in the two diastereomeric *O*-methylmandelates of propan-2-ol-1,1,1-d_3 should be similar to those of the diastereotopic methyl groups in the undeuterated ester, the only difference being due to the substitution of a deuteriomethyl group for the other methyl group; the deuterium isotope effect on the chemical shift should be negligible, in this instance certainly not more than 1 Hz. This indicates that the NMR method may be used to determine the optical purity of propan-2-ol-1,1,1-d_3 (49).

The optical purity of a sample of (*S*)-propan-2-ol-1,1,1-d_3 (50) ($[\alpha]_D$ $+0.27°$ (neat)) was determined by complete reaction with an excess of the acid chloride prepared from optically pure (*R*)-*O*-methylmandelic acid. The NMR spectrum of the resulting ester was identical to that of the undeuterated analog except that the isopropyl methine signal occurred as a broadened quartet rather than as a multiplet, and that the doublet corresponding to the low-field methyl group, which would indicate the presence of the other diastereomer, was absent. The optical purity was thus estimated at 98–100%, in harmony with the fact that the alcohol was prepared from optically pure lactic acid by a series of reactions none of which involved bond breaking at the asymmetric carbon atom (50).

The observation that none of the diastereomer that would have given rise to the low-field doublet in the ester was formed from the (*S*)-alcohol and the (*R*)-acid also indicates that the (*R*)-acid was at least 98% optically pure. If either the alcohol or the acid had not been optically pure, some of the low-field diastereomer would have resulted. If some (*R*)-alcohol had been present, some of the (*R*,*R*) isomer would have been formed, and if some of the (*S*)-acid had been present, some of the enantiomeric (*S*,*S*) isomer would have resulted. Both of these isomers give rise to resonance at the position of the low-field doublet.

As discussed above, the determination of optical purity by NMR may involve the conversion of a mixture of enantiomers into a mixture of diastereomers (Scheme 1) or conversion of a mixture of diastereomers into a mixture of enantiomers (Scheme 2). When the compound whose optical purity is to be determined contains a "handle" by which a suitable B reagent may be attached, Scheme 1 will, in general, be the approach of choice. In some cases, however, it may be more convenient to remove a chiral moiety to produce a mixture of enantiomers rather than to attach one. Such will be the case especially when the route to the optically active compound involves its conversion from a mixture of diastereomers. For instance, the optical purities of sulfoxides are most conveniently estimated using NMR spectroscopy according to Scheme 2. In an example studied in our laboratory (46a), a mixture of diastereomeric sulfinate esters was prepared by reaction of inactive *p*-toluenesulfinyl chloride with (*S*)-pinacolyl alcohol; this reaction involves an asymmetric synthesis and an unequal mixture of diastereomeric sulfinate esters is formed (51a). Since the pinacolyl alcohol was nearly (96%) optically pure, only two of the four possible stereoisomers were formed in appreciable concentration. These two isomers have the same configuration at carbon and are epimeric at sulfur.

The diastereomeric mixture of sulfinate esters, a mixture of A_+B_+ and A_-B_+, where A represents the *p*-toluenesulfinyl moiety, was treated with excess methyl magnesium iodide to remove the pinacolyl moiety (B) and to produce a mixture of enantiomers, A_+ and A_-, of methyl *p*-tolyl sulfoxide. This reaction, which occurs with inversion of configuration at sulfur (51b), is highly stereospecific and as a consequence the ratio of product enantiomers is very nearly the ratio of the precursor diastereomers.

The NMR spectrum (Fig. 2) of the mixture of sulfinates as a 70% solution in carbon tetrachloride clearly reveals the presence of the two diastereomers (46a). The resonances of the methine hydrogens occur as an apparent unsymmetrical pentuplet, centered at δ 4.03 ppm which results from the superposition of two quartets centered at δ 4.08 and 3.97 ppm due to the two diastereotopic methine hydrogens in the two diastereomers. The two diastereotopic pinacolyl methyl group resonances occur as doublets centered at δ 1.30 and 1.08 ppm ($J = 6.5$ Hz) and the two diastereotopic *t*-butyl groups are revealed as singlets at δ 0.88 and 0.83 ppm. Integration of the methyl group doublets, as well as the *t*-butyl singlets, indicates a ratio of diastereomers of 60.5:39.5 or a diastereomeric purity of 21%. The starting pinacolyl alcohol is 96% optically pure and the product mixture of enantiomeric methyl *p*-tolyl sulfoxides is calculated to be 20% optically pure. Since the rotation of the sulfoxide product is $[\alpha]_D$ +29° (ethanol), the absolute rotation is calculated as $[A]_D$ +145° (ethanol), in fair agreement with the highest

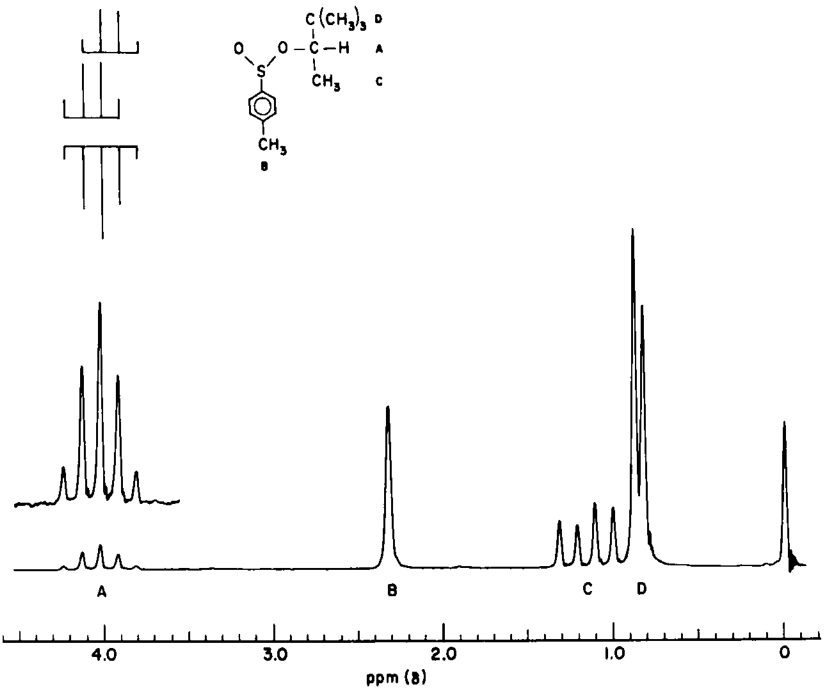

Figure 2

reported (52) rotation for presumably optically pure methyl *p*-tolyl sulfoxide, $[\alpha]_D$ +155° (ethanol).

Two further examples may be mentioned. Treatment of optically pure methyl-α-naphthylphenylbenzoylsilane (Si*COPh) with methylmagnesium bromide gives a mixture of optically active diastereomeric carbinols (Si*C(OH)MePh), which is rearranged to a mixture of optically active diastereomeric silyl ethers (Si*OCHMePh) on treatment with Na–K alloy (53). In the carbinol Si*C(OH)MePh, the ratio of relative intensities of the diastereotopic Si—CH_3 signals (at δ 0.65 and δ 0.72) is 81:19 (54). In the product of rearrangement, the ratio of relative intensities of diastereotopic Si—CH_3 signals (δ 0.65 and δ 0.61) and C—CH_3 signals (δ 1.44 and δ 1.38) is 78:22 (54). It follows that the rearrangement is nearly 100% stereospecific. Since reduction of the rearrangement product with lithium aluminum hydride gives 1-phenylethanol which is 58% optically pure by polarimetry (54), it follows that the ratio of enantiomers produced (79:21) in the reduction equals the ratio of precursor diastereomers, the reduction proceeds with 100% stereospecificity, and the absolute rotation of 1-phenylethanol has been confirmed.

Gerlach (9) used the NMR method to determine the optical purity of benzylamine-1-*d*, in another example which illustrates the usefulness of this method in the determination of the optical purity of compounds which owe their chirality to dissymmetric deuterium substitution. Benzylamine-1-*d*, obtained by an asymmetric synthesis (55), was converted to the *N*-benzylphenylglycine derivative by reaction with racemic phenylchloroacetic acid. Reduction (lithium aluminum hydride), optical "resolution," and cyclization with thiophosgene yielded a mixture of diastereomeric *N*-benzyl-α-*d*-4-phenyloxazolidine-2-thiones (cf. Table I).

This compound is configurationally homogeneous with regard to the asymmetric carbon C-4. In undeuterated *N*-benzyl-4-phenyloxazolidine-2-thione, the diastereotopic *N*-benzyl methylene protons occur as signals centered at δ 5.52 and δ 3.85 with a ratio of intensities of unity; in the deuterated compound the ratio of intensities (after correction for undeuterated material) is 81 : 19 and corresponds to an optical purity of about 62% in the precursor amine. Hence the absolute rotation of benzylamine-1-*d* is calculated to be $[\alpha]_D$ 1.8° (neat).

In chiral solvents, enantiotopic nuclei reside in diastereomeric environments and will therefore be anisochronous; the ratio of intensities is thus a means of establishing optical purity. Pirkle has adduced several examples (56,57). In 2,2,2-trifluoro-1-phenylethanol, the trifluoromethyl groups are enantiotopic by external comparison: in the achiral solvents carbon tetrachloride and *dl*-α-phenylethylamine, the fluorine resonance of racemic 2,2,2-trifluoro-1-phenylethanol appears as a doublet (H–F spin coupling), whereas in a chiral solvent (optically active α-phenylethylamine) it appears as two doublets of equal intensity.

The chemical shift difference between the atoms in optically active solvents is independent of the optical purity of the solute but does depend on the optical purity of the solvent. The magnitude of the chemical shift difference is expected to be quite small (in the preceding example, $\Delta\nu = 0.04$ ppm). Conversely the ratio of integrated intensities of the two doublets equals the ratio of abundances of the two enantiomers of the solute and is independent of the nature or optical purity of solvent. Similarly the enantiotopic carbinyl methine protons in the enantiomers of isopropylphenylcarbinol are isochronous in achiral solvents but are chemically shifted in the chiral solvent (+)-α-(1-naphthyl)-ethylamine ($\Delta\nu = 0.025$ ppm).

It should be noted that in the above treatment solvents are regarded as achiral whether this condition arises as a consequence of molecular symmetry (as in carbon tetrachloride) or because the medium is racemic (e.g., *dl*-α-phenylethylamine). This point of view is legitimate because solvent–solute interactions are averaged on the NMR time scale. Thus, when a racemic compound $A_\pm$ is dissolved in a racemic solvent $B_\pm$, the diastereomeric interactions (A_+/B_+) and A_+/B_-) are averaged out, as are the diastereomeric interactions in the enantiomeric set (A_-/B_-) and (A_-/B_+). Since enantiomeric conditions are indistinguishable by NMR, only one signal due to the averaged diastereomeric solvent interactions is detected. However, on a shorter time scale (e.g., electronic or vibrational transitions) such diastereomeric solvent–solute interactions would not be averaged and should, in principle, be distinguishable: in that case, a difference might be discerned between solvents which are achiral on the molecular level and those which are achiral on the bulk level by reason of being racemic mixtures.

Pirkle's NMR method (56), like Gil-Av's GLC method using optically active substrates (44), is absolute, in the sense that no reference to a standard of optical purity is required. The chemical shift difference between enantiotopic nuclei in chiral solvents increases with increasing optical purity of the solvent, even as the retention-time difference between enantiomers increases with increasing optical purity of the substrate in the GLC method. However, since the relative intensities of the integrated signals are independent of the separation, optical purity may be determined by either method on an absolute scale.

VI. THE CALORIMETRIC METHOD

A method has been devised by Fouquey and Jacques (58,59) for determining the enantiomeric composition of optically impure substances by differential microcalorimetry.

The method depends on the phase relationship of the component enantiomers. Generally, racemic forms are either conglomerates, i.e., equimolar mixtures of crystals of the pure enantiomers, or they are 1:1 compounds of the enantiomers (so-called "true" racemates*); only

---

* In contrast to "true" racemates, "anomalous" racemates are compounds in which the ratio of enantiomeric components is not unity. For a recent example, see M. Andersson, A. Fredga, and B. Jerslev, *Acta Chem. Scand.*, **20**, 1060 (1966).

rarely do enantiomers form a continuous series of solid solutions (60). In the binary phase diagram of a mixture of enantiomers there is but a simple eutectic, which corresponds to the racemic conglomerate. The eutectic temperature T_e is also the melting point of the racemic conglomerate T_r. For any other mixture of enantiomers the thawing point (i.e., the temperature corresponding to the solidus) is also T_r and, characteristically, the melting point (i.e., the temperature corresponding to the liquidus) T is always above T_r, regardless of the composition (i.e., optical purity) of the mixture. By contrast, there are two eutectic points in the binary phase diagram of a racemic compound (racemate). The melting point of a racemate T_r is always above the eutectic temperature T_e, though it may be either above or below the melting point of the pure enantiomers. The identity of the racemic form (i.e., as a conglomerate or a racemate) may be established by its phase behavior, or by a comparison of its infrared spectrum or x-ray powder diagram with that of the pure enantiomers.

If the enantiomers form a racemic compound, determination of the optical purity of an optically impure sample by this method requires the following information: the heat of fusion of the racemate, ΔH_r; the melting point of the racemate, T_r; the melting point (liquidus temperature) of the unknown sample, T. All these quantities can easily be determined by differential microcalorimetry (58,59).

Using the relationship (61) given in eq. (25)

$$ln \frac{F_+F_-}{0.25} = \frac{\Delta H_r}{R}\left(\frac{1}{T_r} - \frac{1}{T}\right) \tag{25}$$

the product F_+F_- can thus be evaluated, where F_+ is the mole fraction of one enantiomer and F_- that of the other. Since $F_+ + F_- = 1$, the required information is in hand for calculating the optical purity of the sample. The method requires that the optical purity of the sample be less than that of the eutectic mixture; if the sample has an optical purity greater than that of the eutectic mixture, a known weight of racemate may be added to the sample to bring its composition into the useful range. To determine which side of the eutectic composition the sample is on, one need only add a small amount of the racemate; if the melting point is lowered, the optical purity of the sample is greater than that of the eutectic mixture, whereas, if the melting point is raised, the optical purity of the sample is less than that of the eutectic mixture.

If the enantiomers form a conglomerate, eq. (25) is not applicable, but the optical purity of the sample may nonetheless be estimated by differential microcalorimetry (58,59) as follows. The sample of unknown composition is heated. When the eutectic temperature T_r is reached, all of the eutectic component of the mixture (i.e., all of the minor enantiomer plus a correspondingly equal amount of the major enantiomer) will melt before the temperature rises above T_r. The amount of heat required to melt the eutectic component, Q_1, is compared with the amount of heat required to melt a sample of racemic, i.e., eutectic, composition, Q_2. The ratio Q_1/Q_2 equals the fraction of racemic material in the unknown sample. The optical purity may thus be calculated.

The method of differential microcalorimetry appears to have wide applicability and high precision, and has the further advantage that very small quantities of material suffice to carry out the measurements (59).

Acknowledgments

We gratefully acknowledge the kindness of those of our colleagues who provided us with results of their work prior to publication: Professors A. Brook, E. Gil-Av, A. Horeau, J. Jacques, and W. H. Pirkle, and Dr. H. Gerlach.

References

1. E. L. Eliel, *Stereochemistry of Carbon Compounds*, McGraw-Hill, New York, 1962, pp. 61, 62, 83–85.
2. (a) J. A. Berson and D. Willner, *J. Am. Chem. Soc.*, **86**, 609 (1964); (b) G. W. O'Donnell and M. D. Sutherland, *Australian J. Chem.*, **19**, 525 (1966).
3. J. P. Greenstein and M. Winitz, *Chemistry of the Amino Acids*, Wiley, New York, 1961.
4. (a) J. H. Brewster, *J. Am. Chem. Soc.*, **81**, 5475, 5483, 5493 (1959); (b) J. H. Brewster in *Topics in Stereochemistry*, Vol. 2, N. L. Allinger and E. L. Eliel, Eds., Interscience, New York, 1967, p. 1.
5. K. Mislow, R. Graeve, A. J. Gordon, and G. H. Wahl, Jr., *J. Am. Chem. Soc.*, **86**, 1733 (1964); H. Wynberg, G. L. Hekkert, J. P. M. Houbiers, and H. W. Bosch, *ibid.*, **87**, 2635 (1965); C. Djerassi, *Optical Rotatory Dispersion*, McGraw-Hill, New York, 1960, pp. 235–236.
6. S. Graff, D. Rittenberg, and G. L. Foster, *J. Biol. Chem.*, **133**, 745 (1940).
7. J. A. Berson and D. A. Ben-Efraim, *J. Am. Chem. Soc.*, **81**, 4083 (1959).
8. H. L. Goering and J. T. Doi, *J. Am. Chem. Soc.*, **82**, 5850 (1960).
9. H. Gerlach, *Helv. Chim. Acta*, **49**, 2481 (1966).
10. J. A. Berson and S. Suzuki, *J. Am. Chem. Soc.*, **81**, 4088 (1959).

11. H. L. Goering, M. M. Pombo, and K. D. McMichael, *J. Am. Chem. Soc.*, **85**, 965 (1963).
12. H. L. Goering and D. L. Towns, *J. Am. Chem. Soc.*, **85**, 2295 (1963).
13. H. L. Goering, J. T. Doi, and K. D. McMichael, *J. Am. Chem. Soc.*, **86**, 1951 (1964).
14. J. R. Beckwith and L. P. Hager, *J. Org. Chem.*, **26**, 5206 (1961).
15. A. C. Cope, W. R. Funke, and F. N. Jones, *J. Am. Chem. Soc.*, **88**, 4693 (1966).
16. K. Mislow, *Introduction to Stereochemistry*, Benjamin, New York, 1965, p. 122 ff.
17. A. Horeau, *J. Am. Chem. Soc.*, **86**, 3171 (1964); *Bull. Soc. Chim. France*, **1964**, 2673; A. Horeau, J. P. Guetté, and R. Weidmann, *ibid.*, **1966**, 3513.
18. A. Horeau and A. Nouaille, *Tetrahedron Letters*, **1966**, 3953.
19. H. Weber, J. Seibl, and D. Arigoni, *Helv. Chim. Acta*, **49**, 741 (1966).
20. J. Casanova, Jr. and E. J. Corey, *Chem. Ind.* (*London*), **1961**, 1664.
21. E. Gil-Av and D. Nurok, *Proc. Chem. Soc.*, **1962**, 146.
22. J. Petránek, M. Kolínský, and D. Lim, *Nature*, **207**, 1290 (1965).
23. F. Weygand, A. Prox, L. Schmidhammer, and W. König, *Angew. Chem. Intern. Ed. Engl.*, **2**, 183 (1963).
24. Y. Gault and H. Felkin, *Bull. Soc. Chim. France*, **1965**, 742.
25. R. Charles, G. Fischer, and E. Gil-Av, *Israel J. Chem.*, **1**, 234 (1963).
26. S. V. Vitt, M. B. Saporovskaya, I. P. Gudkova, and V. M. Belikov, *Tetrahedron Letters*, **1965**, 2575.
27. B. Halpern and J. W. Westley, *Chem. Commun.*, **1965**, 246.
28. J. P. Guetté and A. Horeau, *Tetrahedron Letters*, **1965**, 3049.
29. G. E. Pollock, V. I. Oyama and R. D. Johnson, *J. Gas Chromatog.*, **3**, 174 (1965).
30. G. E. Pollock and V. I. Oyama, *J. Gas Chromatog.*, **4**, 126 (1966).
31. E. Gil-Av, R. Charles, and G. Fischer, *J. Chromatog.*, **17**, 408 (1965).
32. (a) E. Gil-Av, R. Charles-Sigler, G. Fischer, and D. Nurok, *J. Gas Chromatog.*, **4**, 51 (1966); (b) R. Charles-Sigler and E. Gil-Av, *Tetrahedron Letters*, **1966**, 4231.
33. B. Halpern and J. W. Westley, *Chem. Commun.*, **1965**, 421.
34. B. Halpern and J. W. Westley, *Chem. Commun.*, **1966**, 34.
35. B. Halpern and J. W. Westley, *Biochem. Biophys. Res. Commun.*, **19**, 361 (1965).
36. B. Halpern, J. W. Westley, I. Wredenhagen, and J. Lederberg, *Biochem. Biophys. Res. Commun.*, **20**, 710 (1965).
37. B. Halpern, J. Ricks, and J. W. Westley, *Anal. Biochem.*, **14**, 156 (1966).
38. B. Halpern and J. W. Westley, *Tetrahedron Letters*, **1966**, 2283.
39. B. Halpern, J. W. Westley, and B. Weinstein, *Nature*, **210**, 837 (1966).
40. D. M. Feigl and H. S. Mosher, *Chem. Commun.*, **1965**, 615.
41. M. Raban and K. Mislow, *Tetrahedron Letters*, **1965**, 4249.
42. G. Karagounis and E. Lemperle, *Z. Anal. Chem.*, **189**, 131 (1962); G. Karagounis and G. Lippold, *Naturwiss.*, **46**, 145 (1959).
43. C. B. Coleman, G. D. Cooper, and J. F. O'Donnell, *J. Org. Chem.*, **31**, 975 (1966).
44. E. Gil-Av, B. Feibush, and R. Charles-Sigler, *Tetrahedron Letters*, **1966**, 1009.

45. C. E. Dalgliesh, *J. Chem. Soc.*, **1952**, 3940.
46. (a) M. Raban, Ph.D. thesis, Princeton University, 1966; (b) W. Leitke, *Monatsh.* **51**, 381 (1929).
47. P. M. Nair and J. D. Roberts, *J. Am. Chem. Soc.*, **79**, 4565 (1957); M. Raban, *Tetrahedron Letters*, **1966**, 3105, and references cited therein.
48. F. A. Loewus, F. H. Westheimer, and B. Vennesland, *J. Am. Chem. Soc.*, **75**, 5018 (1953); H. R. Levy, F. A. Loewus, and B. Vennesland, *J. Am. Chem. Soc.*, **79**, 2949 (1957) and references cited therein.
49. M. Raban and K. Mislow, *Tetrahedron Letters*, **1966**, 3961.
50. K. Mislow, R. E. O'Brien, and H. Schaefer, *J. Am. Chem. Soc.*, **84**, 1940 (1962).
51. (a) M. M. Green, M. Axelrod, and K. Mislow, *J. Am. Chem. Soc.*, **88**, 861 (1966). (b) P. Bickart, M. Axelrod, J. Jacobus, and K. Mislow, *J. Am. Chem. Soc.*, **89**, 697 (1967) and references cited therein.
52. K. Mislow, M. Axelrod, D. R. Rayner, H. Gotthardt, L. M. Coyne, and G. S. Hammond, *J. Am. Chem. Soc.*, **87**, 4958 (1965).
53. A. G. Brook and W. W. Limburg, *J. Am. Chem. Soc.*, **85**, 832 (1963).
54. W. W. Limburg, Ph.D. thesis, University of Toronto, 1965; A. G. Brook, private communication.
55. A. Streitwieser, Jr., J. R. Wolfe, Jr., and W. D. Schaeffer, *Tetrahedron*, **6**, 338 (1959).
56. W. H. Pirkle, *J. Am. Chem. Soc.*, **88**, 1837 (1966).
57. T. G. Burlingame and W. H. Pirckle, *J. Am. Chem. Soc.*, **88**, 4294 (1966).
58. C. Fouquey and J. Jacques, *Bull. Soc. Chim. France*, **1966**, 165.
59. C. Fouquey and J. Jacques, *Tetrahedron*, in press; J. Jacques, private communication.
60. J. T. Melillo and K. Mislow, *J. Org. Chem.*, **30**, 2149 (1965).
61. H. Mauser, *Chem. Ber.*, **90**, 307 (1957).

Topics in Stereochemistry, Volume 2
Edited by Norman L. Allinger, Ernest L. Eliel

Author Index

Numbers in parentheses are reference numbers and indicate that the author's work is referred to although his name is not mentioned in the text. Numbers in *italics* show the pages on which the complete references are listed.

Topics in Stereochemistry, Volume 2
Edited by Norman L. Allinger, Ernest L. Eliel

Subject Index